

*A PALAEOECOLOGICAL ANALYSIS OF  
LATE QUATERNARY SAPROPELS FROM  
THE MEDITERRANEAN RIDGE*

By

**Darren Barry**

Supervisor: Dr Angela Cloke-Hayes

*A thesis submitted for the degree of*  
DOCTOR OF PHILOSOPHY

Department of Geography  
Mary Immaculate College  
(Coláiste Mhuire Gan Smál)  
University of Limerick





## **Abstract**

### *A PALAEOECOLOGICAL ANALYSIS OF LATE QUATERNARY SAPROPELS FROM THE MEDITERRANEAN RIDGE*

By Darren Barry

The sedimentary sequences of the Eastern Mediterranean Sea are interspersed by black-coloured, organic rich deposits called sapropels. Ranging in thickness from a few millimeters to as much as tens of centimetres these sedimentary layers have been deposited throughout the late Cenozoic. Despite intensive research the exact environmental conditions that led to the deposition of these sapropels are not yet fully understood. Using planktonic foraminifera as a proxy, this research focuses on the deposition of several sapropels. In addition to the more commonly studied sapropels (S1 and S5) S3 and S6 have also been investigated. The principle aim of this research is to reconstruct the palaeoenvironmental conditions during these depositional events. In addition to using the traditional method of analysing faunal assemblages, particular emphasis will be placed on accessing the test size variation of individual species of planktonic foraminifera. This technique has been applied to other events in Earth's history but not in relation to sapropel deposition.

The research is based on data extracted from ODP core 969A (latitude 33.84N, longitude 24.88E, water depth 2200.3 m). With the exception of S1 (7cm), the thickness of each sapropel (S3 – 28cm; S5 – 28cm; S6 – 41cm) allows each event to be analysed at a sufficiently high resolution. One aspect of this study related to the palaeoenvironmental reconstruction of two cores from open ocean sites. Using micropalaeontological data along with multivariate statistical analysis has allowed detailed analysis of palaeoenvironmental variability since the Last Glacial Maximum (LGM). In addition, estimates of sea surface temperature (SST) shows a gradual climate amelioration from the LGM to present. A unique aspect of this research examined the mean test size data of two shallow and one deep dwelling planktonic foraminiferal species over two sapropel events. Particular attention was paid to both biotic and abiotic factors in the understanding of their effects on species growth. While no obvious

increase in mean test size was noted as a direct response to sapropel deposition, variability throughout these timeframes is observed. It is concluded that the mean test size of each species responds differently depending on their SST and nutrient requirements. For the Eemian interglacial sapropel S5 and glacial sapropel S6, a palaeoecological analysis utilising palaeoenvironmental indices reconstructed the water column dynamics and trophic status during these depositional events. Sapropel S5 exhibited considerable variability in response to the position of the Cretan gyre while a two phase depositional event in S6 indicated extreme shoaling of the pycnocline.

## **Declaration**

I, Darren Barry, declare that this thesis is my own work and has never been previously submitted by me or any other individual for the purpose of obtaining a qualification.

Signed:

---

Darren Barry

Date:

---

## Acknowledgements

There is no doubt that this has been an enjoyable (and long) process from start to finish but none of it would have been possible without the immense support of my supervisor Dr. Angela Cloke-Hayes, her unwavering encouragement, long chats and many laughs has kept me on the right track. From our first discussions where I wanted to do something with dinosaurs to showing me a path of research that I would never have imagined possible not only has she been a fantastic supervisor but a great friend.

I would like to thank Mary Immaculate College and all the wonderful friends I have met there. A very special mention must go to my Micro-Madness group, Margaret Browne and Dr. Joyce Novak, thank you for listening, offering me advice, supporting me through this entire process and for believing in me, even at times when I didn't believe in myself. I know this process was made all the better for having you as my friends and my colleagues.

Of course they are only a few of the friends that I have made along the way, many thanks to Dr. Shane O Sullivan, Niall Walsh, Marie Taylor, Dr. Britta Jung, Dr Julie McGrath, Ruth Guiry, Dr. Teresa Broggy, Bernie McCarthy, Sean Halligan, Patrick Morrissey and the wider postgrad community (Emma, Paul, Aideen and Cillian, to name a few)...it was always good to know that I wasn't the only one who wanted to hide and binge watch Netflix.

Special recognition must go to all the members of the Geography Department, Prof Des McCafferty, Dr Helene Bradley-Davies, Dr Brendan O'Keefe, Dr Catherine Dalton, Dr Anne Kane and Dr Julian Bloomer for being great colleagues and for their continual friendship and support.

Further thanks must go to Dr. Lucilla Capotondi and Dr. Aggeliki Georgiopoulou for making the Viva Voce an enjoyable experience and for their comments and support.

My sincerest thanks go to my brothers & sisters, Thomas, Anthony, Liam, Amy, Amanda and Kellie, my nephews, nieces and indeed to all my family (my grandmother Agnes, aunts Caroline, Mary and Majella, cousins and in-laws especially my Mother-in-law Celine) for whose love support and understanding over the years has enabled me to remain in college. Further thanks must go to all my friends Aisling, Orla, Nadine & Pamela for helping me to have some resemblance of life outside of research.

The words THANK YOU don't seem enough in order to return all the love and support my wife Caroline has given me over the years, nothing I do would be possible without her by my side, not only has she been an amazing wife but also my very best friend. To our children Taylor and Zachary, you are the best children a father could hope for, happy, loving and a joy to be around.

Finally, my thanks have to go to Madonna, whose music kept me sane during many long hours working in the lab....it is now time for a 'Holiday'

Dedicated to the memory of an amazing & unforgettable Mother

Ann Barry (1962 – 2014)

*In my dreams I'll always see you soaring by the sky,  
In my heart there'll always be a place for you,  
For all my life  
I'll keep a part of you with me,  
And everywhere I am there you'll be.*

# TABLE OF CONTENTS

|  |    |
|--|----|
| <b>Chapter 1</b> .....   | 1  |
| Introduction .....   | 1  |
| 1.1 Area of Study.....   | 3  |
| 1.2 Planktonic foraminifera .....  | 4  |
| 1.3 Purpose and Aims of this research .....                                      | 5  |
| <b>Chapter 2</b> .....   | 7  |
| Present Day Climatology and Physical Oceanography of the Mediterranean Sea ..... | 7  |
| 2.1 Introduction .....   | 7  |
| 2.2 Present Day Climatology.....   | 8  |
| 2.2.1 Prevailing Winds .....   | 10 |
| 2.2.2 African Monsoon .....  | 13 |
| 2.2.3 North Atlantic Oscillation.....  | 14 |
| 2.3 Physical Oceanography .....  | 15 |
| 2.3.1 Atlantic Surface Waters .....  | 16 |
| 2.3.2 Levantine Intermediate Water (LIW) .....                                   | 18 |
| 2.3.3 Deep Water Formation .....   | 20 |
| <b>Chapter 3</b> .....   | 22 |
| Eastern Mediterranean Sedimentary Deposits (Sapropels).....                      | 22 |
| 3.1 Introduction .....   | 22 |
| 3.2 Geochemical Characteristics of Sapropels .....                               | 22 |
| 3.3: Chronology of Sapropels.....  | 24 |
| 3.3.1 Marine Isotope Stages.....   | 24 |
| 3.3.2 Astronomical Forcing .....   | 25 |
| 3.5 Sapropel Formation .....   | 29 |
| 3.5.1 Stagnation/Anoxia Model.....   | 30 |
| 3.5.2 Insolation Model .....   | 32 |
| 3.5.3 Productivity Model .....   | 33 |
| 3.6 Faunal Characteristics of Sapropels .....                                    | 36 |

|  |           |
|--|-----------|
| 3.6.1 Benthic Foraminifera .....   | 36        |
| 3.6.2 Planktonic Foraminifera .....  | 39        |
| 3.6.3 Sapropel Interruption .....  | 40        |
| <b>Chapter 4</b> .....   | <b>42</b> |
| Planktonic Foraminifera.....   | 42        |
| 4.1 Introduction .....   | 42        |
| 4.2: Planktonic foraminifera development .....   | 44        |
| 4.2.1 Lifecycle .....  | 44        |
| 4.2.2 Shell Composition and Morphology.....  | 45        |
| 4.3: Distribution of planktonic foraminifera .....   | 46        |
| 4.3.1 Temperature and Salinity.....  | 46        |
| 4.3.2 Productivity.....  | 48        |
| 4.3.3 Vertical distribution of Foraminifera.....   | 49        |
| 4.4 Distribution in the Mediterranean Sea.....   | 52        |
| 4.6 Transfer Functions.....  | 54        |
| <b>Chapter 5</b> .....   | <b>56</b> |
| Materials and Methods.....   | 56        |
| 5.1 Introduction .....   | 56        |
| 5.2 Materials .....  | 56        |
| 5.2.1 Core Lithostratigraphy.....  | 57        |
| 5.3 Methods .....  | 62        |
| 5.3.1 Micropalaeontological analysis .....   | 62        |
| 5.3.2 Accelerator mass spectrometry (AMS) <sup>14</sup> C dating .....   | 65        |
| 5.3.3 Artificial Neural Networks .....   | 65        |
| <b>Chapter 6</b> .....   | <b>67</b> |
| Palaeoenvironmental variability of the eastern Mediterranean Sea (Mediterranean Ridge) since the Last Glacial Maximum (LGM)..... | 67        |
| 6.1 Introduction .....   | 67        |
| 6.2 Chronological Framework.....   | 69        |
| 6.3 Palaeoenvironmental Proxies .....  | 71        |

|   |            |
|---|------------|
| 6.4 Results .....   | 73         |
| 6.4.1 Distribution of planktonic foraminifera.....  | 73         |
| 6.4.2 Principal Component Analysis .....  | 81         |
| 6.4.3 Sea Surface Temperatures .....  | 84         |
| 6.5: Discussion .....   | 85         |
| 6.5.1 Palaeoenvironmental Reconstruction .....  | 85         |
| 6.5.2. The Late Glacial (~21,000 – 15,000 cal yrs BP) .....   | 85         |
| 6.5.3 Deglaciation (~15,000 – 10,500 cal yrs BP).....   | 90         |
| 6.5.4 Holocene Climatic Optimum.....  | 91         |
| 6.5.6 Modern day (~5,000 – Present cal yrs BP).....   | 92         |
| 6.6: Conclusions .....  | 93         |
| <b>Chapter 7 .....</b>  | <b>95</b>  |
| Does Size Matter? Test size variability of planktonic foraminifera in response to biotic/abiotic factors during the deposition of sapropel S3 and S5. A case study from the Mediterranean Ridge (ODP core 969A) ..... | 95         |
| 7.1: Introduction .....   | 95         |
| 7.2: Materials and methods .....  | 97         |
| 7.2.2 Species Measurement .....   | 100        |
| 7.3 Results .....   | 101        |
| 7.3.1 Test size of planktonic foraminifera .....  | 101        |
| 7.3.2 absolute abundance of planktonic foraminifera.....  | 105        |
| 7.3.3 Sea Surface temperatures (SSTs) during S3 and S5 .....  | 105        |
| 7.3.4 Summary of results .....  | 106        |
| 7.4 Discussion .....  | 109        |
| 7.4.1 Sea Surface Temperatures .....  | 110        |
| 7.4.2 Nutrients .....   | 114        |
| 7.4.3 Irradiance .....  | 117        |
| 7.4.4 Salinity.....   | 117        |
| 7.5 Conclusions .....   | 118        |
| <b>Chapter 8 .....</b>  | <b>121</b> |

|   |     |
|---|-----|
| Palaeoecological variability of Eastern Mediterranean sapropels S5 and S6: a case study from the south of crete ..... | 121 |
| 8.1 Introduction .....  | 121 |
| 8.2 Palaeoenvironmental Proxies .....   | 123 |
| 8.3 Results .....   | 124 |
| 8.3.1 distribution of planktonic foraminifera.....  | 124 |
| 8.3.3 Summary of Sea Surface Temperatures (SSTs) .....  | 130 |
| 8.4 Discussion .....  | 131 |
| 8.4.1 PalaeoEcological varaibility of sapropels s5 and s6.....  | 131 |
| 8.5 Conclusions .....   | 137 |
| <b>Chapter 9</b> .....  | 139 |
| Conclusions and further work .....  | 139 |
| 9.1 Conclusions .....   | 139 |
| 9.2 Limitations and Recommendations .....   | 141 |
| <b>Bibliography</b> .....   | 143 |

# LIST OF FIGURES

|  |           |
|--|-----------|
| <i>Figure 1.1: Example of a Mediterranean Core (ODP core 969A), sapropel layers are indicated by the dark colour change in the sediments (courtesy of Ocean Drilling Program).....</i>   | <i>1</i>  |
| <i>Figure 1.2: Map of the Mediterranean Sea displaying the main basins, sub basins and straits 1=Alboran Sea, 2=Balearic Basin, 3=Gulf of Lion, 4=Algerian Sea, 5=Tyrrhenian Sea, 6=Adriatic Sea, 7=Ionian Sea, 8=Cretan Sea, 9=Aegean Sea, 10=Levantine Basin. ....</i>   | <i>4</i>  |
| <i>Figure. 2.1: Map of the Mediterranean Sea displaying the main basins, sub basins and straits 1=Alboran Sea, 2=Balearic Basin, 3=Gulf of Lion, 4=Algerian Sea, 5=Tyrrhenian Sea, 6=Adriatic Sea, 7=Ionian Sea, 8=Cretan Sea, 9=Aegean Sea, 10=Levantine Basin.....</i>   | <i>7</i>  |
| <i>Figure 2.2: Schematic representation of the global atmospheric circulation during the Northern Hemisphere summer. Global wind patterns are indicated by the black arrows. Note that the dominant winds influencing the climate of the Mediterranean Sea are the westerlies. ITCZ = Inter-Tropical Convergence Zone; H = areas of high sea-level pressure; L = areas of low sea-level pressure (courtesy of Rohling et al., 2015).....</i>                         | <i>8</i>  |
| <i>Figure 2.3: Mean sea surface temperature in the Mediterranean Sea (°C) exhibiting annual (A), spring (B), summer (C), autumn (D) and winter (E) averages. Note that during spring and winter the dominant wind systems are the westerly winds with the Etesian prevailing during the summer months and Sirocco winds occurring throughout the year (courtesy of Shaltout and Omstedt, 2014).....</i>  | <i>9</i>  |
| <i>Figure 2.4: Map illustrating the direction and location of the prevailing winds across the Mediterranean region. Cold winds include the Westerly, Mistral, Bora and the Etesian which extend over the northern borderlands of the Mediterranean while the warm winds include Sirocco which extend over the southern parts of the sea. ....</i>  | <i>11</i> |
| <i>Figure 2.5: Map illustrating the seasonal changes of the Inter Tropical Convergence Zone with emphasis on its location over the River Nile. The red line represents its location during summer and the blue line represents its winter location.....</i>  | <i>14</i> |
| <i>Figure 2.6: Schematic representation of the positive and the negative phases of the North Atlantic Oscillation, showing centres of high and low pressure together with significant anomalies in atmospheric and oceanic conditions (courtesy of Bojariu and Gimeno, 2003). ....</i>   | <i>15</i> |
| <i>Figure 2.7: Surface water circulation in the Mediterranean Sea. Note that the shaded areas indicate the formation of intermediate and deep water production, in particular note how the transportation of MAW and the formation of the intermediate and deep water are aligned with the main gyres of the Mediterranean (Modified from Rohling et al., 2008). ....</i>  | <i>17</i> |
| <i>Figure 2.8: Map illustrating the circulation of LIW within the Mediterranean Sea. Note how at several points through its path LIW breaks off and is recirculated throughout the entire Sea (Modified from Millot and Taupier-Letage, 2005). ....</i>  | <i>19</i> |
| <i>Figure 3.1: Marine isotope stages of the last 500,000 years depicting the main stages and sub stages (courtesy of Railsback et al. 2015). ....</i>  | <i>25</i> |
| <i>Figure 3.2: Illustration of the Earth’s precessional cycle depicting the wobble of the Earth’s axis between pointing towards Polaris and Vega during this cycle. ....</i>   | <i>27</i> |
| <i>Figure 3.3: Relationship between sapropel deposition, associated oxygen isotope record (for eastern Mediterranean core RC9-181) and the Milankovitch cycles (eccentricity and precession). Note that not all precession minima produced sapropels, but instead sapropel deposits occur in discrete groups. Also with the exception of S4, S6 and S8, sapropels coincide with intervals of <math>\delta^{18}O</math> depletion (courtesy of Hilgen, 1991).....</i> | <i>28</i> |

|   |           |
|---|-----------|
| <i>Figure 3.4: Map of Mediterranean Sea highlighting some of the main contributing rivers of the northern borderlands including Ebro, Rhone, Po and Danube. A number of smaller rivers also contribute to the freshwater influx into the Mediterranean. ....</i>  | <i>31</i> |
| <i>Figure 3.5: Nutrient cycling and circulation patterns during deposition of sapropel S5 deposition in the Eastern basin. Over most of the basin, moderate primary productivity is supported by increased nutrient input from rivers re-circulated in the basin by estuarine flow. Extensive N-fixation occurs in surface waters overlying shallow redox boundaries due to additional phosphorus originating from the deep water column (modified form Struck et. al. 2001). ....</i>              | <i>35</i> |
| <i>Figure 3.6: Conceptual model explaining the benthic foraminifera living depths (black area) in terms of food availability and oxygen concentration (modified after Jorissen at al., 1995). ....</i>  | <i>38</i> |
| <i>Figure 4.1: Diagram illustrating the three main supergroup families of planktonic foraminifera: Microperforate (G. glutinata), Globorotaloidea (non-spinose species e.g. G. truncatulinoides) and Globigerinidea (spinose species e.g. G. ruber. A close up image of the wall structure displays the difference between the supergroups) (courtesy of Kucera, 2007).....</i>   | <i>43</i> |
| <i>Figure 4.2: Depiction of the sexual reproduction cycle of planktonic foraminifera. All planktonic foraminiferal species are considered to be diploids and so complete the full life cycle as shown (courtesy of Topa et al., 2017). ....</i>   | <i>45</i> |
| <i>Figure 4.3 Map showing the five major planktonic foraminiferal faunal provinces which largely correspond to the main hydrographic regions of the modern global ocean. Also depicted is the relative abundance profiles of planktonic foraminifera within each of the global provinces (courtesy of Kucera, 2007). ....</i>   | <i>47</i> |
| <i>Figure 4.4: Modern day depth profiles of planktonic foraminifera (courtesy of Schiebel and Hemleben, 2005). ....</i>   | <i>50</i> |
| <i>Figure 4.5: Distribution map of sampling locations during Vicomed I (summer), II (winter) and III (spring) cruises (modified after Pujol and Vergnaud-Grazzini, 1995; base map courtesy of www.google.com/earth). ....</i>   | <i>52</i> |
| <i>Figure 4.6: Graphs representing the summer/winter densities (number of species/1000m<sup>3</sup> of filtered water) of defined planktonic foraminiferal species within the eastern basin of the Mediterranean Sea (data from Pujol and Vergnaud-Grazzini, 1995). The Y-axis represents number of specimens and the X-axis signifies the station number. (Stations 10=Malta; 11=Ionian Sea; 14/17(winter) =Anaximander Trough; 15/16= Cyprus; 17(Summer) =Crete; 18= Rhodes; 19= Crete). ....</i> | <i>54</i> |
| <i>Figure 5.1 Map illustrating the location of Eastern Mediterranean ODP Cores 969A located along Mediterranean ridge and ODP core 964A located within the Ionian Sea. ....</i>   | <i>57</i> |
| <i>Figure 5.2: Lithological log and corresponding photograph of ODP core 969A with sapropel layers and sampling section marked within each unit. Photograph of ODP core 964A with sampling section also defined. Orange bar represents the areas from which sampling at 2cm (969A) and 4cm (964A) intervals was taken. (Photograph courtesy of Ocean Drilling Programme).....</i>   | <i>60</i> |
| <i>Figure 5.3: Depiction of some of the equipment that was used for the processing of samples where (A) Oven; (B) Sieves; (C) Random Micro Splitter (D) Microscope (E) Cushman Slides.....</i>  | <i>63</i> |
| <i>Figure 6.1: Map illustrating the location of Eastern Mediterranean ODP Cores 969A, located along the Mediterranean Ridge and 964A situated within the Ionian Sea.....</i>  | <i>68</i> |
| <i>Figure 6.2 Age-depth profile for Mediterranean ridge core 969A (red) and Ionian Sea core 964A (black) with AMS dating control points marked by dashed lines relative to each core. ....</i>  | <i>70</i> |
| <i>Figure 6.3 Faunal assemblage for ODP core 969A presented with winter (blue), annual (purple) and summer (red) SSTs. The grey shaded area represents Sapropel S1 and the results of the cluster analysis are also identified with respect to their location within the core (see figure 6.5 and tables 6.4 and 6.5 for details). ....</i>   | <i>74</i> |

|  |     |
|--|-----|
| Figure 6.4 Faunal assemblage for ODP core 964A presented with winter (blue), annual (purple) and summer (red) SSTs. The grey shaded area represents Sapropel S1 and the results of the cluster analysis are also identified with respect to their location within the core (see figure 6.6 and tables 6.4 and 6.5 for details) .....   | 75  |
| Figure 6.5: Dendrogram resulting from Q-mode cluster analysis and the clusters identified in core 969A. On the right hand side, the relevant clusters have been identified and colour coded; Cluster 1 = glacial assemblage (blue), Cluster 2A = modern assemblage (orange), Cluster 2B = deglaciation assemblage (red) and Cluster 3 = Holocene Climatic Optimum assemblage (green) .....   | 77  |
| Figure 6.6: Dendrogram resulting from Q-mode cluster analysis and the clusters identified in core 964A. On the right hand side, the relevant clusters have been identified and colour coded; Cluster 1 = glacial assemblage (blue), Cluster 2A = modern assemblage (orange), Cluster 2B = deglaciation assemblage (red) and Cluster 3 = Holocene Climatic Optimum assemblage (green). .....  | 78  |
| Figure 6.7: Depiction of the intricate relationship of environmental factors determining the results of the principal component analysis. ....   | 84  |
| Figure 6.8: Comparison between down-core score plots of the factors revealed from PCA analysis, micropalaeontological indexes and ANNs for core 969A. Indexes include <i>G. bulloides</i> / <i>G. ruber</i> ratio (S-index), Eutrophication index (E-index), PCI (Principal component scores), Sea Surface Temperature (constructed from ANNs), SSTs for winter (blue), annual (purple) and summer (red), shaded purple area is the Last Glacial maximum (LGM), green relates to Heinrich Event 1, red area refers to the Bølling-Allerød, Shaded blue area relates to the Younger Dryas and Shaded yellow area represents Sapropel S1 ..... | 86  |
| Figure 6.9: Comparison between down-core score plots of the factors revealed from micropalaeontological indexes, PCA analysis, and ANNs for core 964A. Indexes include <i>G. bulloides</i> / <i>G. ruber</i> ratio (S-index), Eutrophication index (E-index), PCI (Principal component scores), Sea Surface Temperature (constructed from ANNs), SSTs for winter (blue), annual (purple) and summer (red), shaded purple area is the Last Glacial maximum (LGM), green relates to Heinrich Event 1, red area refers to the Bølling-Allerød, Shaded blue area relates to the Younger Dryas and Shaded yellow area represents Sapropel S1..... | 87  |
| Figure 6.10: Comparable results of TEX86 (based on glycerol dialkyl glycerol tetraethers) and $U^{k}_{37}$ (based on the ratio of long-chain diunsaturated and triunsaturated ketones produced by haptophyte algae) reconstructed SSTs based on core GEOB7702-3 collected off the Israeli coast. The calibration of Kim et al. [2008] was applied for TEX86, while the calibration of Conte et al. [2006] was used for $U^{k}_{37}$ (courtesy of Castañeda et al., 2010). .....  | 91  |
| Figure 7.1: Scanning electron microscope images of the chosen species <i>Orbulina universa</i> , <i>Globigerinella siphonifera</i> and <i>Neogloboquadrina incompta</i> (courtesy of <a href="http://www.marinespecies.org">http://www.marinespecies.org</a> ). .....  | 98  |
| Figure 7.2: Diagram depicting the relationship between sapropel layers and Marine Isotope Stages (MIS). Note that both S3 and S5 were deposited during MIS 5 but at different sub stages. ....   | 100 |
| Figure 7.3: Illustration of the measuring technique utilised for <i>O. universa</i> , <i>G. siphonifera</i> and <i>N. incompta</i> . Measurements were taken along the longest axis of each species. ....  | 101 |
| Figure 7.4: Line graphs representing the test size variations of predefined planktonic foraminiferal species before, during and after sapropel deposition, Sapropel S3 (A) and Sapropel S5 (B) (sapropel is defined by the shaded area). Also represented is SSTs for each depositional event, winter (blue), Annual (purple) and summer (red). Cooling events during sapropel deposition are labelled as points 1,2 and 3. ....   | 103 |
| Figure 7.5 Line graphs representing the numbers per gram variations of predefined planktonic foraminiferal species before, during and after sapropel deposition, Sapropel S3 (A) and Sapropel S5 (B) (sapropel is defined by the shaded area). Also represented is SSTs for each depositional event, winter (blue), Annual (purple) and summer (red). .....  | 104 |

|   |     |
|---|-----|
| <i>Figure 7.6: Box and whisker plots summarising micropalaeontological data for sapropel S3. Displayed within the graphs are test size data (A), the absolute abundances shown by specimens per gram (B) and the sea surface temperatures (C).</i> .....  | 107 |
| <i>Figure 7.7: Box and whisker plots summarising micropalaeontological data for sapropel S5. Displayed within the graphs are test size data (A), the absolute abundances shown by specimens per gram (B) and the sea surface temperatures (C).</i> .....  | 108 |
| <i>Figure 7.8: Graph summarising the relationship between the most recent sapropels (S1-S9), the Late Quaternary glaciations (MIS 1-8) and the insolation variations dominated by the 22 kyr orbital procession (courtesy of Bard et al., 2002).</i> .....  | 110 |
| <i>Figure 7.9: Schematic illustration depicting a temperature growth model for both warm and cold water species (courtesy of Schmidt et al., 2014).</i> .....   | 111 |
| <i>Figure 7.10: Graphs displaying the correlation between species mean test size and SSTs. Winter correlations are denoted in blue and summer correlations are signified by red.</i> .....  | 112 |
| <i>Figure 7.11: growth rates of selected species in relation to experimental temperature (°C). Large dots signify mean population at one temperature while smaller dots represent individual growth rates. Model results (line) and 95% confidence intervals of the model are shown by dashed lines. Stepped filled bars represent observations from Be and Tonderlund, 1971, flux observed in sediment traps (Zaric et al., 2005) are shown in terms of overall distribution as a line and as optimal SST as an open bar (courtesy of Lombard et al., 2009).</i> ..... | 113 |
| <i>Figure 7.12: Correlation between species test size and specimens/g for each of the defined species.</i> .....  | 116 |
| <i>Figure 8.1: Sapropel occurrence in relation to timing of the SPECMAP normalized <math>\delta^{18}O</math> record showing glacial/interglacial cycles [Imbrie et al., 1984] and summer insolation at 65°N [Laskar et al., 1993] (Courtesy of Emeis et al. 2003).</i> .....  | 122 |
| <i>Figure 8.2: Locations of cores utilised for comparative analysis, ODP Core 969 (A and E), ODP Core 971A and Core BAN89GC09.</i> .....  | 123 |
| <i>Figure 8.3: Faunal records throughout the deposition of sapropel S5 (shaded area) for core 969A presented with winter (blue), annual (purple) and summer (red) SSTs</i> .....  | 126 |
| <i>Figure 8.4: Comparison between plots of the ODP core 969A for Sapropel S5. Analysis includes, Total specimens per gram and total number of species, Diversity index, Herbivorous index, G. inflata %. The shaded area represents sapropel S5.</i> .....  | 127 |
| <i>Figure 8.5: Faunal records throughout the deposition of sapropel S6 (grey shaded area) for core 969A presented with winter (blue), annual (purple) and summer (red) SSTs.</i> .....  | 129 |
| <i>Figure 8.6 Comparison between plots of the ODP core 969A for Sapropel S6. Analysis includes, Total specimens per gram and total number of species, Diversity index, Herbivorous index, G. inflata %. The shaded grey area represents Sapropel S6.</i> .....  | 130 |
| <i>Figure 8.7: Diagram illustrating spatial variability of export and carbonate productivities during sapropel S5 and suggested method of nutrient delivery and their magnitude at the different locations (courtesy of Weldeab et al., 2003).</i> .....  | 135 |

# LIST OF TABLES

|   |           |
|---|-----------|
| <i>Table 3.1: Table depicting the timing of sapropel deposition in the eastern Mediterranean Sea for S1 (MIS1), S3 and S5 (MIS 5) and S6 (MIS6) showing the estimated depositional timeframe and references for each interval. ....</i>                                     | <i>29</i> |
| <i>Table 5.1 Summary of data for core 969A and 964A including depth below seafloor, the total thickness of sediment layer, the number of samples studied within the layer and the data extracted. ....</i>  | <i>61</i> |
| <i>Table 5.2 Summary of data for core 969A and 964A including depth below seafloor, the total thickness of sediment layer is illustrated with the sapropel intervals displayed in brackets, the number of samples studied within the layer and the data extracted. ....</i> | <i>61</i> |
| <i>Table 5.3: Sample of processing data showing weights before and after wet sieving .....</i>  | <i>62</i> |
| <i>Table 5.4: List of planktonic foraminiferal species that have been identified and utilised throughout this research. ..</i>  | <i>64</i> |
| <i>Table 6.1: AMS <sup>14</sup>C dating control points utilised for the construction of an age-depth model for core 969A. ....</i>  | <i>70</i> |
| <i>Table 6.2: AMS <sup>14</sup>C dating control points utilised for the construction of an age-depth model for core 964A. ....</i>  | <i>70</i> |
| <i>Table 6.3: Average sedimentation rates for cores 969A and 964A based on AMS dating control points highlighted in figure 6.2 .....</i>  | <i>71</i> |
| <i>Table 6.4: Inferred age range of each cluster in both cores 969A and 964A. Figures 6.3 and 6.4 illustrate the position of each cluster within the individual core.....</i>   | <i>78</i> |
| <i>Table 6.5: This table highlights the dominant species and relative abundance within the faunal assemblages of the individual clusters. ....</i>  | <i>79</i> |
| <i>Table 6.6: PCA factors and their percentages of the total variability for core 969A (Levantine basin).....</i>   | <i>82</i> |
| <i>Table 6.7: PCA factors and their percentages of the total variability for core 964 (Ionian Sea).....</i>   | <i>82</i> |
| <i>Table 6.8: Planktonic foraminifera rankings and factor loadings for PCI in core 969A and 964A.....</i>   | <i>83</i> |
| <i>Table 7.1: Classification of chosen species within the Protozoa Kingdom .....</i>  | <i>97</i> |

## LIST OF ABBREVIATIONS

|                  |                                  |
|------------------|----------------------------------|
| AMS              | Accelerated Mass Spectrometry    |
| ADW              | Adriatic Deep Water              |
| AeDW             | Aegean Deep Water                |
| ANN              | Artificial Neural Networks       |
| AW               | Atlantic Water                   |
| Ba               | Barium                           |
| cm               | Centimetres                      |
| DCM              | Deep Chlorophyll Maximum         |
| EMDW             | Eastern Mediterranean Deep Water |
| EMT              | Eastern Mediterranean Transient  |
| H1               | Heinrich 1                       |
| HCO              | Holocene Climatic Optimum        |
| IKM              | Imbrie-Kipp Method               |
| ITCZ             | Inter Tropical Convergence Zone  |
| Fe               | Iron                             |
| FeS <sub>2</sub> | Iron Pyrite                      |
| LIG              | Last Interglacial Period         |
| LIW              | Levantine Intermediate Water     |
| $\Delta R$       | Local Reservoir Ages             |
| Mn               | Manganese                        |
| MIS              | Marine Isotope Stage             |
| MDW              | Mediterranean Deep Water         |
| MIW              | Mediterranean Intermediate Water |
| MO               | Mediterranean Oscillation        |
| mbsf             | Metres below sea floor           |

|      |   |
|------|---|
| µm   | Micrometres                                   |
| MMJ  | Mid-Mediterranean Jet                         |
| MAT  | Modern Analog Technique                       |
| MAW  | Modified Atlantic Water                       |
| Mo   | Molybdenum                                    |
| NAO  | North Atlantic Oscillation                    |
| NBEM | Northern Borderlands of Eastern Mediterranean |
| ODP  | Ocean Drilling Program                        |
| Corg | Organic Carbon                                |
| PETM | Palaeocene-Eocene Thermal Maximum             |
| PCA  | Principal Component Analysis                  |
| Re   | Rhenium                                       |
| SST  | Sea Surface Temperature                       |
| Na   | Sodium  |
| S    | Sulphur                                       |
| V    | Vanadium                                      |
| WMDW | Western Mediterranean Deep Water              |
| YD   | Younger Dryas                                 |

# CHAPTER 1

## INTRODUCTION

Since they were first discovered during the Swedish Deep Sea Expedition in 1947-1948, the sedimentary sequences of the Mediterranean Sea have been subjected to a plethora of research due to the presence of distinctive organic rich sediments known as sapropels (Bouloubassi et al., 1998; Cramp and O'Sullivan, 1999; Bernasconi and Pika-Biolzi, 2000; Meyers and Arnaboldi, 2008; Scheiderich et al., 2010; Liu et al., 2012; Grant et al., 2015 among others). Numerous sapropels have been deposited throughout the Quaternary Period, the most recent of which is sapropel S1, these continue through but are not limited to S2, S3, S4, S5, S6, S7, S8 and S9.

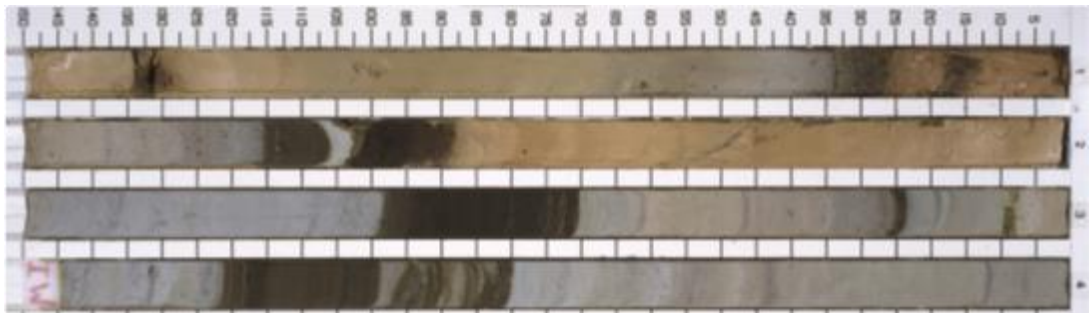


*Figure 1.1: Example of a Mediterranean Core (ODP core 969A), sapropel layers are indicated by the dark colour change in the sediments (courtesy of Ocean Drilling Program)*

Sapropels are defined as organic rich sediments that are dark in colour when compared to adjacent sedimentary layers (Rohling et al., 2015) (figure 1.1). In general Kidd et al. (1978) was the first to define these layers and recommended that sediments that contained  $> 2\%$  total organic carbon were to be defined as sapropels, this has since been updated with many researchers suggesting that anything  $> 1\%$  organic carbon should be defined as a sapropel (Kidd et al., 1978). Depending on the duration of the depositional event, these layers have been shown to have up to 30% organic carbon (Emeis et al., 1996). Chemically an enrichment of iron and sulphur, usually in the form of pyrite, is noted within these layers and is indicative of poor oxygen levels during production (Van Os et al., 1995; Azrieli-Tal et al., 2014). Furthermore high barium concentrations have been noted throughout these sedimentary sequences in conjunction with elevated levels of rhenium and vanadium (Grant et al., 2016; Tachikawa et al., 2015).

The timing of sapropel deposition is important as most sapropels are deposited within interglacial periods, such as S1 during the current interglacial and S5 deposited during the last interglacial approximately 125 kyr years ago however, S6 and S8 were inconsistent with this and were deposited during glacial periods (Cramp and O'Sullivan, 1999; Liu et al., 2012). Each sapropel layer is attributed to a Marine Isotope Stage (MIS), some existing within a single stage (e.g. S1 = MIS1, S6 = MIS6) and some within similar stages (e.g. S3 and S5 = MIS 5, but different sub stages MIS5a and MIS 5e respectively) (Cramp and O'Sullivan, 1999).

The actual formation of these distinctive sedimentary layers has been a topic of much consideration since their discovery and numerous proposals have been put forward. Succinctly, the main premise relates to astronomical forcing which is based on the correlation between the timing of sapropel deposition and Milankovitch cycles. It notes that the accumulation occurs in conjunction with eccentricity maxima and precession minima, when the earth is closest to the sun during boreal summer (Hilgen, 1991; Negri et al., 2003). Models to explain the increased presence of organic carbon within sediments have also been proposed. The stagnation/anoxia model suggests that the influx of freshwater created a blanket within the Mediterranean which led to a stagnant water column and anoxic levels within bottom waters aiding in the preservation of extended organic content (Cramp and O'Sullivan, 1999). Another model that has been proposed relates to increased productivity, whereby the influx of freshwaters led to an increase in nutrients in the form of a Deep Chlorophyll Maximum and so increased the organic carbon that would be stored within the sediments (Rohling and Gieskes, 1989).

Over the past number of decades, the topic of sapropel deposition has been at the forefront of Mediterranean palaeoceanographic research. This research has taken many forms, with analysis ranging from geochemistry, hydrography, and benthic and planktonic foraminiferal habitats. Geochemical analysis examines the chemical compounds that are contained within these depositional layers as a way to unravel some of the mystery that surrounds their deposition (Sutherland et al., 1984; de Lange and Nijenhuis, 2000; De Lange et al., 2001; Halbach et al., 2003; Jiang et al., 2012; Moller et al., 2012; Ganssen et al., 2013). Hydrographic studies examine the influence/influx of external waters (such as monsoonal rainfall) into the Mediterranean Sea (Rossignol-Strick, 1985; Toucanne et al., 2015; Williams et al., 2015; Grant et al., 2016; Tesi et al.,

2017). Foraminiferal ecology of these depositional events has been intrinsically linked with two types of foraminifera, namely benthic and planktonic. Benthic studies utilises the variations in the assemblage of these species, who reside at the sediment water interface, and the role of anoxia in the absence of this species during sapropel deposition (Corliss and Nolet, 1990; Nolet and Corliss, 1990; Jorissen, 1999b; Schmiiedl et al., 2003; Weldeab et al., 2003; Cooke et al., 2008; Morigi, 2009). Similarly the presence and assemblage size of planktonic foraminifera have been used to understand changes within the marine environment during these depositional timeframes. However, as planktonic foraminifera reside within the upper reaches of the water column palaeoceanographers and palaeoecologists can examine the variability in parameters such as productivity and sea surface temperatures and salinities (Tang and Stott, 1993; Negri et al., 1999; Bernasconi and Pika-Biolzi, 2000; Corselli et al., 2002; Principato et al., 2003; Triantaphyllou et al., 2009).

## 1.1 AREA OF STUDY

The Mediterranean Sea is almost completely landlocked, bounded to the north by Europe, Asia to the East and Africa on the southern border. Exchange with the Atlantic Ocean is controlled through the Straits of Gibraltar, an opening of approximately 14km. A second passageway at the Straits of Sicily divides the Sea into two main basins, namely the western and the eastern (Demirov and Pinardi, 2002). A number of seas and sub basins are also present throughout the Mediterranean, these include but are not limited to the Ionian Sea and the Levantine basin (figure 1.2).

The transitional location of the Mediterranean Sea is one of the controlling factors within its climate regime. The wet climates associated with central Europe to the dry arid desert climates of Northern Africa create a varied climate over the basins. The migration of the Inter Tropical Convergence Zone (ITCZ), allows for the movement of the Azores sub-tropical high pressure system to progress north and create hot dry conditions currently experienced throughout the Mediterranean but in particular in the eastern basin during the summer season. The retreat of the ITCZ then places the Mediterranean under the influence of the temperate westerly winds, creating a mild but wet season. Localised mountainous regions such as the Alps and the Pyrenees aid in funnelling air into the Mediterranean Sea. The main winds associated with the

Mediterranean Sea are the Westerlies, however there are more localised winds that are important, from the north the Mistral, Bora, Etesian and the southerly warm dry Sirocco winds. These localised winds play an integral role in the formation of deep water within each of the basins (Pinardi and Masetti, 2000).

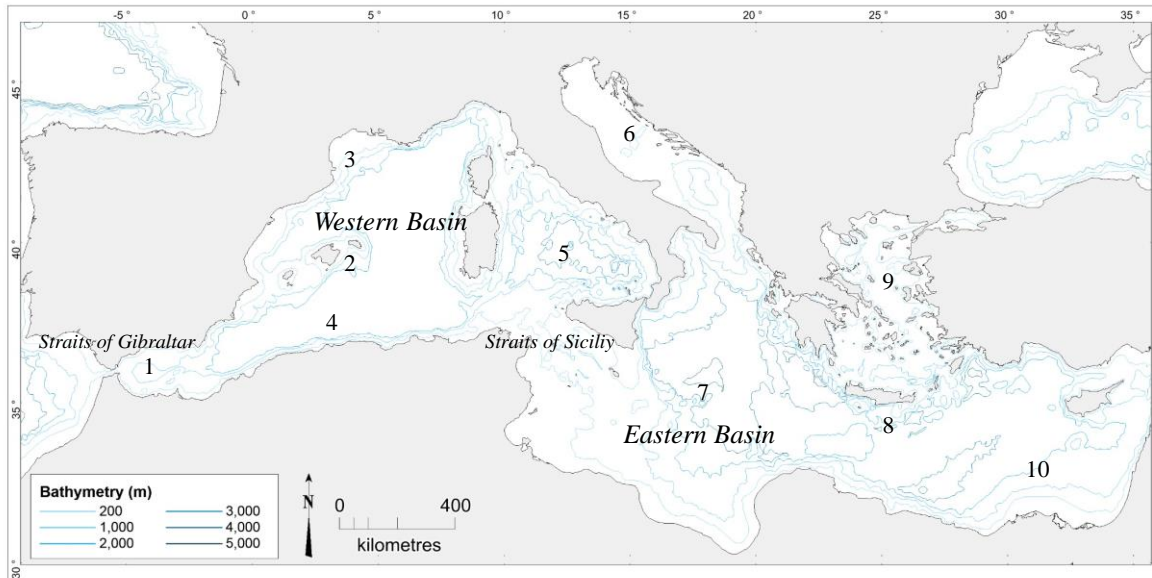


Figure 1.2: Map of the Mediterranean Sea displaying the main basins, sub basins and straits 1=Alboran Sea, 2=Balearic Basin, 3=Gulf of Lion, 4=Algerian Sea, 5=Tyrrhenian Sea, 6=Adriatic Sea, 7=Ionian Sea, 8=Cretan Sea, 9=Aegean Sea, 10=Levantine Basin.

The circulation patterns of the Mediterranean Sea are controlled by the different water masses that are formed within the two basins. The surface layer, referred to as Modified Atlantic Water, enter through the Straits of Gibraltar and can be traced throughout both basins (Send et al., 1999). This overlies the Levantine Intermediate Waters, this high salinity water mass is formed in the Levantine sub basin of the eastern Mediterranean (Pinardi and Masetti, 2000). However, deep water formation within the Mediterranean Sea occurs individually within both the eastern and western basins. Western basin deep water primarily forms in the Gulf of Lion and the eastern basin sees this occur within the Adriatic/Aegean seas (Robinson et al., 2001).

## 1.2 PLANKTONIC FORAMINIFERA

Planktonic foraminifera are microscopic uni-cellular marine protozoans that are comprised of a soft cytoplasm surrounded by a shell/test. They are thought to have first appeared during the mid-Jurassic period and have inhabited the world's oceans since the

mid-cretaceous period. The calcareous test of planktonic foraminifera have aided in their enhanced preservation within marine sediments. The abundance and diversity of species has meant that they have been used extensively in palaeoceanographic, palaeoecological and palaeoclimatological research (Cita, 1976; Thunell, 1978; Rohling et al., 2004; Hayes et al., 2005; Boussetta et al., 2012; Corbí and Soria, 2016).

The distribution of planktonic foraminiferal species is intrinsically linked to a number of environmental parameters. Individual species of planktonic foraminifera have a preferential and optimum temperature range in which they reside. Modern assemblages are categorised by five predefined hydrographic zones; tropical, subtropical, transitional, subpolar and polar (Kucera, 2007). The abundance of planktonic foraminifera within an assemblage can be then interpreted in order to reconstruct the sea surface temperatures (SSTs) related to the timeframe in which it was formed. Like temperature, planktonic foraminifera have particular preferences when it comes to salinity and are known to occupy marine environments with salinities ranging between 30-40‰ on average (Arnold and Parker, 1999; Kucera, 2007). Similarly each species has a depth preference within the water column, with species existing within a shallow mixed layer to deeper waters (Pujol and Vergnaud Grazzini, 1995; Kuroyanagi and Kawahata, 2004; Birch et al., 2013). Downcore observations of deviations within planktonic foraminiferal assemblages allow for Palaeoclimatic reconstructions as these species record changes within the marine environment through their calcium carbonate tests.

### 1.3 PURPOSE AND AIMS OF THIS RESEARCH

After seven decades of research much knowledge has been acquired regarding the formation, composition and faunal characteristics of eastern Mediterranean sapropels. However, with advancements in technology and the extraction of new cores there is still much to discover about these unique sediments and the circumstances surrounding their deposition. To this end the primary component of this research is to undertake a palaeoecological analysis of the Late Quaternary sapropels (S1, S3, S5 and S6) at a site located to the south of Crete.

In order to fulfil the research objectives a single core (ODP core 969A) was primarily used containing 4 sapropel layers and the following aims were set out:

1. To assess the variations in planktonic foraminiferal assemblages from two eastern Mediterranean cores spanning the time since the Last Glacial Maximum (LGM). Particular emphasis is placed on the palaeoecological/palaeoenvironmental interpretation of faunal occurrences employing the use of multivariate statistical analysis and Artificial Neural Networks (ANN).
2. To investigate the changes in mean test size from three defined planktonic foraminiferal species (*Orbulina universa*, *Globigerinella siphonifera* and *Neogloboquadrina incompta*) during the deposition of sapropels S3 and S5. Emphasis is placed on gaining an understanding of the role of biotic and abiotic factors in influencing the growth of these species.
3. To provide a comparative palaeoecological analysis between sapropel S5, deposited during the last interglacial period, and sapropel S6 deposited during a glacial period.

## CHAPTER 2

# PRESENT DAY CLIMATOLOGY AND PHYSICAL OCEANOGRAPHY OF THE MEDITERRANEAN SEA

## 2.1 INTRODUCTION

Bordered to the north by Europe, Africa to the south and Asia to the east, the location of the Mediterranean Sea exhibits a transitional climatic regime due to its relative position between 30° and 45°N. The unique climate of this sea is related to its location within the global atmospheric system lying between a sub-tropical high pressure system to the south and westerly wind belts to the north (Harding et al., 2009). Influences from the Hadley cell and the secondary circulation system of the Ferrel cell also play an important role in this system. The Mediterranean Sea is a semi enclosed basin which is connected to the Atlantic Ocean via the Strait of Gibraltar. A second narrow passageway at the Strait of Sicily divides the sea into the distinctive western and eastern basins. Within these two basins are a number of sub-basins namely the Aegean, Alboran and Adriatic Seas (figure 2.1).

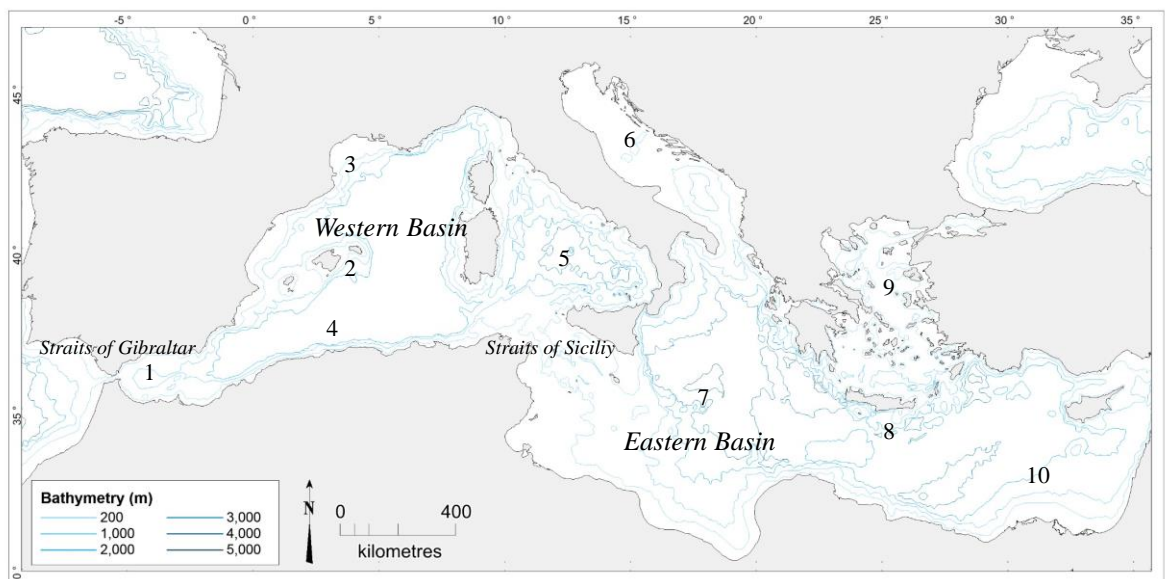


*Figure 2.1: Map of the Mediterranean Sea displaying the main basins, sub basins and straits 1=Alboran Sea, 2=Balearic Basin, 3=Gulf of Lion, 4=Algerian Sea, 5=Tyrrhenian Sea, 6=Adriatic Sea, 7=Ionian Sea, 8=Cretan Sea, 9=Aegean Sea, 10=Levantine Basin.*

The semi-enclosed nature of the Mediterranean Sea has a significant control over its circulation patterns. Variability in temperature, salinity and pressure has a combining effect on sea water density and ultimately the formation of water masses (Turley, 1999; Robinson et al., 2001; Millot and Taupier-Letage, 2004; Rohling et al., 2009; Rohling et al., 2015). Controlled by differential heating and evaporation, variations in surface water density control the vertical movement of seawater. This is particularly significant within the Mediterranean Sea where evaporation greatly exceeds precipitation and river run-off particularly within the eastern basin.

## 2.2 PRESENT DAY CLIMATOLOGY

The transitional location of the Mediterranean region positioned to the north of the arid climates of northern Africa and to the south of the wet climates of central Europe creates a varied climate over the western and eastern basins (Giorgi and Lionello, 2008). The overall location of the Mediterranean Sea is influenced by both subtropical and mid-latitude atmospheric systems as is illustrated in figure 2.2. The transition between the Ferrel and Hadley cells forces hot, dry air to descend creating a high pressure system in the subtropical latitudes. As a result diverging winds are forced both poleward (westerly winds) and equatorward (trade winds). In particular the westerly winds are seen to be influential in affecting the climate of the Mediterranean Sea.

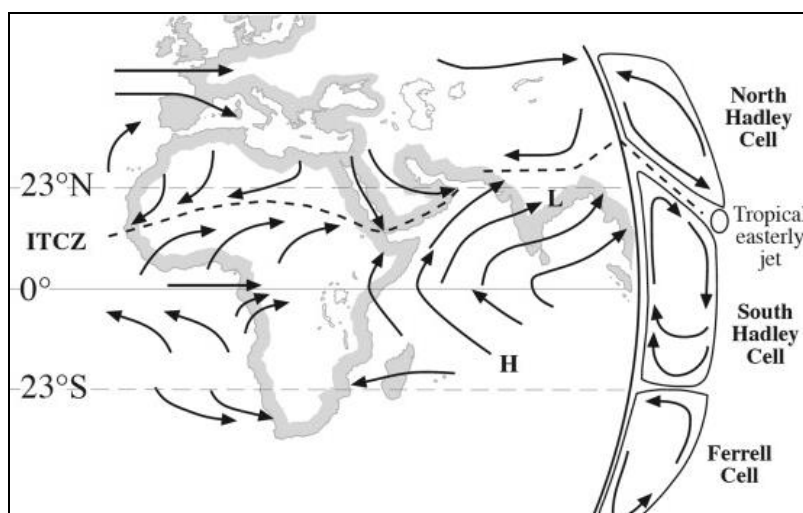


*Figure 2.2: Schematic representation of the global atmospheric circulation during the Northern Hemisphere summer. Global wind patterns are indicated by the black arrows. Note that the dominant winds influencing the climate of the Mediterranean Sea are the westerlies. ITCZ = Inter-Tropical Convergence Zone; H = areas of high sea-level pressure; L = areas of low sea-level pressure (courtesy of Rohling et al., 2015).*

During the summer months the migration north of the Inter Tropical Convergence Zone (ITCZ) pushes the Azores sub-tropical high pressure system north. As such the climate over the Mediterranean Sea is dominated by this, experiencing hot and dry conditions, particularly in the eastern basin (Cramp and O’Sullivan, 1999). Conversely during the winter when the ITCZ retreats so does the high pressure system leaving the region largely under the influence of the temperate westerly winds resulting in mild but wet winters (Cramp and O’Sullivan, 1999). The eastern Mediterranean Sea is predominately closer to the truly continental influences of central Europe and Asia with drier climates incorporating higher summer temperatures and much cooler winter temperatures (figure 2.3) (Lionello et al., 2006; Finné et al., 2011).

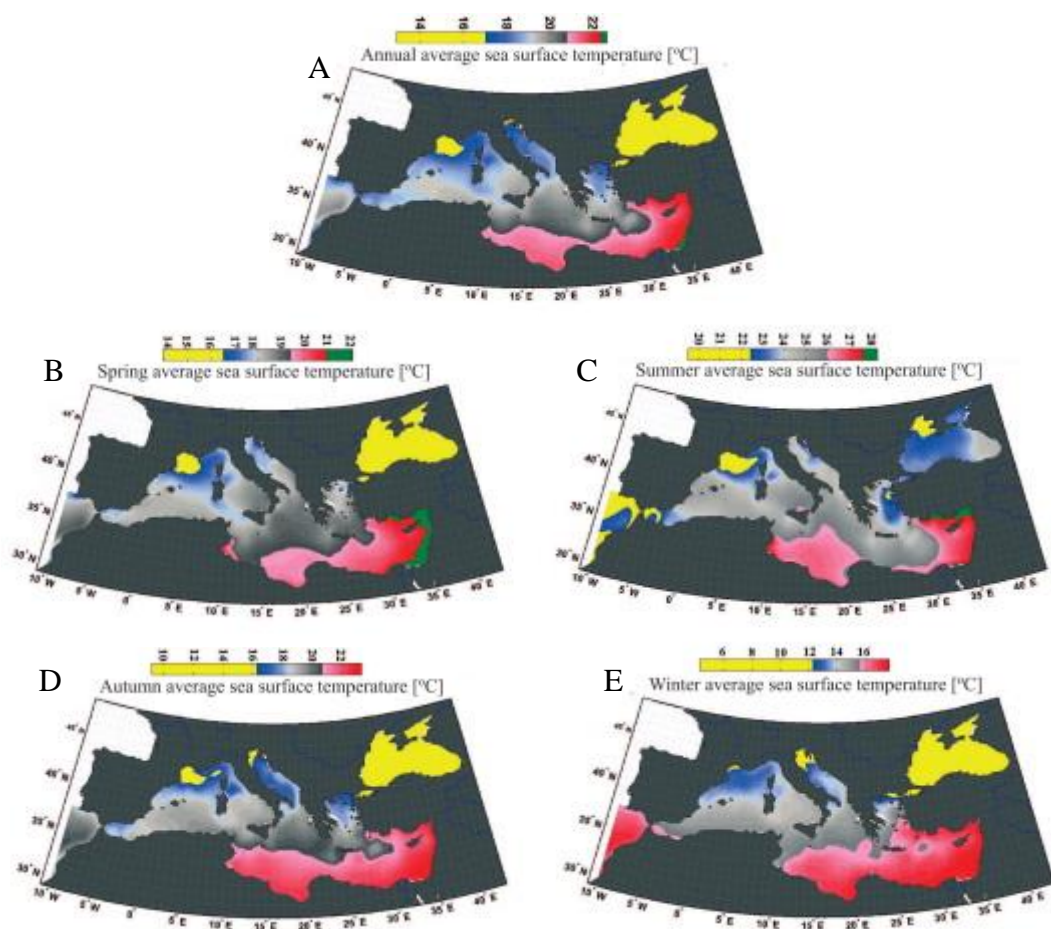


Figure 2.3: Mean sea surface temperature in the Mediterranean Sea (°C) exhibiting annual (A), spring (B), summer (C), autumn (D) and winter (E) averages. Note that during spring and winter the dominant wind systems are the westerly winds with the Etesian prevailing during the summer months and Sirocco winds occurring throughout the year (courtesy of Shaltout and Omstedt, 2014).

## 2.2.1 PREVAILING WINDS

The surrounding topography of the Mediterranean Sea plays a significant role in the regions climate. Localised mountainous regions of the Alps and Pyrenees channel the local winds towards the Mediterranean Sea. The main winds associated with the Mediterranean are the Mistral, Westerly, Levante, Bora, Etesian and Sirocco (figure 2.4), all of which have varying influences on the climatology of the Mediterranean Sea. The western basin is predominately associated with the winds of the Mistral and Levante while the westerlies affect both basins. As the focus of this research, it is the Bora, Etesian and Sirocco wind systems that have a direct influence on the eastern Mediterranean basin. Resulting from the movement of polar and continental air masses over Europe, the Bora winds are a cold and characteristically dry gusty katabatic wind which are forced into the Adriatic Sea through gaps in the Dinaric Alps (figure 2.4). These winds have been known to reach as far as the Ionian and Tyrrhenian Seas. The Bora winds are more common in winter and can reach speeds in excess of  $30\text{ms}^{-1}$ . Typically divided into two main types, the white Bora (anticyclonic pattern), produces a high pressure cell while the black Bora (cyclonic pattern) has a low pressure centre (Ciceran, 2002). The Etesian winds influence many aspects of the eastern Mediterranean climate due to their positioning and persistent wind pressure wielded on water columns of the Aegean Sea. These strong winds flow in a north-west direction through both the Rhodope Mountains in Turkey and the Pindus Mountains in Greece into the Aegean Sea and can extend over the eastern basin. These winds occur throughout the summer months from mid-May to mid-September, mainly due to the monsoonal influence preceding to a thermal low pressure trough over Turkey (Ciceran, 2002; Adloff et al., 2011; Tyrlis and Lelieveld, 2013).

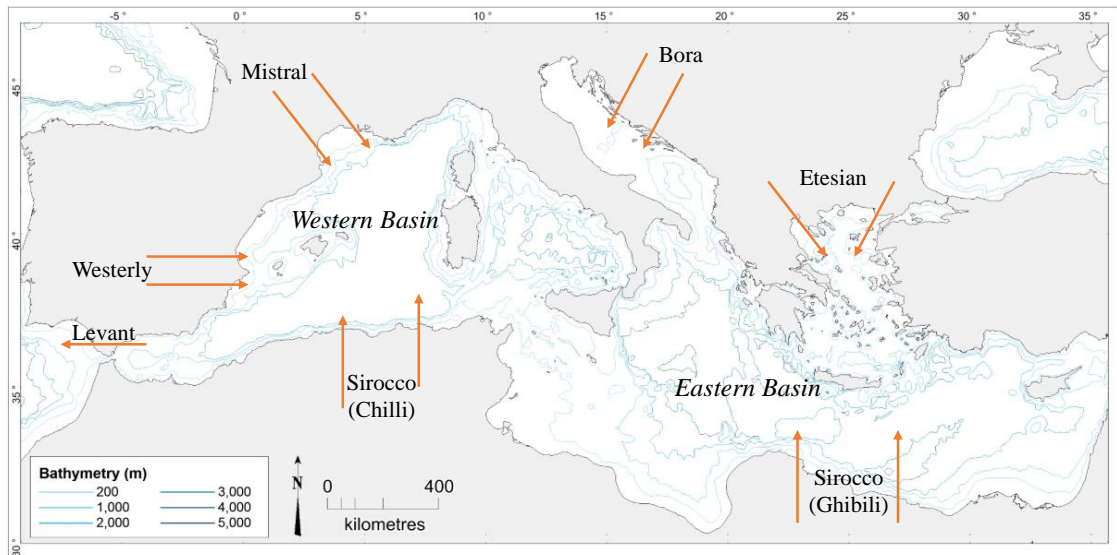


Figure 2.4: Map illustrating the direction and location of the prevailing winds across the Mediterranean region. Cold winds include the Westerly, Mistral, Bora and the Etesian which extend over the northern borderlands of the Mediterranean while the warm winds include Sirocco which extend over the southern parts of the sea.

Unlike the other two prevailing winds of the eastern basin, the Sirocco winds are not forced through a mountainous landscape and actually extend from the desert regions in Egypt, Tunisia and Libya. These winds occur as a result of the eastward movement of both surface and upper level depressions across North Africa. The mass movement of hot, dry air produced north of the Sahara desert flows through Libya and Egypt continuing across the Mediterranean collecting moisture which results in rain and fog within the northern borderlands of the eastern Mediterranean such as Italy and Greece (Ciceran, 2002; Metlink 2017). The wind force of both the Bora and Etesian winds on the Adriatic and Aegean seas has been shown to initiate the formation of Eastern Mediterranean Deep Water (EMDW), which will be discussed in detail later.

### 2.2.1.1 Cyclogenesis

Many of the local winds that are found in the Mediterranean Sea are associated with a process called cyclogenesis. These mid-latitude cyclones are significant atmospheric structures which effect the climate conditions of the Mediterranean basin. Often characterised according to their depth, cyclones can be shallow (weak) or deep (strong) and originate in three principal areas of the northern part of the Mediterranean, the Gulf of Genoa, the Aegean Sea and the Black Sea. These cyclones are general sub-synoptic

in scale (this is determined by the maximum radius of the cyclone which is on average >500km, while North-Atlantic cyclones are synoptic with a radius of between 1000-2000km) and are usually generated due to exchanges with local topography by the residue of the North Atlantic synoptic systems (Harding et al., 2009). Overall cyclones within the Mediterranean region have an average lifespan of 28 hours, this is far less than those noted within the North Atlantic cyclogenesis systems (3 - 3.5 days). In the western basin, one of the main centres is the Gulf of Genoa, where cyclones form throughout the year but are most frequent in the winter. According to the UK Meteorological Office report (HMSO, 1962) observations of the cyclonic regime over the course of a year found that Genoa produced the most cyclones with approximately 60 cyclones per year while 51 cyclones originated in the Ionian Sea. This was further examined by Maheras et al. (2001) who, over a period of 40 years (1958-1997), observed higher intensity cyclones in the western basin than those seen in the eastern basin. Within the eastern basin three systems of cyclogenesis are noted, the southern, the northern and the eastern border (Almazroui and Awad, 2016). The development of cyclones is prominent within the eastern basin during November and the spring months, while fewer are developed during the warmer summer months. The southern cyclogenesis events are directed from the Libyan coast with the dry subtropical African deserts and high precipitation levels providing the heat and moisture required for cyclogenesis (Lionello et al., 2006). Northern developments occur along the coast of Turkey and travel over the Aegean Sea. Throughout the full year a major cyclogenesis pattern is noted over the Black Sea, with intensities in the summer months of July and August with approximately one cyclogenesis event per week (Trigo et al., 1999). The presence of a strong cyclonic exchange over the Arabian Peninsula with an eastward shift of relative weak upper level wind, support the eastern development of cyclogenesis (Almazroui and Awad, 2016). Due to the scale and intensity, the eastern basin cyclogenesis systems have been somewhat overlooked when compared to the strength of those seen within the western basin.

## 2.2.2 AFRICAN MONSOON

The seasonal migration of the ITCZ, the narrow latitudinal zone of wind convergence and precipitation, determines the onset, duration and termination of the monsoon-rainy season in the tropics and subtropics. This is particularly significant in the south east of the Mediterranean Sea which, during the summer months, is influenced by the African subtropical monsoon system. The monsoonal system, which originates in the tropical Atlantic and the southern Indian Ocean, passes over northeast Africa and is associated with the low-latitude rainfall system that while does not directly penetrate the Mediterranean Sea it does influence the hydrology of the Levantine basin through Nile River Outflow (Rohling et al., 2009). These changes are linked with the precession minima cycle, which caused an intensity in the summer monsoon rain belt along with a northern migration over river catchments and North African wadi systems that empty into the eastern Mediterranean basin including the River Nile (Grant et al., 2016). This discharge through the Nile River Outflow system has been restrained since the construction of the Aswan high Dam in 1964, which reduced the overflow from an average of  $8.4 \times 10^{10} \text{ m}^3 \text{ yr}^{-1}$  to an insignificant amount (Rohling et al., 2009). The intensity of the summer African/Asian monsoon rainfall is mainly controlled by the amount of solar radiation received at low latitudes, which is regulated by the Earth's astronomical precessional cycle (Hennekam et al., 2014). Changes in solar radiation (based on seasonal and orbital timescales) and consequently fluctuations in temperature and pressure in the tropics, result in net changes in atmospheric heat export from the ITCZ to higher latitudes and the relative strength of the Hadley Cell circulation in both hemispheres. Because solar heating is the basic driving force behind the Hadley Cell circulation, seasonal shifts of the Sun between hemispheres affects the location of the ITCZ. The ITCZ (figure 2.5) moves northward during the northern hemisphere summer and southward during the southern hemisphere summer tracking the location of peak sea surface temperature (SST) (Flohn, 1984; Broccoli et al., 2006).

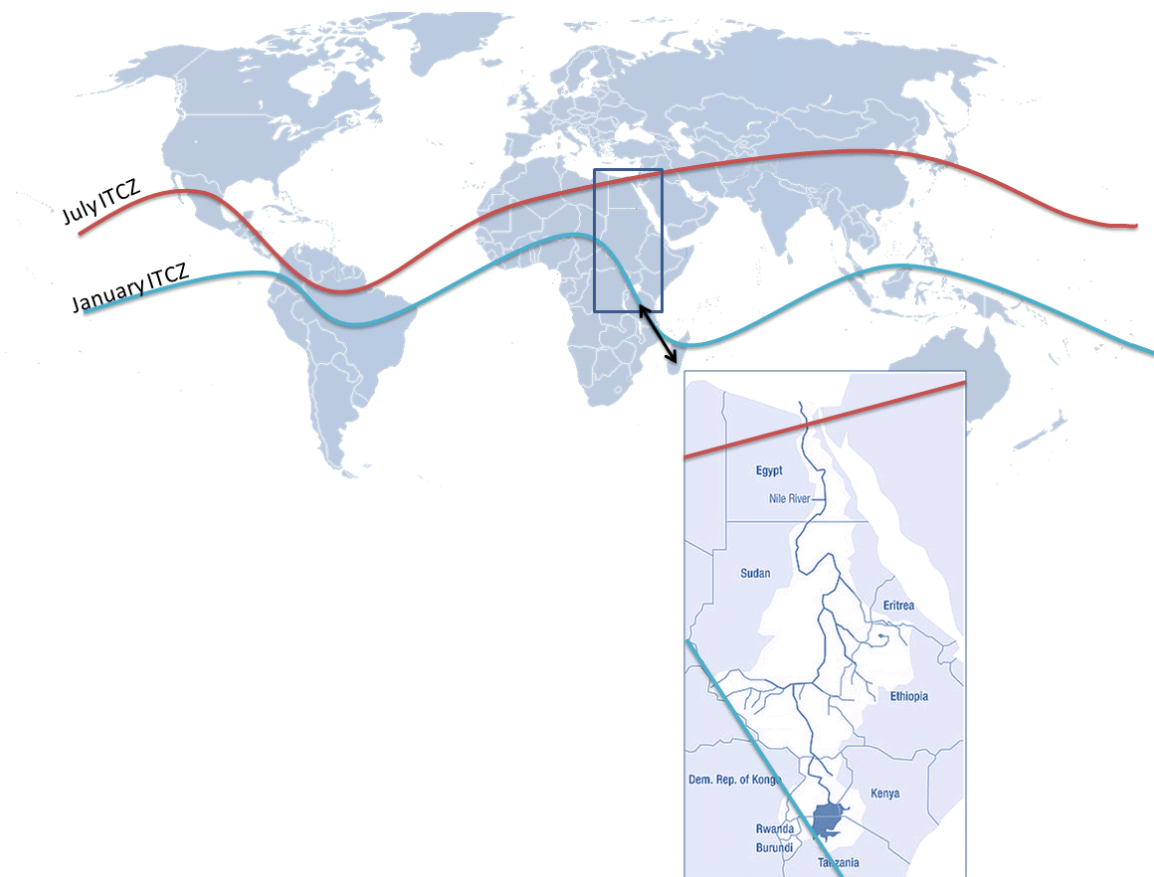


*Figure 2.5: Map illustrating the seasonal changes of the Inter Tropical Convergence Zone with emphasis on its location over the River Nile. The red line represents its location during summer and the blue line represents its winter location*

### 2.2.3 NORTH ATLANTIC OSCILLATION

The predominant atmospheric circulation system that influences the Mediterranean region is referred to as the North Atlantic Oscillation (NAO). The NAO is a climatic phenomenon in the North Atlantic Ocean relating to the fluctuations in the difference between the Icelandic low and the Azore high pressure systems with influences on mean wind speed and direction, temperature and precipitation (Suselj and Bergant, 2005; Vallis and Gerber, 2008). This atmospheric circulation system is presented in two formats which are dependent on the relative pressure exerted on the system (figure 2.6). A positive NAO arises from a strong subtropical high pressure centre and a deep Icelandic low pressure. The subsequent increase in pressure difference results in stronger winter storms crossing the North Atlantic in a north-westerly direction. These storms result in cold, dry winters in the Mediterranean region. The comparative negative NAO occurs when only a small pressure difference exists between the Azores and Icelandic pressure systems. This results in fewer and significantly weaker winter storms.

Following a more west to east track this atmospheric pattern brings warm, moist air to the Mediterranean region (Visbeck et al., 2001; Bojariu and Gimeno, 2003). It should be noted that the NAO primarily affects the western basin and is only weakly established in the eastern basin. However, the climate dynamics in the eastern basin are further complicated by the presence of the Mediterranean Oscillation (MO). The MO is strongly linked to the low NAO phase that gives rise to wet conditions in the western basin. Simply put, the MO is described as two opposing pressure systems lying in a west – east trajectory within the Mediterranean Sea. The result of this pressure see-saw produces opposing temperatures and rainfall patterns between the basins particularly during the winter and spring months (Martin-Vide and Lopez-Bustins, 2006; Rohling et al., 2009; Törnros, 2013).

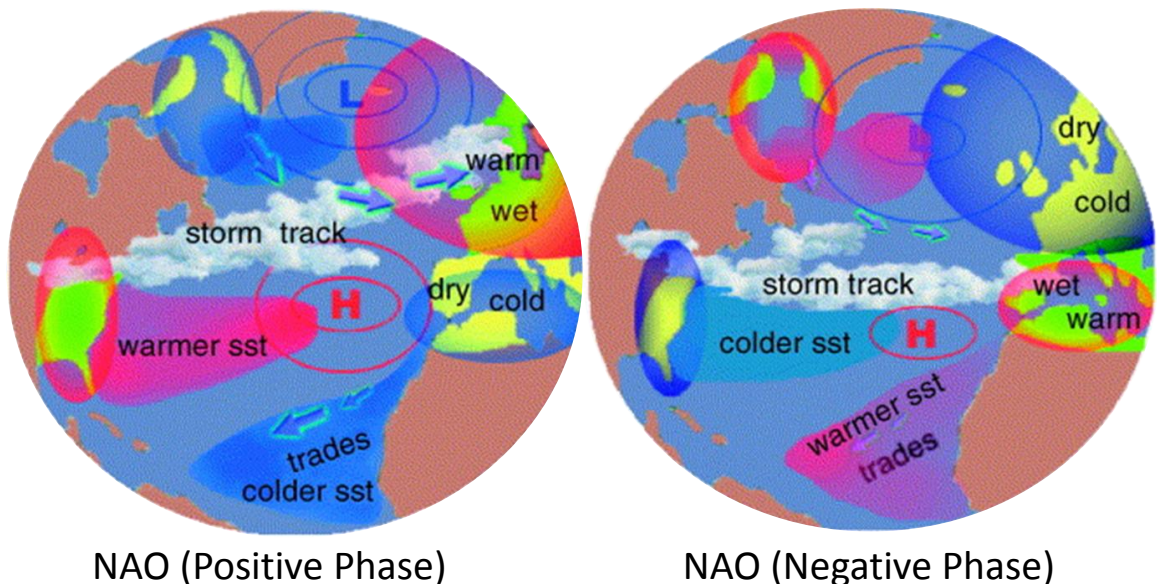


Figure 2.6: Schematic representation of the positive and the negative phases of the North Atlantic Oscillation, showing centres of high and low pressure together with significant anomalies in atmospheric and oceanic conditions (courtesy of Bojariu and Gimeno, 2003).

## 2.3 PHYSICAL OCEANOGRAPHY

The circulation system of the Mediterranean Sea, a semi-enclosed sea, is known to contain many of the same characteristics that are found within the open ocean. Surface water circulation within the Mediterranean is primarily driven by wind stress while deep water formation is dependent on thermohaline conditions (Send et al., 1999; Klein et al.,

2003; Tanhua et al., 2013). The Strait of Gibraltar controls the interchange of Atlantic and Mediterranean waters, which plays a significant role in the circulation and productivity of the Mediterranean Sea. Both Mediterranean basins can be described as evaporation basins as evaporation levels greatly exceed those of precipitation levels. The results of this exhibit clear sea surface temperature and salinity gradients particularly in a west-east direction (Tanhua et al., 2013). These gradients initiate a net buoyancy loss which is facilitated by a two level water exchange through the Strait of Gibraltar, comprising of a relatively fresh surface water inflow and a saline subsurface outflow (Tachikawa et al., 2015). It is the complexity of the water circulation pattern in the basins that has held the interest of oceanographers and has provoked much research. Wüst (1961) was the first to introduce a schematic general circulation pattern of the deep and intermediate waters of the Mediterranean basins. Theocharis et al. (1998) proceeded to give a much broader description of the circulation pattern. These schematic descriptions have aided in understanding the complexity of these water formations. The following sections will include a breakdown of the water masses within the Mediterranean Sea listing their main characteristics.

### 2.3.1 ATLANTIC SURFACE WATERS

On entering the Mediterranean Sea through the Strait of Gibraltar the surface inflowing Atlantic Water (AW) (figure 2.7), has a typical temperature of 15-16 °C, a salinity of 36-37 ‰ (Milot, 2004) and a density of 1.026-1.027 g/cm<sup>3</sup>. This incoming water mass becomes continuously modified due to the mixing effect it encounters with older Atlantic waters. It also mixes with the upwelled Levantine Intermediate Waters (LIW), thus creating Modified Atlantic Waters (MAW). The temperature of MAW increases as it progresses along its course eastwards. Increasing temperatures has the effect of increasing density and although this creates a markedly modified water mass, it remains at the surface.

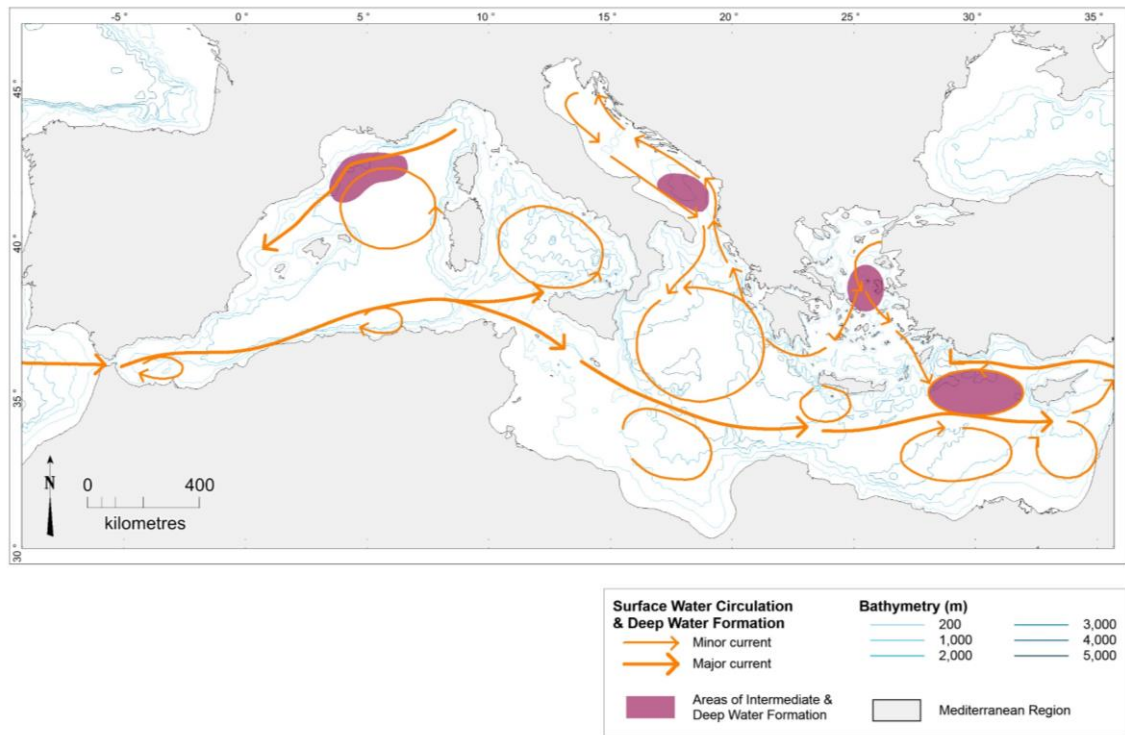


Figure 2.7: Surface water circulation in the Mediterranean Sea. Note that the shaded areas indicate the formation of intermediate and deep water production, in particular note how the transportation of MAW and the formation of the intermediate and deep water are aligned with the main gyres of the Mediterranean (Modified from Rohling et al., 2008).

Upon entering the western Mediterranean through the Straits of Gibraltar, the AW is initially guided in a north-east direction due to the positioning of the Straits before proceeding into a clockwise gyre situated between Spain and Morocco (West Alboran Gyre). The surface water is further entrained into a second gyre (East Alboran Gyre) before being deflected off the coast of Spain (Almeria) in a southerly direction towards the Algerian coast (Oran) (La Violette, 1990). The subsequent well defined frontal zone forms the eastern boundary of the Alboran Sea. The circulation patterns with the Alboran-Algerian Seas provide an excellent example of how local hydrography strongly influences the distribution of planktonic foraminifera, with research demonstrating the dominance of *Globigerina bulloides* and *Globorotalia inflata* in conjunction with the formation of the frontal systems (Rohling et al., 1995). Upon exiting the Alboran Sea the MAW proliferates along the coast of Africa, its spreading mainly associated with the influence of the Coriolis force, and becomes part of the Algerian Current (El-Geziry and Bryden, 2010) (figure 2.7). MAW can also be traced along the Spanish coast as a strong jet (approximately 20 km wide and 150 m deep) which has shown to reach speeds up to several kilometres per hour (Pistek et al., 1985). Hamad et al. (2005) also concluded that the thermal signature of MAW can be tracked along the southern

continental slopes of both the western and eastern basins. The flow of this water mass in both basins forms currents that are unstable at the mesoscale. They continue to meander and proceed to generate anticyclonic eddies that extend downwards and can have lifetimes of several months (Font et al., 1998; Houpert, 2013). In combining satellite thermal images and in-situ observations Millot et al. (1997, 2004) showed how these meso-scale eddies entrain AW and Mediterranean water from the outer edge towards the central part of the Algerian sub-basin potentially diverting part of the water flow from its expected path (Arnone et al., 1990; Perkins and Pistek, 1990).

MAW possesses relatively low salinity levels ( $< 37.5 \text{ ‰}$ ) and can be traced migrating through the Straits of Sardinia and Corsica and entering into the eastern basin via the Strait of Sicily and into the Ionian Sea however, a portion of MAW remains circulating within the western basin (figure 2.7) (Font et al., 1998; Ciappa, 2014). Once in the eastern basin MAW is entrained into the Ionian Current and the Mid-Mediterranean Jet (MMJ) as it flows into the Levantine Basin (Malanotte-Rizzoli et al., 1997). At this point the MMJ splits several times forming a series of cyclonic gyres in the south-eastern basin (e.g. Mersa-Matruh) and anti-cyclonic gyres off the coast of Turkey (e.g. Rhodes Gyre) which are interconnected by currents such as the Cilician and Asia Minor Currents flowing at estimated speeds of  $20\text{-}30 \text{ cm s}^{-1}$  (figure 2.7) (POEM-group, 1992; Hamad et al., 2005). With the passage of MAW into the eastern basin and its continuation in an easterly direction, it is noted that salinity levels continue to increase as the climate becomes more continental facilitating an increase in evaporation (Baringer and Price, 1999).

### 2.3.2 LEVANTINE INTERMEDIATE WATER (LIW)

The Levantine Intermediate water mass (LIW) is formed in the eastern basin, specifically in the northern part of the Levantine sub-basin (figure 2.8) (Emelianov et al., 2006). Its formation generally occurs under the influence of dry, cold winds from the Anatolian Mountains which enhance mixing, eddy formation and decay as well as evaporation (Rohling, 2001; Ozer et al., 2016). While winter cooling reduces sea surface temperatures (to approximately  $17^{\circ}\text{C}$ ), the area between Cyprus and Rhodes is substantially cooled further by these continental winds (approximately  $16^{\circ}\text{C}$ ). The

cooling of sea surface temperatures, accompanied by relatively high salinities (approximately 39.2 ‰) has a decreasing effect on the density of water and vertical convection ensues with the water mass sinking to a depth between 200-600 m where it spreads out (Rohling, 2001). The newly formed water mass is characterised by a salinity maximum between the overlying MAW and the underlying Mediterranean Deep Water (MDW) (Cristofalo and Serravall 1999; Ozer et al., 2016).

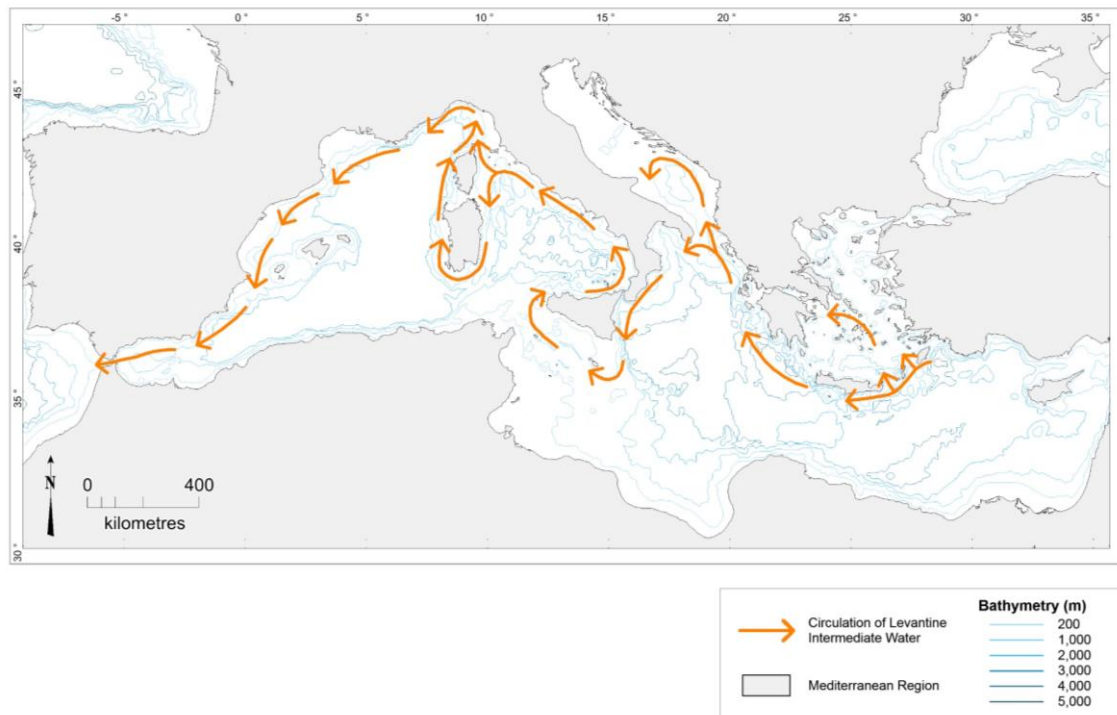


Figure 2.8: Map illustrating the circulation of LIW within the Mediterranean Sea. Note how at several points through its path LIW breaks off and is recirculated throughout the entire Sea (Modified from Millot and Taupier-Letage, 2005).

From its source, the LIW flows westward eventually penetrating both the Ionian and Adriatic seas. Spilling through the Strait of Sicily, this water mass is partially re-circulated back towards the eastern basin while the rest continues to flow into the western basin, making sure that this intermediate water mass is found throughout the entire Mediterranean Sea (Roether et al., 1998) (figure 2.8). The high salinity levels of the water mass provide an enormous subsurface supply of salt to the entire basin, particularly in the Aegean and Adriatic seas, which is critical for Mediterranean deep circulation and the formation of eastern Mediterranean deep water (Millot and Taupier-Letage, 2005). At the Strait of Sicily the LIW remains distinctive within the water column, although due to mixing it has both a lower temperature (13°C – 13.5°C) and salinity (38 ‰) compared to the source area (Ozturgut, 1976; Said et al., 2011). From

the Strait of Sicily, at a depth of approximately 200-600 m, LIW circulates around the Tyrrhenian Sea in an anticlockwise direction with part of the water mass flowing through the Channel of Corsica (Angue Minto'O et al., 2015). The remainder continues along the west coasts of Sardinia and Corsica (part of this then becomes entrained with Atlantic waters in the wintertime formation of western Mediterranean deep water) and continues to be recognisable while continuing along the Spanish continental slope before flowing through the Strait of Gibraltar as a subsurface outflow (figure 2.8) (Millot and Taupier-Letage, 2005).

### 2.3.3 DEEP WATER FORMATION

It should be noted that both the eastern and western basins of the Mediterranean Sea have their own source of deep water formation which settles below the LIW. Western Mediterranean Deep Water (WMDW) is primarily associated with the Gulf of Lions while the Aegean and Adriatic seas are the principal areas of Eastern Mediterranean Deep Water (EMDW). The presence of this deep water formation in both basins signifies that these regions are characterised by the presence of well oxygenated deep water (Rohling et al., 2009). Since this research is primarily concerned with the eastern basin only the formation of Eastern Mediterranean deep water will be discussed here.

#### 2.3.3.1 *Eastern Mediterranean Deep Water (EMDW)*

Initial studies stated that EMDW formation was confined to the Adriatic Sea (Roether and Schlitzer, 1991; Schlitzer et al., 1991; Lascaratos et al., 1999). However, recent research agrees that the Aegean Sea also plays a role in the development of deep waters (Bensi et al., 2016; Cornuault et al., 2016; Filippidi et al., 2016). During the winter months low salinity water on the Adriatic shelf is subjected to extreme cooling initiated by the strong localised cold, dry Bora winds (Lascaratos et al., 1999). These dense cold waters sink beneath the LIW and progress from the northern region towards the central and southern Adriatic following the western coastline. As it flows it combines with the warmer more saline LIW causing the formation of a much denser water mass in the southern Adriatic (Cornuault et al., 2016). This mixing creates a water mass which has

lower temperatures (13°C) and salinities (38.65‰) than the LIW, and therefore higher densities (Gacic et al., 1996; Filippidi et al., 2016). The newly created water mass, known as the Adriatic Deep water (ADW) settles below the LIW where it forms part of the EMDW (Rohling et al., 2009). The EMDW advances out of the Adriatic Sea progressing through the Strait of Ontranto, firstly filling the deepest parts of the Ionian Sea and then the Levantine Sea (POEM–group, 1992; Rohling et al., 2009). In their research, Roether and Schlitzer (1991) indicated that deep water circulation within the eastern basin was confined to a single vertical cell with the Adriatic Sea contributing approximately 0.29 Sv via the ADW.

The role of the Aegean Sea as a contributor to the formation of the EMDW has caused much controversy and debate over the past number of years. Initially Pollak (1951) dismissed the idea that the Aegean Sea played any role in this water formation, contending that the Adriatic Sea was the original source. However, Wüst (1961) stated that the Aegean Sea, although only a minor input, could not be entirely dismissed. This view was further supported by Miller (1963) who suggested that EMDW was formed intermittently before flowing into the Levantine basin. As this controversy reigned much research continued into the extent of the input from the Aegean Sea. First recognised in 1989, a competing addition of deep water from the Aegean Sea was noted after decades of constant replenishment of deep water from the Adriatic Sea. Further research throughout the next decade detected prominent Aegean influence throughout the Eastern Mediterranean (Roether et al., 1996; Klein et al., 1999; Malanotte-Rizzoli et al., 1999). The establishment of deep water originating from the Aegean Sea has been dated to the early 1990s with Aegean deep water (AeDW) accounting for approximately 20% of the EMDW during this period, although by the mid-1990s this contribution had reduced (Roether et al., 2007). It has been suggested that the contribution of the Aegean Sea to deep water formation coincides with a series of meteorological events that occurred during the late 1980s and early 1990s. Such variability in atmospheric forcing increased dense water formation in the Aegean Sea which facilitated its contribution to deep water formation (Lascaratos et al., 1999). This phenomenon between deep water formation in the Aegean and Adriatic Seas has become known as the Eastern Mediterranean Transient (EMT) (Roether et al., 2007).

## CHAPTER 3

### EASTERN MEDITERRANEAN SEDIMENTARY DEPOSITS (SAPROPELS)

#### 3.1 INTRODUCTION

The sedimentary sequences from the eastern Mediterranean Sea are characterised by intermittent, black coloured, organic rich deposits named sapropels. Ranging in thickness from a few millimetres to tens of centimetres these sedimentary layers have been deposited throughout the Late Cenozoic. Numerous studies have concentrated on explaining the formation of these layers since their discovery in cores collected during the 1947–1948 Swedish Deep Sea Expedition (Kullenberg, 1952; Todd, 1958; Rohling, 1994; Casford et al., 2003; Sangiorgi et al., 2006; Capozzi and Negri 2008; Zhao et al., 2011; Grant et al., 2016). Faunal and oxygen isotope research, indicate that these sapropel layers formed not only during Quaternary warm phases but, to a lesser extent during cold phases (Thunell et al., 1977; Thunell and Williams, 1983; Vergnaud–Grazzini, 1985; Cita et al., 1997; Bard et al., 2002; Melki et al., 2010; Liu et al., 2012). A number of separate sapropel layers have been deposited within the eastern Mediterranean basin during the Quaternary period, the deposition of which is also defined by Marine Isotope Stages (MIS), these include but are not limited to S1 (MIS1); S2 (the existence of which is controversial, as it does not appear in many areas); S3, S4, S5 (MIS 5); S6, S7 (MIS6); S8 and S9 (MIS7) (Bard et al., 2002; Schmiedl et al., 2003; Weldeab et al., 2003b; Melki et al., 2010; Liu et. al., 2012; Williams et al., 2015).

#### 3.2 GEOCHEMICAL CHARACTERISTICS OF SAPROPELS

Mediterranean sapropels are very distinctive due to their dark colouring, ranging from olive green to black. These sediments are primarily characterised by a high content of organic carbon concentrations ( $C_{org}$ ) when compared to the surrounding sediments and in particular modern surface sediments which have a very low concentration of  $C_{org}$ .

(Emeis et al., 1998; Rohling et al., 2015). Kidd et al. (1978) proposed that sediments containing over 2% organic carbon by weight are sapropels while layers which contain between 0.5% and 2% organic carbon should be termed sapropelic. In general the organic carbon content levels of these sediments range up to 10% (however some older sediments range up to 30%) while many argue that the lower levels should range above 1%  $C_{org}$  (Emeis et al., 1998; Nijenhuis and De Lange, 2000). However, this determination can be overly reliant on the mass sedimentation rates for the definition of sapropels and so they are only loosely clarified by modern day researchers (Rohling et al., 2015). To complicate matters,  $C_{org}$  can undergo a process known as post depositional oxidation, commonly referred to as 'burn down'. The outcome of this process are sharp upper boundaries to the sapropel layer caused by the deposition of chemical fronts. However, these boundaries are no longer representative of the actual top of the sapropel and as such caution should be made when identifying sapropels based solely on their lithological characteristics (van Santvoort et al., 1996; Higgs et al., 1994; Thomson et al., 1995; De Lange et al., 2008; Rohling et al., 2015). The elevated concentrations of barium (Ba) within sapropels has helped to alleviate this problem. Specifically the Ba/Al ratio is useful for determining the extent of sapropel deposition particularly in the event of post depositional oxidation. In contrast to  $C_{org}$ , once deposited Ba is fixed within the sediment thus Ba/Al profiles allow the determination of the actual position of the sapropel (high Ba concentrations) compared to the surrounding sediments (lower Ba concentrations) (Higgs et al., 1994; Thomson et al., 1999; Hubner et al., 2003; Galego-Torres et al., 2007; Rohling et al., 2015).

Both an iron (Fe) and sulphur (S) enrichment is also typical of sapropel layers usually occurring in the form of iron pyrite ( $FeS_2$ ) which is indicative of oxygen poor conditions (Van Os et al., 1995; Azrieli-Tal et al., 2014). Similarly Calvert (1983) shows that enhancement of molybdenum (Mo) as being distinctive of fine grained organic rich sediments which are amassed in stable or discontinuous anoxic environments. Scheiderich et al. (2010) also noted that high concentrations of Mo, as well as Re (rhenium) and V (vanadium) are consistent within sapropels.

A noticeable reduction of manganese (Mn) appears constant with the behaviour of this element under anoxic conditions, as would be found under sapropel deposition. Within the sapropel, a reduction of insoluble  $MnO_2$ , due to the related putrefaction of organic matter, releases  $Mn^{2+}$  ions into solution. A concentrated gradient is recognised and the

Mn<sup>2+</sup> ions migrate out of the sapropel. When optimum anoxic conditions are achieved, an oxidation reaction occurs with the dissolved oxygen in the solution and MnO<sub>2</sub> is precipitated out (Sutherland et al., 1984; De Lange et al., 1989; Nijenhuis et al., 1996).

### 3.3: CHRONOLOGY OF SAPROPELS

#### 3.3.1 MARINE ISOTOPE STAGES

The Quaternary Period can be further subdivided into Marine Isotope Stages (MIS), the alternating warming and cooling periods in Earth's climates which are constructed from the oxygen isotope record. This record can be used to display changes in temperature and are obtained from both deep sea sediment cores and ice cores. Further examination of the oxygen isotope record reveals sub stages within the MIS (figure 3.1). However, while MIS were generally agreed upon universally, the sub stages have become an issue of consternation as there was no universally agreed method for defining them. Identified by Shackleton (1969), MIS 5 and its associated sub stages (a, b, c, d and e) are perhaps the most well-known of all the MIS. Since then numerous attempts have been introduced to identify the sub stages within MIS however, a universal scheme has never been agreed on. More recently Railsback et., al. (2015) proposed a complete and optimised scheme for the MIS sub stages for the past 1.0 million years. Railsback et. al. (2015) suggested that results obtained from a LRO4 stack of marine benthic oxygen isotope records, which extends to MIS28, be used as the definitive marker for the creation of these sub stages. The results of the work outlined in this research were then incorporated into a complete time scale which is presented in figure 3.1.

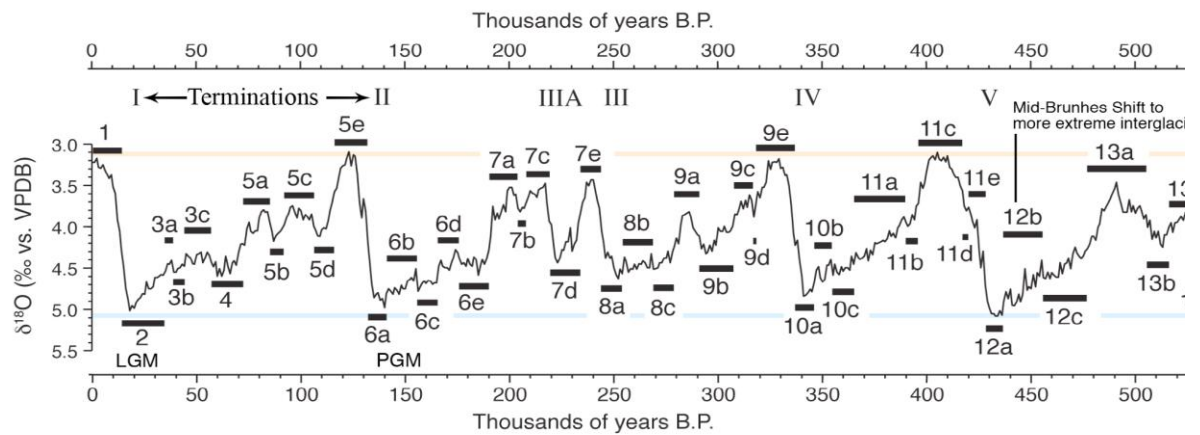


Figure 3.1: Marine isotope stages of the last 500,000 years depicting the main stages and sub stages (courtesy of Railsback et al. 2015).

Sapropels are distributed throughout many MIS however, when examining the occurrence of these depositional events many appear to correlate with a depletion in  $\delta^{18}\text{O}$  values and are generally associated with warm sub humid climates (Kallel et al., 2000; Grant et al., 2016). However, as with all data some anomalies do occur, Sapropel S6 (~172 kyr BP) and S8 were deposited during the glacial periods of MIS 6 and MIS 7 respectively. S6 and S8 are indicative of cold, dry climates noted by the absence of warm water fauna such as *Globigerinoides ruber* and increased abundances of cold-water fauna (Cramp and O’Sullivan, 1999). The most recent sapropel S1 accumulated during the current interglacial ~ 6-10 kyr BP during MIS 1, while sapropel S5 (~124 kyr BP) occurred at during the start of the last interglacial period, MIS5e (Liu et al., 2012). Furthermore sapropel S4 and S3 also formed within the same MIS but at different sub stages (MIS5c and MIS5a respectively). The controversial sapropel deposit of S2 is thought to have taken place during MIS3 but its presence is not validated within the entire Mediterranean Sea. Several older sapropels have also been noted, these include but are not limited to S9 (MIS7), S10 (MIS9) and sapropels 11 and 12 (MIS11) (Cramp and O’Sullivan, 1999; Murat, 1999; Helmke et al., 2008).

### 3.3.2 ASTRONOMICAL FORCING

Maiorano (2008) specifies that the presence of Mediterranean sapropels is an expression of orbitally forced palaeoclimatic and palaeoceanographic changes occurring in a cyclical manner. It was Hilgen (1991) who first presented this correlation between

Pliocene-Pleistocene sapropels and the Milankovitch precessional cycles. The theory of the Milankovitch cycles is based on the premise that the temperature of the Earth's climate would respond in various ways to the regular and predictable changes in the Earth's orbit and axis. This hypothesis was based on three cycles, the eccentricity of orbit, axial tilt and the precession of the equinoxes. The deposition of sapropels can be directly linked to that of the precession cycles and to a much lesser degree the eccentricity cycle (Hilgen, 1991; Negri et al., 2003; Capozzi and Negri, 2009; Kuhlmann et al., 2015).

The precession cycle highlights the Earth's rotational axis relative to the plane of its orbit around the sun is not fixed but rather it sways on its axis which is often referred to as a 'wobble'. In essence this explains the changing direction of the North Pole to whether it is pointing towards Polaris or Vega during the full (26,000 yrs) and half (13,000) precession cycle respectively (figure 3.2). This wobble generates the difference in seasons experienced throughout the globe based on its position along its orbit. Furthermore the hemisphere at perihelion (which at present is the southern hemisphere) will experience increased summer solar radiation but a cooler winter, while the opposite hemisphere will experience 'warmer' winters and cooler summers. The astronomical seasons are noted at 90° intervals on their orbit divided between the winter solstice, the March (vernal) equinox, the summer solstice and the September (autumnal) equinox with the locations between exhibiting the climatic seasons (Timm et al., 2008).

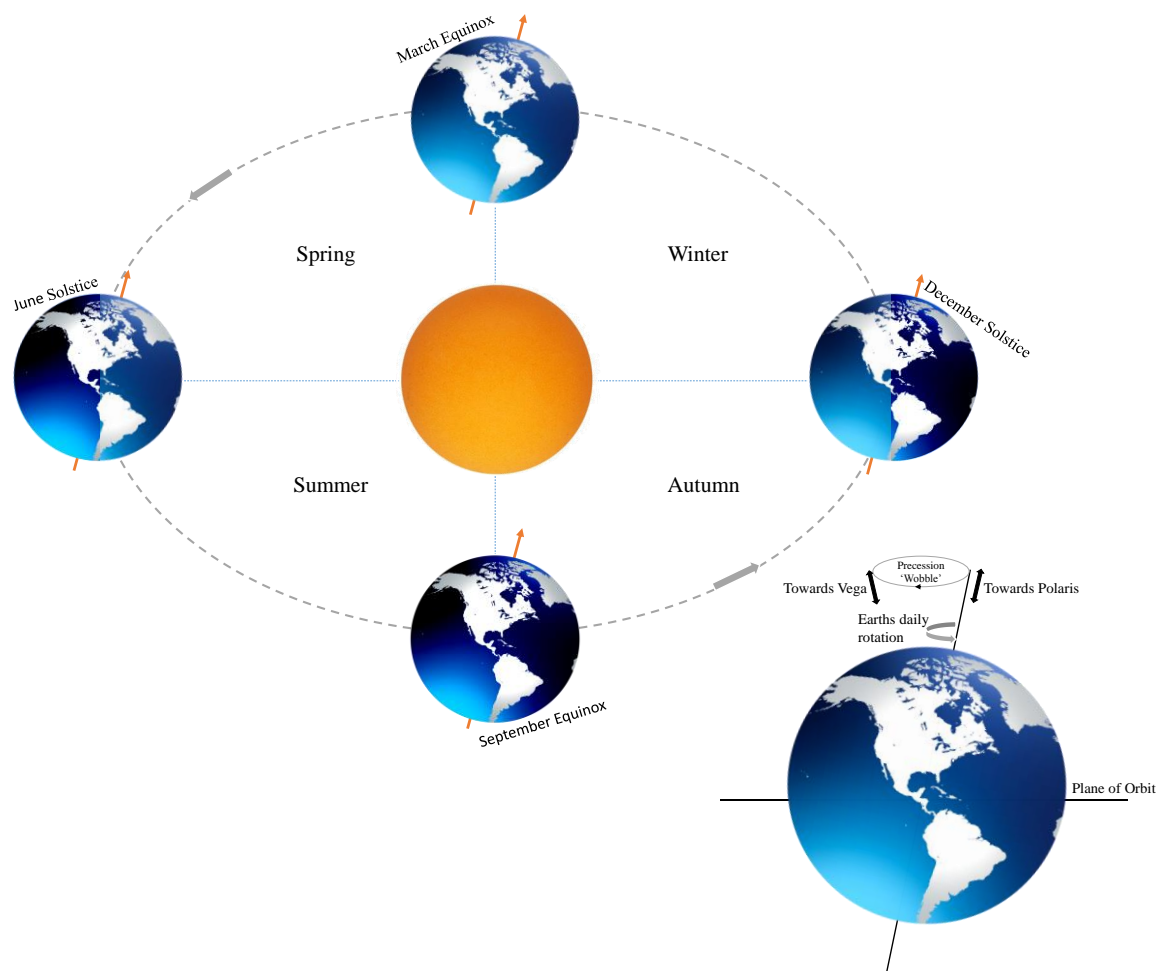


Figure 3.2: Illustration of the Earth's precessional cycle depicting the wobble of the Earth's axis between pointing towards Polaris and Vega during this cycle.

Rohling (2001) continues to state that further to this precession cycle, that once in every four precession periods the Earth's orbit itself rotates around the sun. This is shown to result in the insolation to the Earth's surface in two distinct periods centred at 23,000 yrs (major) and 19,000 yrs (minor) which is often averaged to a period of 22,000 yrs. It is these precession cycles that ultimately affect Earth's climate as it causes a slow change in the dates of the solstices and equinoxes along the orbit (figure 3.2). The eastern Mediterranean core RC9-181, located to the south of Crete, contains a nearly complete record of sapropel deposition throughout the Quaternary Period. Consisting of 11 sapropels, their deposition highlights a clear relationship with precession minima (figure 3.3). However, upon closer examination the occurrence of sapropels seems to demonstrate a particular pattern, sometimes occurring in clusters and others individually. It has been suggested that the clusters occur in conjunction with

eccentricity maxima, showing a periodicity of 100 and 400 kyr. Further work confirmed that sapropels developed at times when Earth is at the point in orbit where it is nearest the sun during boreal summer. It was also observed that not all precession minima produced sapropels, but instead sapropel deposits occur in discrete groups. Each group was shown to be a representation of maximum orbital eccentricity, in agreement with eccentricity modulation of the impact of precession (Hilgen, 1991; Hilgen et al., 1995; Lourens et al., 2001) (figure 3.3).

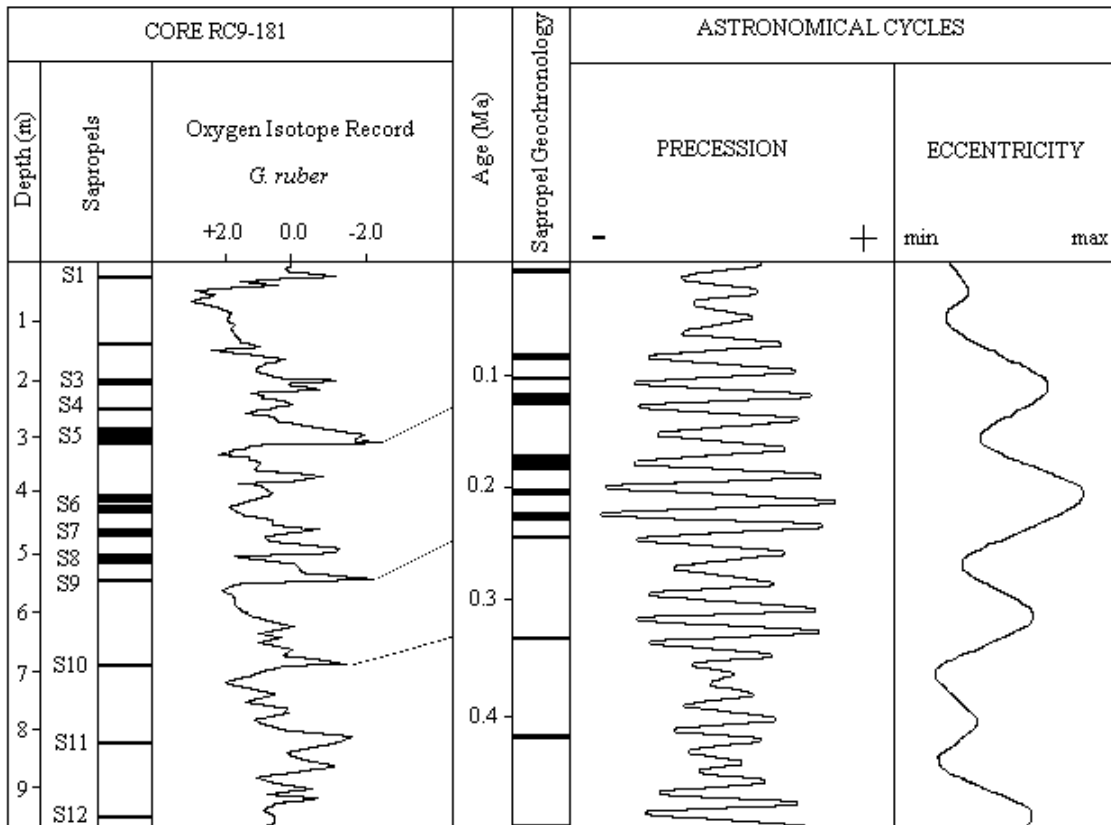


Figure 3.3: Relationship between sapropel deposition, associated oxygen isotope record (for eastern Mediterranean core RC9-181) and the Milankovitch cycles (eccentricity and precession). Note that not all precession minima produced sapropels, but instead sapropel deposits occur in discrete groups. Also with the exception of S4, S6 and S8, sapropels coincide with intervals of  $\delta^{18}O$  depletion (courtesy of Hilgen, 1991).

According to Nijenhuis and de Lange (2000) there is a complete astronomically calibrated timescale for the eastern Mediterranean linking each sapropel since the Late Miocene, to numbered (i-coding) precessional cycles of ~21,000 years duration. One uncertainty surrounding the formation of sapropels relates to the timeframe of deposition. Table 3.1 illustrates the approximate duration of sapropel deposition during the last 180 kyr, highlighting the specified depositional interval for each sapropel with reference to some texts. The given timeframe for each sapropel is an approximation,

with the exception of sapropel S1, which was deposited within the Holocene and therefore is recent enough to be radiocarbon dated. As it has been noted that sapropels and precession cycles are closely related, it can be stated that an individual cycle of sapropel/homogenous sediment deposition must have lasted 21,000 years on average. Notably though it remains uncertain whether or not sedimentation rates changed during a cycle, and so therefore how long sapropel formation itself occurred (Nijenhuis et al., 1996; Wehausen and Brumsack, 1998).

| <b>Sapropel</b> | <b>Deposition Timeframe (yrs BP)</b> | <b>Source</b>                       |
|-----------------|--------------------------------------|-------------------------------------|
| <b>S1</b>       | 9,500 - 6,000                        | <i>Martinez-Ruiz et al.,(2003)</i>  |
| <b>S3</b>       | 85,000 - 78,000                      | <i>Martinez-Ruiz et al., (2003)</i> |
| <b>S5</b>       | 127,000 - 122,000                    | <i>Schmiedl et al., (2003)</i>      |
| <b>S6</b>       | 176,000 - 170,000                    | <i>Schmiedl et al., (2003)</i>      |

*Table 3.1: Table depicting the timing of sapropel deposition in the eastern Mediterranean Sea for S1 (MIS1), S3 and S5 (MIS 5) and S6 (MIS6) showing the estimated depositional timeframe and references for each interval.*

### 3.5 SAPROPEL FORMATION

The formation of these organic rich deposits has been the subject of much interest since Bradley (1938) predicted the occurrence of these sedimentary layers in the Mediterranean basins from exposures in southern Italy. Through his research he surmised that sapropel formation recorded periods of stagnation throughout the Quaternary Period. Later, Kullenberg (1952) interpreted their development as a result of interstitial salinity variations, a theory based on cores extracted during the 1948 Swedish Deep Sea Expedition. Olausson (1961) presented a glacio-eustatic sea-level change model as an explanation for sapropel formation however, while this model was reinterpreted by several authors (Miller, 1972; Cita et al., 1973) it was eventually disregarded as it was unable to account for the numerous characteristics associated with sapropels. Based on their distinctive colour and cyclical arrangement in the sedimentary sequence Sigl et al. (1978) suggested that sapropels represented short lived, but catastrophic adjustments in oceanographic conditions that were probably caused by climatic changes. Various processes have been put forward to explain sapropel

formation, among these, the several variations on the classic ‘stagnation/anoxia’ and increased productivity models remain the most common. The following sections will provide an overview of these models.

### 3.5.1 STAGNATION/ANOXIA MODEL

According to the stagnation/anoxia model, anoxic bottom conditions are caused by a strong stratification of the water column that prevents vertical mixing and oxygen supply to the bottom waters. Within the Mediterranean basin, the basis of this stratification was explained as a result of increased Nile river runoff linked to the periodic enhancement of African monsoons (Grant et al., 2016; Tesi et al., 2017). The link between astronomical variations and sapropel formation is thought to be the cause of an increase in monsoonal activity (Rossignol-Strick, 1983, 1985; Prell and Kutzbach, 1992) and Mediterranean Atlantic-born depressions (Rohling and Hilgen, 1991) at times correlating to the precession minima. It was Rossignol-Strick (1985) who first provided an in-depth description defining the proposed relationship between a monsoonal maxima and the development of sapropels. In works from 1982 and 1985, Rossignol-Strick emphasised that the increased monsoonal precipitation, caused heavy Nile floods which discharged into the eastern Mediterranean Sea. Freshwater has a depleted oxygen isotope ratio when compared to seawater and this is particularly applicable to freshwater which is derived from heavy, monsoonal rainfall. In essence the mix of freshwater inflow from the monsoonal rainfall creates a digression in the salinity levels within the Mediterranean basin. It was this freshwater outflow which was the proposed causal effect for the formation of sapropels. The Nile outflow reduced the salinity of the coastal waters and increased the density stratification of the water column. The presence of these low-density waters at the surface prevented overturning within the water column subsequently producing water stagnation which in turn led to anoxia in the bottom waters and the increased accumulation of organic matter in the sediments (Rossignol-Strick, 1982; 1985; Taylforth et al., 2014). This theory was partially rejected by several authors such as Jenkins and Williams (1984) and Gudjonsson and Van der Zwaan (1985) as they argued that although an influx of freshwater was part of the reason for the development of these sapropel layers, the source originated from several European rivers, not solely the Nile. Rossignol-Strick

(1987) set about a revision of her earlier work stating that in addition to Nile flooding, precipitation in the Northern Borderlands of the Eastern Mediterranean (NBEM) also played a vital role in the development of sapropels (figure 3.4).

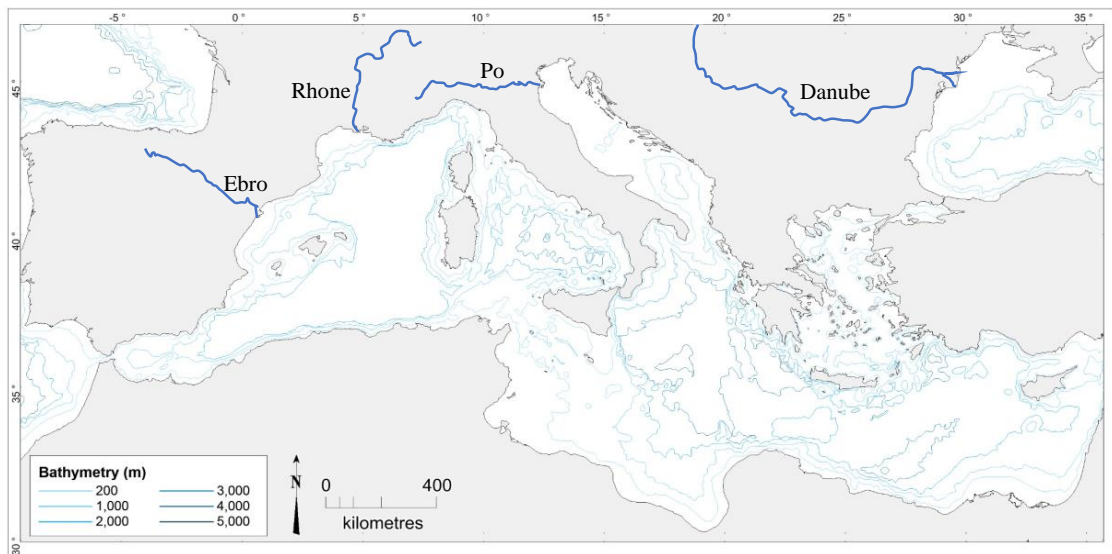


*Figure 3.4: Map of Mediterranean Sea highlighting some of the main contributing rivers of the northern borderlands including Ebro, Rhone, Po and Danube. A number of smaller rivers also contribute to the freshwater influx into the Mediterranean.*

Research conducted by Ducassou et al. (2008) highlighted several high magnitude floods, called pluvial periods, occurring during the Quaternary Period which correlated with the periodic monsoon intensification. The authors conclude that this increase in the Nile outflow during periods of flooding caused a reduction in the salinity of the coastal waters of the Mediterranean Sea. This in turn increased the stratification of the water column, which allowed a reduction of water mixing and allowed for stagnation to occur.

In response to Rossingol-Strick's work, Tzedakis (2007) states that there has been some confusion over the notion that the African monsoon extended over the Mediterranean basin during specific intervals and so has been responsible for increasing precipitation during interglacial periods. He states that this confusion stems from a close grouping of precession minima, boreal summer insolation maxima, northward migration of the ITCZ, intensification of the African monsoon, increased freshwater input into the basin, reduced deep-water ventilation and sapropel deposition which led to a notion of a direct influence of the African monsoon on Mediterranean climates. Tzedakis (2007) indicates this influence may only be indirect and does not infer there was a northward extension of the monsoon over the Mediterranean Sea. In fact, based on his results Tzedakis (2007) concludes that African monsoonal precipitation only penetrated as far as 25°N,

not extending to the North African coast. Supporting evidence from Bar-Matthews et al. (2000) showed the isotopic composition of precipitation in Israel, during the Late Quaternary stages of sapropel deposition, contained a Mediterranean origin, distinct from African monsoon precipitation. Further evidence from the northern Red Sea highlighted the presence of a humid interval coeval with the deposition of sapropel S1 in the Mediterranean Sea. This interval showed no definitive evidence of surface water freshening within the Red Sea suggesting that the increased precipitation could not have originated from a northward extension of the African monsoon but from the Mediterranean itself. Larrasoana et al. (2003) focused their study on the record of Aeolian dust supply to the eastern Mediterranean. It was found that a dust flux minima, corresponding to the insolation maxima, related to the penetration of the African monsoon to the north of the central Saharan watershed ( $> 21^{\circ}\text{N}$ ). Indicators show that this northward monsoon penetration recurred during insolation maxima throughout the last 3 million years.

Tzedakis (2007) discussed ambiguities surrounding the Mediterranean palaeoenvironmental narrative, in which he quantifies several issues surrounding precession minima, sapropel deposition and the seasonality of precipitation in the NBEM. Isotopic records acquired from Israel suggest a distinct rainfall increase during the precession minima – summer insolation maxima concurrent with sapropel deposition. This isotopic record mirrors evidentiary information in the Levantine region which signifies an early Holocene Wet Period between  $\sim 9.5$  and 7 kyr (Robinson et al., 2006). This wet period is believed to be broadly coeval with the deposition of sapropel S1, the most recent sapropel. Mercone et al. (2000) shows that calibrated radiocarbon dates and Ba/Al ratios from rapidly accumulating sapropel sediments suggest a somewhat broader time scale of  $\sim 10.3$ -6.4 kyr.

### 3.5.2 INSOLATION MODEL

The insolation model highlights the comparison between the sapropel record and insolation variations during these depositional phases (Kallel et al., 2000; Negri et al., 2003; Toucanne et al., 2015). In the Northern hemisphere, correlations between the last peak of high summer insolation and the deposition of sapropels have been recorded.

Based on oxygen isotope and sea surface temperature (SST) records from planktonic foraminifera within the Tyrrhenian Sea and Levantine basin, strong surface water salinity decreases occurred within both basins during sapropel deposition (Kallel et al., 2000). This decrease in surface water salinity revealed variations in localised freshwater budgets and is shown to be concurrent to the same processes observed during the deposition of the most recent sapropel (S1). In a response to increasing insolation, the differential heating between land masses and water bodies is the likely cause for a monsoon-like atmospheric circulation over the Mediterranean basin during periods of sapropel deposition. This is also validated by the development of sapropels in conjunction with heavy summer Indian monsoon rains. These heavy monsoonal rains are accumulated within the major river systems which then feed into the Bay of Bengal and Andaman Sea. It showed that each Mediterranean sapropel is coeval with a decrease in the surface salinity of the Andaman Sea and its related summer monsoon increase. Therefore high summer insolation was accountable for the enhanced atmospheric transport of freshwater from the ocean to the land, both towards Asia and the Mediterranean basin (Kallel et al., 2000).

### 3.5.3 PRODUCTIVITY MODEL

It was Rohling and Gieskes (1989) who proposed an increase in productivity combined with a decrease in deep water production, was the cause for the deposition of sapropels. It was noted that increased freshwater inputs into the basin resulted in a shoaling effect of the density gradient between the Mediterranean Intermediate Water (MIW) and the surface water to a depth within the euphotic zone. This resulted in the development of a Deep Chlorophyll Maximum (DCM) between the top of the density gradient and the base of the euphotic layer. Accordingly, the nutrient concentration would have increased as a result of the escalating river fluxes which in turn resulted in a favourable increase in marine organic production. Productivity increases during the deposition of sapropels generally appear to have been of a basin wide nature, especially in relation to the previously discussed formation of the DCM although on shorter timescales there may have been considerable spatial disproportion (Rohling et al., 2008). This shoaling allows stored nutrients in subsurface waters to become utilised for production at the base layer of the euphotic zone. It should be noted that there is ongoing debate

regarding the decisive resource of nutrients that would yield a high organic carbon burial into sediments. Casford et al., (2003) suggests that the nutrient accumulation had been ongoing for approximately 1500 years before the onset of this burial phase, so notably the nutrients may indeed have gathered over longer periods and so was not perceived as being at a fixed state.

It is stated that the productivity theory involves an increase in primary productivity and organic matter supply which resulted in the deposition of elevated organic carbon in what is thought to be well-oxygenated bottom waters. Martinez-Ruiz et al., (2000) investigated the geochemical evidence for the related enhanced productivity during the depositional sequence referred to as sapropel S1. This study has shown that chemical indicators, such as Ba, are seen as strong biogenic associations and is seen to increase with higher biological productivity, and so has been utilised as a marker for this model. Since a high frequency of Ba in suspended particles is barite, which is shown to form in microenvironments within the water column where organic matter decomposes, this is also seen as a very reliable marker when researching the enhanced productivity model. While the concentration of Ba depends on a number of different factors (carriers, diagenetic remobilisation, mineral dissolution and sulphate reduction), the stability of barite is seen as a more indicative model for the hypothesis of productivity. Martinez-Ruiz et al., (2000) showed that the excessive concentrations of Ba within barite crystals derived from marine barite in both the visible sapropel and oxidised horizon of the original sapropel suggests an enhanced productivity zone during the formation of the sapropel layer, so indicating that the origin of at least the sapropel S1 layer is intimately related to an increase in biological production.

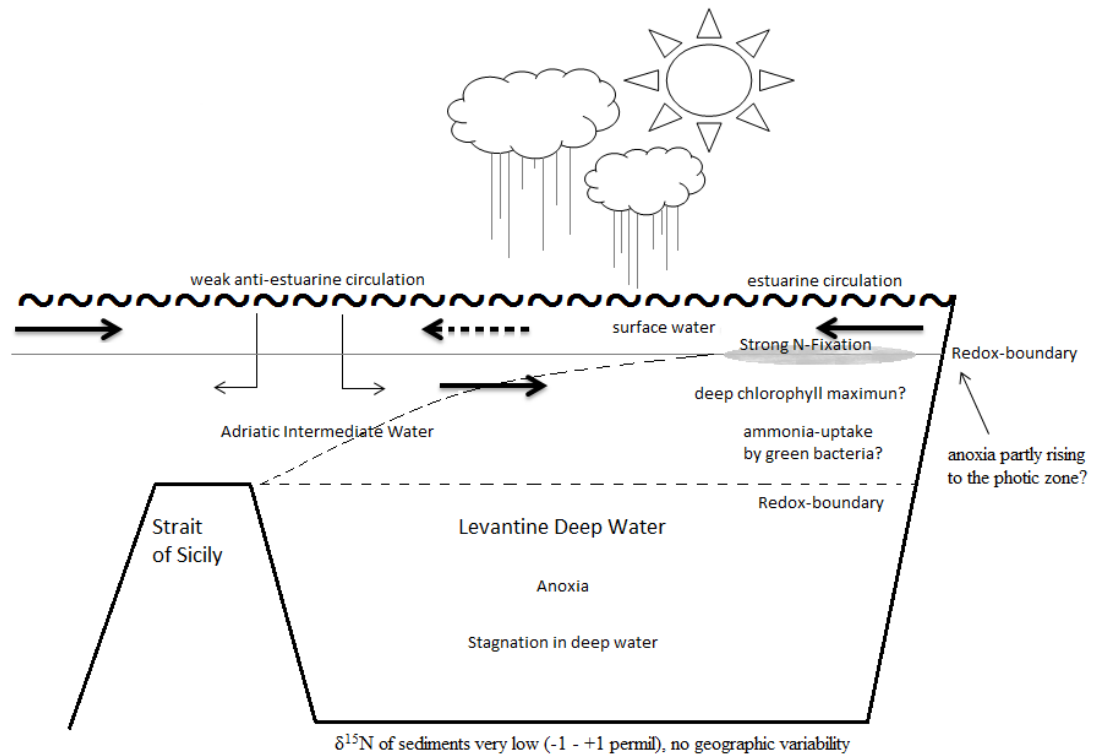


Figure 3.5: Nutrient cycling and circulation patterns during deposition of sapropel S5 deposition in the Eastern basin. Over most of the basin, moderate primary productivity is supported by increased nutrient input from rivers re-circulated in the basin by estuarine flow. Extensive N-fixation occurs in surface waters overlying shallow redox boundaries due to additional phosphorus originating from the deep water column (modified from Struck et. al. 2001).

Gallego-Torres et al. (2011) investigated the productivity patterns associated with sapropel deposition throughout the eastern Mediterranean and its links with N-fixation. Sequences of sapropel deposition were sampled at 4 locations throughout the basin, each location having varied oceanographic settings (deep marine, open marine, shallow water and detrital input waters). Their results showed some basin-wide patterns as well as temporal and spatial differences within the contexts of sapropel deposition. While there were some issues with sapropel S1 results, it was shown that a similar pattern was shown across the basin. A decrease of  $\delta^{15}\text{N}$  values which preceded an enrichment of Ba/Al is found to be typical of sapropel deposition. It was found that although N-fixation is generally linked to an oligotrophic basin, it has created a highly productive environment when correlated to sapropel deposition in the eastern Mediterranean. This data supported the idea that sapropels were deposited during cyclical increases of primary productivity of organic matter principally sustained by N-fixing bacteria (figure 3.5). Increasing productivity within the Mediterranean was initiated by climatic factors which lead to an increase in fluvial discharge, amplified nutrient input in which

preferential N-fixing bacteria was established. This work had followed on from earlier research carried out on sapropel S5 by Struck et al. (2001).

The formation of sapropels throughout the Mediterranean has been the focus of much research regarding its model of deposition from increasing freshwater causing stratification within the water column (stagnation model) to reduced deep water ventilation and increasing productivity (productivity model) (Rossignol-Strick, 1982; Rohling, 1994; Mercone et al., 2001; Casford et al., 2003; Schmiedl et al., 2010).

Influxes of freshwater from the NBEM, an increased Nile outflow and intensification of monsoons were attributed to the freshening of the marine environment associated with the northward movement of the ITCZ. Furthermore shifts within the precession cycle and in particular the insolation model were attributed to the increasing monsoonal activity. This increase again resulted in a shoaling effect within the water column and created the development of a DCM and in turn increased productivity. Each model presented gives part of the overall scenario that is associated with the formation of sapropels and each one is interrelated and has a causal effect within the marine system.

## 3.6 FAUNAL CHARACTERISTICS OF SAPROPELS

### 3.6.1 BENTHIC FORAMINIFERA

Benthic foraminifera are microscopic invertebrates that reside in both fresh and marine environments. These species make up between 50- 80% of the meiofaunal biomass within the sediment water interface and are an essential element in the food chain by preying on other minor organisms. Usually found residing in a vertical column in the upper ~10cm of the sediment, these species are mainly situated in the uppermost centimetre of the sedimentary sequence or even more predominantly at the sediment-water interface (Jorissen, 1999; Fontanier et al., 2002; Friedrich, 2010; Cesbron et al., 2016; ) These organisms are frequently utilised for palaeoceanographic and palaeoenvironmental research due to their morphological diversification, high preservation rates and abundance within marine sediments (Friedrich, 2010). The foremost influence on the distribution of these foraminifera, in both past and present marine environments, is the

oxygen content of the bottom waters and nutrient availability with temperature and salinity of only minor importance (Friedrich, 2010).

Jorissen et al. (1995) reflected on the connection between food availability, oxygen content and benthic foraminiferal abundance patterns in the so called TROX-model. This model follows the assumption of Shirayama (1984) that the depth in the sediment down to which organisms can live is determined by oxygen availability and, that in the presence of oxygen, the vertical distribution of organisms is controlled by food availability. It should be noted though that this model only accounts for total faunal trends and not individual taxa, and so can only be used as an ecological marker-species. Figure 3.6 shows the changing maximum microhabitat as a direct result of a downward organic flux. In oligotrophic areas, all metabolisable food particles will be consumed at the sediment surface as the underlying sediment will only contain minute quantities of organic matter and so infaunal species will be absent. As the marine environment begins its change to a eutrophic state the associated microhabitat deepens due to the fact that metabolisable organic matter is no longer constrained to surface sediments but rather moves by bioturbation to deeper sediments where it now provides the nutritional requirements in order to sustain infaunal taxa. As the marine environments become completely eutrophic, as would be found during sapropel deposition, it is no longer the critical food supply that is the dominant factor in penetration depth of infauna but rather the critical oxygen levels. It is the degradation of organic matter that consumes more oxygen than can be provided by bioturbation and diffusion and as a result creates an excess of nutrients within the sediment. A further increase of the organic flux leads to an increase in oxygen consumption resulting in a shallowing of the oxygenated sediment-layer. In extreme situations all oxygen will be consumed at the sediment surface, leading to anoxic deeper sediment layers and so benthic foraminifera will be found at the sediment-water interface (Favaretto et al., 2008; Friedrich, 2009; Morigi, 2009; Larkin et al., 2009).

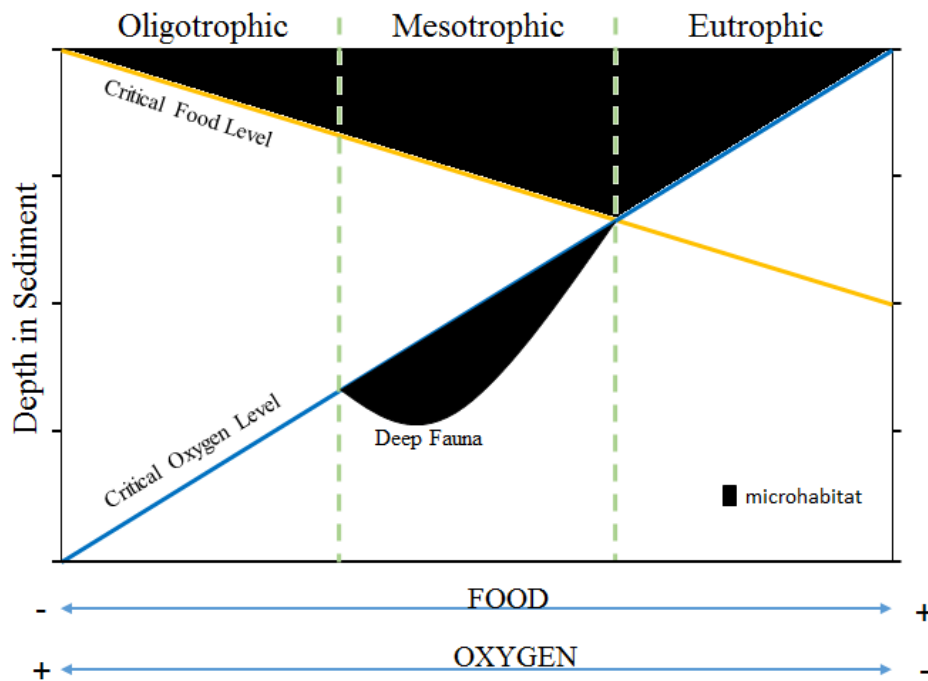


Figure 3.6: Conceptual model explaining the benthic foraminifera living depths (black area) in terms of food availability and oxygen concentration (modified after Jorissen et al., 1995).

While many species of benthic foraminifera are able to tolerate low-oxygen conditions, only a few are able to tolerate a nearly absolute anoxic environment with even smaller numbers able to survive a total anoxic environment for long periods of time. Jorissen (1997a) further examined the characteristics of these benthic foraminifera during sapropel depositional events, particularly S6, S5 and S1, concluding that four main groups of taxa can be associated with sapropel deposition. The first of these groups, *Chilostomella* and *Globobulimina*, usually occur in deep infaunal habitats, often in completely anoxic conditions. Van der Zwann and Jorissen (1991) and Barmawidjaja et al. (1992) suggested that due to decreasing oxygen concentrations, these deep dwelling marine species will reposition themselves in the sediment-water interface. This movement allows these benthic species to ultimately replace species that have much lower tolerance of anoxic environments as seen during sapropel deposition. These deep water taxa have traditionally been considered as opportunistic due to their relatively high abundances in pre-sapropelic sediments. Both biserial and triserial taxa such as *Bolivina* and *Fursenkoina*, belonging to the second group, reside in superficial infaunal microhabitats situated in the sediment but comparatively close to the sediment-water interface. Their relative position within the sediment suggests a certain degree of resistance for low oxygen conditions. *Epistominella*, a species in the third grouping, is

seen as a very opportunistic coloniser. Rapid rises in the abundances of these taxa could be indicative of intervals signified with suitably high oxygen concentrations correlated with an abundant nutrient availability. Nutrient rich environments devoid of biological life are susceptible to colonisation by species *Epistominella* after the re-oxygenation of the marine bottom waters at the termination of sapropel events. The final grouping shows that *Articulina tubulosa* becomes extremely dominant in the foraminiferal densities around sapropels, and is at their most opportunistic in oligotrophic deep sea assemblages (Jorissen, 1999).

### 3.6.2 PLANKTONIC FORAMINIFERA

Although the water column is not entirely oxygen poor, the depositional phases of sapropels can also be identified by specific signals recorded within planktonic foraminiferal assemblages. The abundances of planktonic foraminifera during sapropel deposition can vary quite dramatically from the surrounding sediments, not only in percentages but also in size (Negri et al., 1999). Generally sapropel sediments appear to be dominated by species suited to warm SSTs such as *Globigerinoides ruber* and members of the SPRUDTS-group (Cramp and O'Sullivan, 1999; Principato et al., 2006). However, other environmental parameters associated with these depositional events may favour the occurrence of some species over others. For example the absence of *G. inflata*, a species that thrives in a well-mixed water column, signifies the stratification associated with sapropel formation (Principato et al., 2003; Stefanelli et al., 2005; Capotondi et al., 2006). Similarly the presence / absence of Neogloboquadrinids have been studied extensively in association with the development of sapropels (Rohling and Gieskes, 1989; Rohling et al., 1993a). Predominantly dependent on nutrients, *N. incompta* are associated with the shallowing of the pycnocline and the development of a Deep Chlorophyll Maximum (DCM), as usually seen during sapropel deposition (Rohling and Gieskes, 1989). While these species are always present in older sapropels (S3, S5, S6 and S8) (Rohling et al., 1993a; Capotondi et al., 2006; Sangiorgi et al., 2006), they are unusually absent during the deposition of sapropel S1 (Rohling and Gieskes, 1989; Rohling et al., 1993a; De Rijk et al., 1999; Ariztegui et al., 2000). It has been suggested that conditions favourable towards the development of a DCM were absent during S1 perhaps due to the deepening of the

pycnocline associated with the cessation of Mediterranean Intermediate Water (Rohling and Gieskes, 1989). This would account for the absence of these species as they are dependent on the DCM as their food source. In contrast sapropels S6 and S8, which are deposited during glacial periods are defined by the absence of warm water species such as *G. ruber* and increased associations of cold water species such as *N. incompta* and *T. quinqueloba* (Cramp and O'Sullivan, 1999).

As previously discussed, the top of sapropel layers can undergo 'burn-down' or oxidation this can affect where the 'true' top of the sapropel layer exists. While much research is focused on the geochemistry of these layers, ecological analysis is also important to help signify where the change within the depositional cycle occurs (Passier et al., 1995; van Santvoort et al., 1996; De Lange et al., 1999). Planktonic foraminiferal abundances indeed change within the development of strongly developed sapropels. The reappearance of species within the cores can indicate the end of the unique depositional periods. *N. incompta*'s reappearance after the deposition of the sapropel S1 is one example of this, similarly the reappearance of *G. ruber* after sapropel S6 also indicates the end of sapropel deposition. While oxidation may affect the colour or make-up of the top of the sapropel layer, there is indeed an ecological aspect to defining the top of these layers.

### 3.6.3 SAPROPEL INTERRUPTION

Sapropel interruptions have been documented in the sedimentary record for some time and have been interpreted as reflecting changes in the stability of circulation within the Mediterranean Sea (Rohling et al., 1993b; 1997; De Rijk et al., 1999). Apart from being lithologically distinct, interruptions within a sapropel display anomalous signals within both benthic and planktonic assemblages. Upon examination of the most recent sapropel (S1) Rohling et al. (1997) discovered a significant change within the benthic assemblage throughout the duration of the sapropel. During the initial stages of deposition (S1a) a lack of autochthonous benthic fauna was noted signifying the onset of bottom water anoxia. However, during the interruption a resurgence of benthic species associated with improved oxygenation is displayed. This emergence of benthic foraminifera correlates to a weakening of the anoxic levels within the water column and

an increase within productivity levels. The final phase of sapropel deposition (S1b) sees a return to anoxic bottom waters in association with a decline in oxygen indicative species. Furthermore during the interruption of the sapropel surface water planktonic foraminifera indicate a change in atmospheric temperatures with species such as *G. scitula* and *T. quinqueloba* becoming more prevalent in the assemblage (Rohling et al., 1997). Ruling out sedimentological reasons, the authors interpreted the interruption as a brief (200 years) climatic deterioration resulting in temporary renewed ventilation within the eastern basin. The work of Rohling et al. (1997) was further corroborated by research undertaken by De Rijk et al. (1999). Focusing on planktonic foraminifera, these authors reconstructed a high resolution SST curve throughout the duration of S1 from the Aegean Sea. The results clearly demonstrate faunal assemblages comprised of warm water species during the deposition of sub units S1a and S1b. In contrast a distinct upsurge in cold water species is recorded during the interruption.

# CHAPTER 4

## PLANKTONIC FORAMINIFERA

### 4.1 INTRODUCTION

Belonging to the phylum Protozoa foraminifera are single celled predominantly marine organisms composed of a cell and a test. The cell is comprised of an outer ectoplasm (forms pseudopodia which is used as a feeding mechanism to trap prey e.g. diatoms and dinoflagellates) and an inner endoplasm which is separated by the test. Together, the organism is capable of carrying out the basic functions that are necessary for life.

Foraminifera are classified according to the composition and the structure of the test. Test composition falls into three main categories; organic, agglutinated (composed of sedimentary particles combined together by organic, calcareous, siliceous, or ferruginous cement) or secreted calcium carbonate (Gupta, 1999). Further classification is determined by the morphological characteristics of foraminiferal tests which are employed to differentiate between super families and genera. The appearance of a particular species is generally defined by a number of factors; the simple form of the chambers, the overall shape of the test based on the development and angle of subsequent chambers, the aperture, the number of chambers and the wall structure (Berger, 1969). Determined by their mode of living foraminifera are subdivided into two distinct categories; planktonic and benthic. Planktonic foraminifera spend their lives free floating within the water column and as such occupy the open ocean environments while benthic species are bottom dwelling and occupy environments at the sediment/water interface, and are either infaunal or epifaunal and occupy a wider range of habitats (Benito et al., 2016).

Belonging to the group of foraminifera categorised by a calcareous test, planktonic foraminifera can be sub-divided into three super-groups: Spinose (Globigerinidea), Non-spinose (Globorotaloidae), and Microperforate (figure 4.1). Spinose species such as *Orbulina universa*, *Globigerinoides ruber* and *Globigerina bulloides* have calcite spines ranging from 1-3mm that extend outwards from the test while non-spinose

species such as *Neogloboquadrina incompta* and *Globorotalia inflata* lack these spines (Spero, 1998).

Foraminifera have existed in some form for approximately 540 million years.

Planktonic foraminifera emerged in the fossil record during the mid-Jurassic Period and due to their excellent preservation are one of the most extensively utilised species within palaeoceanography and palaeoecological research (Topa et al., 2017). In particular they have proved useful in the reconstruction of palaeoenvironments with variables such as sea surface temperature (SST), sea surface salinity (SSS) and productivity being the focus of much research (Negri et al., 1999; Melki et al., 2010; Toucanne et al., 2015; Grant et al., 2016). The following sections will outline the main attributes of planktonic foraminifera, and outline their present day distribution in the Mediterranean Sea.

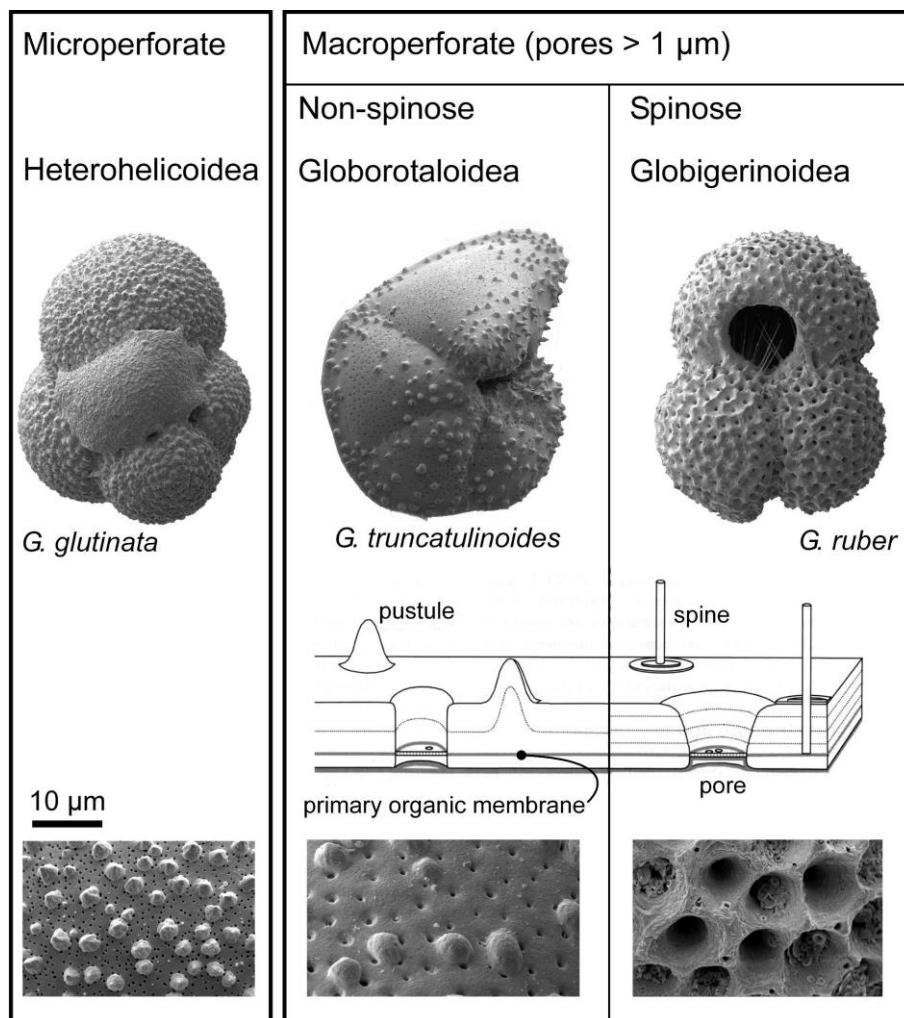


Figure 4.1: Diagram illustrating the three main supergroup families of planktonic foraminifera: Microperforate (*G. glutinata*), Globorotaloidea (non-spinose species e.g. *G. truncatulinoides*) and Globigerinoidea (spinose species e.g. *G. ruber*). A close up image of the wall structure displays the difference between the supergroups) (courtesy of Kucera, 2007)

## 4.2: PLANKTONIC FORAMINIFERA DEVELOPMENT

### 4.2.1 LIFECYCLE

The development of any species is primarily associated with its reproduction/life cycle. The foraminiferal lifecycle is generally categorised by two generations; reproduction by sexual means (gamont generation) and reproduction by an asexual nature (agamont generation). Asexual reproduction occurs when the cytoplasm is drawn into the test, where it splits into numerous haploid daughter cells, each containing half the chromosomal amount of the parental nucleus. While the onset of chamber formation occurs, the new offspring is released into the marine environment to disperse. At the maturity stage, the cytoplasm is once again drawn into the test to divide mitotically to form gametes. Then when released from the parent test, two gametes may fuse together performing the sexual reproduction phase (Armstrong and Brasier, 2009).

The planktonic foraminiferal reproduction cycle is seen as a solely sexual process while benthic foraminifera have an array of reproduction strategies including asexual reproduction (Topa et al., 2017). The reproduction of planktonic foraminifera is also dependent on their location within the water column, with shallow water species completing their breeding phase in sync with the lunar cycle (~ every 28 days) releasing hundreds of thousands of gametes into the marine environment (figure 4.2). Deeper dwelling species such as *Globotalia truncatulinoides* take a longer reproductive cycle only producing gametes once to twice a year (Schiebel and Hemleben, 2005; Kucera, 2007). Planktonic foraminifera are considered to be opportunistic feeders and during the lifetime of a species it obtains nourishment from a variety of sources including unicellular algae, bacteria, dissolved and particulate organic matter and sometimes even metazoans (Lin, 2014; Topa et al., 2017).

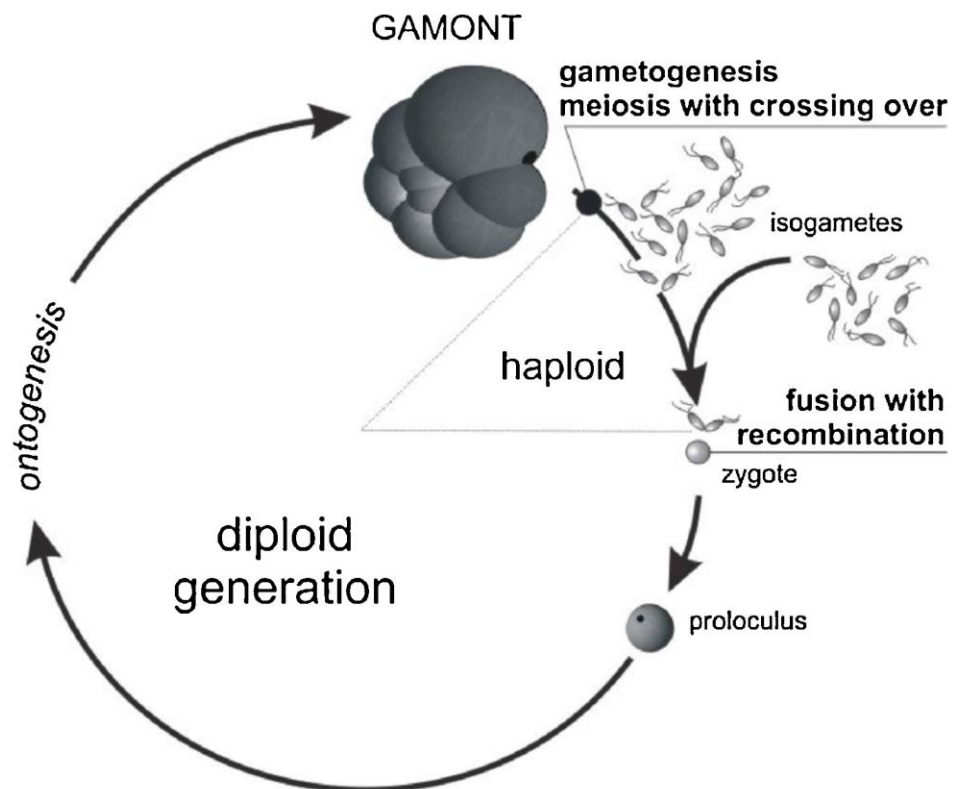


Figure 4.2: Depiction of the sexual reproduction cycle of planktonic foraminifera. All planktonic foraminiferal species are considered to be diploids and so complete the full life cycle as shown (courtesy of Topa et al., 2017).

#### 4.2.2 SHELL COMPOSITION AND MORPHOLOGY

Over the past number of decades much research has focused on the geochemical signals that are contained within the calcareous tests of planktonic foraminifera providing clues to both short and long term changes within the marine environment (Lea et al., 1999; Russell et al., 2004; Salmon et al., 2016; Venancio et al., 2016). Similarly, morphological characteristics of the test of certain species have been used for palaeoenvironmental reconstructions. For example Moller et al. (2013) examined the size of *N. pachyderma* within the North Atlantic Ocean, utilising surface sediment samples from 33 locations. It was noted that shell morphology was only partially controlled by the habitat of the species but that shell size displayed definitive relationships with SSTs. This work showed that within polar environments the test size of *N. pachyderma* is directly related to summer SSTs and as such can be used to develop a SST proxy (Moller et al., 2013). Likewise, the morphology of species can be reflected by whether a species coils to the left (sinistral) or to the right (dextral). Species such as *Globorotalia truncatulinoides* are known to have both coiling variants and as

such extensive research has been undertaken to ascertain the role of environmental variables in controlling the coiling direction (Ericson et al., 1955; Lohmann and Schweitzer, 1990; Ujiie et al., 2010; Broggy, 2011; Quillévére et al., 2013). In contrast other studies suggest that coiling variations are the result of genetic differences within the species (cryptic species) (de Vargas et al., 2001; Ujiie and Lipps, 2009).

In terms of geochemical analysis Salmon et al. (2016) attempted to create a proxy by utilising test composition as a way to reconstruct ocean carbonate chemistry with calcification temperatures being ascertained by  $\delta^{18}\text{O}_{\text{calcite}}$ . It was determined that a correlation existed between test thickness and the Barium/Calcium ratio within all species of planktonic foraminifera but no connection was noted between test size and the Ba/Ca ratio. However, it was noted that the Uranium/Calcium ratio displayed considerable increases with test size in all species which suggested that there may be a link between U/Ca and a biological control such as growth rates.

### 4.3: DISTRIBUTION OF PLANKTONIC FORAMINIFERA

Numerous environmental aspects not only affect the global distribution of planktonic foraminifera but also affect the composition of individual faunal assemblages. Factors such as temperature, salinity and the availability of nutrients are some of the main components that affect the current distribution.

#### 4.3.1 TEMPERATURE AND SALINITY

Analysis of present day foraminifera indicate that temperature, salinity and productivity determine the composition of faunal assemblages with maximum relative abundances correlating to their ecological optima (Bé, 1959, 1960; Thunell, 1978; Bernasconi and Pika-Biolzi, 2000; Hayes et al., 2005; Corbí and Soria, 2016). Principally based on their optimum temperature ranges, modern day assemblages have been categorised into defined hydrographic zones; tropical, subtropical, transitional, subpolar and polar (figure 4.3) (Kucera, 2007). SST is one of the primary factors for the development and growth of foraminifera with each species having an optimum temperature range that

allows for the greatest development (figure 4.3). Conversely adverse temperature ranges can inhibit growth (Kucera, 2007). Specific features of a species such as size, shape and coiling direction may be influenced by temperature, which is also true when referring to the vertical distribution of species.

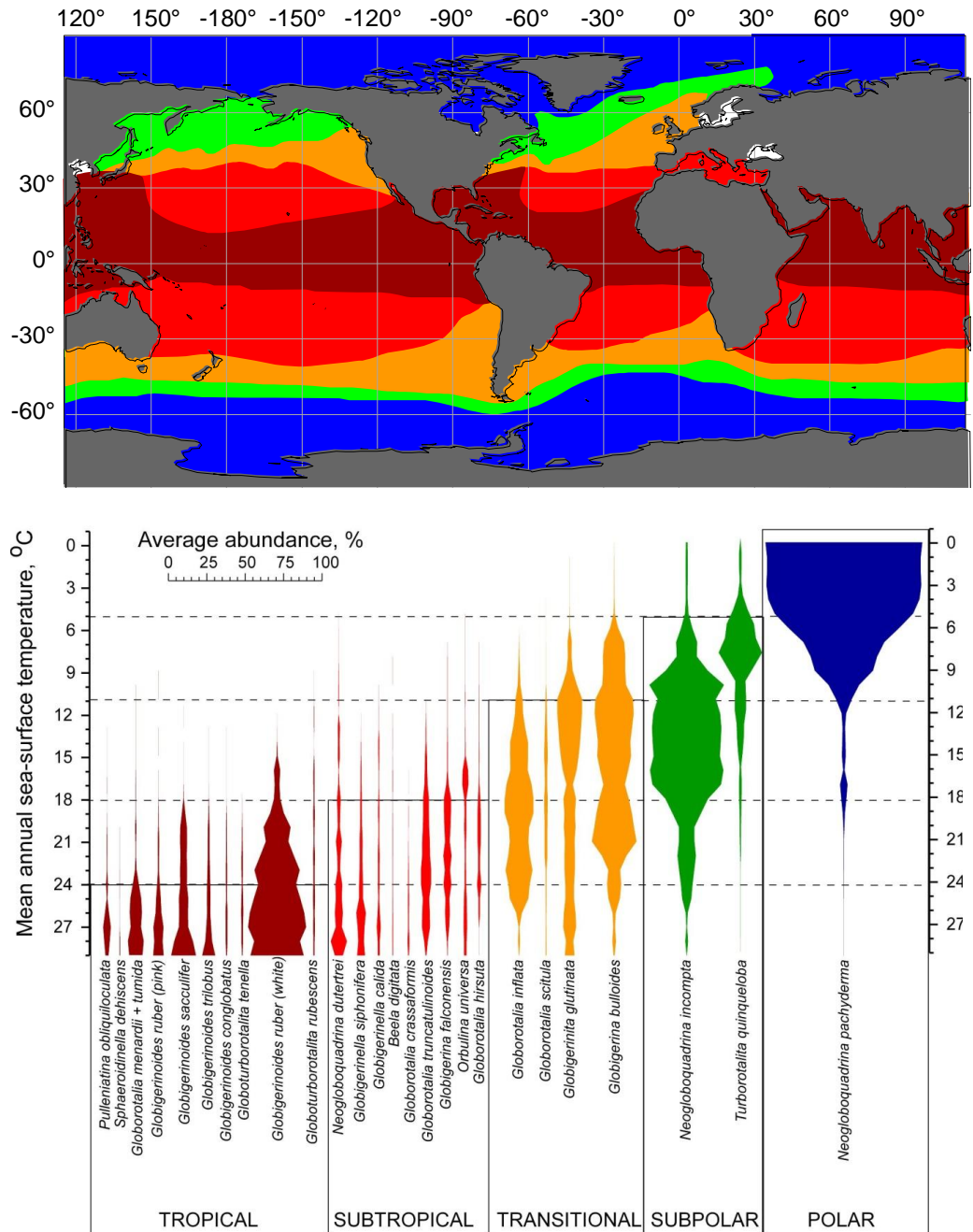


Figure 4.3 Map showing the five major planktonic foraminiferal faunal provinces which largely correspond to the main hydrographic regions of the modern global ocean. Also depicted is the relative abundance profiles of planktonic foraminifera within each of the global provinces (courtesy of Kucera, 2007).

Like temperature, planktonic foraminifera have specific preferences when it comes to salinity, occupying marine environments with salinities ranging on average between 30-

40‰ and demonstrating adaptive capabilities to changes within these parameters (Arnold and Parker, 1999; Kucera, 2007). Several processes such as changes in river discharge, sea ice formation, and the balance between evaporation and precipitation are responsible for determining such salinity levels. Studies have also shown that SSS, in conjunction with SST, decrease during cold periods (the Younger Dryas and Heinrich Event 2) thereby altering the distribution and therefore the composition of foraminiferal assemblages (Melki et al., 2009). Several studies have used planktonic foraminifera to make inferences about changes in SSS. In a study on meltwater fluxes into the Gulf of Mexico, Flower and Kennett, (1995) noted elevated frequencies of *G. ruber* coinciding with influxes of lower salinity meltwater. It is now well documented that *G. ruber* is a species that will tolerate a wide range of salinities but is known to thrive in low salinity lenses within the mixed layer (Bijma et al., 1990; Pujol and Vergnaud-Grazzini, 1995). In a similar study Rasmussen and Thomsen, (2012) highlighted a decrease in SSS (-1.5‰) between the Bølling interstadial and Heinrich Event 1 within the Gulf Stream. This was derived due to an increase in the relative abundance of *N. dutertrei*, which was interpreted to indicate an increase in nutrient supply corresponding to an influx of freshwater. Due to the inherent link between SSS and SST it has proved difficult to reconstruct SSS due to the difficulty in separating the two signals. However, recent research has attempted to use the assimilation of sodium (Na) into foraminiferal calcite as a proxy for the reconstruction of salinity levels (Mezger et al., 2016). Utilising planktonic foraminifera (*G. ruber* and *G. sacculifer*) from the Red Sea it was found that while there seems to be a correlation within the upper parameters of the salinity range, further study is required on individual species development before a complete dataset can be formalised.

#### 4.3.2 PRODUCTIVITY

Varying both seasonally and geographically marine productivity is principally governed by photic levels, nutrient availability and access to phytoplankton (Berger, 1969), ultimately controls the composition and abundance of foraminiferal assemblages. In general terms marine productivity tends to be lower in areas that are characterised by poor circulation and restricted vertical mixing whilst, high rates of primary productivity occur where nutrients are transferred into surface waters via increased vertical mixing

(Casford et al., 2003; Meier et al., 2004; Hernández-Almeida et al., 2011; Incarbona et al., 2011). In a study undertaken by Hernández-Almeida et al. (2011) productivity and planktonic foraminiferal response was examined within the Alboran Sea. The Alboran Sea has high rates of productivity due to local circulation patterns which are regulated by the influx of Atlantic surface waters and the development of anticyclonic gyres which subsequently allow the development of phytoplankton blooms within the region. The authors noted high concentrations of chlorophyll corresponding with the development of specific microplanktonic assemblages (coccolithophores and diatom cells), providing a food source for planktonic foraminiferal species such as *G. bulloides*, a species known to thrive in nutrient rich waters (Hernández-Almeida et al., 2011). Furthermore Rohling and Gieskes (1989) discussed the relationship between the development of a Deep Chlorophyll Maximum (DCM) and the abundance of *Neogloboquadrina incompta*. A DCM occurs when the pycnocline moves within the base of the euphotic zone. This allows the transference of nutrients from the eutrophic intermediate waters into the oligotrophic photic zone. The effect is increased primary productivity and the development of a DCM thus providing the nutrient requirements for *N. incompta* to flourish. Neogloboquadrinids are particularly susceptible to the development of a DCM and high abundances of this species are noted and are attributed to the increased productivity associated with preferential grazing upon phytoplankton blooms (Rohling and Gieskes. 1989).

#### 4.3.3 VERTICAL DISTRIBUTION OF FORAMINIFERA

Like temperature, salinity and nutrient availability, water depth is a significant factor in controlling the distribution of planktonic foraminifera. As is illustrated in figure 4.4 the maximum concentrations of planktonic foraminifera tend to reside in the shallower parts of the photic zone (0-50 m) Species residing at this depth include *G. ruber* (*alba* and *rosea*) and *G. sacculifer*. Subsurface species residing within 50-100m include *O. universa*, *N. incompta*, *G. siphonifera* and *G. bulloides*. Deeper dwelling species (those over 100m depth preference) include *G. menardii*, *G. hirsuta* and *G. truncatulinoides* (whose depth habitat is completed over a yearly cycle associated with their lifecycle) (Tosk, 1988; Pujol and Vergnaud Grazzini, 1995; Kuroyanagi and Kawahata, 2004; Birch et al., 2013; Rebotim et al., 2016) (figure 4.4).

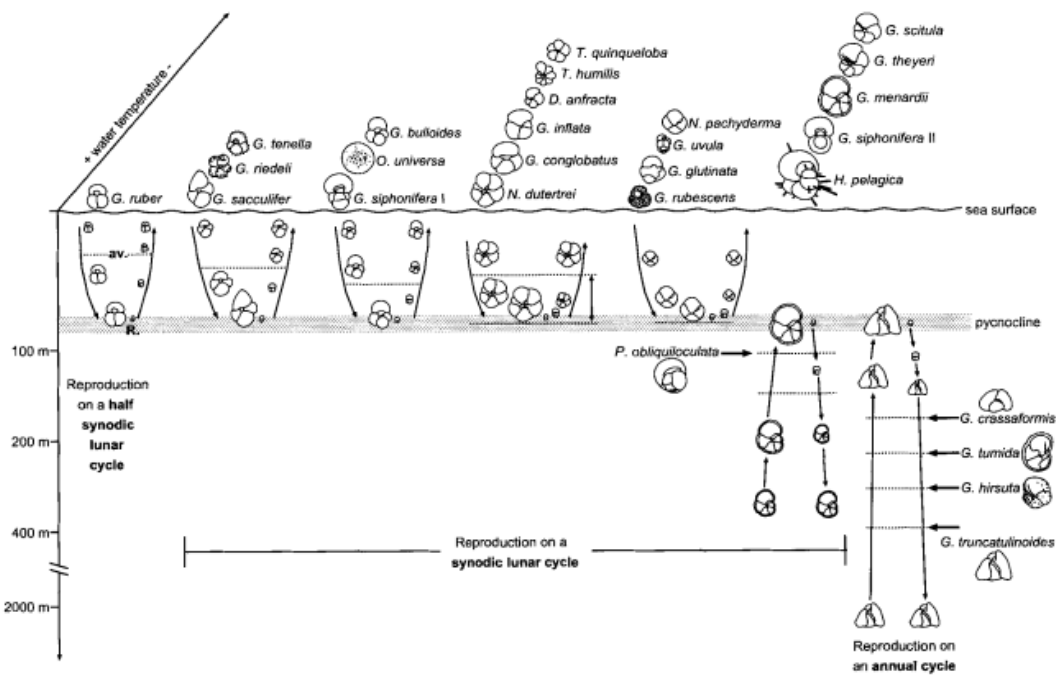


Figure 4.4: Modern day depth profiles of planktonic foraminifera (courtesy of Schiebel and Hemleben, 2005).

Using vertical plankton tows and open-close nets several studies have been initiated to examine the vertical distribution of planktonic foraminifera, in an effort to understand how their distribution is influenced by environmental parameters at different depths (Schiebel et al., 1995; Field, 2004; Kuroyanagi and Kawahata, 2004; Sousa et al., 2014). In a study undertaken in the seas around the island of Japan, Kuroyanagi and Kawahata (2004) attempted to determine the factors that controlled the vertical distribution of living planktonic foraminifera with particular reference to temperature, chlorophyll-a concentrations and light intensity. Highlighting the vertical distribution of *G. ruber*, a warm, shallow dwelling species, Kuroyanagi and Kawahata (2004) distinguished two morphotypes of the species as recognised by Wang (2000). Interestingly the two morphotypes showed differing vertical distributions with one morphotype (*G. ruber* s.s) dominating surface waters and perhaps more dependent on symbionts. The other morphotype (*G. ruber* s.l) was prevalent in deeper waters with lower light intensities suggesting a reliance on feeding rather than symbionts. A similar study was undertaken by Bergami et al. (2009) in the Ross Sea and Pacific sector of the Southern Ocean. Specifically these authors focused on the vertical distribution of *N. pachyderma* (sinistral) at two separate locations. Results indicate that distribution of the

species differed between the two sites due to the variations in the hydrological regimes. Encrusted morphotypes of the species demonstrated preferences towards the stratified water column in contrast to the open water site whereby juvenile specimens dominated the surface waters with encrusted morphotypes showing a preference for deeper waters. However, this research did conclude that, contrary to previous studies in which *N. pachyderma* (sinistral) is referred to as a deep dwelling species (based on the calcification depth), *N. pachyderma* (sinistral) was present at all water depths (< 300m) provided the SST was < 2°C (Bergami et al., 2009). Both these studies highlight the importance of identifying different morphotypes within individual species and how they can affect the accuracy of palaeoenvironmental interpretations.

Equally, a study undertaken by Birch et al. (2013) discusses the effect of foraminiferal size when reconstructing depth profiles. Isotopic reconstructions are based on the isotopic composition of a calcite test being dependent on isotopic ratios and the temperature of the water in which they calcify. An analysis of isotopic composition of various species should therefore reveal ecological aspects at different water depths. This is based on the interpretation that the depth of the environment as determined by whole shell stable isotopes from planktonic foraminifera is isotopically similar to ambient seawater. However, due to variations in chemical and physiological processes this is not always true. To counterbalance this effect utilising a multispecies size specific approach has helped to alleviate these 'vital effects' (Thunell and Sautter, 1992; Peeters, 2002).

Birch et al. (2013) reconstructed the thermal properties of the water column by combining stable isotopic measurements on multiple size fractions from 12 modern day species in the Indian Ocean. Their results indicated size control was significant when using planktonic foraminifera to reconstruct ecological parameters at different water depths. Oxygen isotope data highlighted *G. ruber* as the most appropriate species to reconstruct surface water temperature. Furthermore they suggested as there was no correlation with test size, all sizes of this species would provide unbiased data. In contrast, the deeper dwelling species of *G. scitula* is ideal for reconstructions of subsurface waters. The size fraction becomes more prevalent when referring to *G. bulloides*, *G. scitula* and *G. truncatulinoides*. Indicative of subsurface conditions, the authors suggest that due to a correlation between  $\delta^{18}\text{O}$  and test size, that only specimens greater than 300 $\mu\text{m}$  should be used. This correlates with the maximum depth habitat of

these species and therefore provides a more realistic reconstruction of subthermocline temperatures Birch et al., 2013).

#### 4.4 DISTRIBUTION IN THE MEDITERRANEAN SEA

As with global distribution, planktonic foraminifera in the Mediterranean Sea are influenced by the aforementioned environmental parameters. In 1995 Pujol and Vergnaud-Grazzini presented a comprehensive analysis of the seasonal distribution of planktonic foraminifera as related to the regional hydrography within the Mediterranean Sea (figure 4.5). The following section will examine the results of this paper placing particular emphasis on the focus area of this research, the eastern basin.

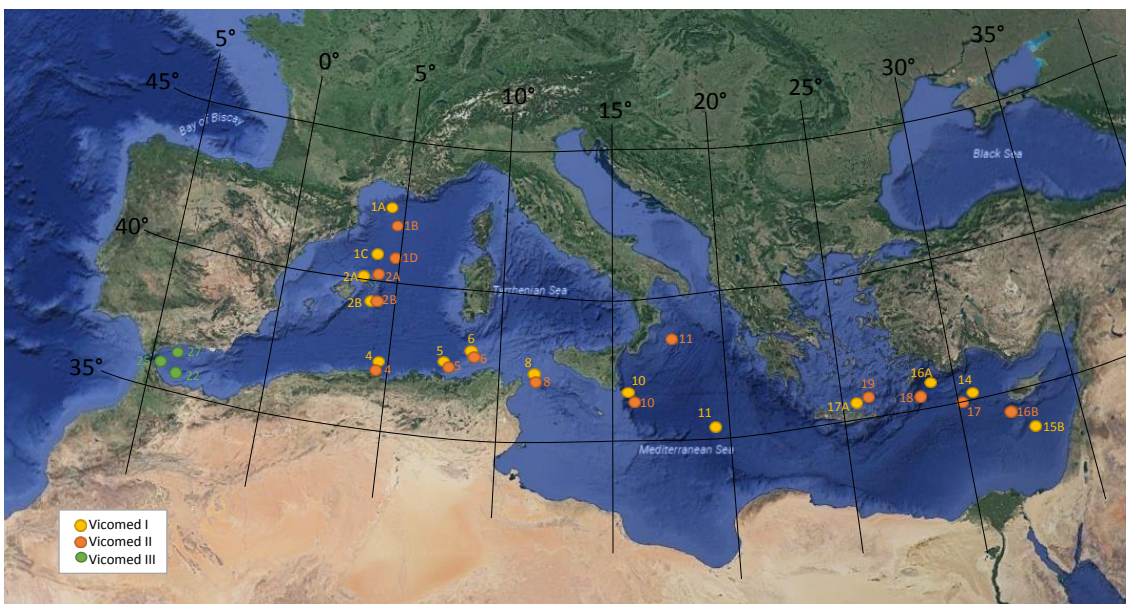


Figure 4.5: Distribution map of sampling locations during Vicomed I (summer), II (winter) and III (spring) cruises (modified after Pujol and Vergnaud-Grazzini, 1995; base map courtesy of [www.google.com/earth](http://www.google.com/earth)).

The eastern basin has an arid climate due to the surrounding continentality. In conjunction with minimal terrigenous runoff to inject nutrients to surface waters, the eastern Mediterranean is typically oligotrophic. This is reflected in the faunal assemblages that occupy these waters (Pujol and Vergnaud-Grazzini, 1995; Morard et al., 2009). Pujol and Vergnaud-Grazzini (1995) collected foraminiferal densities (number of specimens/1000 m<sup>3</sup>) from depths up to 350 m during the late summer and winter seasons across both basins of the Mediterranean Sea. Not surprisingly the eastern basin recorded much lower population densities compared to the western basin with

peak production (1000 – 2000 specimens/1000 m<sup>3</sup>) occurring during the late summer months. At this time peak production is confined to the central Mediterranean with assemblages almost entirely composed of *G. ruber* (*alba* and *rosea*) with smaller contributions of *G. sacculifer* and *O. universa* (figure 4.8). These predatory species dominate the shallow mixed layer (~ 50m) (Pujol and Vergnaud-Grazzini, 1995). In contrast winter assemblages are more diverse particularly in the Ionian Sea (station 9 and to a lesser extent station 10). *G. ruber* is a much smaller component of the assemblage with *G. truncatulinoides*, *G. inflata* and *G. bulloides* dominating (figure 4.8). The change to predominantly grazing species is indicative of nutrient enrichment in the surface waters and subsequent phytoplankton growth. It is likely that the formation of winter eddy structures facilitates the movement of nutrients from the deeper intermediate waters. However, it is noted that diversity and densities decrease in the more eastward stations (Pujol and Vergnaud-Grazzini, 1995). Based on their findings Pujol and Vergnaud-Grazzini (1995) surmise that nutrient availability is the main limiting factor for the development and distribution of planktonic foraminiferal species within the entire Mediterranean Sea. This is particularly prevalent in the eastern basin where standing stocks are low and faunal assemblages are dominated by spinose species.

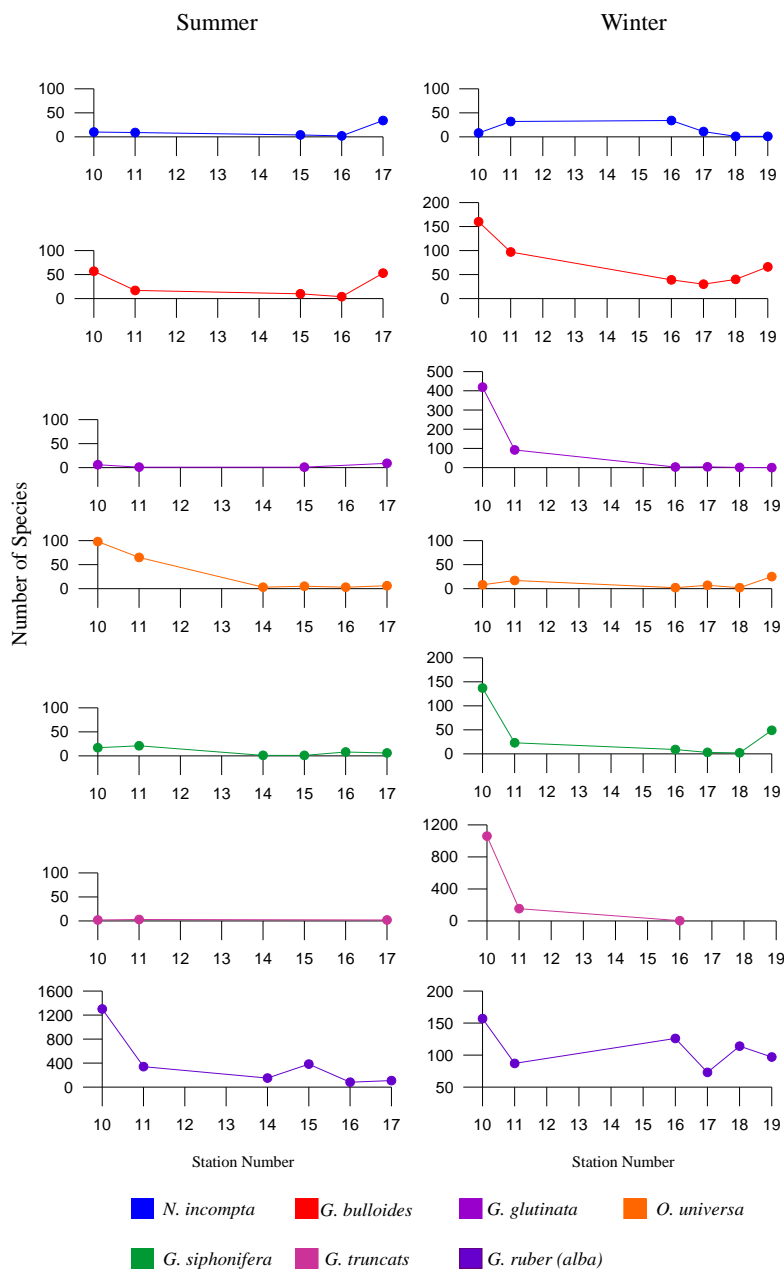


Figure 4.6: Graphs representing the summer/winter densities (number of species/1000m<sup>3</sup> of filtered water) of defined planktonic foraminiferal species within the eastern basin of the Mediterranean Sea (data from Pujol and Vergnaud-Grazzini, 1995). The Y-axis represents number of specimens and the X-axis signifies the station number. (Stations 10=Malta; 11=Ionian Sea; 14/17(winter) =Anaximander Trough; 15/16= Cyprus; 17(Summer) =Crete; 18= Rhodes; 19= Crete).

## 4.6 TRANSFER FUNCTIONS

As previously discussed, modern planktonic foraminiferal assemblages have specific preferences when discussing global SSTs. In knowing the present distribution of species many researchers have developed methods of reconstructing past temperatures, one

such method was the application of transfer functions. Imbrie and Kipp (1971) were one of the first to develop this transfer function as a way of reconstructing past surface water temperatures based on the abundance of planktonic foraminifera. Since it was first devised the process has been utilised and expanded by a number of palaeoceanographic researchers. CLIMAP (1976) utilised the Imbrie-Kipp Method (IKM), employing core top samples which contained a total of 22 different foraminiferal species from the Mediterranean Sea and Atlantic Ocean, in order to reconstruct SST since the Last Glacial Maximum (LGM). However due to issues with cryptic species, this data set was largely discredited. Hayes et al. (2005) expanded this process by utilising 145 core tops from the Mediterranean Sea and 129 from the Atlantic Ocean with a total of 23 planktonic foraminiferal species. Employing the use of Artificial Neural Networks (ANN) and planktonic foraminiferal assemblages as a means to reconstruct SSTs since the LGM was more successful due to the larger calibration set and the development in the taxonomic understanding of planktonic foraminiferal species (Hayes et al., 2005). Further methods included the Modern Analog Technique (MAT), developed by Hutson (1980), this again quantifies faunal changes within palaeoenvironments in order to reconstruct SSTs, this time it utilises the faunal dissimilarity index from modern oceans as a means of reconstruction. This process has been used within numerous palaeoenvironmental reconstructions (Kallel et al. 1997; Dowset and Robinson 1998). Both the IKM and MAT methods have been essential in understanding the changes within SSTs within the Quaternary and the use of planktonic foraminiferal assemblages have been central to the development of these techniques.

# CHAPTER 5

## MATERIALS AND METHODS

### 5.1 INTRODUCTION

The chapter will present a detailed account for the materials and methods that were used to facilitate the completion of this research. The initial sections of the chapter refer to the deep sea cores outlining the locations and their physical attributes. The second part of the chapter will focus on the laboratory procedures employed to extract the micropalaeontological data while addressing the quality and preservation of the material. Finally an examination of the methods utilised throughout the research will be addressed including reference to Accelerated Mass Spectrometry (AMS) and the Artificial Neural Networks (ANN) transfer function.

### 5.2 MATERIALS

The data obtained for this research was primarily based on sediments extracted from core ODP 969A (33°50.399'N, 24°53.065'E; Water depth 2200.3m) (figure 5.1). This core was selected as it contained an undisturbed sequence of Late Quaternary sapropel sediments and was deemed suitable to assess both the test size of species specific planktonic foraminifera and the faunal abundances during several of these depositional events. A second core ODP 964A (36°15.623'N; 17°44.990'E; water depth 3657.7m) situated within the Ionian Sea was also utilised in chapter 6.

Core 969A is located within the Mediterranean Ridge, a significant structural-morphological element, within the eastern basin of the Mediterranean Sea, running along the Hellenic subduction zone, lying to the south of Greece and the island of Crete. It is approximately 300km wide and 2000km long and it owes its formation to the subduction of the African lithosphere beneath Europe and in particular the Aegean microplate (Limonov et al., 1996; Mascle and Chaumillon, 1997; Fruehn et al., 2002; Kopf et al., 2003; Huguen et al., 2004).

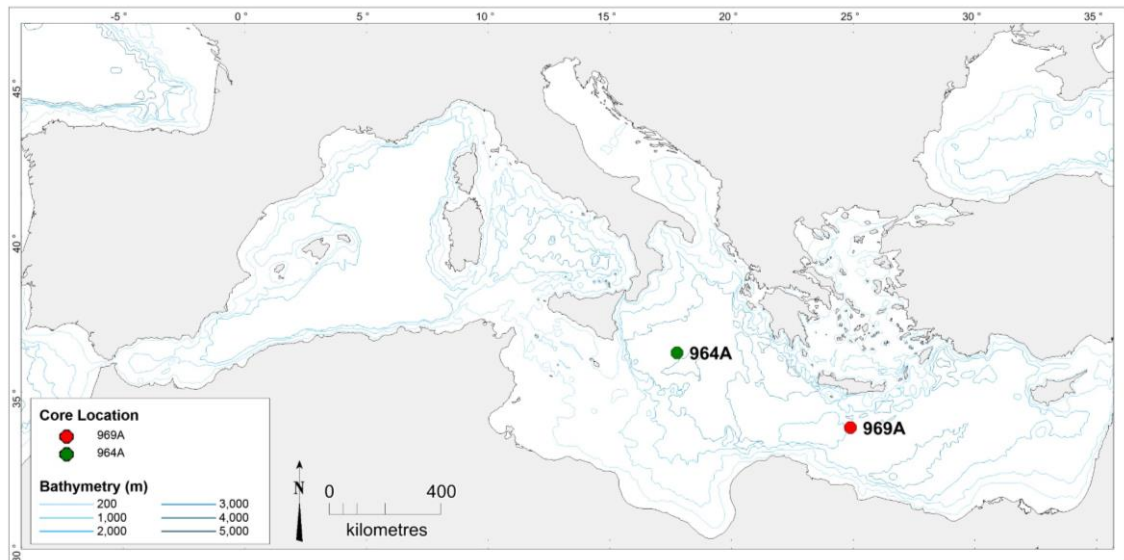


Figure 5.1 Map illustrating the location of Eastern Mediterranean ODP Cores 969A located along Mediterranean ridge and ODP core 964A located within the Ionian Sea.

Both these cores were obtained from the Ocean Drilling Program (ODP) Leg 160. Core 969A was obtained between the 14<sup>th</sup> and 15<sup>th</sup> April 1995, whereby 108.3m of core was recovered with the oldest part exhibiting a calcareous silty clay. Core 969A is located within the shallower inner part of the Mediterranean ridge, in a region of intense deformation. This location was chosen as it contained a comparatively undisturbed section of extended Pliocene-Pleistocene sediment and so a full record of sapropel deposition may be obtained. Colour scanning was completed at 2cm intervals, the reflectance of which provided a superb documentation of sapropel deposition. In total a record of 80 sapropel layers was noted ranging from the Pliocene to the Holocene, these were noted within 5 distinct groupings, interceded by layers of yellow oxidised sediment that showed no signs of preserved sapropels. The upper part of the core contains the most recent sapropels S1, S3, S4, S5, S6 and S7 while S2 was not present in this core. The sapropels appeared to be grey to dark grey in colour. In addition to this there are several ash layers with one most notably adjacent to sapropel S3.

### 5.2.1 CORE LITHOSTRATIGRAPHY

All sapropel layers utilised within this research were contained within unit 1 of core 969A. The lithology of this unit was primarily composed of nannofossil ooze, clayey

nannofossil ooze and foraminiferal nannofossil ooze, interjected by minor intervals of nannofossil clay. Within the core a number of distinct layers were noted at different intervals, the upper 2.5m of the sediment is composed of a pale brown nannofossil ooze, followed by the deposition of sapropel S1, then a clayey nannofossil ooze. The next 20-25m is comprised of both clayey nannofossil ooze and foraminiferal nannofossil ooze that has a distinct colouring from light grey to a yellowish brown. A notable ash layer appears above the location of sapropel S3. The next section of the core is notable due to changes within the colour of each layer. Most commonly this is a light grey to grey foraminiferal clayey nannofossil ooze with sapropel layers. Furthermore some slightly darker clay-rich intervals are noticed. Very little difference in bulk sediment configuration is noted, some red intervals are typified by trace quantities of hematite while the grey sediment is noted to have trace amounts of pyrite. The bottom-most interval of light grey sediment, which contains early Pliocene age sapropels is described as having an elevated clay content (Emeis et al. 1996). Sapropel S6 exhibits a moderately burrowed upper section with some slight colour change intervals, while some reports have identified S6 in other cores as a double sapropel there is no evidence of this throughout the research or from the ship report.

Sapropel identification has been completed based on physical attributes of the cores and in conjunction with the information provided by the Ocean Drilling Program who had previously identified these layers with some analysis. ODP research completed natural gamma-ray spectrometry for U/TH ratios, which is utilised as a organic carbon content indicator and to distinguish changes with oxidation, additionally colour reflectance, magnetic susceptibility and lithological markers such as an ash layers were all identified in order to define the sapropel layer Physical identification is based on changes within the colour sequences of the sapropel layers. In order to allow for the possible burn-down/oxidation of the top/bottom of sapropel layers this research completed further analysis of test and assemblage size of pre and post sapropel layers in order to ensure a full timeframe was completed. The identification of these layers was further supported through the changes within the faunal abundances within each core.

This core is utilised within 3 chapters of this research; 22,000 yrs to present (chapter 6) (table 5.1), sapropel S3 and S5 (chapter 7) (table 5.2) and sapropel S5 and S6 (chapter 8) (table 5.2). A sampling resolution every of 2cms from core 969A and every 4cms

from core 964A was obtained to maximise the observation of faunal changes in response to both short and long term events (Tables 5.1 & 5.2).

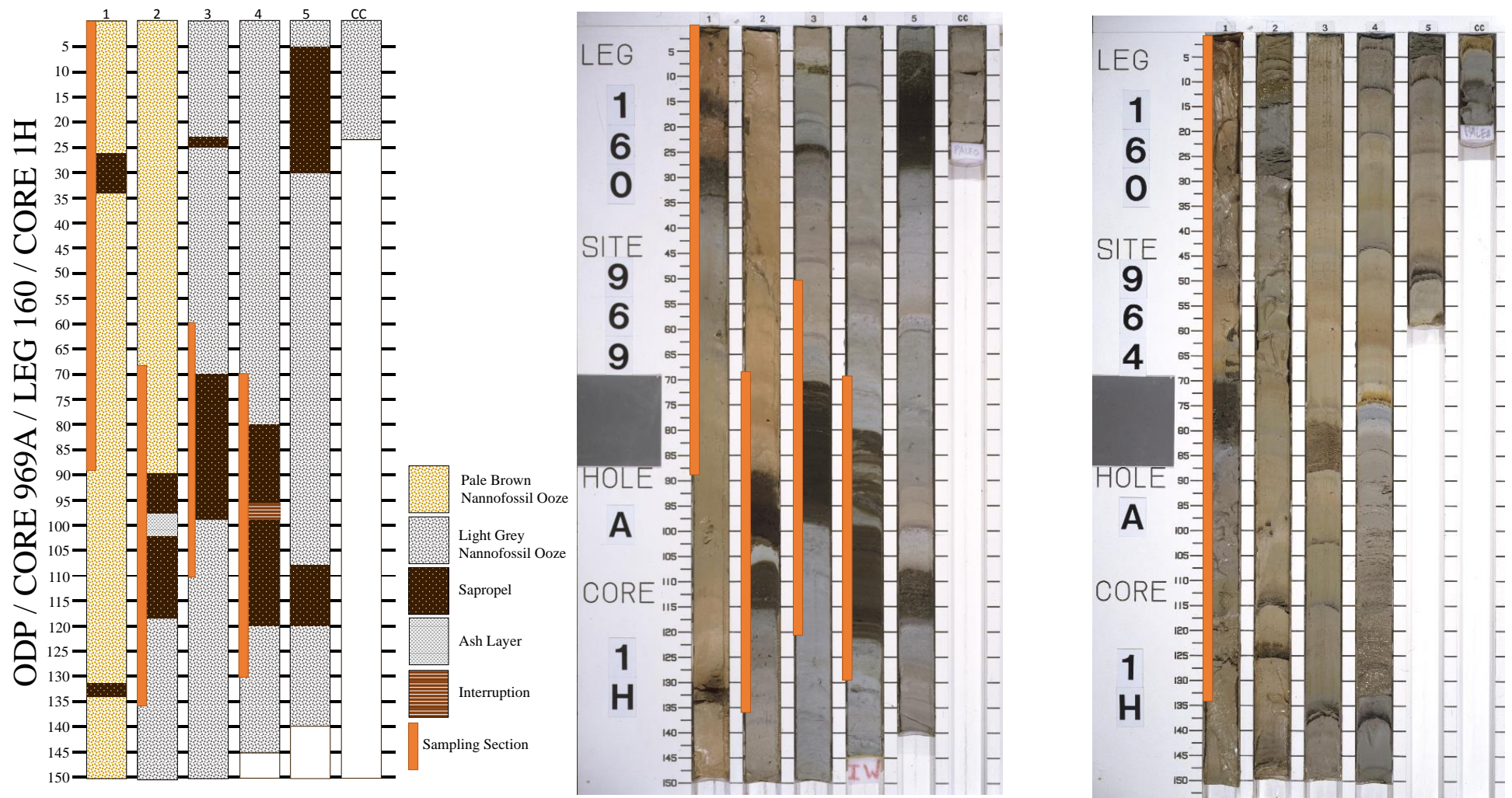


Figure 5.2: Lithological log and corresponding photograph of ODP core 969A with sapropel layers and sampling section marked within each unit. Photograph of ODP core 964A with sampling section also defined. Orange bar represents the areas from which sampling at 2cm (969A) and 4cm (964A) intervals was taken. (Photograph courtesy of Ocean Drilling Programme)

| Core | Project Scope | Metres Below Seafloor (mbsf) | Section Thickness (cm) | Sampling Resolution (cm) | No. of Samples | Core Section | Data Extracted                      |
|------|---------------|------------------------------|------------------------|--------------------------|----------------|--------------|-------------------------------------|
| 969A | LGM - Present | 0.23                         | 69                     | 2                        | 35             | 1H1          | Planktonic foraminifera assemblages |
| 964A | LGM - Present | 0.23                         | 86                     | 4                        | 22             | 1H1          | Planktonic foraminifera assemblages |

*Table 5.1 Summary of data for core 969A and 964A including depth below seafloor, the total thickness of sediment layer, the number of samples studied within the layer and the data extracted.*

| Core | Project Scope | Metres Below Seafloor (mbsf) | Section Thickness (cm) | Sampling Resolution (cm) | No. of Samples | Core Section | Data Extracted  |
|------|---------------|------------------------------|------------------------|--------------------------|----------------|--------------|---|
| 969A | Sapropel S3   | 2.40                         | 80-135 (S3 90-118)     | 2                        | 28             | 1H2          | Planktonic foraminifera assemblages                   |
| 969A | Sapropel S5   | 3.70                         | 60-109 (S5 70-98cm)    | 2                        | 24             | 1H3          | Planktonic foraminifera assemblages<br>Test Size Data |
| 969A | Sapropel S6   | 5.30                         | 70-131 (S6 80-120)     | 2                        | 31             | 1H4          | Planktonic foraminifera assemblages                   |

*Table 5.2 Summary of data for core 969A and 964A including depth below seafloor, the total thickness of sediment layer is illustrated with the sapropel intervals displayed in brackets, the number of samples studied within the layer and the data extracted.*

## 5.3 METHODS

### 5.3.1 MICROPALAEONTOLOGICAL ANALYSIS

Utilising standard foraminiferal procedures, all micropalaeontological samples were placed on a weighed petri-dish and dried overnight in an oven at  $< 40^{\circ}\text{C}$ , these temperatures are low enough to prevent heat damage to the fragile foraminiferal tests. Higher temperatures may result in increased fragmentation of certain species reducing the overall quality of the sample thereby skewing statistical analysis. When this overnight drying process was finished, the samples were weighed to obtain a dry sample weight (table 5.3). Samples were then disaggregated in deionised water and wet sieved through a  $63\mu\text{m}$  sieve again using deionised water. Deionised water is used to prevent contamination of the sample by minerals that occur in natural water. Once disaggregation has occurred the remaining sediment was placed in a petri-dish and redried again in an oven at  $< 40^{\circ}\text{C}$ . The final weight of the dried sample is taken once the drying stage is complete to obtain  $> 63\mu\text{m}$  dry weight. The final stage occurred when the sample was dry sieved through  $150\mu\text{m}$  sieve and resulting in splitting the sediment into two sections  $< 150\mu\text{m}$  and  $> 150\mu\text{m}$ . Each section was then stored in glass bottles which had been clearly marked with details relating to the sample.

| Sample Info    |            | Step 1: Before Wet Sieving |                                |                   | Step 2: After Wet Sieving |                                |                   |
|----------------|------------|----------------------------|--------------------------------|-------------------|---------------------------|--------------------------------|-------------------|
| Sample Section | Depth (cm) | Petri Dish Weight          | Petri Dish Weight & Dry Sample | Dry Sample Weight | Petri Dish Weight         | Petri Dish Weight & Dry Sample | Dry Sample Weight |
| 3A             | 22-23      | 48.24                      | 50.46                          | 2.22              | 46.05                     | 46.28                          | 0.23              |
| 3A             | 24-25      | 48.06                      | 50.78                          | 2.72              | 40.41                     | 40.66                          | 0.25              |
| 3A             | 26-27      | 47.33                      | 50.00                          | 2.67              | 46.01                     | 46.63                          | 0.62              |
| 3A             | 28-29      | 47.95                      | 50.58                          | 2.63              | 47.40                     | 48.01                          | 0.61              |
| 3A             | 30-31      | 46.25                      | 48.67                          | 2.42              | 48.53                     | 49.33                          | 0.80              |

The  $> 150\mu\text{m}$

*Table 5.3: Sample of processing data showing weights before and after wet sieving, all weights are displayed in gams.*

size fraction was

used for foraminiferal analysis as most research associated with planktonic foraminifera utilises this sieve size and so allows for direct comparison between results. This technique was applied to samples taken from sapropels S3, S5 and S6. Samples from

sapropel S1 had already been processed prior to the start of this research (Hayes et al., 2005).

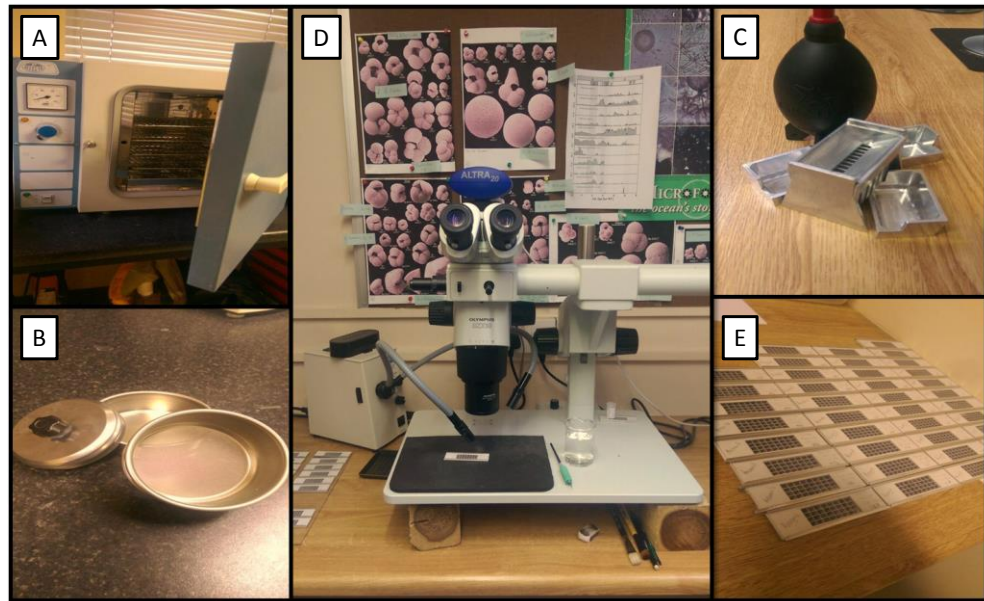


Figure 5.3: Depiction of some of the equipment that was used for the processing of samples where (A) Oven; (B) Sieves; (C) Random Micro Splitter (D) Microscope (E) Cushman Slides.

Where necessary, samples were then split using a random microsplitter, into samples of at least 300 specimens (where possible) from the  $>150\mu\text{m}$  size fraction, Statistically 300 individuals is used to ensure a 95% probability of not encountering an additional species (Shaw, 1964). A maximum total of 16 species was noted throughout all assemblages (table 5.4). General species identification was then completed according to the taxonomy of Hemleben et al. (2012). Some species were further divided into their coiling directions (e.g. *G. truncatulinoides*) or by their varieties (e.g. *G. ruber rosea* and *alba*). While in all instances throughout this research *N. pachyderma* (right coiling) has been redefined as *N. incompta* due to its many genetic differences with *N. pachyderma* (left coiling) which still continues to dominate polar waters (Darling et al., 2006). One exception to this identification process has occurred during sapropel S6 in relation to *N. pachyderma/incompta-dutertrei* where these combined species will be referred to as Neogloboquadrinids group. *N. incompta* and *N. dutertrei* are known to be genetically and morphologically related (Darling and Wade, 2008). Both species exhibit a low trochospiral test with between 4 and 6 chambers that frequent surface waters. Similarly both *N. incompta* and *N. dutertrei* are also herbivorous and exhibit the same feeding

patterns. While much care was taken to ensure correct identification occurred throughout all instances, it was decided to combine these species into one group in order to correctly address any issues that may arise during this sapropel layer. The final data then presented is in percentages of total planktonic foraminifera number and total abundance displayed as specimens/g.

| Species  |
|--|
| <i>Globigerinoides ruber (alba and rosea)</i>                |
| <i>Globigerinella siphonifera</i>                            |
| <i>Globiturbotalita rubescens</i>                            |
| <i>Orbulina universa</i>                                     |
| <i>Beela digitata</i>  |
| <i>Globiturbotalita tenella</i>                              |
| <i>Globigerina bulloides</i>                                 |
| <i>Globigerinita glutinita</i>                               |
| <i>Globorotalia truncatulinoides (dextral and sinistral)</i> |
| <i>Neogloboquadrina incompta</i>                             |
| <i>Neogloboquadrina pachyderma (sinistral)</i>               |
| <i>Turbotalita quinqueloba</i>                               |
| <i>Globigerinioides sacculifer</i>                           |
| <i>Globorotalia inflata</i>                                  |
| <i>Globorotalia scitula</i>                                  |
| <i>Globigerinella calida</i>                                 |

Table 5.4: List of planktonic foraminiferal species that have been identified and utilised throughout this research.

One issue related to the total abundance of planktonic foraminifera that resides within the sedimentary layer relates to the preservation of this material. Marine environment deep waters are undersaturated when dealing with calcium carbonate, so the decomposition procedure of organic matter during settling in conjunction with the acidic environments in predator guts produce extremely corrosive microenvironments that aid in the dissolution of calcite material within the deep waters of the open oceans. Due to this issue, the calcium carbonate tests of deceased planktonic foraminifera is exposed to these corrosive environments. It is estimated about 25% of all planktonic foraminiferal tests reach the sea floor, this is related to the intensity of dissolution within the water column and settling depths. While it is noted that the rate of dissolution within the water column it relatively low compared to the rate of carbon supply. Above the calcium carbonate depth, the dissolution rate increases dramatically and it strongly affects the bulk composition of the sediment in favour of insoluble constituents, this is known as the foraminiferal lysocline. Bottom water carbonate composition is reflected within the position of the lysocline and calcium carbonate depth, this position is

variable in response to fluctuations with in oceanic circulation and the redistribution of carbon (Berger 1970; Kucera, 2007; Schiebl et al., 2002).

### 5.3.2 ACCELERATOR MASS SPECTROMETRY (AMS) $^{14}\text{C}$ DATING

Resulting from advancing procedures, through the application of particle accelerators as mass spectrometers, AMS was developed in the 1980s. The use of mass spectrometers allowed for the detection of the atoms of particular elements, this was conducted through the variations within atomic weights. While traditional mass spectrometers were unable to differentiate between the atomic weight of  $^{14}\text{C}$  and other similarly weighted molecules, the use of accelerating these atoms allowed researchers to distinguish the weighted differences. AMS ascertains the isotopic ratio of  $^{14}\text{C}$  in relation to stable isotopes of Carbon ( $^{13}\text{C}$  or  $^{12}\text{C}$ ), dating then is determined by comparing the resulting ratio to that of the standard  $^{14}\text{C}$  content. The development of AMS dating also allowed for the researchers to use smaller sample sizes for dating processing, commonly  $> 1\text{mg}$  of carbon can be utilised to obtain results, this has sped up the timing of this process also which dating results only taking a number of hours. Furthermore, depending on the size of samples that are being examined, numerous samples can be completed within the same run. Numerous efforts have been made to increase the radiocarbon dating beyond the timescale of eight half-lives, however issues with this relate to very old samples whose residual  $^{14}\text{C}$  activity is so minimal that unreasonably extended counting times are required to get a true estimate of age (Walker 2008).

### 5.3.3 ARTIFICIAL NEURAL NETWORKS

Artificial Neural Networks (ANNs), a branch of artificial intelligence, is a system that allows for the computational defining of a connection between two sets of data. This model can be trained to recognise any correlation from the input of variables (e.g. faunal abundance) into desired output variables (e.g. sea surface temperatures) (Wasserman 1989). ANNs first came into effect in the 1940s with the original network description (Wasserman, 1989) and since have been applied to a wide variety of disciplines ranging from aeronautics to cell analysis. The application of ANN requires the use of a calibration dataset and by observing the present day relationship between the variable

(Sea Surface Temperatures {SST}) and faunal abundances it can then be applied to fossil assemblages. This research employs the Mediterranean Sea calibration dataset already established by Hayes et al. (2005) that presented the relationship between planktonic foraminiferal faunal assemblages and SSTs. The dataset is composed of 23 planktonic foraminiferal species from 145 Mediterranean Sea core tops and 129 North Atlantic Ocean core tops (Hayes et al., 2005). Core tops from the Atlantic Ocean were used as comparable analogues for glacial Mediterranean planktonic foraminiferal assemblages, nevertheless these were employed with restraint in order to avoid an over-representative element of a specific environment (Hayes et al., 2005). Furthermore annual, winter (January-March) and summer (July-September) SST data from the World Ocean Atlas (WOA, Vol. 2) was utilised (10m depth) in conjunction with the core top locations (Hayes et al., 2005). Results of the ANN demonstrated the capability to successfully reconstruct SSTs with average error rates ranging between 0.5°C for the winter and 1.1 °C for the summer months. This research utilises the quantitative variations in planktonic faunal assemblages from specific depositional events (sapropels) and downcore to reconstruct SSTs in the eastern Mediterranean Sea

## CHAPTER 6

# PALAEOENVIRONMENTAL VARIABILITY OF THE EASTERN MEDITERRANEAN SEA (MEDITERRANEAN RIDGE) SINCE THE LAST GLACIAL MAXIMUM (LGM)

### 6.1 INTRODUCTION

The Mediterranean Sea has long been the focus of international research, particularly in the eastern basin, relating to the depositional events associated with sapropels (Rohling & Hilgen, 1991; Myers et al., 1998; Liu et al., 2012; Toucanne et al., 2015; Filippidi et al., 2016; Grant et al., 2016). However, aside from containing these unique sediments, the Mediterranean Sea has made notable contributions to palaeoclimatic and palaeoceanographic studies due to its latitudinal position and configuration as a marginal semi-enclosed sea. Such attributes facilitate the amplification of mid latitude climatic variations which are registered as compositional changes in planktonic foraminiferal assemblages. It is well documented that the distribution of planktonic foraminifera are influenced by environmental parameters such as sea surface temperature (SST), nutrient availability and water column stratification (Thunell, 1978; Kucera, 2007; Lombard et al., 2009). As such it is acknowledged that when variations within the abundance of a particular species is noted within a core, it is shown to represent an ecological, rather than evolutionary, response to environmental variations.

With regards to the eastern Mediterranean Sea many Late Glacial planktonic foraminiferal investigations have been undertaken in the Adriatic and Aegean Seas owing to i) the unusually high sedimentation rates occurring in these regions and, ii) their importance as areas contributing to deep water formation (Triantaphyllou et al., 2009; Geraga et al., 2010; Georgiou et al., 2015; Kontakiotis, 2016 among others). In contrast, with lower sedimentation rates, more oceanic sites such as those in the Ionian and Levantine basins and along the Mediterranean Ridge tend to be less well researched

during this timeframe (Emeis et al., 2000; Geraga et al., 2000; Ehrmann et al., 2007; Kuhnt et al., 2008; Cornuault et al., 2016).

This chapter presents the planktonic foraminiferal records from two deep sea sediment cores located close to the Ionian Abyssal Plain (ODP 964A) and on the Mediterranean Ridge (ODP 969A) (figure 6.1). Both cores provide a continuous faunal record which provides the basis for the palaeoenvironmental reconstruction of the last glacial cycle. The main objective of this chapter is to identify and describe the distributional patterns of planktonic foraminifera from both cores in the context of palaeoclimatic and palaeoceanographic conditions at each location. To do this Q-mode Cluster Analysis and Principal Component Analysis (PCA) are presented to ascertain the relationship between the downcore faunal assemblages and environmental parameters. In addition, other palaeoenvironmental proxies such as SST, water column stratification (S-Index) and productivity (E-Index) were calculated to provide an insight into the hydrography and trophic status of the selected localities during this timeframe. This allows for the establishment of much needed Late Quaternary palaeoclimatic records in the poorly investigated oceanic sites, whilst also facilitating correlation with other palaeoclimatic records in the Mediterranean Sea, particularly in the eastern basin.

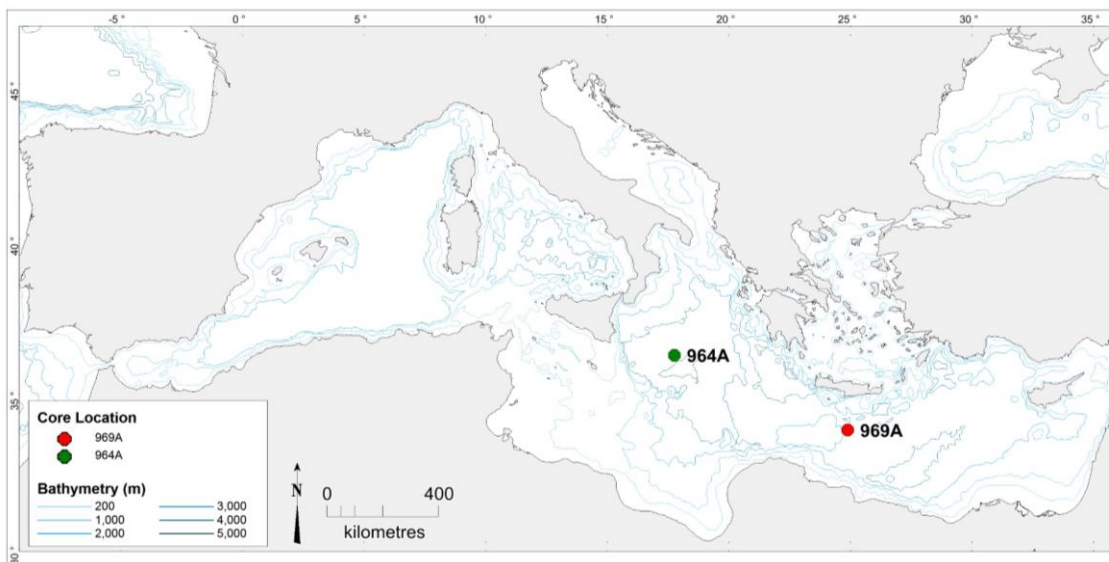


Figure 6.1: Map illustrating the location of Eastern Mediterranean ODP Cores 969A, located along the Mediterranean Ridge and 964A situated within the Ionian Sea.

## 6.2 CHRONOLOGICAL FRAMEWORK

The chronology of both cores was calculated using AMS  $^{14}\text{C}$  dates (tables 6.1 and 6.2). A total of 4 AMS  $^{14}\text{C}$  dates were obtained from core 969A (dating on core 964A was previously completed) and are presented in tables 6.1 and 6.2. These dates were obtained utilising > 10mg of clean processed unbroken non-specific planktonic foraminifera from the > 150 $\mu\text{m}$  size fraction. Radiocarbon dating is generally based on monospecific however, due to the small sample sizes there was an inadequate amount of single species to allow this. It was therefore decided to achieve the desired weight parameters a nonspecific assemblage was needed. AMS  $^{14}\text{C}$  dating was undertaken at Beta Analytics Laboratory in London, UK

Each AMS  $^{14}\text{C}$  date was then transformed into calendar years using computerised software CALIB 7.0.4 (Stuiver and Reimer, 1993), using the Marine13 calibration curve dataset and a standard global ocean reservoir age of 400 yrs (Stuiver and Braziunas, 1993) (tables 6.1 and 6.2). All AMS  $^{14}\text{C}$  dates utilised within this project are expressed to a 2-sigma calibration (95% probability). The use of marine samples uses a marine dataset so that the reservoir effect can be taken into account. This is due to the different replenishment rates of  $^{14}\text{C}$  in the oceans.

The local marine reservoir age has been a subject of recent debate with regards to the Mediterranean Sea. Facorellis and Vardala-Theodorou (2015) attempted to define local reservoir ages ( $\Delta\text{R}$ ) within the Aegean Sea however, while the authors noted inconsistencies in regional deviations they did conclude that the Mediterranean reservoir age was  $390 \pm 85$  yrs. Reimer and McCormac (2002) also noted that  $\Delta\text{R}$  was indistinguishable for different Mediterranean basins but recommended a  $\Delta\text{R}$  of  $58 \pm 85$   $^{14}\text{C}$  yr. This followed on from Siani et al. (2001) who concluded a  $\Delta\text{R}$  of  $35 \pm 70$  yrs with a regional average for the Mediterranean Sea of  $390 \pm 80$  yrs. Oceanographic research has suggested that substantial changes have occurred within the Mediterranean Sea over time and as a response to this, this research has applied the standard global ocean reservoir age (400 yrs) to this research, but omitted a  $\Delta\text{R}$  (Hughen et al., 2004).

| Core 969A  |                     |                 |                    |                    |                    |
|------------|---------------------|-----------------|--------------------|--------------------|--------------------|
| Depth (cm) | <sup>14</sup> C age | Corrected error | Lower cal range BP | Upper cal range BP | Median probability |
| 6.5        | 3340                | 30              | 3090               | 3315               | 3195               |
| 25.5       | 7420                | 30              | 7807               | 7953               | 7886               |
| 34.5       | 9700                | 40              | 10492              | 10713              | 10601              |
| 58.5       | 15240               | 50              | 17871              | 18220              | 18038              |

Table 6.1: AMS <sup>14</sup>C dating control points utilised for the construction of an age-depth model for core 969A.

| Core 964A       |                     |                 |                    |                    |                    |
|-----------------|---------------------|-----------------|--------------------|--------------------|--------------------|
| 964A Depth (cm) | <sup>14</sup> C age | Corrected error | Lower cal range BP | Upper cal range BP | Median probability |
| 2.5             | 1250                | 30              | 714                | 889                | 793                |
| 9.5             | 2360                | 30              | 1888               | 2086               | 1982               |
| 65.5            | 13050               | 60              | 14740              | 15244              | 15036              |
| 87.5            | 17730               | 80              | 20639              | 21166              | 20895              |

Table 6.2: AMS <sup>14</sup>C dating control points utilised for the construction of an age-depth model for core 964A.

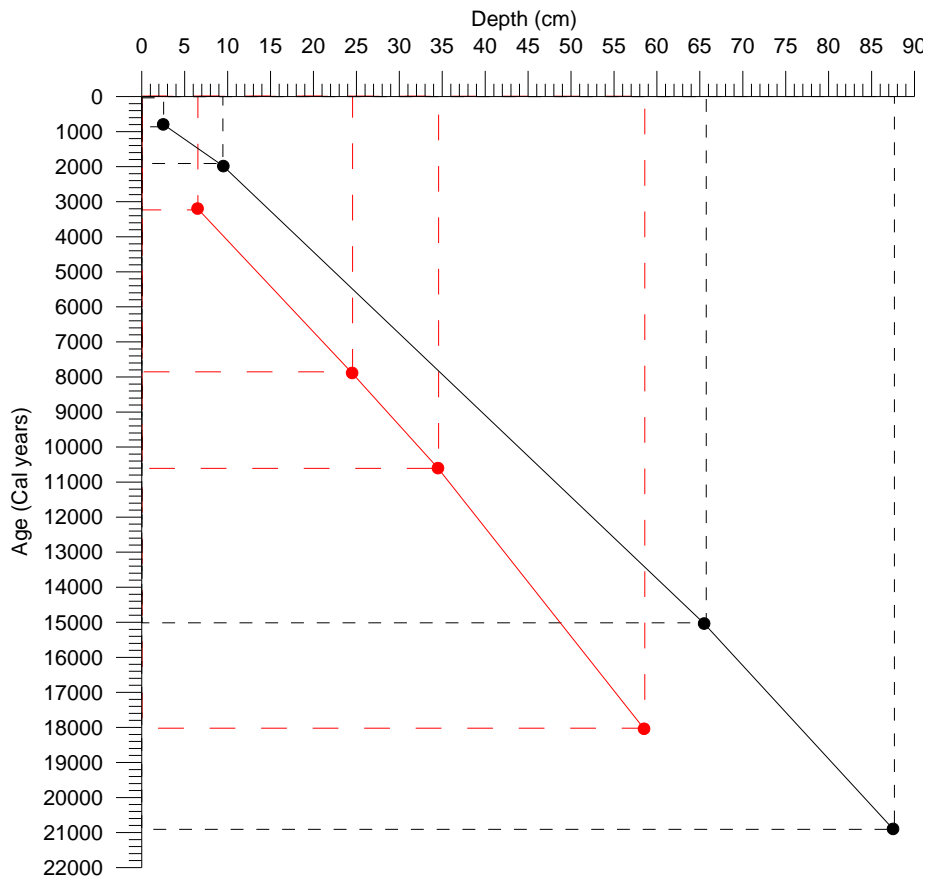


Figure 6.2 Age-depth profile for Mediterranean ridge core 969A (red) and Ionian Sea core 964A (black) with AMS dating control points marked by dashed lines relative to each core.

| 969A  |       |                              | 964A  |       |                              |
|---|-------|------------------------------|---|-------|------------------------------|
| Depth   | Age   | Sedimentation Rate<br>cm/kyr | Depth   | Age   | Sedimentation Rate<br>cm/kyr |
| <b>6.5</b>                                    | 3195  | 2.03                         | <b>2.5</b>                                    | 794   | 3.15                         |
| <b>24.5</b>                                   | 7886  | 3.84                         | <b>9.5</b>                                    | 1983  | 5.89                         |
| <b>34.5</b>                                   | 10601 | 3.68                         | <b>65.5</b>                                   | 15036 | 4.29                         |
| <b>58.5</b>                                   | 18038 | 3.23                         | <b>87.5</b>                                   | 20895 | 3.75                         |
| <i>Average sedimentation rate 3.20 cm/kyr</i> |       |                              | <i>Average sedimentation rate 4.27 cm/kyr</i> |       |                              |

*Table 6.3: Average sedimentation rates for cores 969A and 964A based on AMS dating control points highlighted in figure 6.2*

Figure 6.2 and table 6.3 highlight the age depth profile of both cores based on the AMS dating control points clearly illustrating the sedimentation rates of each core. Core 964A demonstrates a marginally higher sedimentation rate than that of 969A (4.27 cm/kyr and 3.20 cm/kyr respectively) however, it has a lower sampling resolution. As previously mentioned, the Mediterranean ridge generally has a lower sedimentation rate when compared to the Aegean and Adriatic seas with much of the sediment supply coming from localised inflow systems while it is known that much of the sediment deposition for the south-eastern basin comes from the Nile river (Garzanti et al., 2006; Hamann et al., 2008; van Helmond et al., 2015). In the Adriatic Sea the Po River is the prime contributor providing approximately a quarter of the sediment influx, this along with several smaller rivers from the Apennine Mountains are shown to be providing the historic sediment inflows to this area (Cattaneo et al., 2003). Several deltas such as the Po delta and Gargano delta have been studied in order to understand the late-Holocene sediment corridor from source to open sea (Cattaneo et al., 2003; Harris et al., 2008). As such mean sedimentation rates in the Aegean Sea can be seen to vary between 3.8 and 11.5 cm/kyr (Geraga et al., 2000, 2005; İşler et al., 2015) while those in the Adriatic Sea are much higher reaching rates of between 20 and 35 cm/kyr (Sangiorgi et al., 2003; Siani et al., 2010).

### 6.3 PALAEOENVIRONMENTAL PROXIES

Researchers have long used a palaeoenvironmental imprint (known as proxies) to interpret the past. The use of these proxies varies depending on the type of research that

is being completed and the data that is available e.g. stable isotopes, sediment grain size, molecular biomarkers and microfossil assemblages (Wit et al., 2013; McCave and Hall, 2006; Wilhelms-Dick et al., 2012; Cleroux et al., 2013; Annan and Hargreaves, 2015; Martinez-Ruiz et al., 2015). Both benthic and planktonic foraminifera are primarily used as a way to interpret past climates. As previously discussed in chapter 4, foraminifera exist at different depths within the water column and are subjected to changes in temperature, nutrients and salinity as well as changes to the chemistry of their shells (which are composed of calcium carbonate). This chapter utilised several proxies originating from the planktonic foraminiferal assemblages to determine a palaeoenvironmental reconstruction for both cores.

Cluster analysis is used as a means to divide the data into sets (clusters) that are more significant to each other than other sets, this way it is possible to locate which groups are similar and exhibit correlating assemblages. Principal component analysis (PCA) is a mathematical technique that transforms a set of correlated variables. The first variable component accounts for as much of the variability in the data as possible, with each remaining component accounting for less variability. A Stratification Index (S-Index) was used to determine the variability of the water column with respect to being strongly or weakly stratified. Based on previous studies this index measures the ratio between *G. ruber* (a mixed layer species favouring a strongly stratified water column) and *G. bulloides* (a species which flourishes in environments dominated by upwelling and strong vertical mixing) (Sbaffi et al., 2004; Kontakiotis, 2015). The Eutrophication Index (E-index) was utilised in order to investigate the trophic levels with the water column. The E-index uses the formula  $\frac{Sum(E)}{Sum(E+O)}$  where E is the eutrophic species which thrive within nutrient rich waters (*N. incompta*, *N. dutertrei*, *G. bulloides*, *T. quinqueloba*, *G. inflata*) and O corresponds to the oligotrophic species which when considered in conjunction with each other can represent a warmer water column (*G. ruber [rosea and alba]*, *G. rubescens*, *G. sacculifer*, *O. universa*, *G. siphonifera*) (Kontakiotis, 2015). Sea surface temperatures (SSTs) are a proponent of much palaeoclimatic research, the development of this process has grown over the past two decades and currently this method is accomplished using artificial neural networks (further details of this method is outlined in chapter 5) which is based upon 145 cores tops from the Mediterranean Sea and 129 from the Atlantic Ocean (Hayes et al., 2005). It is acknowledged that while the proxies described above can provide an insight into

the environmental conditions of both cores, they are based on our understanding of the environmental preferences of the planktonic foraminiferal species. To confirm such relationships exist analysis of independent variables such as  $\delta^{13}\text{C}$  (a function of productivity) and  $\delta^{18}\text{O}$  (a function of temperature) would be useful. However, such analysis was beyond the scope of this research and so therefore must be taken into account when interpreting the results.

## 6.4 RESULTS

### 6.4.1 DISTRIBUTION OF PLANKTONIC FORAMINIFERA

Throughout this chapter all planktonic foraminiferal species are presented versus age in cal yrs BP and are illustrated in figures 6.3 and 6.4. A total number of 15 species were observed within the faunal records (not all species occurred in both cores) and are listed as follows: *G. ruber* (*rosea* and *alba*), *G. siphonifera*, *G. rubescens*, *O. universa*, *G. digitata*, *G. tenella*, *G. sacculifer*, *G. bulloides*, *G. glutinata*, *G. truncatulinoides* (*left and right coiling*), *G. inflata*, *N. incompta*, *N. pachyderma*, *T. quinqueloba* and *G. scitula*.

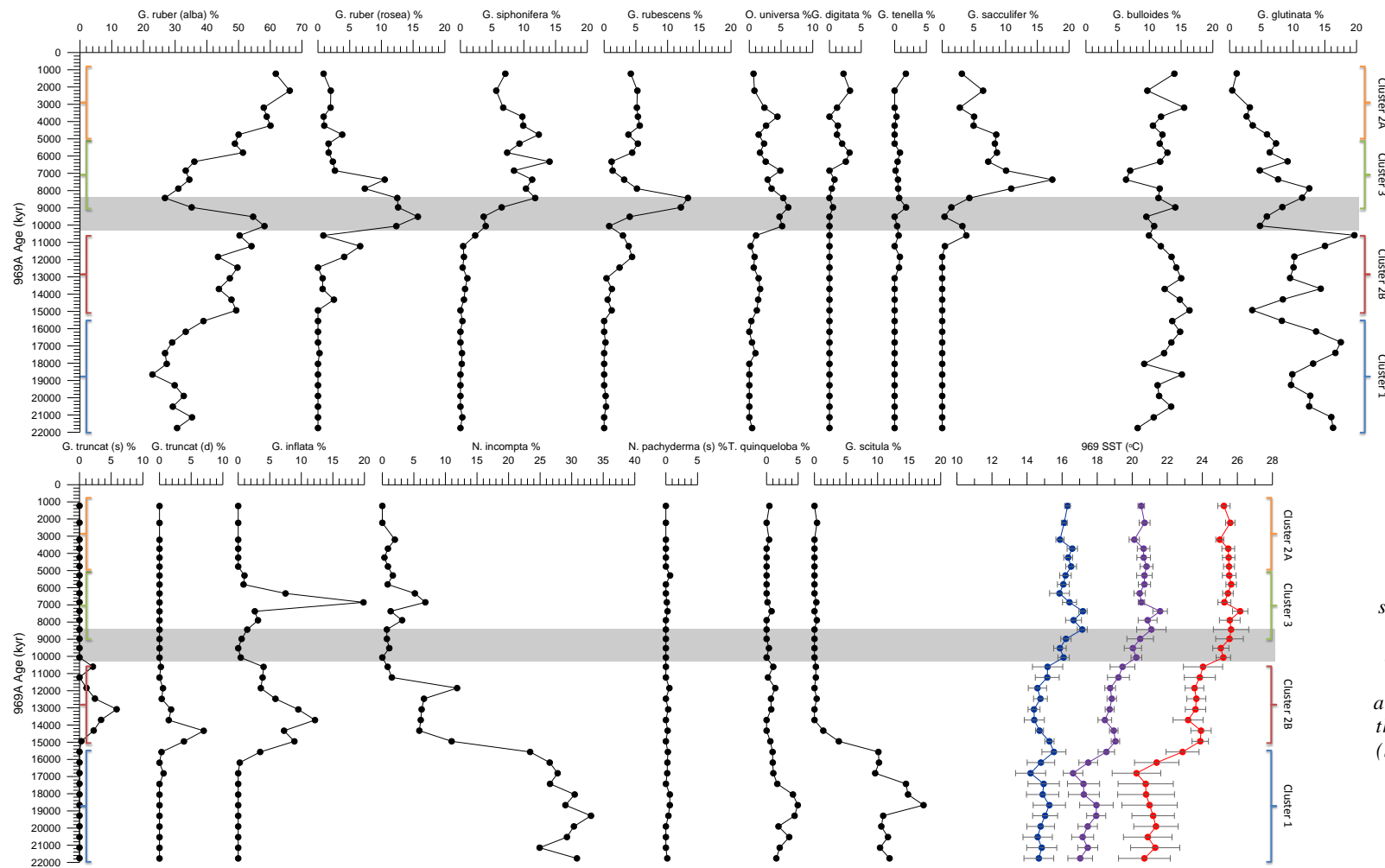


Figure 6.3 Faunal assemblage for ODP core 969A presented with winter (blue), annual (purple) and summer (red) SSTs. The grey shaded area represents Sapropel S1 and the results of the cluster analysis are also identified with respect to their location within the core (see figure 6.5 and tables 6.4 and 6.5 for details).

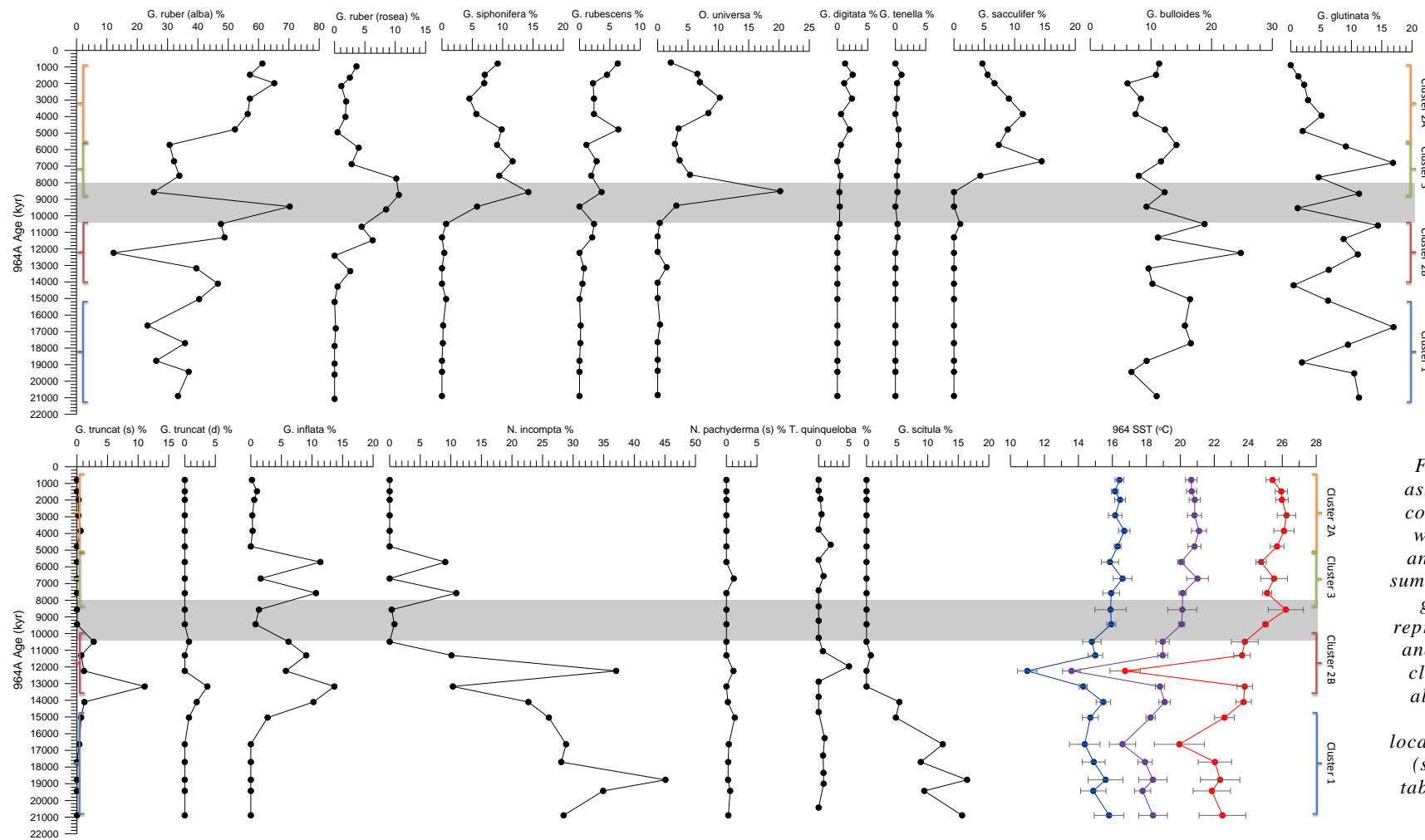


Figure 6.4 Faunal assemblage for ODP core 964A presented with winter (blue), annual (purple) and summer (red) SSTs. The grey shaded area represents Sapropel S1 and the results of the cluster analysis are also identified with respect to their location within the core (see figure 6.6 and tables 6.4 and 6.5 for details)

Distinctive faunal assemblages were further corroborated by Q-mode cluster analysis utilising the unweighted pair-group average (UPGMA) analysis which determine the statistical similarity between samples. The results of the cluster analysis are presented as dendrograms, recording samples on the Y axis and similarity on the X axis (figures 6.5 and 6.6 and summarised in tables 6.4 and 6.5) Four distinct assemblages of planktonic foraminifera were identified for both cores 964A and 969A (figure 6.5 and 6.6). Table 6.4 highlights the approximate age range for each cluster while table 6.5 identifies the dominant species within each cluster. It should be noted that two individual cluster points in core 964A have not been discussed within their clusters. Firstly the sample dated at 12239 yrs BP (cluster 1) appears in conjunction with the glacial cluster. This point occurs during the Younger Dryas, a cold phase, and so exhibits similarities with this cluster. Secondly in cluster 2A the sample dated at 9442 yrs BP is not included within the Modern day cluster as it occurs at the onset of sapropel S1 deposition when faunal assemblages began change and only exhibits some similarities with the modern day assemblages.

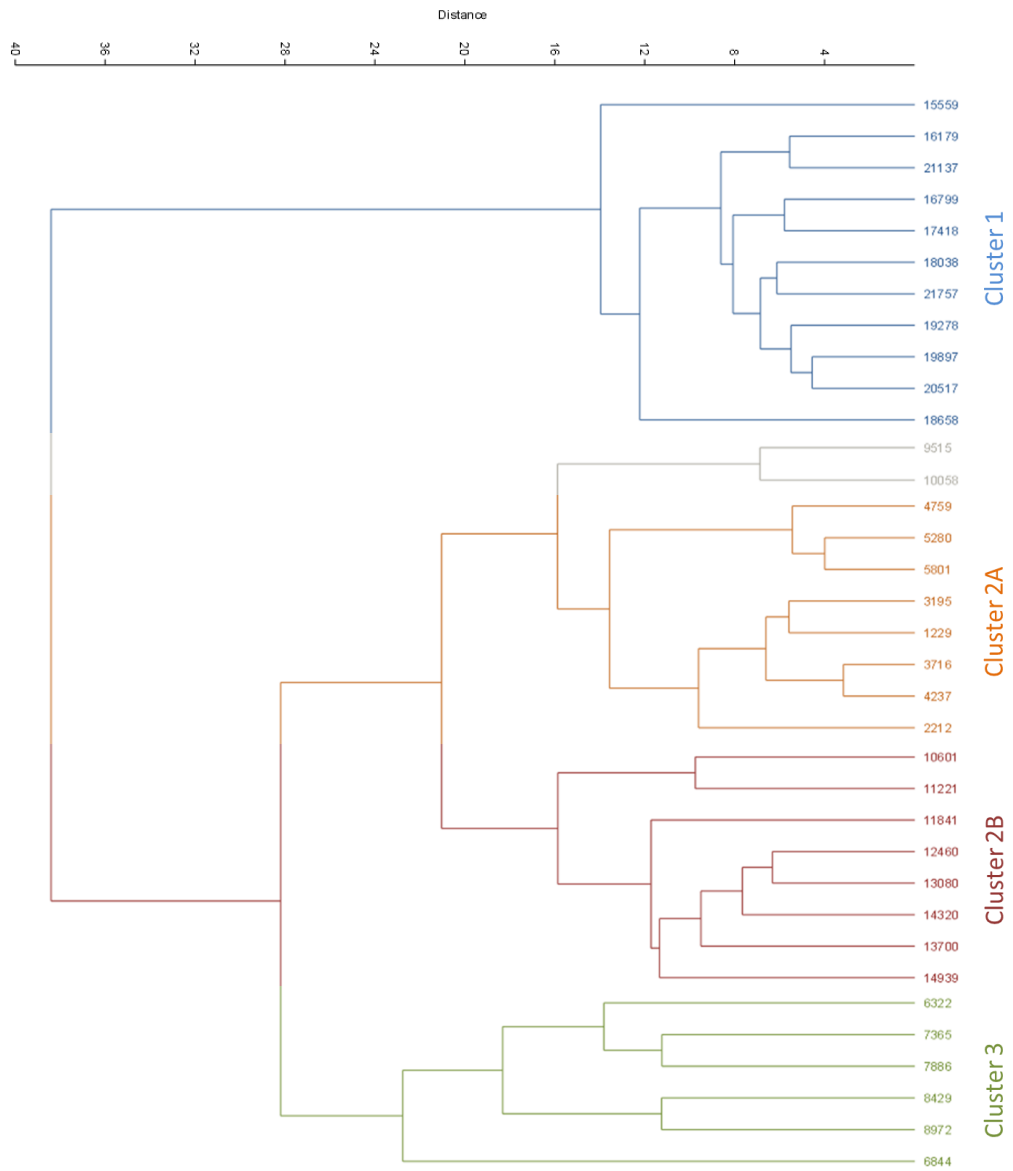


Figure 6.5: Dendrogram resulting from  $Q$ -mode cluster analysis and the clusters identified in core 969A. On the right hand side, the relevant clusters have been identified and colour coded; Cluster 1 = glacial assemblage (blue), Cluster 2A = modern assemblage (orange), Cluster 2B = deglaciation assemblage (red) and Cluster 3 = Holocene Climatic Optimum assemblage (green)

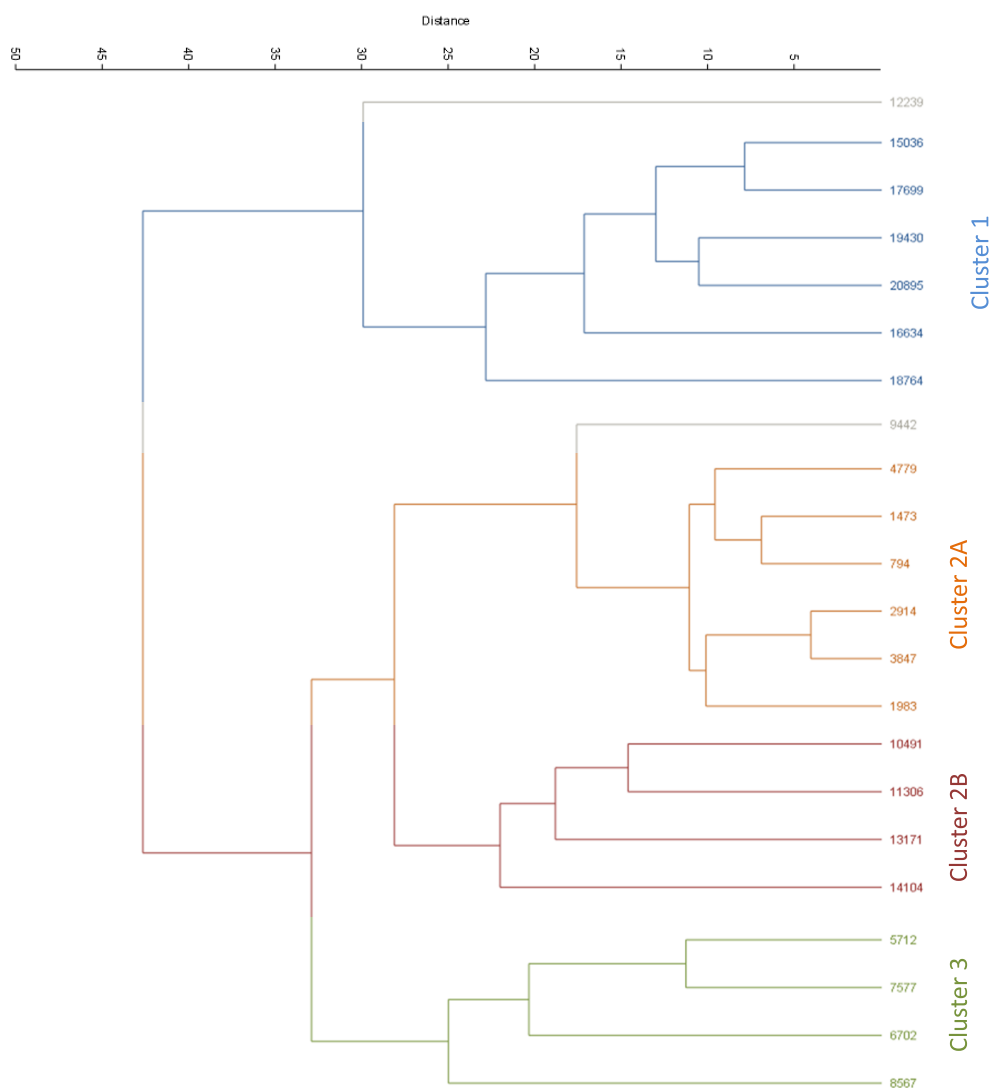


Figure 6.6: Dendrogram resulting from Q-mode cluster analysis and the clusters identified in core 964A. On the right hand side, the relevant clusters have been identified and colour coded; Cluster 1 = glacial assemblage (blue), Cluster 2A = modern assemblage (orange), Cluster 2B = deglaciation assemblage (red) and Cluster 3 = Holocene Climatic Optimum assemblage (green).

| Cluster   | ODP 964A<br>(Cal BP) | ODP 969A<br>(Cal BP) | Assemblage                |
|-----------|----------------------|----------------------|---------------------------|
| <b>1</b>  | ~ 21,000 – 15,000    | ~ 19,000 – 15,500    | Glacial                   |
| <b>2A</b> | ~ 5,000 - Present    | ~ 5,000 - Present    | Modern                    |
| <b>2B</b> | ~ 14,000 – 10,500    | ~ 15,000 – 10,500    | Deglaciation              |
| <b>3</b>  | ~ 8,500 – 5,500      | ~ 9,000 – 5,000      | Holocene Climatic Optimum |

Table 6.4: Inferred age range of each cluster in both cores 969A and 964A. Figures 6.3 and 6.4 illustrate the position of each cluster within the individual core.

| Cluster   | Dominant Species   |  |
|-----------|--|--|
|           | ODP 964A   | ODP 969A   |
| <b>1</b>  | <i>G. ruber alba</i> (35%); <i>N. incompta</i> (30%); <i>G. bulloides</i> (15%); <i>G. scitula</i> (15%); <i>G. glutinata</i> (10%)        | <i>N. incompta</i> (30%); <i>G. ruber alba</i> (30%); <i>G. bulloides</i> (15%); <i>G. glutinata</i> (15%); <i>G. scitula</i> (10%)    |
| <b>2A</b> | <i>G. ruber alba</i> (60%); SPRUDTS-group (25%); <i>G. bulloides</i> (10%)   | <i>G. ruber alba</i> (60%); SPRUDTS-group (20%); <i>G. bulloides</i> (15%)   |
| <b>2B</b> | <i>G. ruber alba</i> (50%); <i>G. bulloides</i> (15%); <i>G. inflata</i> (12%); <i>G. glutinata</i> (10%); <i>G. truncatulinoides</i> (7%) | <i>G. ruber alba</i> (45%); <i>G. truncatulinoides</i> (15%); <i>G. bulloides</i> (12%); <i>G. inflata</i> (12%)                       |
| <b>3</b>  | <i>G. ruber alba</i> (37%); <i>G. siphonifera</i> (10%); <i>G. sacculifer</i> (9%); <i>G. bulloides</i> (10%)                              | <i>G. ruber alba</i> (30%); <i>G. siphonifera</i> (11%); <i>G. bulloides</i> (11%); <i>G. glutinata</i> (10%); <i>G. sacculifer</i> 8% |

Table 6.5: This table highlights the dominant species and relative abundance within the faunal assemblages of the individual clusters.

#### 6.4.1.1 Cluster 1 (Glacial Assemblage)

Cluster 1 contains samples from the lower part of the cores corresponding to Late Pleistocene glacial conditions (figure 6.3 and 6.4). As expected the faunal assemblage is dominated by species with preferences for colder SSTs e.g. *N. incompta* (~ 30%) and *G. scitula* (~ 10-15%) (Thunell, 1978; Hayes et al., 1999; Geraga et al., 2005; Darling, et al., 2006). This correlates well with the SST reconstruction indicating relatively low annual SSTs of between 17°C (ODP 969A) and 18°C (ODP 964A) (figures 6.3 and 6.4). The concurrent occurrence of *G. ruber alba* (~ 30-35%), *G. glutinata* (~ 10-15%) and *G. bulloides* (~ 15%) suggests the cooler surface waters were also well stratified and rich in nutrients (Bé and Tolderlund 1971; Lourens et al., 1994; Pujol and Vergnaud Grazzini 1995).

#### 6.4.1.2 Cluster 2 (*Deglaciation (2B) and Modern Day Assemblages (2A)*)

Cluster 2 is subdivided into 2A and 2B. Cluster 2A is dominated by *G. ruber alba* (~ 60%), a shallow dwelling species that prefers well stratified waters (Pujol and Vergnaud-Grazzini, 1995) (figures 6.3 and 6.4). Species of the SPRUDTS-group, particularly *G. siphonifera* (~ 12%) and *G. sacculifer* (~ 8%) are also present whilst similar percentages of *G. bulloides* (~ 12%) are also observed. Several members of the SPRUDTS-group have optimum temperatures of 20°C or higher and as such would be considered a warm water indicator especially when considered in conjunction with *G. ruber alba* (Tolderlund and Bé, 1971; Thunell, 1978; Rohling et al., 1993; Pujol and Vergnaud-Grazzini, 1995). Indeed SSTs associated with Cluster 2A record temperatures in excess of 20°C (figures 6.3 and 6.4). Cluster 2A appears to be representative of warm oligotrophic surface waters such as those occurring in the modern day water column (Berman et al., 1984; Sarmiento et al., 1988; Yacobi et al., 1995). Cluster 2B highlights assemblages that are indicative of deglaciation, encompassing both the Bølling-Allerød and the Younger Dryas. The Bølling-Allerød interstadial represents a warm, moist climatic period that occurred during the final stages of the last glacial cycle. In contrast, the Younger Dryas records a short lived return to glacial conditions before the onset of the current interglacial. Faunal assemblages are similar to those observed in Cluster 2A however, notable differences include the presence of both *G. truncatulinoides* (dextral and sinistral) and *G. inflata*. Comparatively *G. truncatulinoides* occurs in low frequencies (~ 7-15%) and is representative of vertical mixing during the winter likely associated with the reproductive phase of their life cycle (Pujol and Vergnaud-Grazzini, 1995). Similarly *G. inflata* also prefers a cool, deep mixed layer such as those prevailing in the winter however, the presence of this species appears to coincide with the path of Modified Atlantic Waters suggesting an intrusion of these waters into the eastern basin possibly during the Termination 1A event (Pujol and Vergnaud-Grazzini, 1995; Ariztegui et al., 2000). ODP 964A clearly indicates the occurrence of the Younger Dryas with temporary increases in cold water indicator species *N. incompta*, *G. bulloides* and *T. quinqueloba*. This is corroborated by a marked reduction in both *G. ruber alba* and *G. ruber rosea* and the SST record (figures 6.3 and 6.4).

### 6.4.1.3 Cluster 3 (*Holocene Climatic Optimum*)

Cluster 3 includes samples that were deposited during the latter part of S1. In both cores it is important to note that depositional onset of S1 occurs between approximately 10 and 10.4 kyr (figures 6.3 and 6.4). Rohling (2015) noted that the onset of S1 tended to occur earlier (~10.5 kyr) in more oceanic sites compared to the Adriatic and Aegean Seas which lag by approximately 500 years. Indeed, a study by Capotondi et al. (2011) highlights the deposition of S1 between 9.8 and 5.9 kyr from a core in the Ionian Sea showing strong similarities with the cores used in this research. The faunal assemblage varies within this cluster. Older samples associated with S1 are dominated by *G. ruber* (*alba* and *rosea*), some members of the SPRUDTS-group (*G. siphonifera* and *G. tenella*) and *G. bulloides*. Such an assemblage would be indicative of warm stratified surface waters with lenses of low salinity. Peak occurrences of *G. bulloides* would suggest an increase in nutrient availability associated with a more eutrophic water column (Capotondi et al., 2011). It is suggested that the increased nutrients are as a result of increased river discharge rather than local upwelling (Tanhua et al., 2013; Toucanne et al., 2015). Beyond the termination of S1 the faunal assemblage records increased frequencies of *G. inflata* and *N. incompta* indicating a significant change in the upper water column. The rapid and temporal increase of these species is widely documented within the eastern Mediterranean and is attributed to a return to cooler, well ventilated, nutrient rich conditions following the water column stratification that dominated during sapropel deposition (Geraga, 2000, 2005; Casford, 2002; Principato, 2003). A small but significant decline in annual SSTs corroborates this (figures 6.3 and 6.4).

### 6.4.2 PRINCIPAL COMPONENT ANALYSIS

A standardised Principal Component Analysis (PCA) was performed on each core to determine which environmental variables influenced the distribution of planktonic foraminifera. This process would also examine similarities between both cores and other cores from the wider eastern basin. Tables 6.6 and 6.7 illustrate the results from the PCA. The first component is primarily considered as this accounts for 67.485% and 65.481% of the total variance for ODP cores 969A and 964A respectively.

| PC | Eigenvalue | % variance | Cumulative % of total Variance |
|----|------------|------------|--------------------------------|
| 1  | 311.012    | 67.485     | 67.485                         |
| 2  | 72.2803    | 15.684     | 83.169                         |
| 3  | 26.0622    | 5.6551     | 88.824                         |
| 4  | 20.6331    | 4.477      | 93.301                         |
| 5  | 12.1211    | 2.6301     | 95.931                         |
| 6  | 8.49293    | 1.8428     | 97.774                         |
| 7  | 3.2394     | 0.7029     | 98.477                         |
| 8  | 2.1281     | 0.46176    | 98.939                         |
| 9  | 1.96772    | 0.42696    | 99.366                         |
| 10 | 0.999269   | 0.21683    | 99.582                         |
| 11 | 0.922154   | 0.20009    | 99.783                         |
| 12 | 0.589446   | 0.1279     | 99.910                         |
| 13 | 0.293964   | 0.063785   | 99.974                         |
| 14 | 0.0949934  | 0.020612   | 99.995                         |
| 15 | 0.0271886  | 0.0058995  | 100.001                        |

Table 6.6: PCA factors and their percentages of the total variability for core 969A (Levantine basin).

| PC | Eigenvalue | % variance | Cumulative % of total Variance |
|----|------------|------------|--------------------------------|
| 1  | 420.164    | 65.481     | 65.481                         |
| 2  | 115.429    | 17.989     | 83.470                         |
| 3  | 34.643     | 5.399      | 88.869                         |
| 4  | 24.1028    | 3.7563     | 92.625                         |
| 5  | 16.0969    | 2.5087     | 95.134                         |
| 6  | 14.22      | 2.2161     | 97.350                         |
| 7  | 7.07904    | 1.1032     | 98.453                         |
| 8  | 4.85263    | 0.75627    | 99.210                         |
| 9  | 2.38634    | 0.3719     | 99.581                         |
| 10 | 1.16798    | 0.18203    | 99.764                         |
| 11 | 1.10051    | 0.17151    | 99.935                         |
| 12 | 0.292771   | 0.045627   | 99.981                         |
| 13 | 0.0824985  | 0.012857   | 99.993                         |
| 14 | 0.030308   | 0.0047234  | 99.998                         |
| 15 | 0.00822599 | 0.001282   | 99.999                         |

Table 6.7: PCA factors and their percentages of the total variability for core 964 (Ionian Sea).

The PCA reveals strong similarities between both cores utilised in this research. PC1 explains 67.49% (ODP 969A) and 65.48% (ODP 964A) of the total variance and shows high strong positive loadings of *N. incompta*, with weaker loadings of *G. scitula* and *G. glutinata* (table 6.8). Strong negative loadings are dominated primarily by *G. ruber alba* with weaker loadings accrued from members of the SPRUDTS-group. Initially the bipolar nature of these results appear to separate species that thrive in warm, oligotrophic waters (*G. ruber alba* and the SPRUDTS-group) from those that prefer cooler or cold conditions (*N. incompta*, *G. scitula* and *G. glutinata*) and thus may be interpreted as a temperature indicator (Thunell, 1977; Rohling, 1993; Hayes, 1999; Kontakiotis, 2015). However, it cannot be dismissed that PC1 may be a signal of nutrient availability thus reflecting the trophic status of the water column.

| 969A                           |        | 964A                           |        |
|--------------------------------|--------|--------------------------------|--------|
| Species                        | PC 1   | Species                        | PC 1   |
| <i>G. ruber (a)</i>            | -0.601 | <i>G. ruber (a)</i>            | -0.649 |
| <i>G. siphonifera</i>          | -0.155 | <i>G. siphonifera</i>          | -0.127 |
| <i>G. sacculifer</i>           | -0.110 | <i>G. sacculifer</i>           | -0.119 |
| <i>G. ruber (r)</i>            | -0.102 | <i>O. universa</i>             | -0.107 |
| <i>G. rubescens</i>            | -0.100 | <i>G. ruber (r)</i>            | -0.065 |
| <i>O. universa</i>             | -0.054 | <i>G. rubescens</i>            | -0.064 |
| <i>G. inflata</i>              | -0.037 | <i>G. truncatulinoides (d)</i> | 0.001  |
| <i>G. truncatulinoides (s)</i> | -0.010 | <i>G. truncatulinoides (s)</i> | 0.002  |
| <i>G. truncatulinoides (d)</i> | -0.006 | <i>N. pachyderma (s)</i>       | 0.012  |
| <i>G. bulloides</i>            | 0.005  | <i>G. inflata</i>              | 0.019  |
| <i>N. pachyderma (s)</i>       | 0.005  | <i>T. quinqueloba</i>          | 0.024  |
| <i>T. quinqueloba</i>          | 0.061  | <i>G. bulloides</i>            | 0.099  |
| <i>G. glutinata</i>            | 0.184  | <i>G. glutinata</i>            | 0.123  |
| <i>G. scitula</i>              | 0.299  | <i>G. scitula</i>              | 0.191  |
| <i>N. incompta</i>             | 0.671  | <i>N. incompta</i>             | 0.683  |

Table 6.8: Planktonic foraminifera rankings and factor loadings for PC1 in core 969A and 964A

In fact if the species with the strongest loadings are analysed in more detail a different picture emerges. *N. incompta* (OPD 969A – 0.651; ODP 964A – 0.683), while indicative of cool waters is also associated with an increase in nutrient availability associated with the development of a Deep Chlorophyll Maximum (DCM) at the base of

the euphotic zone (Fairbanks and Wiebe, 1980; Fairbanks et al., 1982; Reynolds and Thunell, 1986; Rohling and Geiskes, 1989). *G. ruber alba* (ODP 969A - -0.635; ODP 964A - -0.649) on the other hand prefers warmer oligotrophic waters (Pujol and Vergnaud-Grazzini, 1995) (figure 6.7). Therefore PC1 could also be considered indicative of nutrient availability within the euphotic zone.

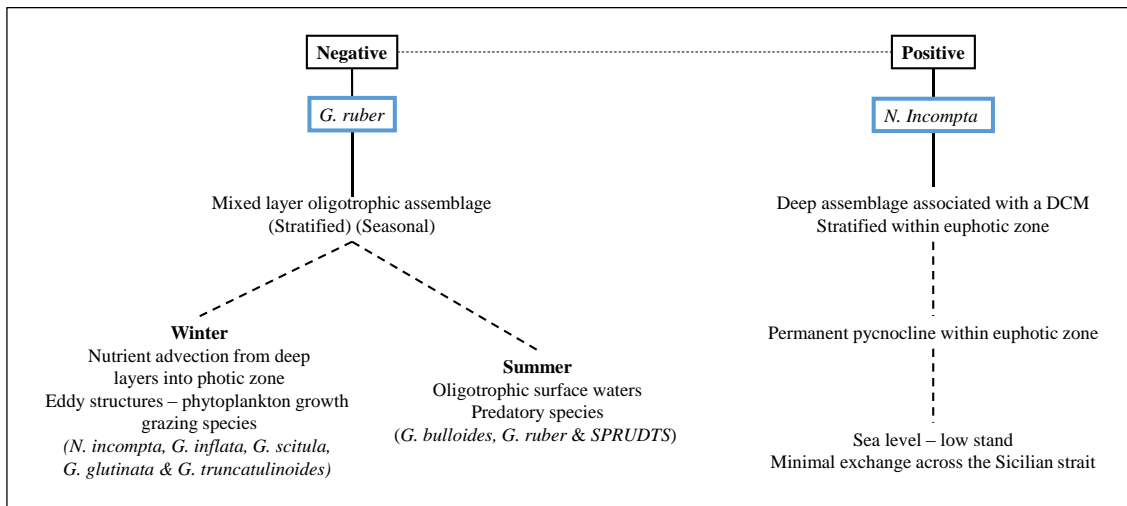


Figure 6.7: Depiction of the intricate relationship of environmental factors determining the results of the principal component analysis.

### 6.4.3 SEA SURFACE TEMPERATURES

Numerous studies have reconstructed SST change since the Last Glacial Maximum (LGM) into the Holocene Epoch (Emeis et al., 2000; Geraga et al., 2000; Hayes et al. 2005; Tzedakis, 2007). Similar trends are noted within the cores utilised in this research. As expected temperatures during the LGM were relatively cold however, SSTs during Heinrich Event 1 displayed colder temperatures with a difference of 1-2°C compared to the LGM notably 16°C (969A) and 16.5°C (964A) (figures 6.8 and 6.9). It is feasible that this decrease in SST during H1 may relate to the re-connection between both basins via the Sicilian Strait. Rising sea levels experienced at this time would have allowed cooler waters from the Atlantic Ocean to flow into the eastern basin (Benjamin et al., 2017). The coldest reported temperature is recorded in 964A during the Younger Dryas at 13.5°C, something that is not seen in core 969A. Higher annual SSTs (20°C) are recorded at the onset of S1 were they remain fairly stable resembling modern day conditions (figures 6.8 and 6.9).

## 6.5: DISCUSSION

### 6.5.1 PALAEOENVIRONMENTAL RECONSTRUCTION

A combination of multivariate statistical methods and micropalaeontological analyses reveal palaeoenvironmental variations throughout four distinct timeframes; the Late Glacial (~21,000 – 15,000 cal yrs BP), deglaciation (~15,000 – 10,500 cal yrs BP), the Holocene Climatic Optimum (~9,000 – 5,000 cal yrs BP) and the late Holocene (~5,000 to present) with the results summarised in figures 6.8 and 6.9. Taking into account the errors associated with ANN and the low sampling resolution of the studied cores (see chapter 5 section 2) it is important to note that only multi-decadal events have been identified. As such significant events such as the 8.2 kyr event (~150 yrs in duration) were not recorded in these cores.

### 6.5.2. THE LATE GLACIAL (~21,000 – 15,000 CAL YRS BP)

The Late Glacial period within these cores encompasses the latter part of the LGM (26.5 to 19 ka BP) (Clark et al., 2009) and Heinrich Event 1 (H1) (18 to 15 ka BP) (Alvarez-Solas et al., 2011). The faunal assemblage is dominated by *N. incompta* and *G. ruber alba* with *G. bulloides*, *G. glutinata*, *G. scitula*, and *T. quinqueloba* comprising the remainder. In corroboration with relatively low SSTs, PCA and high E-Index values (figures 6.8 and 6.9) the faunal assemblage is indicative of cool, well stratified nutrient rich waters (Rohling et al., 1993a; Pujol and Vergnaud-Grazzini, 1995).

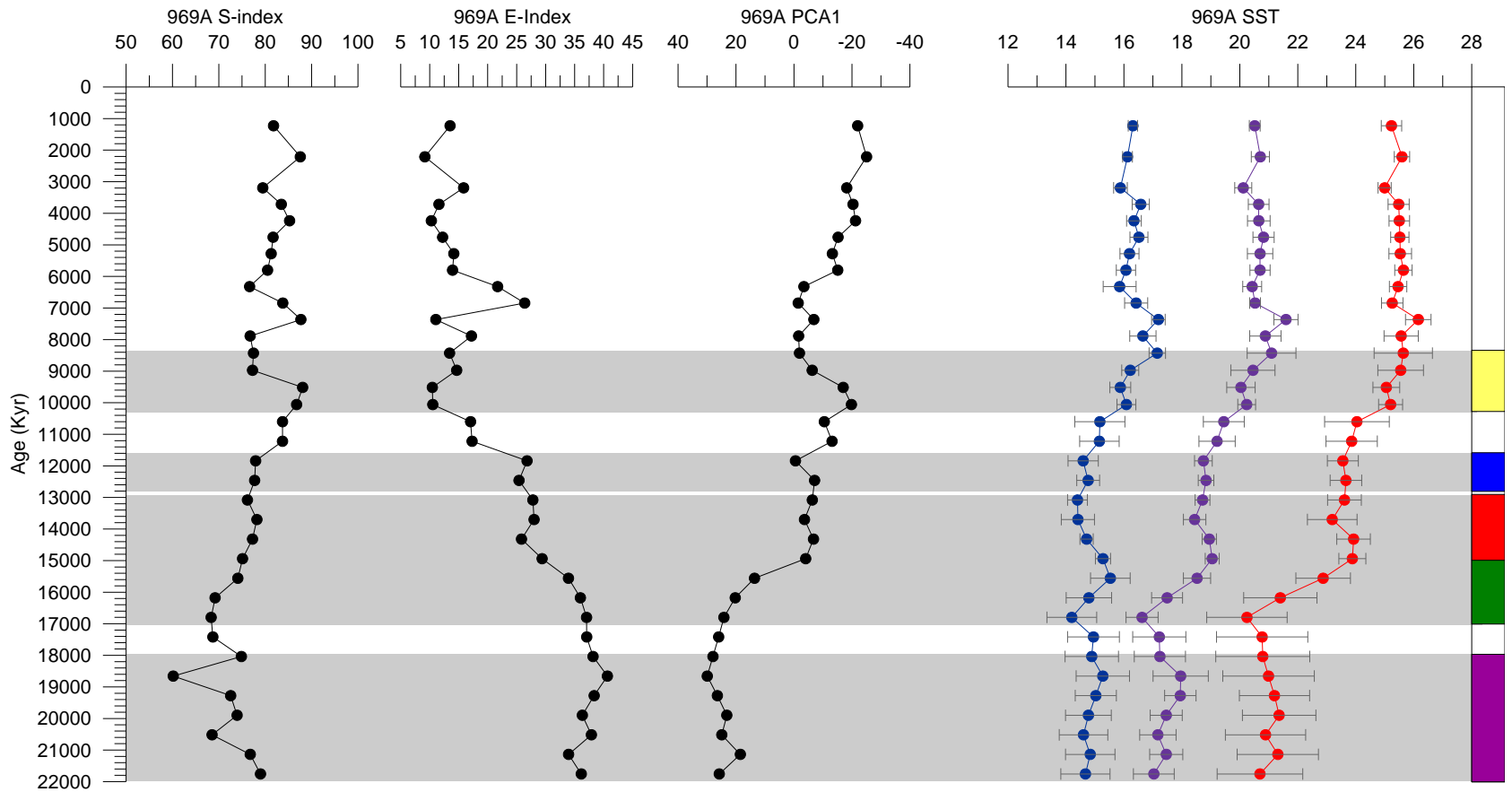


Figure 6.8: Comparison between down-core score plots of the factors revealed from PCA analysis, micropalaeontological indexes and ANNs for core 969A. Indexes include *G. bulloides*/*G. ruber* ratio (S-index), Eutrophication index (E-index), PC1 (Principal component scores), Sea Surface Temperature (constructed from ANNs), SSTs for winter (blue), annual (purple) and summer (red), shaded purple area is the Last Glacial maximum (LGM), green relates to Heinrich Event 1, red area refers to the Bølling-Allerød, Shaded blue area relates to the Younger Dryas and Shaded yellow area represents Sapropel S1.

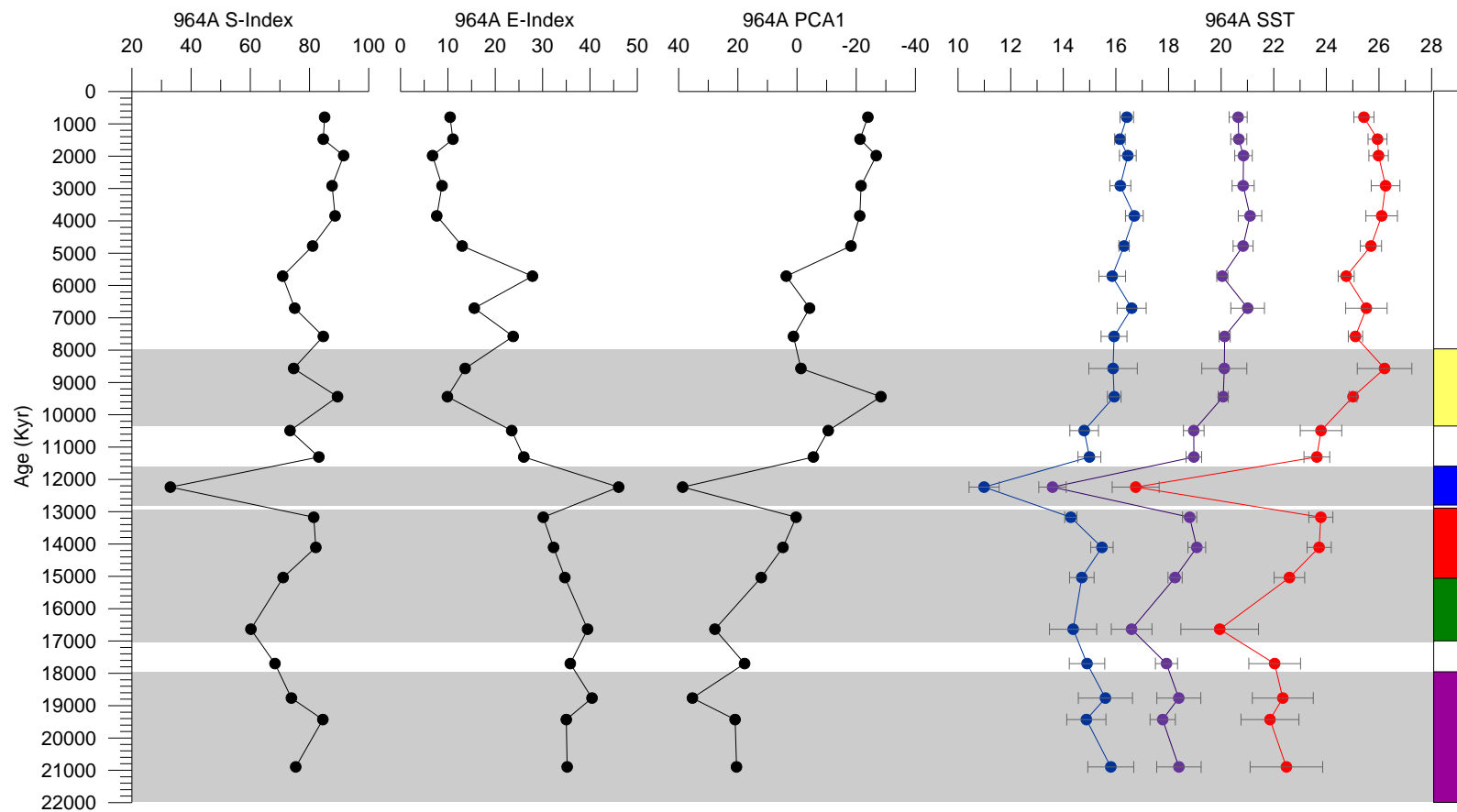


Figure 6.9: Comparison between down-core score plots of the factors revealed from micropalaeontological indexes, PCA analysis, and ANNs for core 964A. Indexes include *G. bulloides/G. ruber* ratio (S-index), Eutrophication index (E-index), PC1 (Principal component scores), Sea Surface Temperature (constructed from ANNs), SSTs for winter (blue), annual (purple) and summer (red), shaded purple area is the Last Glacial maximum (LGM), green relates to Heinrich Event 1, red area refers to the Bølling-Allerød, Shaded blue area relates to the Younger Dryas and Shaded yellow area represents Sapropel S1

In modern day assemblages *N. incompta* has been recorded from subpolar to tropical regions however, it is known to become prevalent in the faunal assemblage when SSTs fall below 12°C (Bé and Tolderlund, 1971). Furthermore a strong relationship is known to exist between the formation of a DCM at the base of the thermocline and peak occurrences of *N. incompta*, implying a preference for deeper (~ 200 m) waters (Fairbanks and Wiebe, 1980; Fairbanks et al., 1982; Reynolds and Thunell, 1986; Rohling and Gieskes, 1989; Rohling et al., 1995). The development of a DCM occurs when the pycnocline lies close to the base of the euphotic zone, due to changes within the water column the shoaling of the pycnocline to within the euphotic zone causes the development of the DCM which appears between the pycnocline and the base of the euphotic zone (Rohling and Gieskes, 1989). Its preference for nutrient rich deep waters would suggest that populations of *N. incompta* are not affected by SST increases provided the DCM remains intact (Pujol and Vergnaud-Grazzini, 1995). This is demonstrated by the differing populations in both the western and eastern basins of the Mediterranean Sea. The species dominates the faunal assemblages (both surface and at depth) in the Gulf of Lions and the Balearic Basin (~ 74%) however, these peak occurrences are likely due to the combination of both low SSTs and high nutrient levels (Pujol and Vergnaud-Grazzini, 1995). In contrast higher annual SSTs in the eastern basin would suggest that *N. incompta* is only present below the thermocline where temperatures are cooler. Using PC1 as an indicator of trophic status, the late glacial records the highest positive loadings as determined by *N. incompta* (Table 6.8 and figures 6.8 and 6.9). As annual SSTs throughout this timeframe are above 12°C it is assumed that the presence of *N. incompta* is associated with the formation of a DCM at the base of the thermocline. Figures 6.8 and 6.9 show this remains the case until approximately 15,000 yrs BP indicating a potentially permanent pycnocline and associated DCM within the euphotic zone. Rohling and Gieskes (1989) proposed that during glacial periods lower sea levels caused a reduction in water exchange at the Sicilian Strait. The subsequent shoaling of the pycnocline was due to the increase in SST gradients between the two basins.

Although this period is characterised by cooler temperatures, *G. ruber*, a warm water species, still constitutes approximately 30% of the faunal assemblage (figures 6.3 and 6.4). This species has a temperature tolerance of between 13.3 and 29.5°C with greatest frequencies being achieved at optimum temperatures of ~ 21°C (Tolderlund and Bé,

1971). With annual SSTs of  $\sim 17^{\circ}\text{C}$  at this time, the presence of *G. ruber alba* would not be uncommon particularly in lower abundances.

During the latter part of the LGM annual SSTs are recorded at approximately  $17^{\circ}\text{C}$  after which a general increase is apparent. A notable exception is the cold episode observed at approximately 17,000 cal yrs where SSTs reach their lowest ( $\sim 16.5^{\circ}\text{C}$ ) (in ODP 969A). Similarly low SSTs have been observed within the same timeframe from both the western (Cacho et al., 1999; Melki et al., 2009) and eastern (Geraga et al., 2005; Rouis-Zorgourni et al., 2009) basins corresponding to H1. It is generally well documented, particularly in the North Atlantic, that faunal assemblages often record elevated frequencies of *N. pachyderma* (s) during these cold Heinrich Events (Pérez-Folgado et al., 2003; Sierro et al., 2005). Similar faunal signals have also been noted in cores from the Alboran Sea (Cacho et al., 1999; Perez-Folgado et al., 2003), the Balearic basin (Frigola et al., 2008) and the Gulf of Lions (Melki et al., 2009) where small, but significant, frequencies of *N. pachyderma* (s) have been recorded (5-10% of the faunal assemblage). In contrast, while a decrease in SSTs has been noted in cores from the eastern basin, *N. pachyderma* (s) is virtually absent from the faunal assemblages during the Heinrich Events, synonymous with this research (Geraga et al., 2005). Geraga et al. (2005) suggest that the lack of *N. pachyderma* (s) is as a result of annual SSTs being too high, stating that the species only occurs when annual SSTs fall below  $7^{\circ}\text{C}$ . While this is true to some extent, the presence of *N. pachyderma* (s) is known to be significant in faunal assemblages if year round SSTs remain below  $17^{\circ}\text{C}$ , particularly in regions of high nutrient availability (Giraudeau, 1993). Based on the data obtained from this research, while the trophic conditions at this time do not appear to be the limiting factor, annual SSTs do not remain below  $17^{\circ}\text{C}$  rendering conditions unsuitable for *N. pachyderma* (s) (figures 6.8 and 6.9). Other research from both terrestrial and marine sources within the eastern Mediterranean region (Tierney et al., 2008; Castañeda et al., 2010) have indicated warming trends following the LGM. In particular Castañeda et al (2010) observed evidence of strong warming after the LGM and prior to H1 using alkenones as a proxy. In contrast to this, SST records from the western basin fail to highlight the same trends during this time period (Cacho et al., 1999; Melki et al. 2009) and it has been suggested that both basins responded differently to the deglaciation process (Castañeda et al., 2010).

### 6.5.3 DEGLACIATION (~15,000 – 10,500 CAL YRS BP)

The onset of deglaciation coincides with a notable increase in SST (figures 6.8 and 6.9). Consistent with other records from the eastern basin this increase determines the beginning of the Bølling-Allerød (Asioli et al., 2001; Kontakiotis, 2015). The change in climate is reflected in the faunal assemblage whereby notable decreases in the cold water species (e.g. *G. scitula*) is concurrent with maximum frequencies of *G. ruber* and the appearance of *G. inflata* and *G. truncatulinoides*. *G. bulloides* and *G. glutinata*, make up the remainder of the assemblage. Collectively these species are indicative of seasonal mixing within the water column and enhanced nutrient availability. The simultaneous strengthening of water column stratification (as determined by the S-Index) suggests a seasonality between summer stratification (dominated by *G. ruber*) and winter mixing (dominated by *G. bulloides*, *G. inflata* and *G. truncatulinoides*). Similar faunal sequences have been recorded in the Tyrrhenian Sea (Capotondi, 1995) the Adriatic Sea (Asioli et al., 2001) and the Aegean Sea (Kothoff et al., 2011; Kontakiotis, 2015). While increased vertical convection will enhance primary productivity, Kontakiotis (2015) suggests that the input of terrestrial material, due to rapid sea level rise and increased riverine discharge, also contribute to the influx of nutrients at this time. Additionally an influx of freshwater into the basin will create an increase in the density gradient potentially explaining the development of seasonal stratification (Kontakiotis, 2015).

The onset of the Younger Dryas at ~ 12.9 kyr is well documented from sediment cores across both basins within the Mediterranean Sea (e.g. Capotondi, 1995; Pérez-Folgado et al., 2003; Geraga et al., 2005; Frigola et al., 2008; Melki et al., 2009; Kontakiotis, 2015). However, in this research the event only seems to be recorded in core 964A (Ionian Sea) (figures 6.8 and 6.9). The brief return to glacial conditions is illustrated by an abrupt SST decrease (~ 5°C) which is reflected in the temporary increase in cold water species, particularly *G. scitula* and *N. incompta* (figure 6.3). Water column dynamics during this time display a weakened stratification corresponding to elevated frequencies of *G. bulloides* (an upwelling indicator). Concomitant high E-Index values strengthens the case for strong vertical mixing and subsequent eutrophication (Kontakiotis, 2015). Other research within the Mediterranean Sea have recorded the presence of the Younger Dryas as two distinct phases (Cacho et al., 2001; Geraga et al.,

2008, 2010; Kontakiotis, 2015). However, this is not evident in core 964A, possibly due to the low sampling resolution.

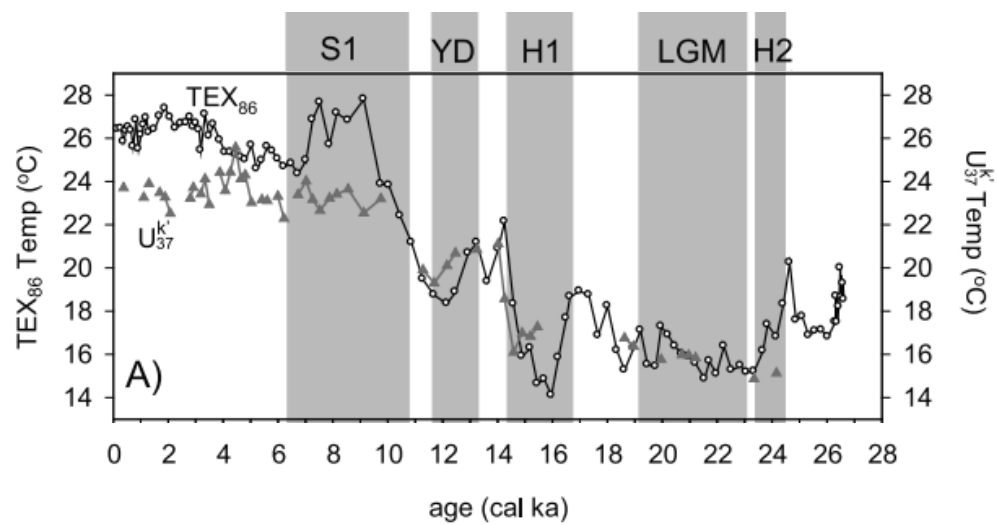


Figure 6.10: Comparable results of TEX<sub>86</sub> (based on glycerol dialkyl glycerol tetraethers) and  $U^{k'_{37}}$  (based on the ratio of long-chain diunsaturated and triunsaturated ketones produced by haptophyte algae) reconstructed SSTs based on core GEOB7702-3 collected off the Israeli coast. The calibration of Kim et al. [2008] was applied for TEX<sub>86</sub>, while the calibration of Conte et al. [2006] was used for  $U^{k'_{37}}$  (courtesy of Castañeda et al., 2010).

Within the western basin the Younger Dryas represented lower oxygenation and improved productivity which corresponded with maximum intensity of LIW flow within the central Mediterranean however, data from the western basin suggests that there was a marked difference between the eastern and western basins and that the eastern Mediterranean was more prone to alterations within the water column than seen within the western Mediterranean (Jiménez-Espejo et al., 2015).

#### 6.5.4 HOLOCENE CLIMATIC OPTIMUM

Broadly associated with the deposition of sapropel S1, the Holocene Climatic Optimum (HCO) covers the period between 10 – 6 ka BP. The onset of sapropel deposition is marked by the disappearance of *G. inflata* and *N. incompta* and subsequent increases in shallow mixed layer species such as *G. ruber* (particularly *G. ruber rosea*) and members of the SPRUDTS-group (figures 6.3 and 6.4). The presence of *G. ruber rosea* is significant of maximum warming which is further corroborated by elevated SSTs and (figures 6.8 and 6.9). However, the reconstructed SSTs recorded in this research are 2-

3°C higher than those estimated in studies undertaken by Giunta et al. (2001) and Emeis et al. (2000b). Despite these differences elevated SSTs can induce stratification within the water column due to the development of a strong thermocline. Indeed this is corroborated by a strengthened S-Index at this time (figures 6.8 and 6.9). Furthermore a significant decrease in the calcareous nannofossil species *Reticulofenestra* spp., (an upwelling indicator) was recorded by Principato et al. (2003) at this time. The reappearance of *G. inflata* and *N. incompta* signifies the return to a homothermal water column induced by vertical mixing and an end to the stratification and anoxia that defined the sapropel.

A review of the E-Index during this time displays an apparent decrease in primary productivity (figures 6.8 and 6.9). It is well documented that sapropel deposition is associated with nutrient enhancement in surface waters due to freshwater inputs (Rohling et al., 2015; Simon et al., 2017; Tesi et al., 2017). It is probable that the signal is driven by the dominance of *G. ruber* (*alba* and *rosea*) and to a lesser extent *O. universa* and *G. siphonifera*, species indicative of oligotrophic conditions. These species are also known to tolerate a wide range of salinities particularly *G. ruber*, and therefore would be expected to inhabit the surface waters at this time hence skewing the E-Index values throughout the deposition of the sapropel (Kontakiotis et al., 2011).

#### 6.5.6 MODERN DAY (~5,000 – PRESENT CAL YRS BP)

The period from 5 ka BP to the present day would be representative of current conditions in the eastern Mediterranean Sea. SSTs have remained relatively stable (winter - 16°C; summer 25°C) and faunal assemblages are dominated by *G. ruber* (*alba*) (60%), *G. bulloides* (12%) *G. siphonifera* (8%) and *G. sacculifer* (6%). Examination of the indexes shows a strongly stratified (high S-Index), oligotrophic (low E-Index) water column. The current distribution of planktonic foraminifera as investigated by Pujol and Vergnaud Grazzini (1995), showed a dispersal pattern related to the productivity models as controlled by hydrographical systems. *G. ruber* (*alba* and *rosea*) are shown to be the dominant species within assemblages during the late summer particularly within the eastern basin.

Overall nutrient availability is the limiting factor within the eastern basin of the Mediterranean, so in general a low availability of food will inhibit the growth of phytoplankton, with an average assemblage being dominated by oligotrophic species. When nutrients are available (as they are in the Ionian Sea during the winter at present) then hydrographic structures become of secondary importance with the development and distribution of assemblages (Pujol and Vergnaud-Grazzini, 1995).

## 6.6: CONCLUSIONS

Gravity cores collected from the Ionian Sea (ODP 964A) and along the Mediterranean Ridge (ODP 969A), were used to examine the variability in the relative abundance of planktonic foraminifera. The use of micropalaeontological data along with multivariate statistical analysis has allowed us to elucidate the palaeoenvironmental variability of the studied area since the LGM. Despite the low sampling resolution, distinct climatic phases can be identified in both cores facilitating comparisons with other studies, particularly in the Adriatic and Aegean Seas but also with other open ocean sites such as the Ionian Sea and Levantine Basin.

During the LGM northern hemisphere ice sheets had reached their maximum southerly extent and global sea levels were approximately 120m lower than they are today. In correlation with similar studies this period was dominated by low SSTs with water column dynamics displaying homogeneity facilitating high levels of primary productivity. The subsequent period of deglaciation reflects a time of instability within the basin. Incorporating the climate amelioration associated with the Bølling-Allerød and the subsequent climate deterioration of the Younger Dryas, hydrographic patterns within the basin are subjected to significant changes. During the warmer more humid interval of the Bølling-Allerød conditions within the water column display a strong seasonality with vertical mixing prevalent during the winter contrasting with summer stratification. The onset of the Younger Dryas marks a temporary return to glacial conditions and, similar to the LGM, the hydrological regime displays strong vertical convection accompanied by enhanced eutrophication. The termination of the Younger Dryas is expressed by an abrupt increase in SSTs before the onset of sapropel deposition. Coinciding with the HCO the deposition of sapropel S1 is associated with subtropical humid conditions and a return to water column stratification. This

depositional phase is somewhat unique in that while water column stratification usually favours oligotrophic conditions, high primary productivity levels are prevalent at this time, probably as a result of enhanced riverine input into the surface waters. Shortly after the termination of the sapropel S1 SSTs remain consistently high maintaining water column stratification due to the presence of a well-developed thermocline. The resultant oligotrophic surface waters would be representative of present day conditions in the eastern basin highlighting nutrient availability as the dominant limiting factor in the distribution of planktonic foraminifera. Indeed the overall impression of the faunal record clearly indicates a gradual SST warming concomitant with a reduction in levels of eutrophication over the last 22 kyr.

## CHAPTER 7

# DOES SIZE MATTER? TEST SIZE VARIABILITY OF PLANKTONIC FORAMINIFERA IN RESPONSE TO BIOTIC/ABIOTIC FACTORS DURING THE DEPOSITION OF SAPROPEL S3 AND S5. A CASE STUDY FROM THE MEDITERRANEAN RIDGE (ODP CORE 969A)

### 7.1: INTRODUCTION

Chapter 4 highlights the main factors that control the distribution of planktonic foraminifera but what about how these organisms react to changing environmental conditions? Each species has a well-recognised stratigraphic range and palaeogeographic distribution that allows for the optimum growth of each organism. Every species has a set of environmental conditions which lead to an optimal growth rate allowing for faster growth rates and an increase in both test and assemblage size. (Hecht, 1976; Schmidt et al., 2004). Conversely when these ideal environmental parameters are not reached a decline or complete halt in growth/reproduction rates will be observed. Increasing or decreasing temperatures outside of the optimum will directly affect the maximum size of foraminiferal growth and so correlations between positive/negative growth and temperature is possible within a species. Species such as *N. incompta*, *G. bulloides*, *G. ruber*, *G. sacculifer* and *O. universa* have had the same temperature adaptation over the past 300 kyr as they do today and so their environmental optima can be used to distinguish any environmental changes within recent geological past (Schmidt et al., 2008). Furthermore increases within temperatures ranges have been shown to directly affect the cell physiology of foraminifera, for example increases in temperature by 10°C has been shown to accelerate cell physiology by as much as double (Caron et al., 1987a, 1987b; Bijma et al., 1990; Spero et al., 1991). While temperature can have a direct effect on the size of a species indirect changes within the water column can also have significant consequences on species size. For example water column stratification, induced by a strong thermocline, creates

larger and more defined vertical temperature gradients and subsequent ecological niches. Such niches create a decrease in species competition and those within their optimum environment can reach larger growth sizes (Schmidt et al., 2004a).

Bé and Duplessy (1976) reviewed the test size of *O. universa* within the Indian Ocean and found that the diameter size of this species is directly related to shifts within the location of the subtropical convergence zone and so is directly related to temperature. This direct comparison of test size allowed for the development of this species as an indicator of changing hydrographic conditions and in doing so allowed for the understanding of the displacement of the subtropical convergence zone. They found that assemblages with the largest size were located within tropical/subtropical regions, medium sized shells within the mid-latitudes and smaller shells in the lower latitudes. Similarly Kaiho et al. (2006) looked at foraminifera test size, this time examining the changes associated with a global warming event at the Palaeocene-Eocene boundary (PETM). The authors noted an increase in the maximum test size for the mixed-layer planktonic foraminiferal species while deep-water benthic species saw a reduction within their test size. The decreased test sized was indicated to be related to the reduction in dissolved oxygen levels while increases within the surface layer species correlated to increasing thermal stratification and an ensuing increase of nutrients.

Further aspects of the marine environment can also affect the size of foraminifera such as water turbulence in zones of upwelling and frontal systems. Enhanced primary productivity and a potential reduction in oxygen levels may lead to a decline in foraminiferal respiration and a subsequent restriction in growth (Schmidt et al. 2008). Biotic features can also be a factor when discussing the changes within test size of any foraminiferal species. Factors such as high productivity rates lead to high oxygen consumption and in turn creates an oxygen deficiency allowing for a reduction within foraminiferal respiration and creating a reduced growth rate setting. Biotic factors are known to control species diversity and many palaeo/ecologists have sought out reasoning for the dispersal of species. Diversity of species relates to the influx of change within species by immigration or increasing abundances. These new species within a new location can be a source of enhanced nutrients of existing species and so aid in the growth of a species (Mohd et al., 2017). These biotic factors can include but are not limited to spatial heterogeneity, competition, predation and productivity (Pianka, 1966; Mohd et al., 2017).

Eastern Mediterranean sapropels have been the subject of much research particularly those deposited in the Late Quaternary Period. The cause of these deposits have instigated a plethora of research focusing on geochemical analysis (de Lange and Nijenhuis, 2000; Jiang et al., 2012; Liu et al., 2012) and the distinctive changes within faunal assemblages, both benthic (Corliss and Nolet, 1990; Jorissen, 1999; Morigi, 2009) and planktonic (Bernasconi and Pika-Biolzi 2000; Capotondi et al., 2006; Corselli et al. 2002) foraminifera. Based on our knowledge of abiotic and biotic factors influencing the growth of foraminifera, this research intends to investigate the size variation in species specific planktonic foraminifera throughout the deposition of sapropels S3 and S5. Sapropels are unique depositional environments associated with bottom water anoxia and elevated levels of primary productivity in surface waters (Toggweiler et al. 1988; Gallego-Torres et al. 2007). It is the intention of this research to provide detailed records of planktonic foraminiferal size variations to aid in the interpretation of the palaeoecological conditions associated with sapropel formation.

## 7.2: MATERIALS AND METHODS

A total of three species were utilised for the purpose of this research. Each species of planktonic foraminifera within the marine environment is unique and although many belong to the same family, their needs and development are very much individual to the individual species (table 7.1).

| <b>Classification</b> | <b>Species 1</b>         | <b>Species 2</b>                  | <b>Species 3</b>                 |
|-----------------------|--------------------------|-----------------------------------|----------------------------------|
| <b>Kingdom</b>        | Protozoa                 | Protozoa                          | Protozoa                         |
| <b>Phylum</b>         | Protozoa                 | Protozoa                          | Protozoa                         |
| <b>Class</b>          | Granuloreticulosea       | Granuloreticulosea                | Granuloreticulosea               |
| <b>Order</b>          | Foraminiferda            | Foraminiferda                     | Foraminiferda                    |
| <b>Family</b>         | Globigerinidae           | Globigerinidae                    | Globorotalidae                   |
| <b>Genus</b>          | Orbulina                 | Globigerinella                    | Neogloboquadrina                 |
| <b>Species</b>        | <i>Orbulina universa</i> | <i>Globigerinella siphonifera</i> | <i>Neogloboquadrina incompta</i> |

Table 7.1: Classification of chosen species within the Protozoa Kingdom

The species on which the data is based, were selected using a number of different criteria, firstly the availability and preservation within the sedimentary sequence. It was

also necessary to ensure that each species was the only genetic morphotype of that species within the Mediterranean Sea. Finally each species could be distinguished by different depth habitats within the water column. With these criteria in mind three species were chosen: (i) *Orbulina universa*, (ii) *Globigerinella siphonifera* and (iii) *Neogloboquadrina incompta* (figure 7.1). All samples were extracted from the > 150µm size fraction as this allowed for optimum comparison between species and eliminated juvenile specimens. The sample processing details can be found outlined in chapter 5.

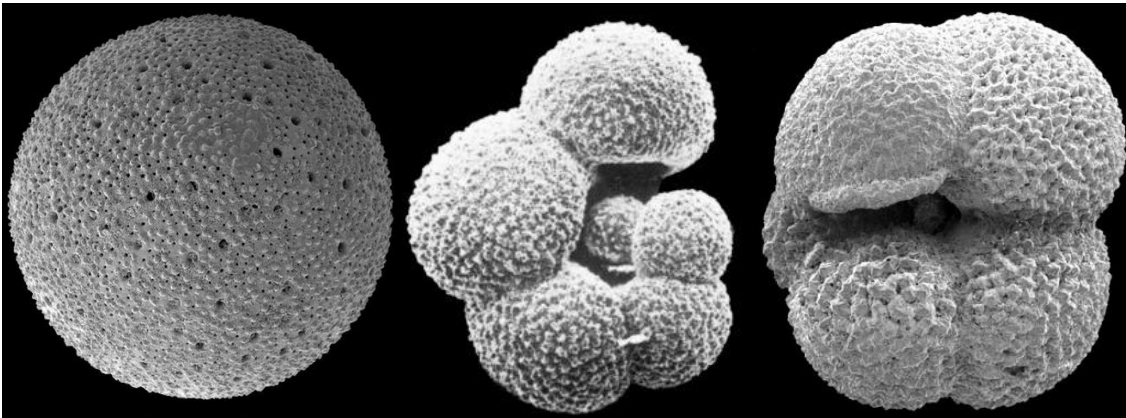


Figure 7.1: Scanning electron microscope images of the chosen species *Orbulina universa*, *Globigerinella siphonifera* and *Neogloboquadrina incompta* (courtesy of <http://www.marinespecies.org>).

*Orbulina universa* is a shallow dwelling (50 - 100m) species and is very distinctive in fossil assemblages as a single spherical chamber. It is only the spherical shell of *O. universa* that is readily preserved within the marine sediment whereas living specimens of this species are surrounded by numerous spines. Residing within the photic zone *O. universa* has a symbiotic relationship with dinoflagellates (*Gymnodinium béii*) (Spero, 1987). They are known to have a salinity range of 23 - 46‰ and an optimum of 30.5 – 31‰ (Bé and Tonderlund, 1971; Hemleben et al., 1988). Their temperature range is between ~10 – 31°C with an optimum of 13-24.5°C (Bé and Tonderlund, 1971), however this has since been updated to 24-29°C (Lombard et al., 2009). *O. universa* is a carnivorous species that preys on species such as copepods when fully matured. Hemleben et al., (1988) noted that *O. universa* is considerably affected by its feeding and light regimes controlling its life span, reproduction and final size much more than temperature and salinity.

*G. siphonifera* is a spinous mixed layer species residing within the surface waters. As with *O. universa* the spines facilitate a symbiotic relationship with dinoflagellates

(orders gymnodiniales and peridiniales). Parasites are often noted to feed on these species, darting between the spines and feeding on the cytoplasm (Hemleben et al., 1988). *G. siphonifera* is a carnivorous species that preys on multiple food sources throughout its lifespan, such as copepods, hyperiid amphipods and tunicates. Existing within temperature ranges of ~10 - 31°C, *G. siphonifera* exhibits an optimum of  $\geq 22^{\circ}\text{C}$  (Žarić et al., 2005; Lombard et al., 2009). Salinity ranges from 27 to 45‰ (Hemleben et al., 1998; Bijma et al., 1990).

Previously referred to as *N. pachyderma* (right coiling), *N. incompta*, was renamed due to the genetic distinction between *N. pachyderma* (left coiling) which dominates sub polar to polar waters (Darling et al., 2006). *N. incompta* is a surface-dwelling (although it does reside at deeper habitats than the other defined species) non-spinose herbivorous species that grazes on phytoplankton. Due to their feeding preferences Neogloboquadrinids are generally associated with the development of a deep chlorophyll maximum at the base of the euphotic zone. *N. pachyderma* (left-coiling) is generally found in areas where temperatures are  $< 9^{\circ}\text{C}$  (Hemleben et al., 1998) while *N. incompta* exhibits preferences for slightly higher temperatures of  $\geq 15^{\circ}\text{C}$  (Rohling et al., 1993).

The modern distribution of the predefined species shows that *O. universa* and *G. siphonifera* are a mixed layer species and are most prevalent within late summer assemblages. While *N. incompta* is a deeper dwelling species and is most common within winter assemblages as temperatures are cooler.

This chapter focuses on the deposition of sapropels S3 and S5 (further details about the depositional framework associated with this depositional event can be found in chapter 3). Both sapropels were deposited during Marine Isotope Stage 5 (MIS5) (Figure 7.2), with S5 accumulating earlier between 127 – 122 kyr BP (substage MIS5e). The younger sapropel S3 was deposited in substage MIS5a between approximately 85 – 78 kyr BP (Bouloubassi et al., 1998; Emeis et al., 1998; Cramp and O'Sullivan, 1999; Bar-Matthews, et. al., 2003; Schmeidl et. al., 2003; Lang and Wolff, 2011; Railsback et al., 2015; Grant et al., 2016; İŞLER et al., 2016).

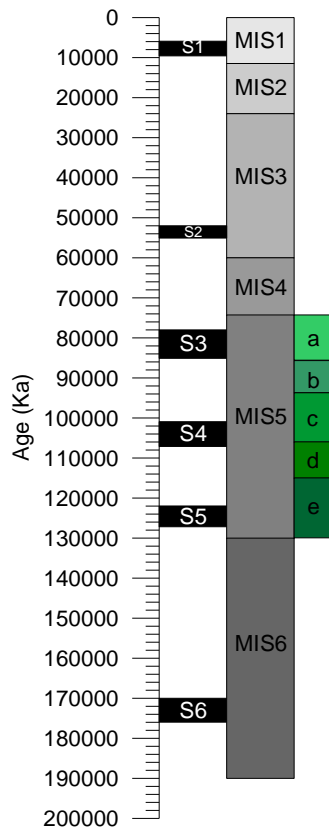


Figure 7.2: Diagram depicting the relationship between sapropel layers and Marine Isotope Stages (MIS). Note that both S3 and S5 were deposited during MIS 5 but at different sub stages.

### 7.2.2 SPECIES MEASUREMENT

Each sample was picked to obtain the individual proposed species. Using a random microsplitter each sample was split to obtain a minimum of 100 specimens (where available) from the >150µm size fraction, this minimum was utilised as it is believed that this gave the best chance for statistical analysis as a representative of the assemblage. The use of this minimum size data set represents an artificial cut off point of the natural size distribution and therefore has no biological significance. Using a fine tipped (00000) paintbrush each chosen specimen was placed onto Cushman slides and using Cell^b imaging software the longest axis of each specimen was measured individually by hand (figure 7.3). Finally, the mean size was calculated for each species within each interval providing a representative measurement of test size before, during and after sapropel deposition.

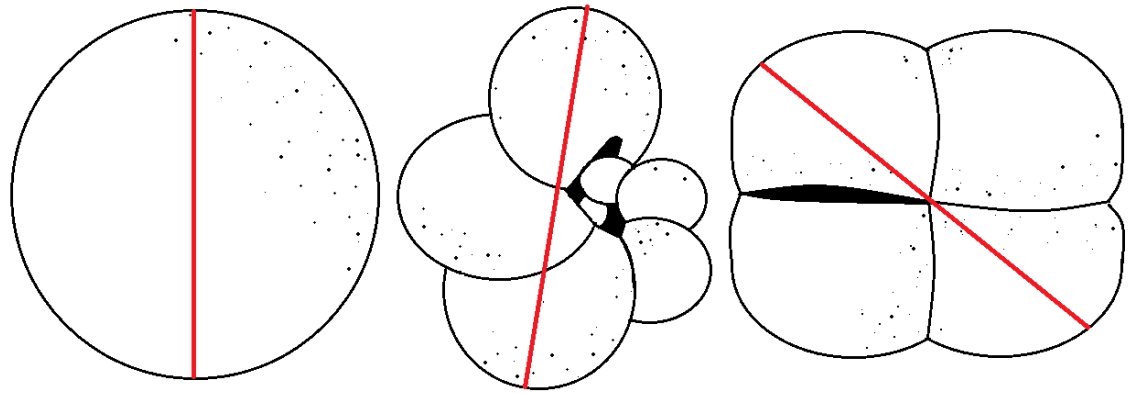


Figure 7.3: Illustration of the measuring technique utilised for *O. universa*, *G. siphonifera* and *N. incompta*. Measurements were taken along the longest axis of each species.

## 7.3 RESULTS

The following section consists of a series of graphs illustrating the variation in the test size of the three planktonic foraminiferal species outlined in the previous section. All graphs are presented versus depth (in cm) and the test size in micrometres ( $\mu\text{m}$ ). In addition annual, summer and winters SSTs, as derived from the ANN transfer function, will also be included, with SSTs recorded in degrees Celsius ( $^{\circ}\text{C}$ ).

### 7.3.1 TEST SIZE OF PLANKTONIC FORAMINIFERA

#### 7.3.1.1 Sapropel S3

In the first instance the most obvious observation is the difference in test size between surface water dwelling species (*G. siphonifera* and *O. universa*) and the deeper dwelling species (*N. incompta*) (figure 7.4A). It is clear that throughout the studied time period the test size of *N. incompta* is consistently smaller ( $252\mu\text{m}$ ) than those of *G. siphonifera* ( $447\mu\text{m}$ ) and *O. universa* ( $493\mu\text{m}$ ). Furthermore, with the exception of a single point (figure 7.4A), the mean test size of *N. incompta* illustrates less variability ( $15\mu\text{m}$ ) than its shallow water counterparts. However, a slight increase is noted at the onset of S3.

In contrast the variability in mean test size between *O. universa* and *G. siphonifera* is more apparent with both species illustrating similar trends. Prior to the onset of S3, the

larger of the two species, *O. universa*, demonstrates a gradual increase in the mean test size (from 450µm – 550µm) (figure 7.4A). This is less apparent with regards to *G. siphonifera*, which shows very little change. As the deposition of S3 commences the mean test size of *O. universa* displays an initial decrease before returning to pre-sapropel sizes. However, the increase in size is short lived and continues to decline for the remainder of the sapropel. With the exception of the initial size decrease at the onset of S3, *G. siphonifera* displays a similar size trend throughout the deposition of the sapropel. Both species behave somewhat differently post sapropel with *G. siphonifera* displaying a smaller size (~400µm) than during the sapropel and *O. universa* displaying a larger mean test size (~540µm). The period after the deposition of S3 *O. universa* records a general increase in mean test size reaching a maximum of ~600µm. This is followed by a rapid decline in size and sees the species reach its smallest (~250µm) over the studied time period (figure 7.4A). In contrast *G. siphonifera* displays much less variability recording a gradual decline post sapropel.

### 7.3.1.2 Sapropel S5

During sapropel S5 it is noted that while the mean test size of *N. incompta* does not seem to change overall (~250µm), there is far more variability recorded over the studied time frame (figure 7.4B). Once again it is the mixed layer species that display the greater variabilities in mean test size however, notable differences between the species are apparent (figure 7.4B). Interestingly in comparison to sapropel S3 *G. siphonifera* appears to record an overall larger mean test size while *O. universa* remains similar in size. In the period prior to the onset of sapropel S5 both species show a gradual increase in test size, before recording an initial decline at the onset of the sapropel depositional phase (figure 7.4B). For the first part of sapropel deposition both species behave similarly and record increases in mean test diameter midway through the sapropel (figure 7.4B). At this point the mean size of *G. siphonifera* remains at its highest (~570µm) before declining at the termination of the sapropel. *O. universa*, on the other hand, displays a much earlier decline in its test size (figure 7.4B). The differences continue post sapropel with *G. siphonifera* demonstrating a significant decline in test size reaching its lowest size ~340µm. In contrast *O. universa* displays a marked increase in test size reaching sizes of ~610µm.

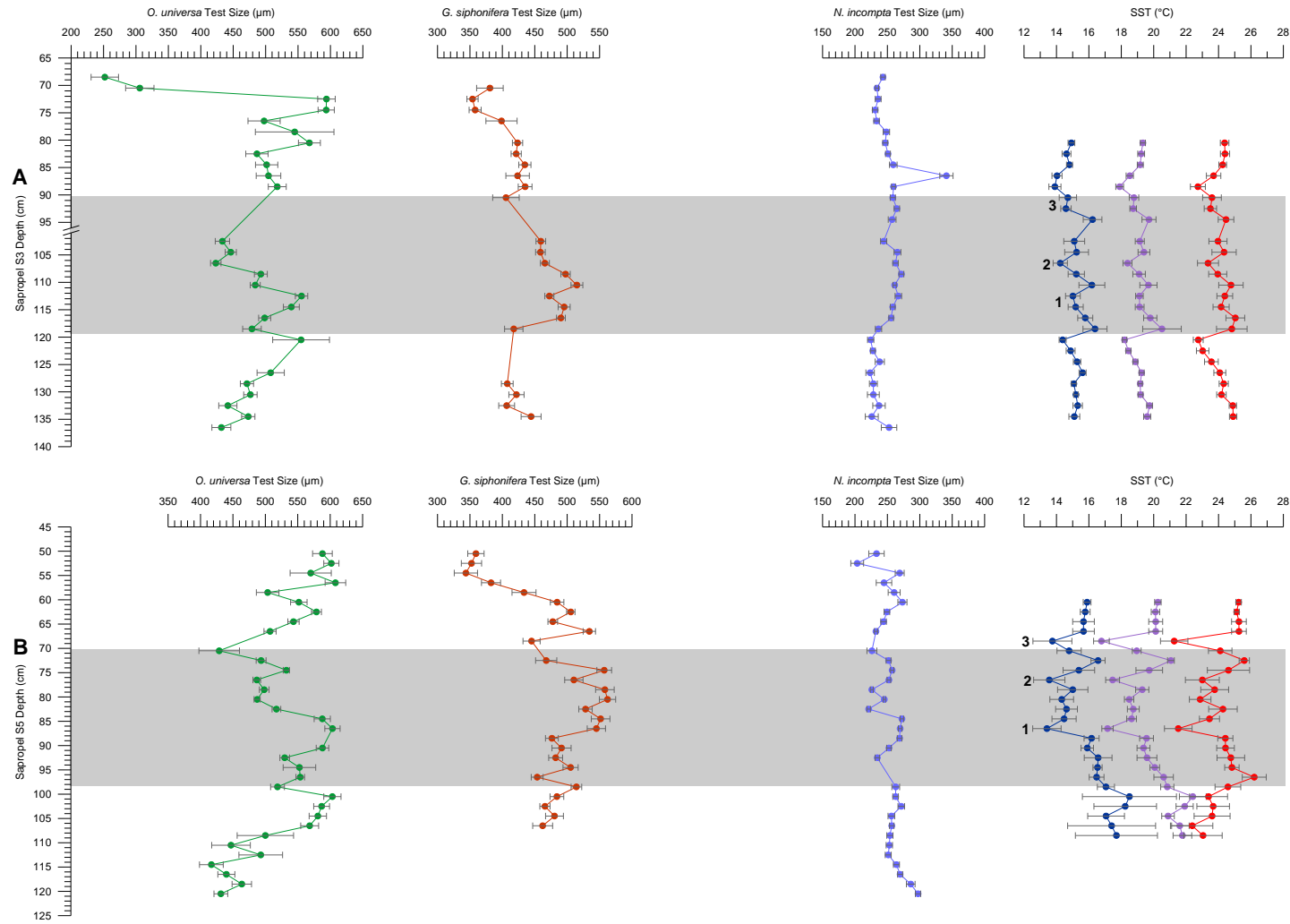


Figure 7.4: Line graphs representing the test size variations of predefined planktonic foraminiferal species before, during and after sapropel deposition, Sapropel S3 (A) and Sapropel S5 (B) (sapropel is defined by the shaded area). Also represented is SSTs for each depositional event, winter (blue), Annual (purple) and summer (red). Cooling events during sapropel deposition are labelled as points 1, 2 and 3.

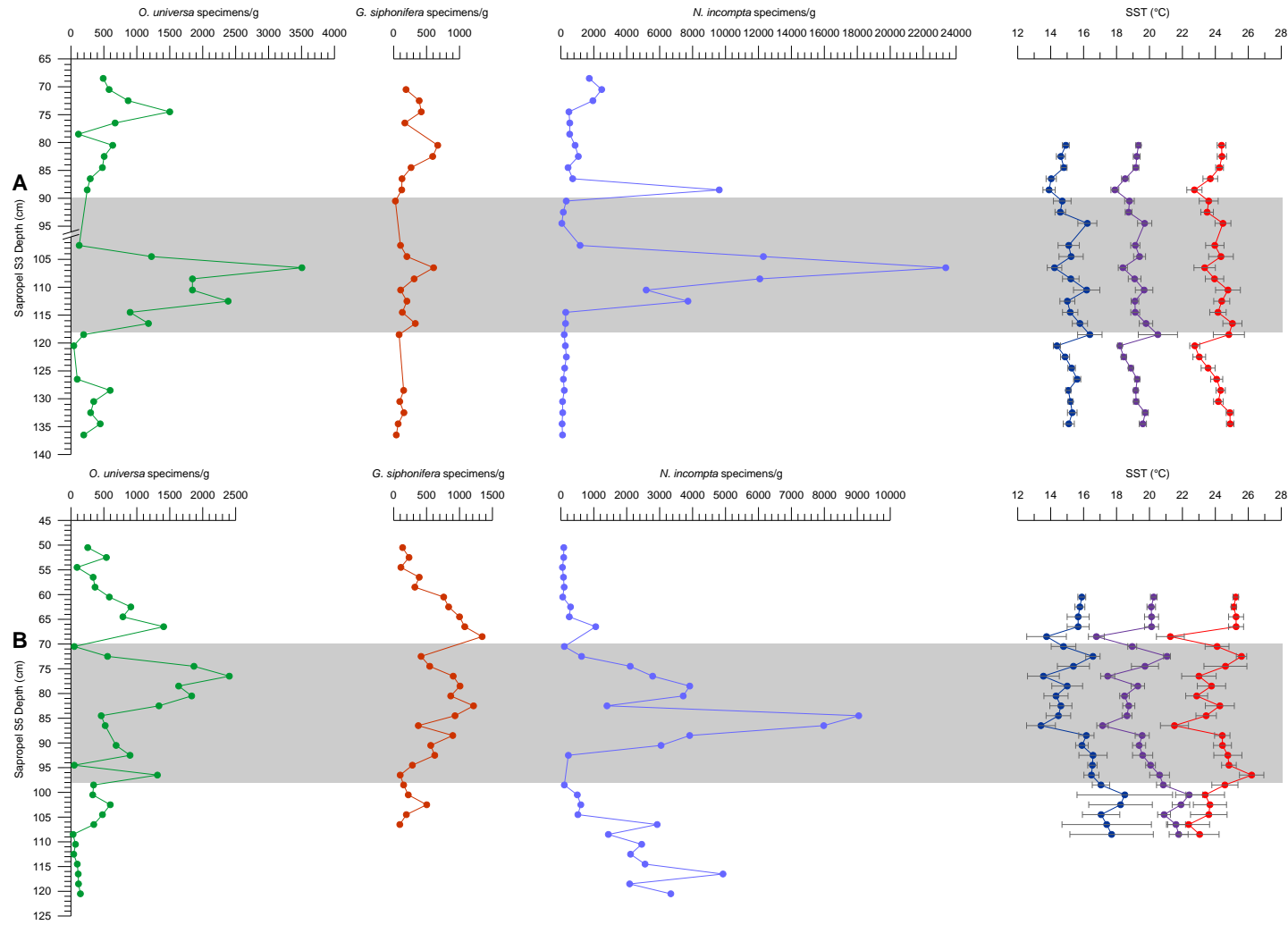


Figure 7.5 Line graphs representing the numbers per gram variations of predefined planktonic foraminiferal species before, during and after sapropel deposition, Sapropel S3 (A) and Sapropel S5 (B) (sapropel is defined by the shaded area). Also represented is SSTs for each depositional event, winter (blue), Annual (purple) and summer (red).

### 7.3.2 ABSOLUTE ABUNDANCE OF PLANKTONIC FORAMINIFERA

The absolute abundance data for the three species are illustrated in figure 7.5. It is immediately clear that during the depositional event of sapropel S3 the specimens/g of both *O. universa* and *N. incompta* increase significantly compared to pre and post sapropel values. In contrast the same signal is not observed for *G. siphonifera* where specimens/g are generally much lower throughout the entire timeframe (figure 7.5A). While *O. universa* and *N. incompta* display similar trends during the deposition of S3 and S5, *G. siphonifera* appears to behave differently. Compared to the low specimens/g in S3, during S5 *G. siphonifera* records a gradual increase throughout the sapropel before declining at the termination of the event. Despite this increase *G. siphonifera* records the lowest specimens/g of the three species (figure 7.5B).

### 7.3.3 SEA SURFACE TEMPERATURES (SSTs) DURING S3 AND S5

Annual, summer and winter SSTs are present in figures 7.4 and 7.5. Despite the difference in variability the SST reconstructions are remarkably similar during both depositional events. What is particularly interesting is evidence of climate cooling within the sapropel compared to both before and after sapropel deposition (figure 7.4 and 7.5). Prior to deposition of sapropel S5 annual SSTs averages  $\sim 21.5^{\circ}\text{C}$ , however at the onset of S5 annual SSTs are recorded at  $\sim 22.5^{\circ}\text{C}$  before a gradual decline culminates in a low of  $\sim 17^{\circ}\text{C}$ , the lowest during the sapropel. Taking into account the errors associated with the SST reconstruction, this is a significant reduction of between  $4\text{-}5^{\circ}\text{C}$  since the onset of sapropel deposition. A further two cooling events are noted, one later in the sapropel and one immediately after the termination of the sapropel, recording SSTs of  $\sim 17.5^{\circ}\text{C}$  and  $16.5^{\circ}\text{C}$  respectively (figure 7.4 and 7.5). Beyond the sapropel, SSTs average  $\sim 20^{\circ}\text{C}$  similar to those prior to the depositional event. While a similar pattern is noted during the deposition of S3 the range in SSTs is much smaller ( $\sim 1\text{-}2^{\circ}\text{C}$ ) from the onset of the sapropel to its termination (figures 7.4 and 7.5).

### 7.3.4 SUMMARY OF RESULTS

A summary of results are presented as a series of box and whisker plots in figures 7.6 and 7.7. During S3, the mean test size demonstrates more variability than during S5 with *G. siphonifera* recording a size increase during the sapropel. In contrast *O. universa* and *N. incompta* appear to be larger post sapropel (figure 7.6A). This does not seem to be the case in S5, with minimal variation in size recorded throughout the studied period (figure 7.7A). With regards to the absolute numbers of each species, S3 displays much higher frequencies than S5, particularly with reference to *N. incompta*. With the exception of *G. siphonifera*, absolute abundance records an increase during the deposition of S3 and S5 compared to pre and post sapropel sediments (Figures 7.6B and 7.7B). Finally SST reconstructions illustrate an interesting pattern between the different depositional events (figure 7.6C and 7.7C). The average SST before, during and after S3 deposition show little change with winter SSTs recorded at  $\sim 15^{\circ}\text{C}$  and summer SSTs at  $\sim 24.5^{\circ}\text{C}$ . The variability in SSTs during S5 is much more striking. Prior to sapropel deposition, winter SSTs are  $\sim 17.5^{\circ}\text{C}$  decreasing to  $\sim 15^{\circ}\text{C}$  during the anoxic events. Post sapropel SSTs only return to  $\sim 16^{\circ}\text{C}$ . However, this trend is not repeated during the summer with SSTs recording an increase of  $\sim 1.5^{\circ}\text{C}$  from before the sapropel to its termination (figures 7.6C and 7.7C).

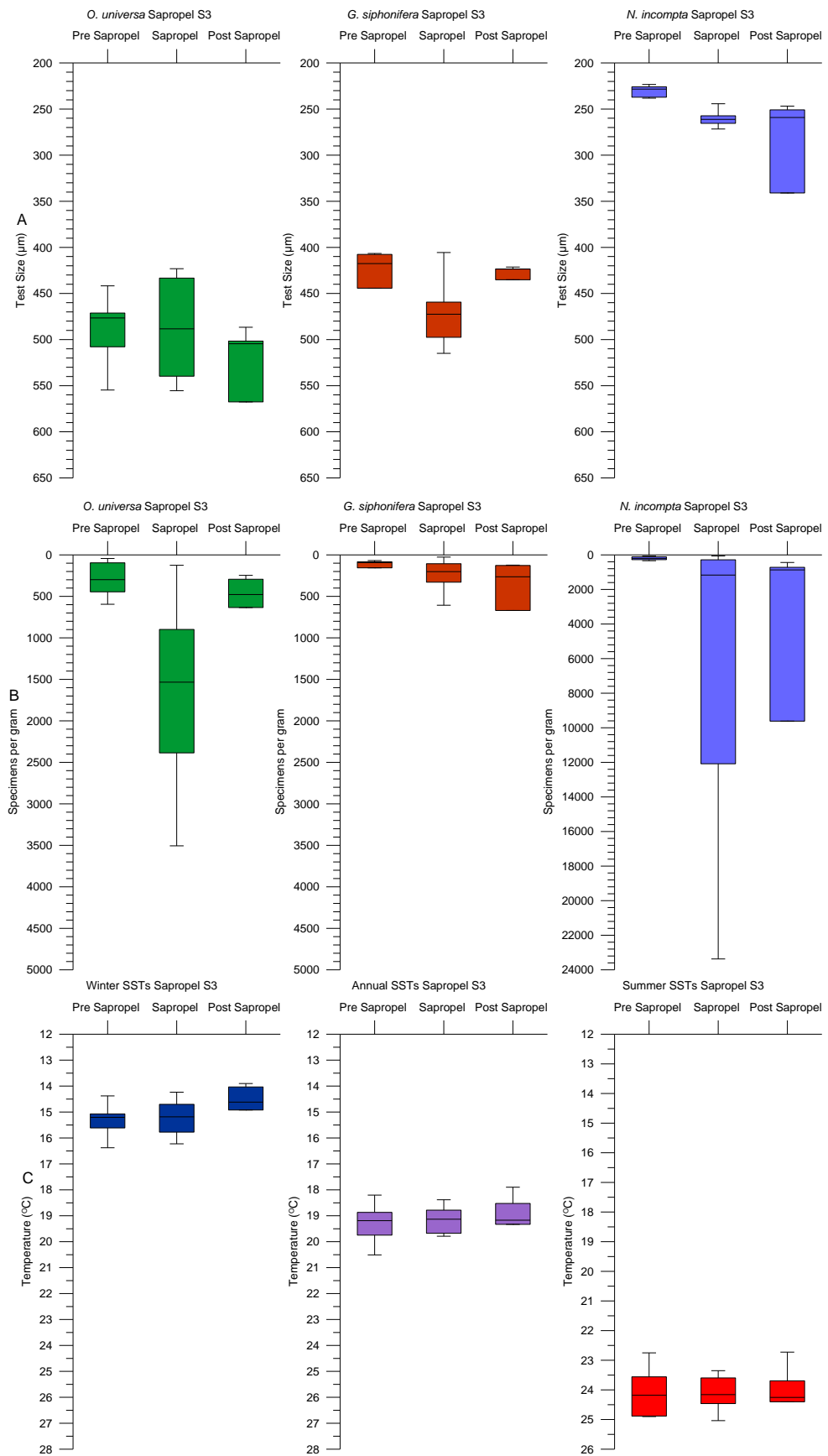


Figure 7.6: Box and whisker plots summarising micropalaeontological data for sapropel S3. Displayed within the graphs are test size data (A), the absolute abundances shown by specimens per gram (B) and the sea surface temperatures (C).

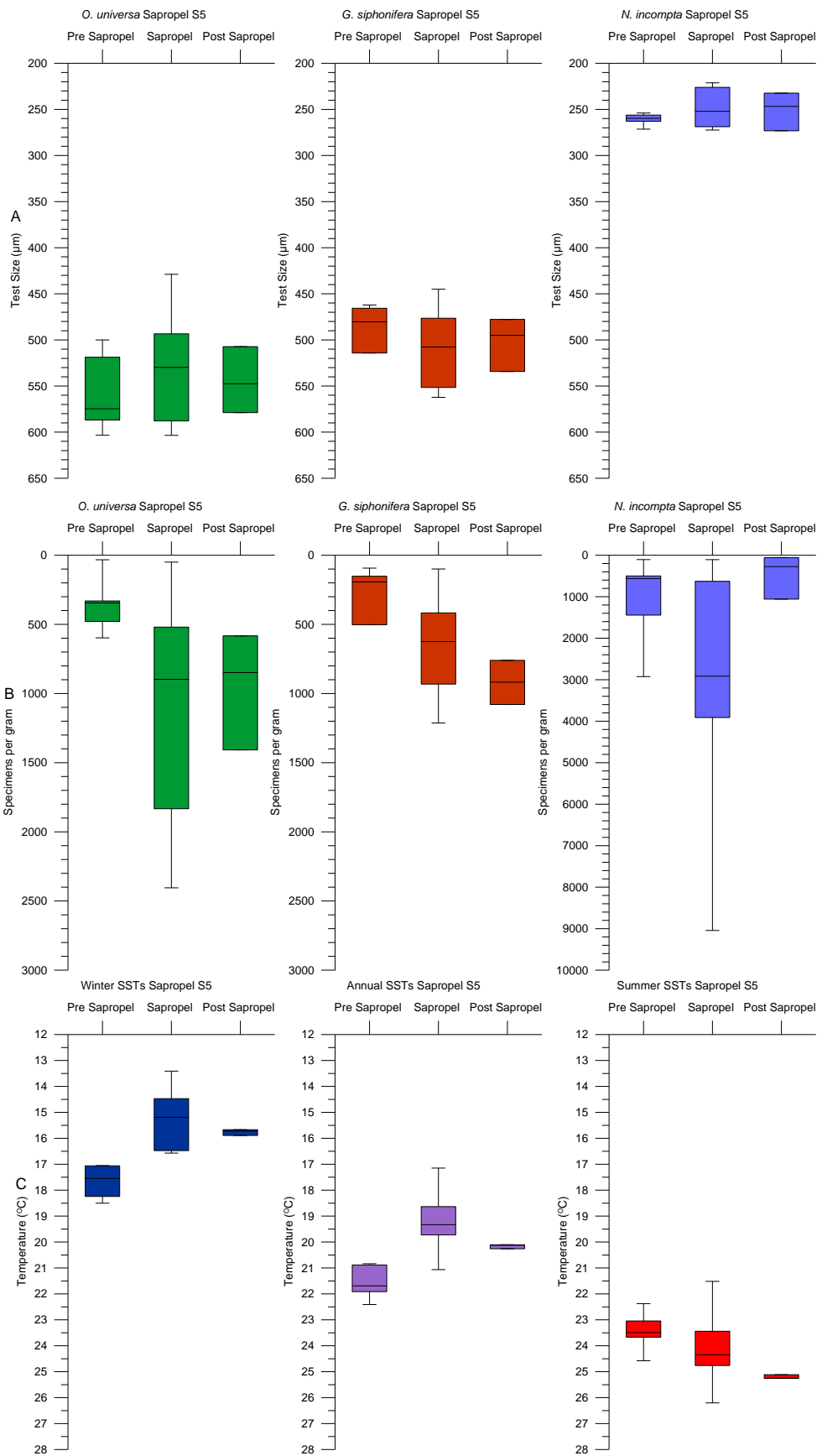


Figure 7.7: Box and whisker plots summarising micropalaeontological data for sapropel S5. Displayed within the graphs are test size data (A), the absolute abundances shown by specimens per gram (B) and the sea surface temperatures (C).

## 7.4 DISCUSSION

A combination of statistical and micropalaeontological analysis reveal changes throughout both timeframes; Sapropel S3 and S5, including pre and post sapropel analysis. The results of the size analysis of *O. universa*, *G. siphonifera* and *N. incompta* are presented in figures 7.4 and 7.5. Further analysis of the test size, species abundance and SSTs can be found in 7.6 and 7.7.

MIS 5 occurred from ~130 kyr BP to ~70 kyr BP and is defined by 5 separate sub stages (a, b, c, d, and e). Sapropel S5 was deposited during substage MIS 5e and sapropel S3 was deposited during MIS5a (Bouloubassi et al., 1998; Emeis et al., 1998; Cramp and O'Sullivan, 1999; Bar-Matthews, et. al., 2003; Schmeidl et. al., 2003; Lang and Wolff, 2011; Railsback et al., 2015; Grant et al., 2016; İşler et al., 2016). MIS 5 is noted as the last interglacial complex, which includes the last interglacial (MIS 5e) and early glacial (MIS 5a) periods (Milner et al., 2016). Substage 5e is well documented throughout the literature with a slight warming of SSTs noted at the beginning of the substage (~1-2°C) while substage 5a experiences cooler temperatures (Oppo et al., 1997). MIS 5a correlates to Northern Hemisphere insolation maxima and it is suggested that global mean sea level during this substage ranged between -18m and +1m relative to present day sea level (Creveling et al., 2017) while Cutler et al., (2003) stipulated that sea levels during substage 5e were similar to present levels (figure 7.8).

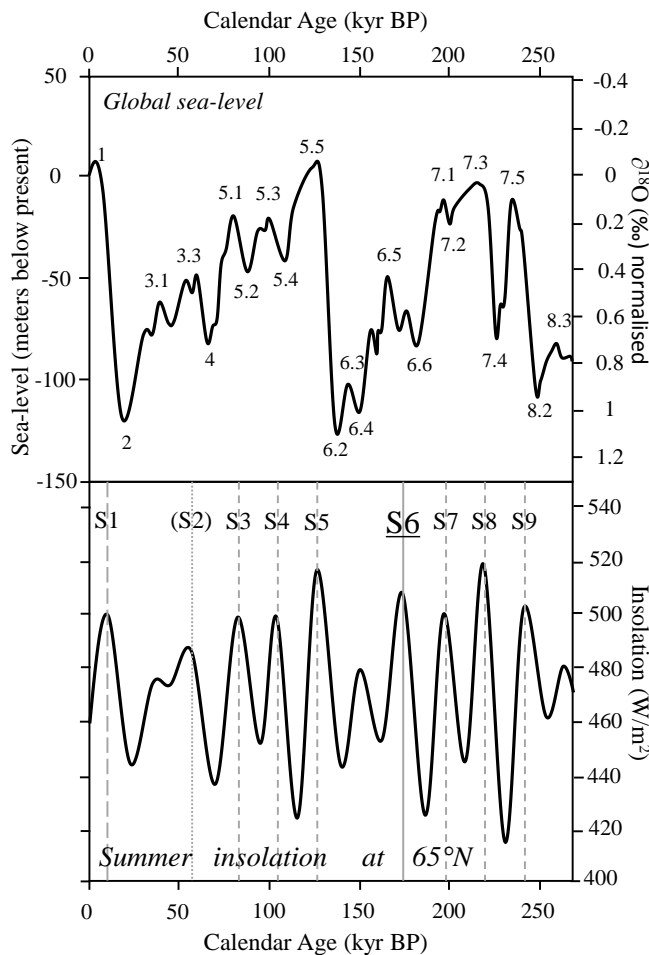


Figure 7.8: Graph summarising the relationship between the most recent sapropels (S1-S9), the Late Quaternary glaciations (MIS 1-8) and the insolation variations dominated by the 22 kyr orbital procession (courtesy of Bard et al., 2002).

### 7.4.1 SEA SURFACE TEMPERATURES

As outlined earlier in this chapter, past research has attempted to correlate changes in the test/assemblage size of planktonic foraminifera to changes in SST (Be and Duplessy, 1976; Schmidt et al., 2004; Kaiho et al., 2006). This is under the premise that each species has a maximum growth rate optimum associated with a particular set of environmental variables (figure 7.9). Beyond the limits of this optima, growth rates and reproduction will diminish. As such in theory correlations between test size and SST should be possible (Hecht, 1976; Schmidt et al., 2004). Obviously such situations are much more complex with the interplay of other environmental parameters affecting the growth rate of planktonic foraminifera. However, in the first instance, it is necessary to address the role of SST and the potential impact on test size throughout the depositional

events of S3 and S5. Figure 7.10 illustrates the relationship between SSTs and mean test size for each of the studied species during S3 and S5. It is immediately apparent that no linear relationship exists between these parameters which is not unexpected. However, upon closer inspection some interesting details can be extracted. The largest mean test size exhibited by *G. siphonifera* occurs during the deposition of both sapropels, associated with summer SSTs ranging between 24 - 25°C and 21.5 – 25°C for S3 and S5 respectively (figure 7.4A and 7.4B). In contrast the largest test size of *O. universa* are not restricted to the sapropels occurring before and after the event also.

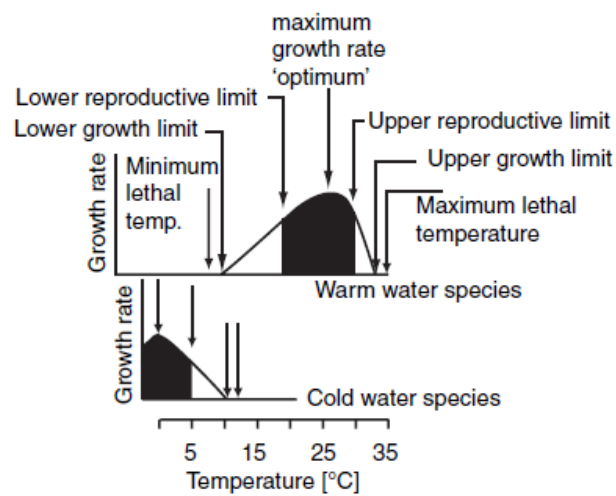


Figure 7.9: Schematic illustration depicting a temperature growth model for both warm and cold water species (courtesy of Schmidt et al., 2014).

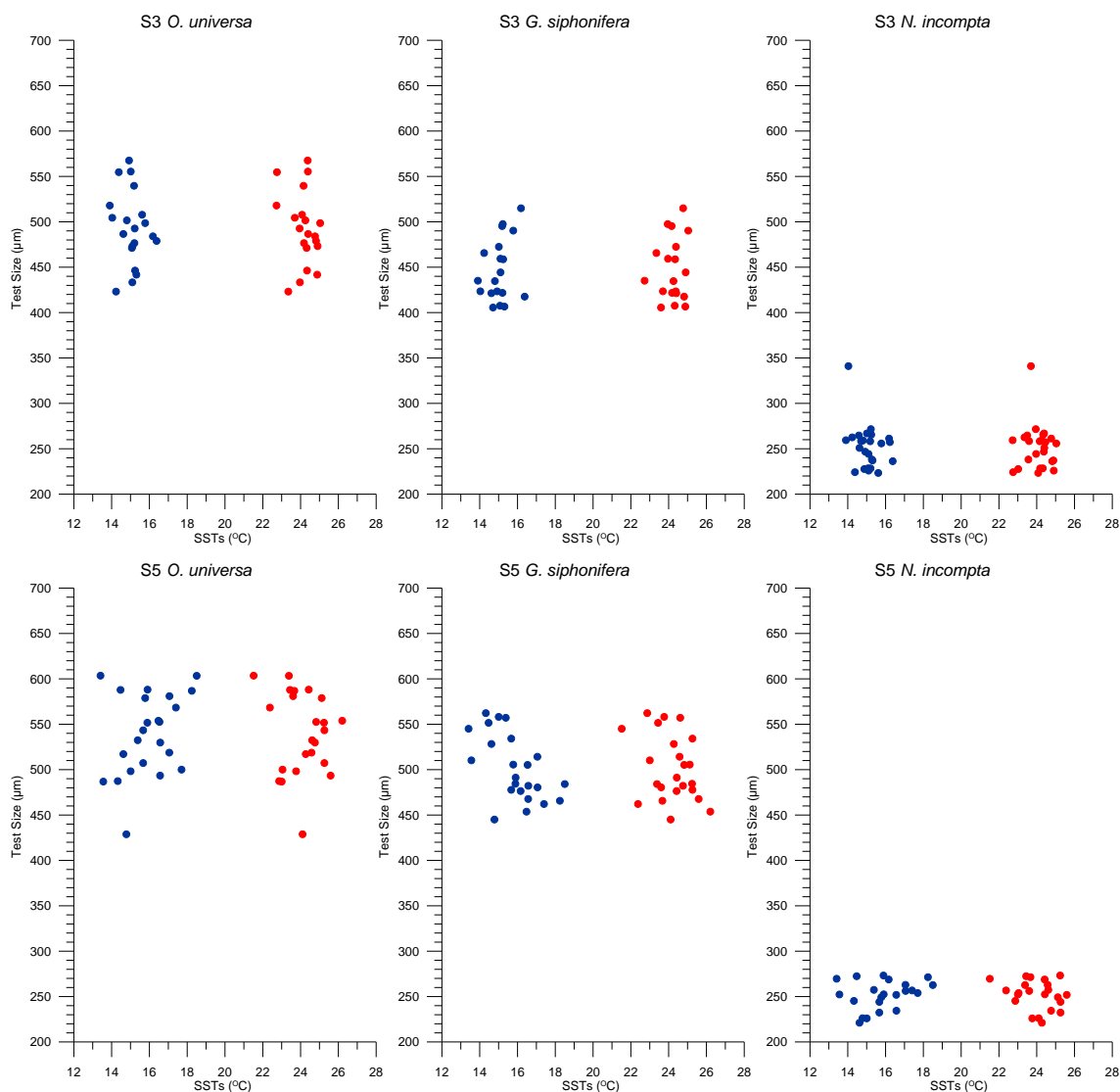


Figure 7.10: Graphs displaying the correlation between species mean test size and SSTs. Winter correlations are denoted in blue and summer correlations are signified by red.

Reviewing experimental data on planktonic foraminiferal growth rates, Lombard et al. (2009) presents optimum SSTs for a number of species (figure 7.11). Specifically, the maximum growth rate of *G. siphonifera* seems to occur between 24°C and 29°C, whilst *O. universa* has a slightly larger SST optimum (21°C - 30°C). In contrast the maximum growth rates of *N. incompta* span a much wider SST range from 5°C to 20°C (figure 7.11). Putting this into the context of sapropel deposition an interesting picture begins to emerge. Before, during and after the deposition of sapropel S3, summer SSTs only peak above 24°C periodically during the depositional phase coinciding with the largest specimens of *G. siphonifera* (figure 7.4). Furthermore minimum summer SSTs do not fall below 21°C falling well within the optimum range for *O. universa* and as such the

larger specimens of this species are not restricted to the sapropel. On the other hand whilst SSTs favour maximum growth for *N. incompta* there is little difference in the

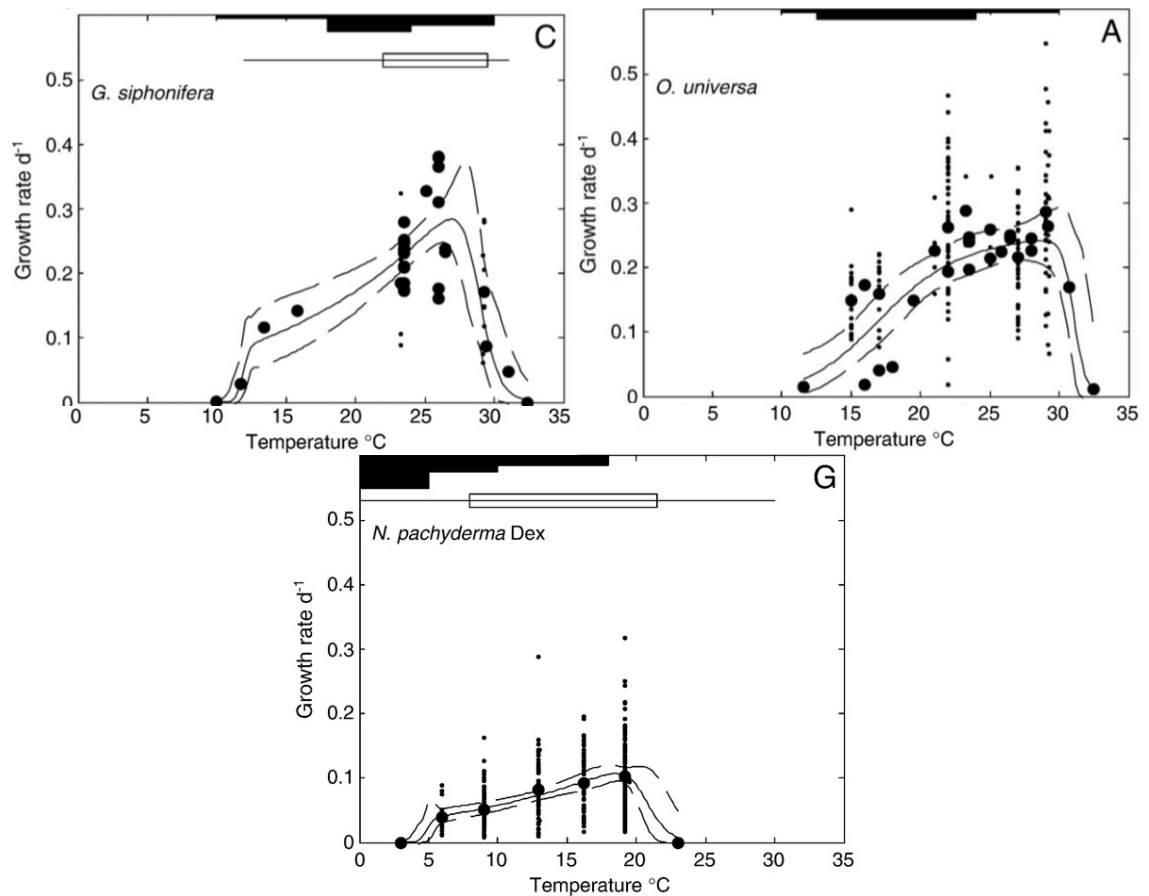


Figure 7.11: growth rates of selected species in relation to experimental temperature (°C). Large dots signify mean population at one temperature while smaller dots represent individual growth rates. Model results (line) and 95% confidence intervals of the model are shown by dashed lines. Stepped filled bars represent observations from Be and Tonderlund, 1971, flux observed in sediment traps (Zaric et al., 2005) are shown in terms of overall distribution as a line and as optimal SST as an open bar (courtesy of Lombard et al., 2009).

mean test size before, during and after sapropel deposition (figure 7.4). A similar pattern is noted during the deposition of sapropel S5. From these observations we can conclude that the variability observed in the mean test size of *G. siphonifera* does seem to be influenced to some degree by SST whilst other factors seem to determine the mean test size of *O. universa*. In contrast the size of *N. incompta* is not affected by changes in SST.

## 7.4.2 NUTRIENTS

While much research has focused on the importance of SST when discussing test/assemblage size, the importance of nutrient availability cannot be discarded as both parameters show a degree of interrelatedness. As summarised earlier in the chapter, each species has specific nutrient preferences and their optimum growth and maturation will only occur once adequate volumes of nutrition is regularly provided (Hemleben et al., 1988). These preferences generally relate to the consumption of zooplankton prey by spinose species and the non-spinose species consuming phytoplankton. Caron and Hutchins, (2013) outline the interdependence of species upon each other within a food ladder. Each level of the ladder has specific needs and requirements to enable the growth of the species. For example the development of a phytoplankton bloom attracts herbivorous species which graze on phytoplankton and allow for the expansion of these species. This enhanced productivity and increase in zooplankton will then attract omnivorous species.

However, does an increase in nutrients signify an increase in individual test size or will size remain constant and the absolute abundance of species increase? Through geochemical analysis many studies have indicated that primary productivity increased during the depositional phase of sapropels (Thomson et al. 1999; Nijenhuis and De Lange, 2000). With particular reference to this research Gallego-Torres et al. (2007) and Weldeab et al. (2003b) computed high productivity levels in sapropels S3 and S5 respectively, using biogenic Ba. The faunal response to nutrient enhanced surface waters is markedly different between the mixed layer carnivorous species (*O. universa* and *G. siphonifera*) and the deeper dwelling herbivorous species (*N. incompta*). Using absolute abundances (number of specimens / gram of sediment) to reflect productivity levels, all three species (with the exception of *G. siphonifera* in sapropel S3) record increases during the deposition of both sapropels (figure 7.5). However, the absolute numbers of *N. incompta* are far greater than those of *G. siphonifera* and *O. universa*. It is interesting to note that none of the species record an increase in mean test size in response to increased primary productivity (figure 7.12).

In their study Weldeab et al. (2003) noted that the spatial distribution of primary productivity varied during the deposition of sapropel S5. Based on four cores from the

eastern basin the authors noted that the area to the south of Crete (ODP 969E - the same core as the one used in this study) recorded maximum surface water productivity. The authors attributed this to different modes of nutrient delivery to the surface waters, within the basin, during the deposition of the sapropel. ODP core 969E is a significant distance from the outflow of the river Nile excluding riverine nutrient input as the source. More likely, and in agreement with Rohling and Gieskes (1989), the introduction of nutrients into the surface waters was as a result of the shoaling of the pycnocline. The subsequent development of a DCM provides an ecological niche that favours large numbers of herbivorous species such as *N. incompta*. Weldeab et al (2003b) further suggested that aside from the shoaling of the pycnocline, the site south of Crete would require additional entrenchment of nutrients to explain such high productivity values. The authors suggest an intensification of upward mixing could be encouraged by submesoscale cyclonic vortices, enabled by the weakened circulation comparable to modern day, and the southeastward movement of the Cretan gyre. This is enabled by a reduction in the density gradient between the surface and intermediate waters favouring the continuation of upward mixing of nutrients. This extended phase of nutrient availability within the DCM that is favoured by *N. incompta* could account for the increase within the absolute abundance of this species.

A further study undertaken by Kaiho et al. (2006) reported an increase in the test size of planktonic foraminifera in response to SST changes at the PETM. The authors concluded the size increase as a result of low nutrient supply due to increased water column stratification. As previously discussed, at times of sapropel deposition, the nutrient levels in the surface waters were high. However, Brown (1997) has indicated that high nutrient levels may inhibit calcification and ultimately growth of a species. This is entirely plausible for a species like *N. incompta*, the smallest of the three species studied and the only herbivorous species. In contrast it has been suggested that mixed layer foraminifera with algal symbionts may have a distinct advantage in that symbiosis can aid in calcification. Planktonic foraminifera with a symbiont, such as *O. universa* and *G. siphonifera*, can utilise sunlight rather than nutrient resources as their source of energy and so can significantly increase calcification by light (Hallock et al., 2000).

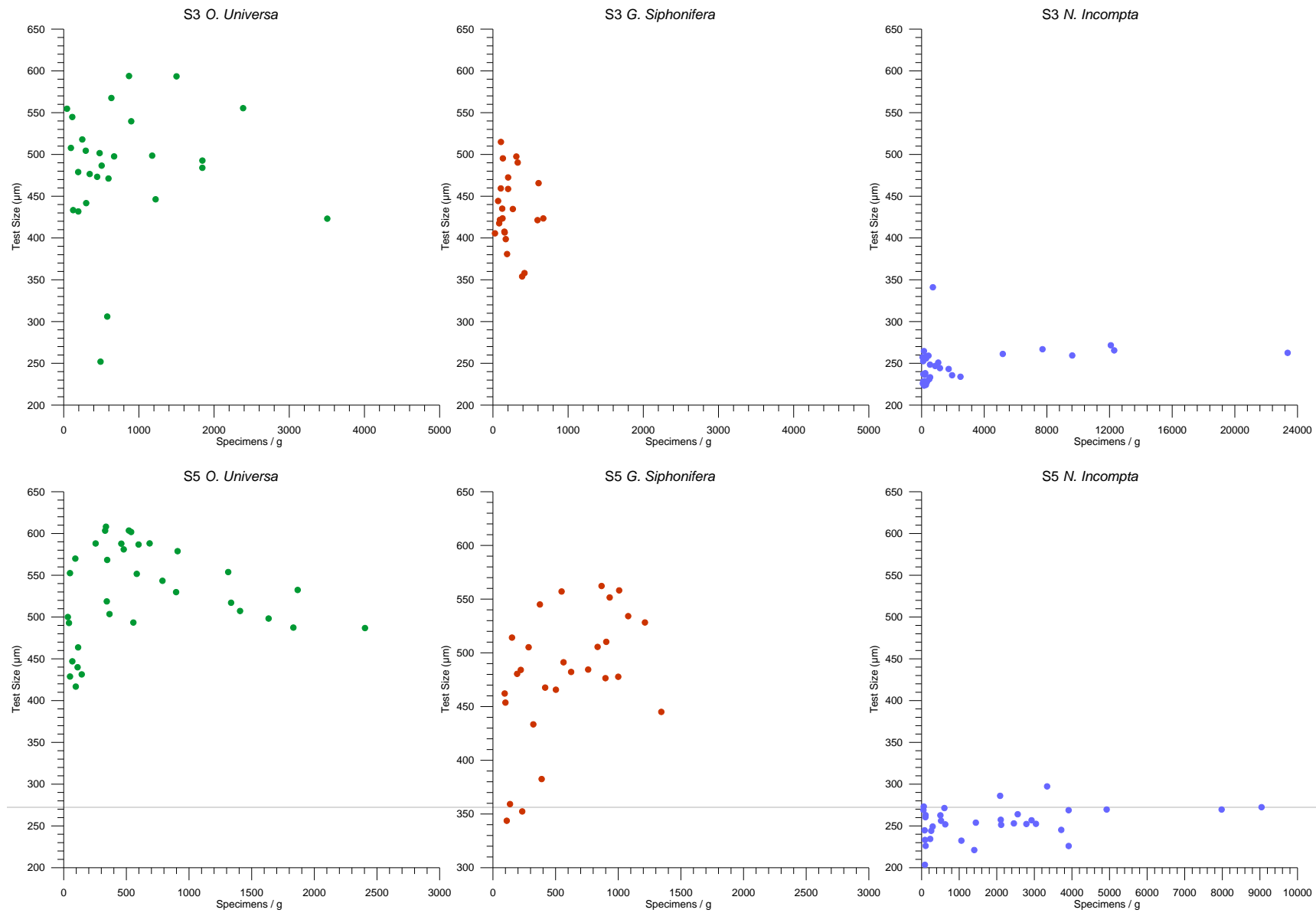


Figure 7.12:  
Correlation between  
species test size and  
specimens/g for  
each of the defined  
species.

### 7.4.3 IRRADIANCE

Symbiont bearing foraminifera reside within the euphotic zone, where the symbionts are exposed to light levels that are required for photosynthesis (Rink et al., 1998). Caron and Hutchins (2013) noted that increased thermohaline stratification within the marine environment, associated with the freshening of the surface waters, leads to species within the upper mixed layer experiencing amplified irradiance. This increasing irradiance may indeed have a direct effect on the growth and behaviour of certain heterotrophic protists. Bemis et al. (2000) conducted laboratory experiments on 100 specimens of *O. universa* and contrasted this with 230 specimens of *G. bulloides* to see the effect of irradiance on species test size. In the case of *O. universa* it was noted that it responds to SST differently depending on the amount of light that it receives. The  $\delta^{13}\text{C}$  of *O. universa* tests developed under low light levels are less sensitive to SST and registers the  $\delta^{13}\text{C}$  value of seawater  $\Sigma\text{CO}_2$ , whereas the  $\delta^{13}\text{C}$  of high light tests intensifies somewhat with SST ( $0.05\text{‰ }^\circ\text{C}^{-1}$ ). *O. universa* is a symbiont bearing species and so exists within the upper water column, so this may have a direct effect on why an increase within test size is not observed. The increased nutrient levels are needed for the symbiont species but there may be a trade off with the access to nutrients and the position within the water column that is required for irradiance.

### 7.4.4 SALINITY

One of the primary suggestions for sapropel formation relates to the increase of freshwater into the Mediterranean Sea due to increased monsoonal activity. Freshwater is much less dense than sea water and so creates a blanket on top of the marine environment leading to stagnation within deeper waters. It is possible that the subsequent decrease in surface water salinity may affect the growth of planktonic foraminifera and therefore the size of the test. While it is commonly known that salinity levels during sapropel S1 were reduced, the case for reduced salinity during S3 and S5 may not be so straight forward. Sea levels were much lower than those of today, creating a longer residency time of water circulating throughout the eastern basin as the connection at the Strait of Sicily was cut off (Grant et al., 2016). The stagnant environment along with evaporation would have led to increased salinities. The influx of fresh water through monsoonal activities into these areas that previously had

increased salinity levels may have counterbalanced this. Again as increases within sea levels began to change it is important to understand the role salinity changes may have on planktonic foraminiferal test size. Unfortunately, while not much work has been completed on the effect of salinity levels on the direct size of these species, research from Bijma et al. (1990) exhibited maximum and minimum salinity tolerances on individual species within a laboratory setting. At maximum salinity tolerances some species such as *O. universa* would reabsorb their final chamber while at reduced salinities the behaviour does not change from its normal pattern. So while it may be conceived that salinity did decrease or at least alternate, reducing salinity levels may not have much impact on the normal functioning of individual growth rates.

## 7.5 CONCLUSIONS

A completed analysis for planktonic foraminifera mean test size from sediment core 969A along the Mediterranean ridge was completed. The results were based on sapropels S3 and S5 both deposited during Marine Isotope Stage 5. Examining the mean test size of planktonic foraminifera gives us the chance to see how the most basic (yet diverse) marine organisms react to changes within the environment particularly in relation to SSTs and nutrients. Overall the mean test size of the three defined species did not show a significant increase across the deposition of the sapropel however, the general variability noted within each species enables us to understand something about their requirements.

Individual species results can be defined as follows:

*Orbulina universa*: A spinous symbiont bearing species, the largest of the three defined species. Optimum temperature ranges for this species are reached at several points throughout core and as would be expected the maximum test sizes are therefore not restricted to the sapropel. Research related to the effects of irradiance on *O. universa* indicated that this species is affected by SSTs only within high light and noting this that size does not increase may indicate that *O. universa* moved within lower depths within their optimum in order to create easier access to nutrients for symbionts. There is no observed relationship between elevated nutrient levels and mean test size although increases in the

number of specimens/g could be as a result of an enhanced reproductive cycle. Furthermore, it is noted that *O. universa* is known to prefer a summer-mixed layer conditions, this furthermore signifies its preference for a warmer water column and its size not being restricted to the sapropel layer. As it moves through its life cycle, it is only affected by the freshwater-dilution at the very surface.

*Globigerinella siphonifera*: Also a spinose species *G. siphonifera* records its largest test sizes within the sapropel. This corresponds to the only time in the core were SSTs reach above 24°C (the lower end of the optimum temperature range for this species). It is the only species that records a slight correlation between SST and mean test size. Specimens /g also show elevated levels during the sapropel although not to the same extent as *O. universa*. *G. siphonifera* is a carnivorous species and so may have benefited from the increased availability of prey brought about by the development of increased nutrients. This species did not show a greater growth rate in conjunction with specimens/g and so it may be possible to surmise that reproduction of this species is not affected by the increased nutrients. *G. siphonifera* thrives winter mixed layer water column that is well ventilated and eutrophic. This is confirmed by the increased large test size noted within the sapropel when nutrients were increased.

*Neogloboquadrina incompta*: A non-spinose herbivorous species that prefers cooler waters showed the least significant change within mean test size throughout both depositional events. However this species did see dramatic increases with specimens/g in both of the sapropels. This increase in the number of specimens is very telling of the way *N. incompta* reacts to elevated nutrient levels and may indicate that enhanced productivity increases the reproduction of the species rather than the size of the species.

Sea surface temperature reconstructions were presented for annual, summer and winter for both S3 and S5 depositional events. The results noted that while there was some variability during the time periods, they illustrated some similarities. Within both sapropel events evidence of cooling event was noted when compared to pre and post sapropel. However the range of changes within the events was different with S3 exhibiting a ~1-2°C change.

Further work needs to be completed on species size in order to get a broader understanding of what is occurring through these sapropel events within different areas of the Mediterranean Sea. It would also aid to open this size research to other species that are prevalent within defined marine environments such as *G. bulloides* in an upwelling area.

## CHAPTER 8

# PALAEOECOLOGICAL VARIABILITY OF EASTERN MEDITERRANEAN SAPROPELS S5 AND S6: A CASE STUDY FROM THE SOUTH OF CRETE

### 8.1 INTRODUCTION

The dark coloured organic rich deposits that are commonly associated with Late Quaternary sedimentary sequences in the eastern Mediterranean Sea, have been the subject of much palaeoceanographic research (Capotondi et al., 2006; Capozzi and Negri, 2009; Corliss and Nolet, 1990; Cramp and O'Sullivan, 1999; Emeis et al. 1998; Emeis et al. 2000; Gallego-Torres et al., 2010; Mangini and Schlosser, 1986; Rohling et al. 1998; Rohling et al., 2015). Orbital forcing corresponding to precession minima and subsequent insolation maxima is thought to support the northward penetration of the African Monsoon across the eastern Mediterranean Sea (Grant et al., 2016; Rossignol-Strick 1985; Simon et al., 2017; Tesi et al., 2017). The consequence of this increases the discharge of freshwater into the eastern basin. Whether the origin of these freshwater influxes are sourced from the North African margin or the northern borderlands of the eastern Mediterranean, is still the subject of debate (Ducassou et al., 2008; Gudjonsson and Van der Zwaan, 1985; Rossignol-Strick, 1985). Nevertheless a freshening of surface waters facilitates an increase in the surface water buoyancy subsequently reducing deep water ventilation and promoting bottom water anoxia (Ducassou et al., 2008). A concomitant increase in surface water productivity increases the export of organic matter to the sea floor becoming preserved in the sediments as organic matter (Rohling and Gieskes, 1989).

While much of the research on sapropels relates to the most recent sapropel deposited during the current interglacial, this chapter focuses on the environmental conditions associated with sapropels S5 and S6. Sapropel S5 was deposited during the Last Interglacial Period (LIG), during Marine Isotope Stage (MIS) 5 and more specifically during MIS substage 5e. MIS 5e was characterised by a reduction of  $-2^{\circ}\text{C}$  in global

mean surface temperatures when compared to modern day, with sea levels approximately 4-6m higher than seen at present (Kopp et al., 2009). In contrast sapropel S6 was deposited during the glacial MIS 6 (figure 8.1). At this time the eastern basin of the Mediterranean Sea was influenced by two extreme climatic systems, the glacial conditions associated with continental ice coverage across Europe and the wet tropical conditions resulting from the enhancement of the African monsoon (Ayalon et al. 2002).

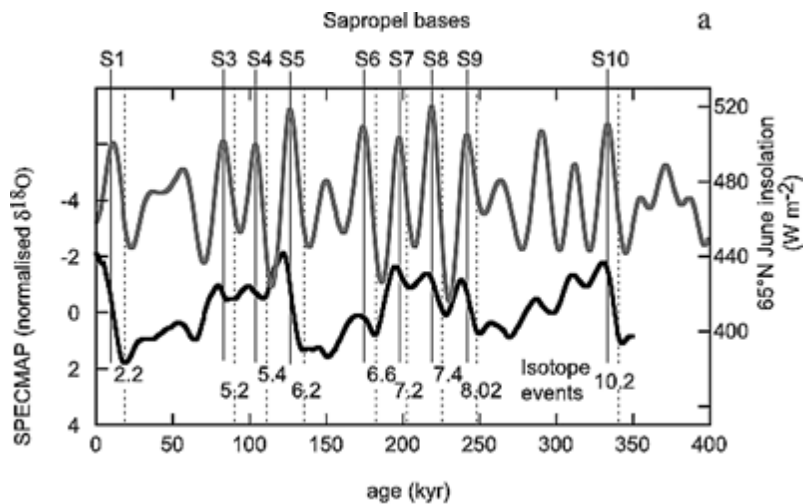


Figure 8.1: Sapropel occurrence in relation to timing of the SPECMAP normalized  $\delta^{18}O$  record showing glacial/interglacial cycles [Imbrie et al., 1984] and summer insolation at 65°N [Laskar et al., 1993] (Courtesy of Emeis et al. 2003).

The analysis of planktonic foraminifera enables us to examine ecosystem changes in response to sapropel deposition however, much of the planktonic foraminiferal research that has been previously done has focused on the interglacial periods (S1, S3 and S5). In this regard this chapter presents the distribution patterns of planktonic foraminifera across interglacial sapropel S5 and glacial sapropel S6 at a site south of Crete (figure 8.2). Specifically the aim of the chapter is to examine the response of the ecosystem to changes in climate variability during these depositional events. It should be noted that in reference to the literature that is present on Sapropel S6 it is stated that the Neogloboquadrinids species is dominated by *N. dutertrei*, however this was not overly evident on examination of the faunal characteristics of this interval, so in deference to this *N. pachyderma* (d), *N. incompta* and *N. dutertrei* will be referred to as Neogloboquadrinids group for sapropel S6 only.

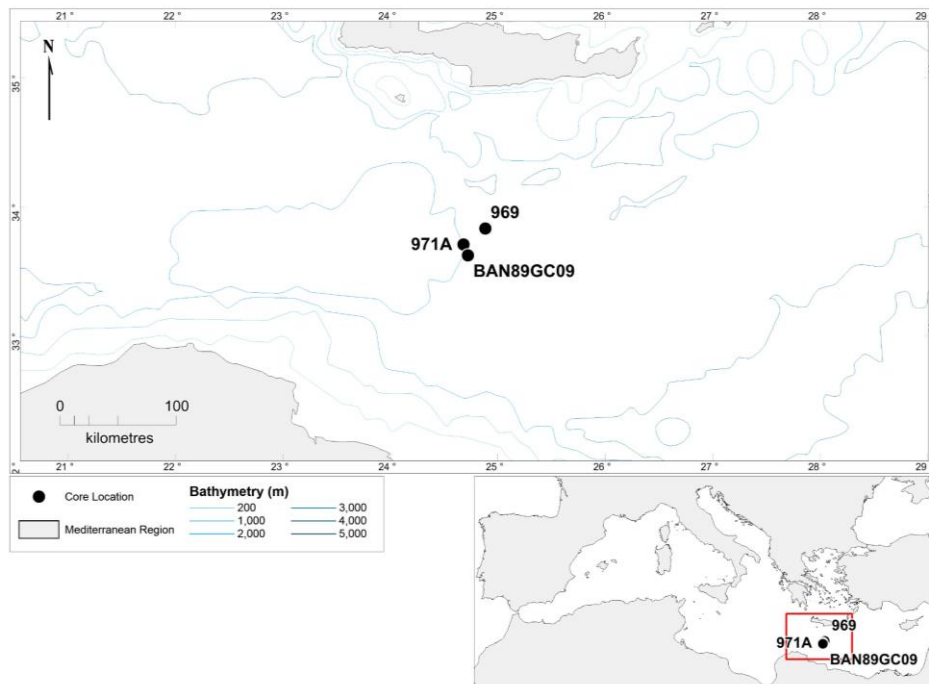


Figure 8.2: Locations of cores utilised for comparative analysis, ODP Core 969 (A and E), ODP Core 971A and Core BAN89GC09.

## 8.2 PALAEOENVIRONMENTAL PROXIES

Employing planktonic foraminifera as a means to interpret palaeoenvironmental variability is one of the primary proxies that is often utilised within Mediterranean palaeoceanographic research. As this research is based on two sapropels that exhibit diverse foraminiferal assemblages a number of proxies will be used to aid in the palaeoenvironmental reconstruction. In addition to Artificial Neural Networks (ANN) (outlined in Chapter 6, Section 6.3) this chapter employs the use of alternative proxies to determine water column stratification and productivity. This is primarily due to the absence of the warm water species *G. ruber*, in sapropel S6 sediments which was integral in calculating water column stratification (S-Index) and productivity (E-Index) (Kontakiotis, 2015). As such the presence / absence of *G. inflata* will be used to determine the variability within the water column reflecting whether the marine environment was strongly or weakly stratified. Based on previous studies *G. inflata* is known to favour seasons of strong vertical mixing with a homothermal water column (Tolderlund and Bé, 1971; Van Leeuwen, 1989; Rohling at al., 1993a; Pujol and Vergnaud-Grazzini, 1995). The Herbivorous index, used to estimate productivity levels,

is the abundance of species including *G. glutinata*, *G. bulloides*, *T. quinqueloba* and Neogloboquadrinids group/*N. incompta*, species known to thrive in nutrient-enriched waters (Rohling et al., 1993a; Pujol and Vergnaud-Grazzini, 1995; Sangiorgi et al., 2006). Finally the Shannon-Wiener diversity index is calculated to examine species diversity (accounting for both abundance and evenness of the species) throughout the deposition of the sapropels. The index measures the difficulty in predicting the next species that will be picked (Harper, 1999). For example if a sample is dominated by a single species then it is easy to determine what the next species will be therefore the Shannon-Wiener Index = 0. The more diverse a sample the higher the index will be (Hammer et al., 2004).

## 8.3 RESULTS

### 8.3.1 DISTRIBUTION OF PLANKTONIC FORAMINIFERA

Planktonic foraminiferal analysis was completed before, during and after sapropel deposition for both periods. After the preparation of the samples faunal analysis was performed every two centimetres throughout the core (further details on core processing can be seen in chapter 5). Only samples within the > 150µm were analysed and a sample size of 300 specimens was obtained where possible. A total of 15 species were identified, including *G. ruber (alba)*, *G. ruber (rosea)*, *G. siphonifera*, *G. rubescens*, *O. universa*, *B. digitata*, *G. tenella*, *G. bulloides*, *G. glutinata*, *G. inflata*, Neogloboquadrinids group/*N. incompta*, *N. pachyderma (s)*, *T. quinqueloba* and *G. scitula*. Faunal profiles and proxy indicators are presented against the depth (cm) of the core section in which the sapropel was located rather than the total depth within the core (mbsf).

#### 8.3.1.1 Eemian warm sapropel S5

Figures 8.3 and 8.4 illustrate the faunal characteristics, SST profiles and palaeoenvironmental indicators associated with the deposition of Eemian sapropel S5. Prior to the onset of the sapropel the total number of planktonic foraminifera per gram of sediment (planktonic foraminifera/g) average approximately 40,000 specimens/g.

Comparable to the rest of the record this would represent relatively high frequencies. The faunal assemblage at this time (prior to S5) is dominated by *G. ruber (alba)* (~ 25%), *G. bulloides* (~ 20%) and *N. pachyderma* (sinistral) (~ 20%) with smaller abundances of the SPRUDTS-group, *G. scitula*, *G. inflata* and *G. glutinata*. This diversity of species is reflected in the Shannon-Weiner diversity index displaying a value of ~ 2 (figure 8.4). SSTs range from 17-18°C during the winter to between 22 and 23°C in the summer. The productivity and stratification indexes would be indicative of strong vertical mixing within the water column sustaining high levels of productivity within the surface waters (figure 8.4).

Significant changes are observed during the deposition of the sapropel. At the onset of deposition *G. inflata* disappears from the faunal assemblage, only re-appearing at the termination (figure 8.3). This signifies a change in the water column dynamics, shifting to a more stratified state. The concurrent increase in *N. incompta* would thus be expected perhaps also signalling the development of a Deep Chlorophyll Maximum (DCM). Both *N. incompta* (~ 35%) and *G. bulloides* (~ 25%) dominate the water column during the sapropel however, significant variability is noted. Similarly *G. ruber (alba)* records an initial increase (~ 50%) in the early sapropel but also displays its lowest frequencies (~ 20%) during the latter phase of deposition (figure 8.3). The productivity index indicates increasingly higher trophic levels as the sapropel progresses culminating in the highest levels just prior to the termination of the sapropel. As would be expected the planktonic foraminiferal numbers mirror the productivity indicator (figure 8.4). SST variability is evident within the sapropel with three distinct cold events evident. In fact these events coincide with the lowest recorded annual SSTs (~ 17°C) throughout the entire record (figure 8.3).

Post sapropel the faunal assemblage changes quite dramatically with significant increases in *G. ruber (alba)* (up to 60%). This is mirrored by the significant decrease in *N. incompta* (< 5%). The SPRUDTS-group and *G. bulloides* constitute the remainder of the faunal assemblage (figure 8.2). *G. inflata* makes a brief appearance but never returns to pre sapropel levels. A concomitant decrease in the herbivorous species suggests that nutrients are no longer being supplied to the photic zone and the prevalence of symbiont bearing mixed layer species is testament to this. SSTs remain relatively stable during this time ranging from 16°C in the winter season to ~ 25°C during the summer (figure 8.3).

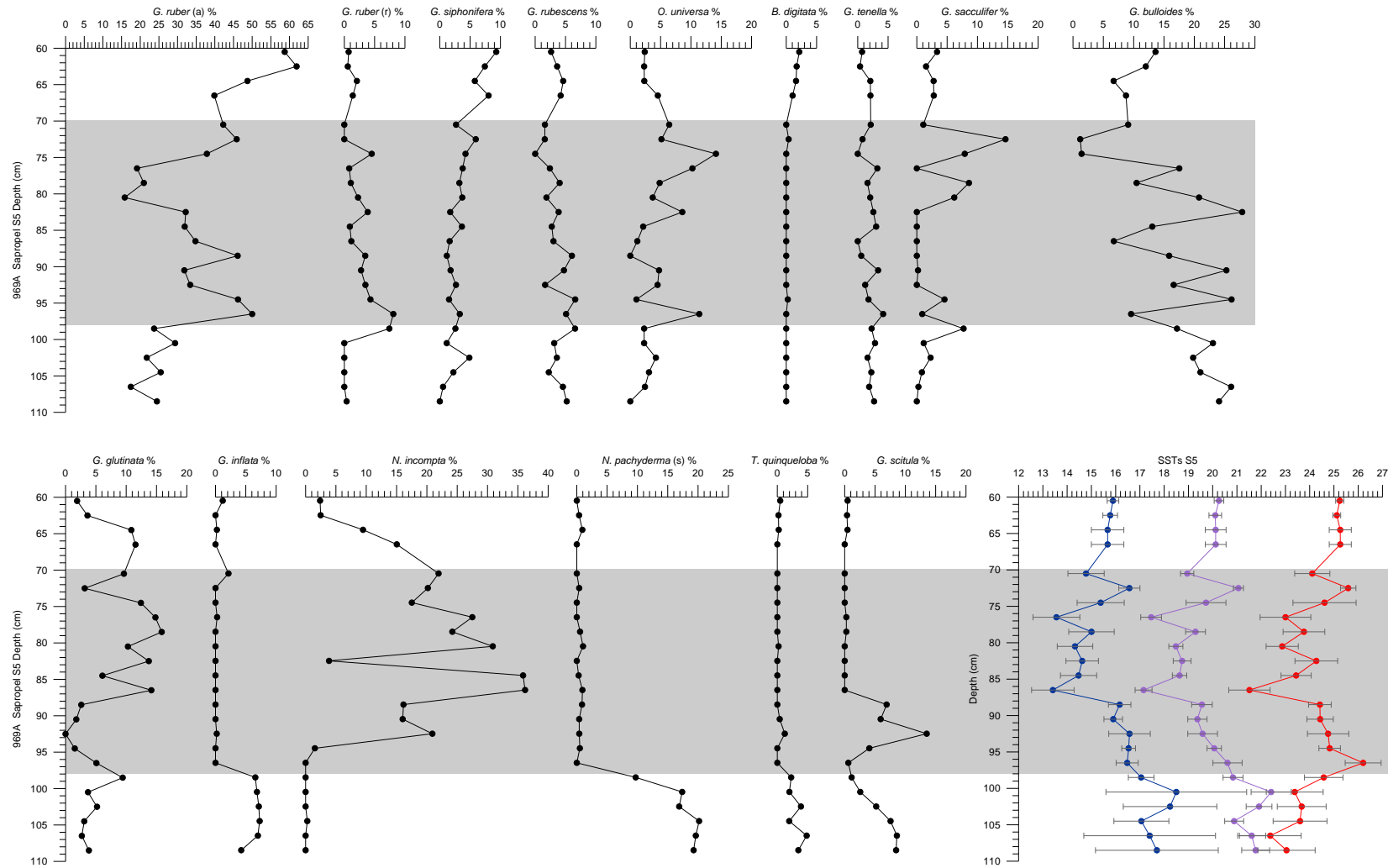


Figure 8.3: Faunal records throughout the deposition of sapropel S5 (shaded area) for core 969A presented with winter (blue), annual (purple) and summer (red) SSTs

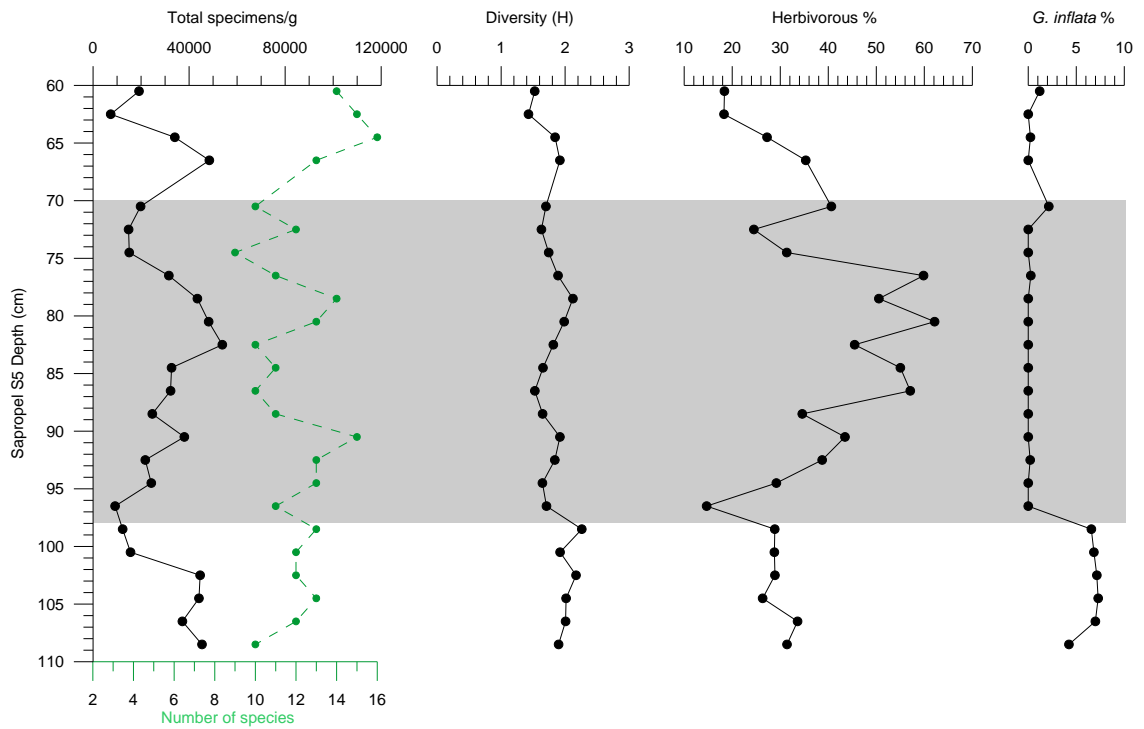


Figure 8.4: Comparison between plots of the ODP core 969A for Sapropel S5. Analysis includes, Total specimens per gram and total number of species, Diversity index, Herbivorous index, *G. inflata* %. The shaded area represents sapropel S5.

### 8.3.1.2 Glacial sapropel S6

Deposited within a glacial period, the faunal assemblages in sapropel S6 are significantly different than those described in the previous section.

It is immediately apparent that the warm water species (*G. ruber* and the SPRUDTS-group) are poorly represented during the deposition of sapropel S6. In fact prior to sapropel deposition *G. ruber (alba)* only represents ~ 5% of the faunal assemblage. Together Neogloboquadrinids group and *G. bulloides* comprise ~ 75% of the entire assemblage with *G. scitula*, *T. quinqueloba* and *G. glutinata* making up the remainder. It is also important to note the significant, albeit low (~ 5%), contribution of *G. inflata* at this time (figure 8.5). An abrupt decline in SSTs is displayed towards the onset of sapropel deposition. Annual SSTs record a decline from ~ 16°C to ~ 10°C (figure 8.5). The productivity indicator would suggest high levels of nutrients however, the near absence of *G. inflata* would indicate that stratification was prominent within the water column (figure 8.6).

The onset of the sapropel sees some significant changes within the faunal assemblage dividing the sapropel into two distinct phases. In the early part of the sapropel the faunal assemblage is dominated by *G. bulloides* (28%), Neogloboquadrinids group (35%) and *T. quinqueloba* (35%). This faunal assemblage coincides with the colder part of the sapropel with winter temperatures falling as low as 6°C, while summer temperatures only reaching 12°C (figure 8.5). The second phase of sapropel deposition records a significant decline in both *T. quinqueloba* and *G. bulloides* and an increase in Neogloboquadrinids group. At this point Neogloboquadrinids group completely dominates the faunal assemblage (65-90%). As expected the Shannon-Winer diversity index notes low diversities at this time (figure 8.6). This change coincides with SSTs increases to 9°C during the winter and 15°C in the summer. The productivity indicator remains high (100%) throughout the sapropel while the stratification index would suggest strong year round stratification. While it might be expected that planktonic foraminiferal numbers might be high in response to the suggested high productivity, the profile does not reflect that. Some degree of variability is noted recording both its lowest (~ 10,000 specimens/g) and highest (~ 120,000 specimens/g) values during the sapropel.

Post sapropel sees a decline in Neogloboquadrinids group to pre sapropel levels (~ 35%) and an abrupt increase in *G. ruber* (~ 20%). *G. bulloides*, *G. glutinata*, *G. inflata* and *G. scitula* comprise the remainder of the assemblage is also reflected in the increase in the Shannon-Wiener diversity index (figure 8.6). An abrupt increase in SST records the return to high (~ 22°C) summer temperatures with winter temperatures averaging just below 14°C. This period also notes a decrease in productivity as suggested by a decline in the percentage of herbivorous species to 60% (figure 8.6).

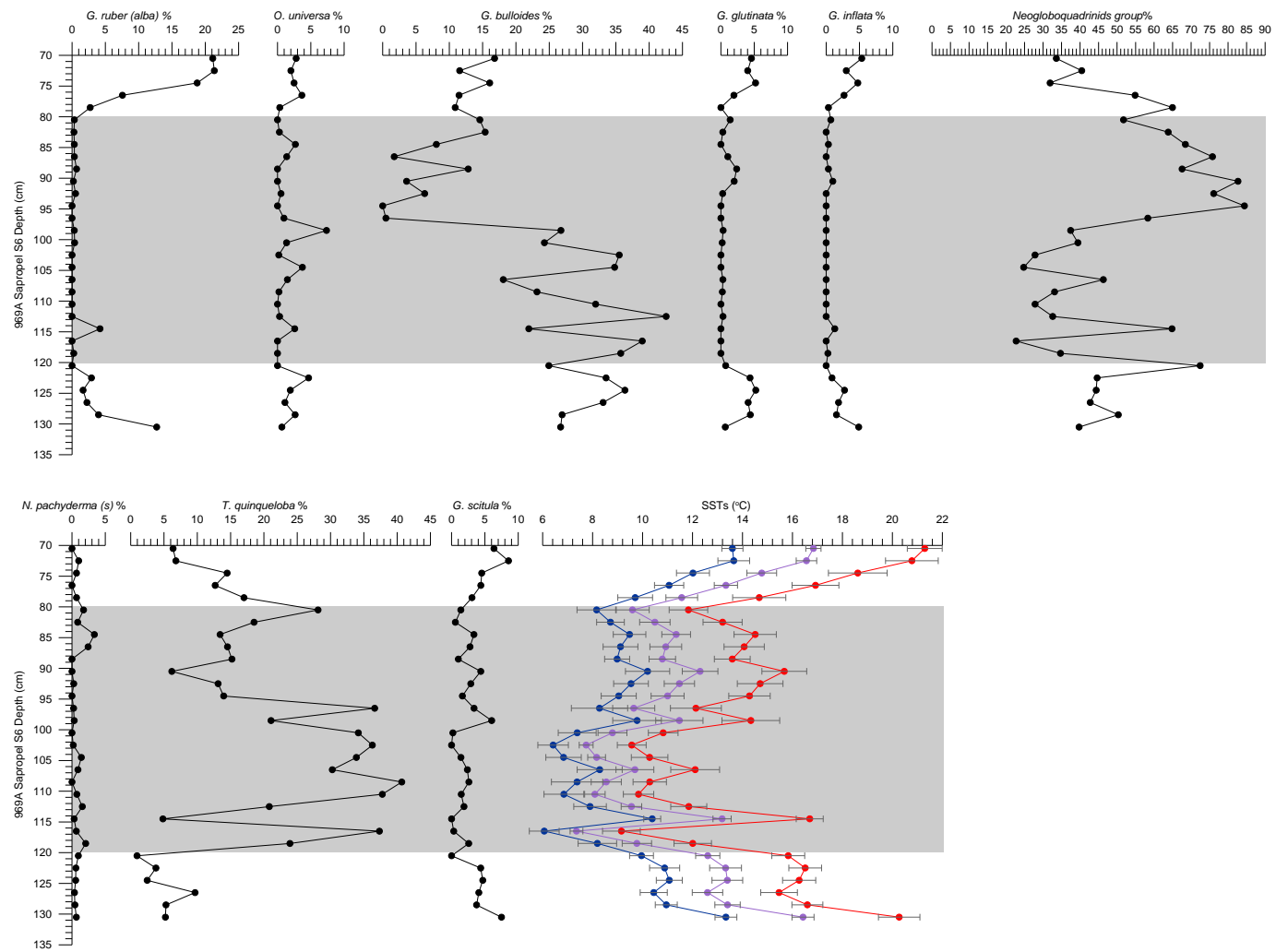


Figure 8.5: Faunal records throughout the deposition of sapropel S6 (grey shaded area) for core 969A presented with winter (blue), annual (purple) and summer (red) SSTs

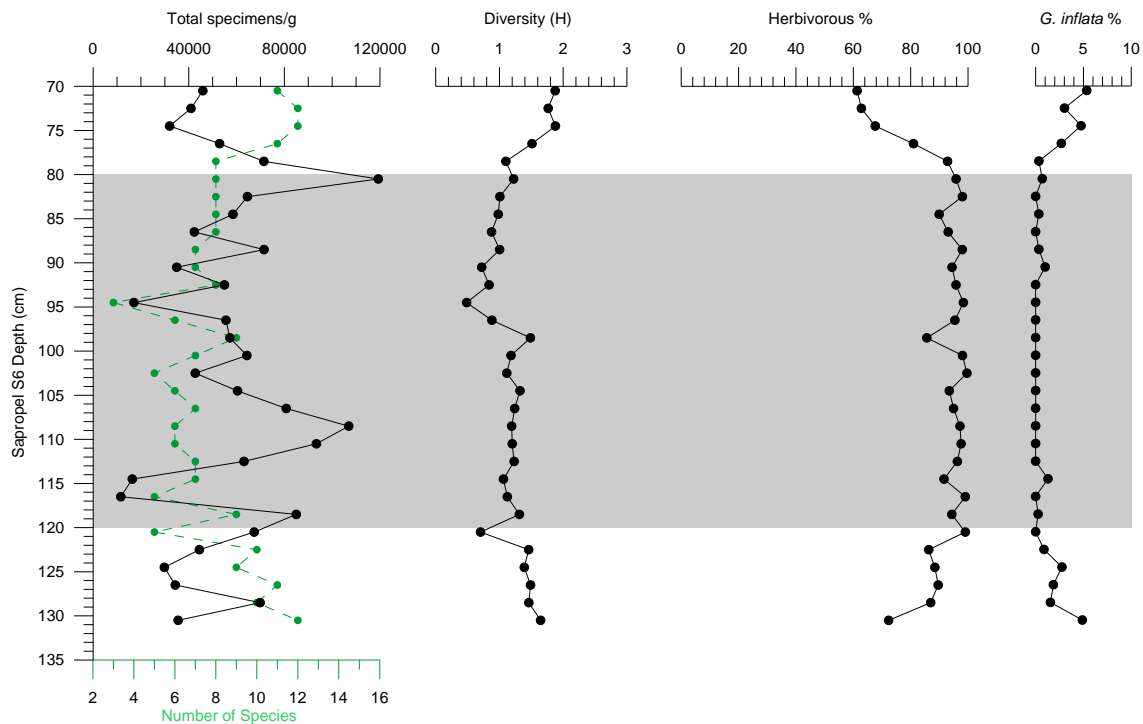


Figure 8.6 Comparison between plots of the ODP core 969A for Sapropel S6. Analysis includes, Total specimens per gram and total number of species, Diversity index, Herbivorous index, *G. inflata* %. The shaded grey area represents Sapropel S6.

### 8.3.3 SUMMARY OF SEA SURFACE TEMPERATURES (SSTS)

Annual, summer and winter SSTS are presented in figures 8.3 and 8.5. As both these sapropel events were deposited during two different time frames, an interglacial (S5) and a glacial (S6) a significant difference in temperature ranges would be expected.

While S5 was deposited in a warm period it is particularly interesting to observe climatic cooling within the depositional period when compared to pre and post results. Preceding the deposition of Eemian sapropel S5 annual SSTS averages at  $\sim 21.5^{\circ}\text{C}$ , yet at the commencement of S5 annual SSTS are documented at  $\sim 22.5^{\circ}\text{C}$  prior to a gradual weakening which concludes in a low of  $\sim 17^{\circ}\text{C}$ , the lowest during the sapropel. An additional two cooling events are observed, one later in the sapropel and one instantaneously following the conclusion of the sapropel; documenting SSTS of  $\sim 17.5^{\circ}\text{C}$  and  $16.5^{\circ}\text{C}$  respectively (figure 8.2). Outside the sapropel SSTS average at  $\sim 20^{\circ}\text{C}$ , similar to those prior to the depositional event.

Prior to the deposition of glacial sapropel S6 annual SSTs averaged at,  $\sim 13.5^{\circ}\text{C}$ , yet at the onset of S6 annual SSTs are noted at  $\sim 9^{\circ}\text{C}$ , a decline of almost  $5^{\circ}\text{C}$ , before increasing to pre sapropel results. A further climatic deterioration concludes to its lowest point of  $\sim 7.5^{\circ}\text{C}$  midway within the sapropel. Beyond this point temperatures increase slightly (up to  $\sim 12^{\circ}\text{C}$ ) before further cooling is witnessed at the conclusion of the sapropel at  $\sim 9.5^{\circ}\text{C}$ . Post sapropel SSTs increase significantly reaching annual highs of  $\sim 17^{\circ}\text{C}$  (figure 8.4).

## 8.4 DISCUSSION

### 8.4.1 PALAEOECOLOGICAL VARIABILITY OF SAPROPELS S5 AND S6

#### *8.4.1.1 Sapropel S5*

The following section will discuss the faunal results for sapropel S5 extracted from ODP core 969A, this will be done in conjunction with other cores located within close proximity in order to give basin wide context to these results (figure 8.2). The planktonic foraminiferal data will enable a reconstruction of the marine environment at a time when the water column was undergoing many changes. Specifically this section will draw on data from other research namely Sangiorgi et al. (2006) and Weldeab et al. (2003b) to facilitate a more holistic approach. Furthermore, SST reconstructions will be used to highlight some of the changes that are noted throughout the depositional event.

The pre-sapropel palaeoenvironmental indexes suggest a water column that is homogenous in its composition, at least during the winter, facilitating the transfer of nutrients into the upper water column. This is consistent with geochemical records presented by Sangiorgi et al. (2006) which indicate a well oxygenated environment undergoing normal pelagic sedimentation. However, while the productivity index is moderate ( $\sim 30\%$ ) it is low comparative to the rest of the record and there is no evidence of the formation of a DCM. Before the onset of the sapropel, SST reconstructions estimate an average annual temperature of  $\sim 21.5^{\circ}\text{C}$  ( $\sim 17.6^{\circ}\text{C}$  in winter and  $\sim 23.4^{\circ}\text{C}$  in summer). These results are

higher than those observed by Sangiorgi et al. (2006) whose temperature results are based on alkenones and recorded pre-sapropel SSTs in the range of 15.3-19.8°C. The error rates associated with both reconstructions can account for some imbalances with the records. Rohling et al. (2004) noted that faunal based SST reconstructions are considerably higher than alkenone-based reconstructions. While the reason for this difference may not be thoroughly understood, it may relate to seasonal changes within the production of alkenones by phytoplankton (Rohling et al, 2004). This relatively stable environment is further corroborated by the high diversity and concentration of benthic foraminifera as observed by Sangiorgi et al. (2006).

The onset of the sapropel observes the first major changes within the depositional environment. The notable absence of *G. inflata* is considered a response to an increase in water column stratification and has been noted by other research during the deposition of sapropels (Cane et al., 2002; Capotondi et al., 2006; Sangiorgi et al., 2006). This stratification is thought to be related to a rapid increase in the freshwater input into the region, which subsequently impedes deep water ventilation and mixing due to an increased density gradient between the surface and intermediate waters. Furthermore, in a study located close to the core utilised in this research, Rohling et al. (2006) noted that during the very early stages of sapropel deposition, *N. incompta* and *G. scitula*, normally indicative of the establishment of a DCM, are nearly non-existent synonymous with this research. However, this quickly changes as both species recover to higher relative abundances as upward nutrient advection begins to occur and the growth of a well-developed DCM occurs (Rohling et al (2006). The productivity index mirrors these observed faunal signals however, they are still relatively low compared to later in the sapropel (figure 8.4). Sangiorgi et al. (2006) suggest this is due to the slow increase in diatom productivity, the main food source for these species. After the initial SST increase at the onset of sapropel a gradual decline in temperatures are evident as sapropel deposition continues. This is consistent with studies undertaken by Rohling et al. (2004) and Sangiorgi et al. (2006) also on sapropel S5.

As deposition of the sapropel continued the first of several cold events is noted, with annual SSTs dipping to ~ 17°C. This cooling event occurred in conjunction with peak abundances

of *N. incompta*, *G. ruber* and the overall increase in the abundance of the herbivorous species. Sangiorgi et al. (2006) recorded similar trends within the temperature regime but more importantly noted a disparity within the oxygen isotopes values displayed by *G. ruber* (indicative of surface waters) and *N. incompta* (indicative of subthermocline temperatures). It would be expected that oxygen isotope values of these species would differ due to their different water depths however, the authors reported a similarity in the results during this stage of sapropel deposition. The authors interpret this signal to reflect either a temporary return to mixing within the water column (although the absence of *G. inflata* would not support that) or to a change in the habitat of one of the two species. Taking into account the change in the faunal assemblage in conjunction with a SST decrease and an increase in productivity levels, it is plausible that thermally induced stratification is temporarily weakened at this time. A reduction in the Mo / Al ratio and concurrent increase in the concentration of benthic foraminifera at this time support this hypothesis (Sangiorgi et al., 2006). Following this cooling event SSTs begin to increase coinciding with the highest recorded numbers of planktonic foraminifera and elevated levels of productivity (figure 8.4). Enhanced SSTs would see a return to strong stratification within the water column suggesting the source of surface water nutrient enhancement is riverine. Indeed Sangiorgi et al. (2006) noted an increase in both K / Al and Mg<sub>det</sub> / Al ratios suggesting an increase in the contribution of the Nile River to sediments south of Crete.

The final phase of sapropel deposition is marked by environmental conditions similar to the onset of the sapropel. Lower numbers of planktonic foraminifera and a decline in herbivorous species are concurrent with SST increases (figure 8.4). Conditions within the water column signify a breakdown in year round stratification and the destabilisation of the DCM (as indicated by the decline in *N. incompta*). Based on the faunal assemblage it is likely that any convection within the water column would be confined to the winter (as is the case in the present day environment) with stratification prevailing for the remainder of the year. Concentrations of benthic foraminiferal numbers display increases at this time in core BAN89-GC09 reflecting a return to more oxygenated conditions (Sangiorgi et al., 2006).

Post sapropel assemblages would be very similar to modern day assemblages in the Mediterranean Sea for this location (Pujol and Vergnaud-Grazzini, 1995). A prevalence of shallow mixed layer species is indicative of oligotrophic surface waters. Furthermore the low frequencies of *G. inflata* would indicate some vertical convection within the water column but at this point it is apparent that the normal mixing conditions observed prior to the onset of the sapropel have not returned. This is mirrored in the low productivity levels recorded in the herbivorous species (figure 8.3 and 8.4).

Ecosystem variability during the deposition of sapropel S5 is evident from the faunal assemblages and can be explained by examining basin wide hydrological dynamics during this depositional event. Based on geochemical evidence Sangiorgi et al. (2006) highlights the absence of a clear source of nutrient input into the region south of Crete despite temperature and oxygen isotope data clearly indicating surface water freshening. However, as is often stated in association with sapropels, the shoaling of the pycnocline into the base of the photic zone will facilitate nutrient transfer into the surface waters enhancing productivity (Rohling and Gieskes, 1989). As such there would be no reason to suggest the same did not happen during S5. Indeed as indicated by elevated Ba profiles, palaeoproductivity is noted as being significant during the deposition of S5 particularly in the region south of Crete (Weldeab et al., 2003b). Despite this, Weldeab et al. (2003b) indicate that pycnocline shoaling is not enough to account for the high productivity levels recorded in ODP 969E. The authors go on to suggest that under a weakened anti-estuarine circulation the Cretan gyre could have relocated to a position south of Crete. The resultant reduction in density gradients would allow for the establishment of cyclonic vortices. This would provide a further mechanism whereby nutrients could be transferred into the surface waters (Waldeab et al., 2003b). Figure 8.7 presents the mechanisms to facilitate the high levels of productivity observed at this time. With this in mind it is expected that the maintenance and strength of these vortices are sensitive to external forcing, such as changes in SSTs and therefore the variability that is observed within S5 is a direct response to this.

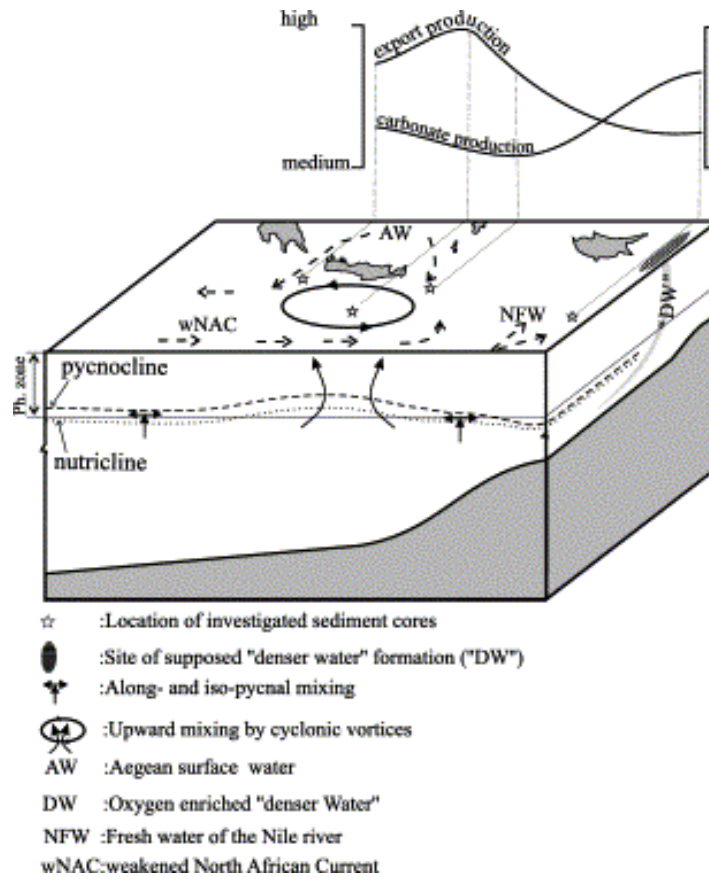


Figure 8.7: Diagram illustrating spatial variability of export and carbonate productivities during sapropel S5 and suggested method of nutrient delivery and their magnitude at the different locations (courtesy of Weldeab et al., 2003).

#### 8.4.1.2 SAPROPEL S6

Prior to the onset of the sapropel, the SSTs indicate a transitional environment associated with climatic deterioration. This significant reduction in annual SSTs (~ 4°C) is comparable to alkenone estimates in the eastern Levantine basin (Kallel et al., 2000). It is suggested that at this time cold surface water favours convection within the water column creating eutrophic conditions. The presence of *G. inflata* and the increasing values of the herbivorous species would testify to this (figure 8.5).

The onset of sapropel formation is marked by significant changes within the faunal assemblages. The elevated abundances of *T. quinqueloba* in association with *G. bulloides* is

suggestive of high productivity levels in subsurface waters (Capotondi et al., 2016). However, in contrast to the upwelling conditions that produce this nutrient enhancement, the absence of *G. inflata* supports water column stratification. Therefore the supply of nutrients must originate from elsewhere. Based on speleothem records Bard et al. (2002) suggest like interglacial sapropels, S6 was deposited in a humid period caused by a basin wide increase in rainfall. The additional inputs of freshwater into the Mediterranean Sea at this time facilitated elevated productivity in the surface waters. Moreover, this is further supported by Ayalan et al. (2002) who suggest that throughout the duration of MIS 6 the Mediterranean region was influenced by two very different climatic extremes; large ice sheet coverage over the European continent and the wet tropical regions associated with the African monsoon. These authors conclude that sapropel S6 was formed in the latter, a period of enhanced pluvial activity. This corroborates previous work undertaken by Kallel et al. (2000).

The later phase of sapropel deposition once again displays a clear shift in the faunal assemblage. Decreases in both *G. bulloides* and *T. quinqueloba* are replaced by significant increases in Neogloboquadrinids group (figure 8.5). The herbivorous species would indicate that productivity is still high so it can only be assumed that increases in SSTs are the cause of change in the faunal assemblage. Indeed it is frequently noted that aside from its nutrient requirements *T. quinqueloba* is a strong cold water indicator (Rohling et al., 1993a; Pujol and Vergnaud-Grazzini, 1995). Albeit at a lower resolution, an increase in SSTs in the latter stages of sapropel deposition are noted by Kallel et al. (2000). The continued dominance of Neogloboquadrinids group would imply that the species is not affected by SSTs providing the food source remains intact (Pujol and Vergnaud-Grazzini, 1995). It is therefore assumed that throughout the duration of the sapropel the development of a DCM has been maintained. The question arises to the dramatic disappearance of *G. bulloides*. Based on results from nannofossil assemblages, Castradori (1993) hypothesised that during the deposition of S6 the pycnocline reached a much shallower position within the photic zone, compared to other sapropels. This was based on the assumption of lower surface water temperatures and higher surface water salinities. The ensuing reduction in the density contrast between the surface and intermediate waters facilitates the shallowing of

the pycnocline. The shallow depth of the pycnocline was determined due to the presence of *Florisphaera profunda* a species usually found in the lower photic zone, but during S6, dominating the upper levels (Castradori, 1993). Given this scenario, it is plausible that the shallow pycnocline and associated DCM created competition between the ecological niches of *G. bulloides* and Neogloboquadrinids group causing the demise of the less dominant species.

The termination of the sapropel marks a climatic amelioration with annual SST estimates of  $\sim 17^{\circ}\text{C}$ . The lower abundances of the herbivorous species suggests reduced surface water nutrient concentrations which is supported by an increase in *G. ruber*, a species that thrives in oligotrophic conditions (Rohling et al., 1993a; Pujol and Vergnaud-Grazzini, 1995). The presence of *G. inflata* would signal a return of vertical mixing, at least within the winter season.

## 8.5 CONCLUSIONS

Occurring during MIS 5e, sapropel S5 was deposited during relatively warm climates. However, analysis of faunal variations across the sapropel has revealed significant variability during this depositional event. The observed variability is indicative of changing environmental conditions related to the strengthening / weakening of cyclonic vortices associated with the Cretan Gyre (Weldeab et al., 2003b). Cooling episodes recorded by SST estimates would be testament to the fluctuating environmental conditions experienced at this time. Previous research has highlighted the region to the south of Crete as an area of exceptionally high productivity during the deposition of S5. The shoaling of the pycnocline into the photic zone has been explained as the mechanism to facilitate the high levels of productivity (Weldeab et al., 2003b). The elevated levels of herbivorous species coeval with an absence of *G. inflata* would support this theory highlighting a strongly stratified water column and the development of a DCM. Palaeoproductivity variability during S5 was marked by spatial differences in areas around Crete and throughout the Levantine basin dependent on the proximity or availability to nutrients (i.e. riverine inputs). The results

from this research compare favourably with those recorded from the nearby core of BAN89-GC09 further corroborating this regional signal.

By comparison, sapropel S6 was deposited during a glacial episode (MIS 6) under significantly lower SSTs. Synonymous with interglacial sapropels research has indicated that S6 was deposited during a period of enhanced pluvial activity (Kallel et al., 2000; Ayalan et al., 2002). Stratification within the water column was prominent evident by elevated abundances of Neogloboquadrinids group however, faunal analysis reveals two distinct phases within the deposition of the sapropel. The initial phase of deposition is characterised by lower SSTs and dominated by cold, nutrient rich species. The latter phase of the sapropel notes the dramatic disappearance of *G. bulloides* in favour of Neogloboquadrinids group. It is suggested that extreme shallowing of the pycnocline created ecological pressures between the species resulting in the decline of *G. bulloides*.

# CHAPTER 9

## CONCLUSIONS AND FURTHER WORK

### 9.1 CONCLUSIONS

The focus of this research was distributed between two distinct topics, firstly the palaeoenvironmental reconstructions utilising planktonic foraminiferal assemblages and secondly to understand how environmental variability within the marine environment affected micro-organisms in terms of their mean test size. Primarily a single core (ODP 969A), located along the Mediterranean Ridge within the eastern basin of the Mediterranean Sea, was the focus of this research. The research aims were; to assess the downcore variations within planktonic faunal assemblages since the Last Glacial Maximum, to investigate the changes in mean test size with reference to biotic and abiotic factors and to provide a comparative palaeoecological analysis between sapropels S5 and S6.

Chapter 6 utilised micropalaeontological data in conjunction with multivariate statistical analysis in order to present a palaeoenvironmental reconstruction since the Last Glacial Maximum. A second core (ODP 964A) located within the Ionian Sea was used in order to provide a comparative analysis whilst also facilitating regional correlations. In order to best elucidate the climatic phases since the LGM a cluster analysis was completed revealing four distinct phases; a glacial assemblage, a deglaciation assemblage, the Holocene Climatic Optimum and finally the modern day assemblages. The planktonic foraminiferal assemblages were further utilised in order to reconstruct the SSTs throughout this time frame. The results of this chapter noted that in conjunction with other work presented, that each defined period showcased some interesting changes within both foraminiferal assemblages and SSTs. The glacial period was characterised by low SSTs with a homogenous water column and high levels of productivity. The period of deglaciation,

which included the Bølling-Allerød and Younger Dryas, was a time of climate instability. Coinciding with the deposition of sapropel S1, The Holocene Climatic Optimum was characterised by enhanced levels of primary productivity linked to increased riverine inputs into the surface waters of the eastern Mediterranean. Finally it noted that the modern Mediterranean Sea is characterised by highly oligotrophic waters with reduced nutrient levels. The resultant faunal record from this chapter has provided valuable Late Quaternary palaeoclimatic data in the more poorly investigated part of the eastern basin. It has also facilitated the correlation with other palaeoclimatic records in the Mediterranean Sea.

Chapter 7 set about establishing the mean test size variations for three predefined species of planktonic foraminifera. This was completed using the species *Orbulina universa*, *Globigerinella siphonifera* and *Neogloboquadrina incompta* selected from the > 150µm size fraction. The use of Cell<sup>^</sup>b imaging software was utilised to take individual images of each species and then measurements of the longest axis were calculated for pre, during and post sapropel intervals. Examining the mean test size of each species may provide an insight into how environmental changes will affect this basic but diverse species. Overall the results did not record an increase in mean test size throughout the deposition of the sapropels. However, distinct trends were observed between the individual species. *O. universa* the largest of the species studied recorded its largest test sizes throughout the entire record. Mean test size did not increase significantly during the sapropel but a notable increase in the number of specimens/g was observed. This indicated that increased nutrients within the water column did not affect test size but may have sped up the reproduction cycle of this species. *G. siphonifera* recorded an increase in mean test size within the deposition of both sapropel layers, although the specimens/g only exhibited minute changes. So it is surmised that increased nutrients within the marine environment benefited this species in terms of mean test size but an increase in its reproduction was not evident. *N. incompta* exhibited the least significant change within its overall size, however its specimens/g increased significantly during both sapropels. This increase in absolute abundance due to the availability of nutrients is very indicative of how this herbivorous species reacts.

Chapter 8 focused on the faunal assemblages associated with the deposition of Eemian warm sapropel S5 and glacial sapropel S6. Analysis of S5 displayed faunal variations across the sapropel associated with water column variability. These changes were noted to be indicative of changes within cyclonic vortices associated with the Cretan gyre. High productivity levels were facilitated by the shoaling of the pycnocline into the photic zone. This strongly stratified water column and the development of a DCM was confirmed by the increased abundance of herbivorous species in conjunction with the absence of *G. inflata*. Glacial sapropel S6 experienced significantly lower SSTs and was deposited during periods of enhanced pluvial activity. Two distinct phases of deposition was noted through faunal analysis, initially deposition is characterised by lower SSTs and dominated by cold, nutrient rich species. The concluding phase exhibits the dramatic disappearance of *G. bulloides* in favour of Neogloboquadrinids group. It is suggested that extreme shallowing of the pycnocline created ecological pressures between the species resulting in the decline of *G. bulloides*.

## 9.2 LIMITATIONS AND RECOMMENDATIONS

Notwithstanding the advantages of utilising planktonic foraminifera as a mechanism for palaeoenvironmental reconstruction, some limitations do exist. One such limitation is the preservation of fossils and the effect of dissolution. While much care has been taken to minimise this in the processing stages, some dissolution cannot be disregarded.

Furthermore recent studies on cryptic diversity on species of planktonic foraminifera, may be an issue with dealing with some species, however, the species studied within chapter 7 were picked with this issue in mind.

The scope of this research relied on the understanding of modern environmental parameters and how they exhibit control over distribution, abundance and diversity. To further advance this research I would suggest that mean test size data to be completed on additional species of planktonic foraminifera such as *G. bulloides* whose penchant for upwelling areas would yield more information about individual species preferences.

The location of the core 969A exhibited high productivity levels during S5, perhaps the selection of a core in another locality would produce different results, ultimately aiding the understanding of species response to environmental parameters. Similarly measuring mean size data in sediments not affected by sapropels might provide some interesting insights.

Glacial sapropel S6 needs further expansion within palaeoenvironmental research, there is not enough focus on the ecological significance of sapropel deposition within cold spells in the Mediterranean Sea and while this project aimed to help fill in some of that data, further cores containing S6 and maybe S8 would help to build up a picture of these cold based sapropels on a more basin wide scale.

## BIBLIOGRAPHY

- Abramovich, S., Keller, G. (2009) "Lilliput effect in late Maastrichtian planktic foraminifera: Response to environmental stress", *Palaeogeography, Palaeoclimatology, Palaeoecology*, 284(1-2), 47-62.
- Adatte, T., Berner, Z., Abramovich, S., Keller, G. (2009) "Biotic effects of the Chicxulub impact, K–T catastrophe and sea level change in Texas", *Palaeogeography, Palaeoclimatology, Palaeoecology*, 271(1-2), 52-68.
- Adloff, F., Mikolajewicz, U., Kučera, M., Grimm, R., Maier-Reimer, E., Schmiedl, G., Emeis, K.-C. (2011) "Upper ocean climate of the Eastern Mediterranean Sea during the Holocene Insolation Maximum – a model study," *Climate of the Past*, 7(4), 1103–1122.
- Aksu, A., Hiscott, R., İslar, E. (2016) "Late Quaternary chronostratigraphy of the Aegean Sea sediments: Special reference to the ages of sapropels S1–S5", *Turkish journal of earth sciences*, 25, 1-18.
- Aldridge, D., Beer, C., Purdie, D. (2012) "Calcification in the planktonic foraminifera *Globigerina bulloides*, linked to phosphate concentrations in surface waters of the North Atlantic Ocean", *Biogeosciences*, 9(5), 1725-1739.
- Al-Sabouni, N., Kucera, M., Schmidt, D. (2007) "Vertical niche separation control of diversity and size disparity in planktonic foraminifera", *Marine Micropaleontology*, 63(1-2), 75-90.
- Andersen, N., Hamann, Y., Ehrmann, W., Schmiedl, G., Kuhnt, T. (2008) "Stable isotopic composition of Holocene benthic foraminifera from the eastern Mediterranean sea: Past changes in productivity and deep water oxygenation", *Palaeogeography, Palaeoclimatology, Palaeoecology*, 268(1-2), 106-115.
- Ariztegui, D., Asioli, A., Lowe, J., Trincardi, F., Vigliotti, L., Tamburini, F., Chondrogianni, C., Accorsi, C., Bandini Mazzanti, M., Mercuri, A., Van der Kaars, S., McKenzie, J., Oldfield, F. (2000) "Palaeoclimate and the formation of sapropel S1: inferences from Late Quaternary lacustrine and marine sequences in the central Mediterranean region", *Palaeogeography, Palaeoclimatology, Palaeoecology*, 158(3-4), 215-240.
- Armstrong, H., Brasier, M. (2009) *Microfossils*, 1st ed, Blackwell Publishing: Malden (Massachusetts).
- Arnold, A., Parker, W. (1999) "Biogeography of planktonic Foraminifera", *Modern Foraminifera*, 103-122.
- Awad, A., Almazroui, M. (2016) "Synoptic regimes associated with the eastern Mediterranean wet season cyclone tracks", *Atmospheric Research*, 180, 92-118.
- Ayalon, A., Bar-Matthews, M., Kaufman, A. (2002) "Climatic conditions during marine oxygen isotope stage 6 in the eastern Mediterranean region from the isotopic composition of speleothems of Soreq Cave, Israel", *Geology*, 30(4), 303.
- Aze, T., Pearson, P., Dickson, A., Badger, M., Bown, P., Pancost, R., Gibbs, S., Huber, B., Leng, M., Coe, A., Cohen, A., Foster, G. (2014) "Extreme warming of tropical waters during the Paleocene-Eocene Thermal Maximum", *Geology*, 42(9), 739-742.
- Azov, Y., Trees, C., El Sayed, S., Townsend, D., Berman, T. (1984) "Optical transparency, chlorophyll and primary productivity in the Eastern Mediterranean near the Israeli coast", *OCEANOLOGICA ACTA*, 7(3).

- Azrieli-Tal, I., Matthews, A., Bar-Matthews, M., Almogi-Labin, A., Vance, D., Archer, C., Teutsch, N. (2014) "Evidence from molybdenum and iron isotopes and molybdenum–uranium covariation for sulphidic bottom waters during Eastern Mediterranean sapropel S1 formation," *Earth and Planetary Science Letters*, 393, 231–242.
- Bard, E., Delaygue, G., Rostek, F., Antonioli, F., Silenzi, S., Schrag, D. (2002) "Hydrological conditions over the western Mediterranean basin during the deposition of the cold Sapropel 6 (ca. 175 kyr BP)", *Earth and Planetary Science Letters*, 202(2), 481-494.
- Bar-Matthews, M., Ayalon, A., Kaufman, A. (2000) "Timing and hydrological conditions of Sapropel events in the Eastern Mediterranean, as evident from speleothems, Soreq cave, Israel", *Chemical Geology*, 169(1-2), 145-156.
- Barrows, T., El Hajaz, Y., Munro, R., El Tom, O., Macklin, M., Woodward, J., Williams, F., Duller, G., Williams, M. (2015) "Causal links between Nile floods and eastern Mediterranean sapropel formation during the past 125 kyr confirmed by OSL and radiocarbon dating of blue and white Nile sediments", *Quaternary Science Reviews*, 130, 89-108.
- Bé, A., Duplessy, J. (1976) "Subtropical Convergence Fluctuations and Quaternary Climates in the Middle Latitudes of the Indian Ocean", *Science*, 194(4263), 419-422.
- Bé, A., Wiebe, P., Free, R., Sverdløve, M., Fairbanks, R. (1982) "Vertical distribution and isotopic fractionation of living planktonic foraminifera from the Panama basin", *Nature*, 298(5877), 841-844.
- Bemis, B., Spero, H., Lea, D., Bijma, J. (2000) "Temperature influence on the carbon isotopic composition of *Globigerina bulloides* and *Orbulina universa* (planktonic foraminifera)", *Marine Micropaleontology*, 38(3-4), 213-228.
- Benito, X., Trobajo, R., Cearreta, A. and Ibáñez, C. (2016) "Benthic foraminifera as indicators of habitat in a Mediterranean delta: implications for ecological and palaeoenvironmental studies", *Estuarine, Coastal and Shelf Science*, 180, pp. 97-113. doi: 10.1016/j.ecss.2016.06.001.
- Benjamin, J., Rovere, A., Fontana, A., Furlani, S., Vacchi, M., Inglis, R., Galili, E., Antonioli, F., Sivan, D., Miko, S., Mourtzas, N., Felja, I., Meredith-Williams, M., Goodman-Tchernov, B., Kolaiti, E., Anzidei, M., Gehrels, R. (2017) "Late Quaternary sea-level changes and early human societies in the central and eastern Mediterranean Basin: An interdisciplinary review," *Quaternary International*.
- Bensi, M., Cardin, V., Meccia, V., Velaoras, D. (2016) "Effects of the eastern Mediterranean sea circulation on the thermohaline properties as recorded by fixed deep-ocean observatories", *Deep Sea Research Part I: Oceanographic Research Papers*, 112, 1-13.
- Berger, W. (1969) "Planktonic Foraminifera: Basic Morphology and Ecologic Implications", *Journal of Palaeontology*, 43(6), 1369-1383.
- Berger, W. (1970) "Planktonic Foraminifera: Selective solution and the lysocline", *Marine Geology*, 8(2), 111-138.
- Bernasconi, S., Pika-Biolzi, M. (2000) "A stable isotope study of multiple species of planktonic foraminifera across sapropels of the Tyrrhenian Sea, ODP Site 974", *Palaeogeography, Palaeoclimatology, Palaeoecology*, 158(3-4), 281-292.
- Bernstein, M., Luz, B. (1976) "Planktonic foraminifera and quantitative paleoclimatology of the eastern Mediterranean", *Marine Micropaleontology*, 1, 307-323.
- Bijma, J., Faber, W. and Hemleben, C. (1990). Temperature and salinity limits for growth and survival of some planktonic foraminifers in laboratory cultures. *The Journal of Foraminiferal Research*, 20(2), pp.95-116.

- Bijma, J., Faber, W., Hemleben, C. (1990) "Temperature and salinity limits for growth and survival of some planktonic foraminifers in laboratory cultures", *The Journal of Foraminiferal Research*, 20(2), 95-116.
- Birch, C.E., Parker, D.J., Marsham, J.H., Copsey, D., Garcia-Carreras, L. (2014) "A seamless assessment of the role of convection in the water cycle of the West African Monsoon," *Journal of Geophysical Research: Atmospheres*, 119(6), 2890–2912.
- Bojariu, R., Gimeno, L. (2003) "Predictability and numerical modelling of the north Atlantic oscillation", *Earth-Science Reviews*, 63(1-2), 145-168.
- Bouloubassi, I., Guehenneux, G., Rullkötter, J. (1998) "Biological marker significance of organic matter origin in sapropels from the Mediterranean Ridge, Site 969", *Proceedings of the Ocean Drilling Program, 160 Scientific Results*.
- Boussetta, S., Kallel, N., Bassinot, F., Labeyrie, L., Duplessy, J., Caillon, N., Dewilde, F., Rebaubier, H. (2012) "Mg/Ca-paleothermometry in the western Mediterranean Sea on planktonic foraminifer species *Globigerina bulloides*: Constraints and implications", *Comptes Rendus Geoscience*, 344(5), 267-276.
- Broccoli, A.J., Dahl, K.A., Stouffer, R.J. (2006) "Response of the ITCZ to Northern Hemisphere cooling," *Geophysical Research Letters*, 33(1).
- Cane, T., Rohling, E., Kemp, A., Cooke, S., Pearce, R. (2002) "High-resolution stratigraphic framework for Mediterranean sapropel S5: defining temporal relationships between records of Eemian climate variability", *Palaeogeography, Palaeoclimatology, Palaeoecology*, 183(1-2), 87-101.
- Capotondi, L., Maria Borsetti, A., Morigi, C. (1999) "Foraminiferal ecozones, a high resolution proxy for the late Quaternary biochronology in the central Mediterranean Sea", *Marine Geology*, 153(1-4), 253-274.
- Capotondi, L., Principato, M., Morigi, C., Sangiorgi, F., Maffioli, P., Giunta, S., Negri, A., Corselli, C. (2006) "Foraminiferal variations and stratigraphic implications to the deposition of sapropel S5 in the eastern Mediterranean", *Palaeogeography, Palaeoclimatology, Palaeoecology*, 235(1-3), 48-65.
- Capozzi, R., Negri, A. (2009) "Role of sea-level forced sedimentary processes on the distribution of organic carbon-rich marine sediments: A review of the Late Quaternary sapropels in the Mediterranean Sea", *Palaeogeography, Palaeoclimatology, Palaeoecology*, 273(3-4), 249-257.
- Cesbron, F., Geslin, E., Jorissen, F., Delgard, M., Charrieau, L., Deflandre, B., Jézéquel, D., Anschutz, P., Metzger, E. (2016) "Vertical distribution and respiration rates of benthic foraminifera: Contribution to aerobic remineralization in intertidal mudflats covered by *Zostera noltei* meadows", *Estuarine, Coastal and Shelf Science*, 179, 23-38.
- Chaumillon, E., Mascle, J. (1997) "From foreland to forearc domains: New multichannel seismic reflection survey of the Mediterranean ridge accretionary complex (Eastern Mediterranean)", *Marine Geology*, 138(3-4), 237-259.
- Chaumillon, E., Mascle, J. (1998) "An overview of Mediterranean ridge collisional accretionary complex as deduced from multichannel seismic data", *Geo-Marine Letters*, 18(2), 81-89.
- Ciappa, A. (2014) "The controversial path of Atlantic water in the eastern Mediterranean", *Progress in Oceanography*, 123, 74-83.
- Ciceran, M. (2002) Istria on the Internet - Geology & Meteorology - Winds: Bora--Adriatic Sea [online], available: <http://www.istrianet.org/istria/geosciences/meteorology/winds/bora-adriatic.htm> [accessed 21 Feb 2017].
- Cita, M. (1976) "Biodynamic effects of the messinian salinity crisis on the evolution of planktonic

foraminifera in the mediterranean", *Palaeogeography, Palaeoclimatology, Palaeoecology*, 20(1-2), 23-42.

Clay Kelly, D., Bralower, T., Zachos, J., Silva, I., Thomas, E. (1996) "Rapid diversification of planktonic foraminifera in the tropical Pacific (ODP Site 865) during the late Paleocene thermal maximum", *Geology*, 24(5), 423.

CLIMAP (1976) "The Surface of the Ice-Age Earth", *Science*, 191(4232), 1131-1137.

Cooke, S., Casford, J., Fontanier, C., Jorissen, F., Rohling, E., Abu-Zied, R. (2008) "Benthic foraminiferal response to changes in bottom-water oxygenation and organic carbon flux in the eastern Mediterranean during LGM to recent times", *Marine Micropaleontology*, 67(1-2), 46-68.

Corbí, H., Soria, J. (2016) "Late Miocene–early Pliocene planktonic foraminifer event-stratigraphy of the Bajo Segura basin: A complete record of the western Mediterranean", *Marine and Petroleum Geology*, 77, 1010-1027.

Corliss, B., Nolet, G. (1990) "Benthic foraminiferal evidence for reduced deep-water circulation during sapropel deposition in the eastern Mediterranean", *Marine Geology*, 94(1-2), 109-130.

Corselli, C., Negri, A., Giunta, S., Maffioli, P., Sangiorgi, F., Morigi, C., Principato, M., Capotondi, L. (2006) "Foraminiferal variations and stratigraphic implications to the deposition of sapropel S5 in the eastern Mediterranean", *Palaeogeography, Palaeoclimatology, Palaeoecology*, 235(1-3), 48-65.

Corselli, C., Principato, M., Maffioli, P., Crudeli, D. (2002) "Changes in planktonic assemblages during sapropel S5 deposition: Evidence from Urania Basin area, eastern Mediterranean", *Paleoceanography*, 17(3), 1-1-1-30.

Cramp, A., O'Sullivan, G. (1999) "Neogene sapropels in the Mediterranean: a review", *Marine Geology*, 153(1-4), 11-28.

Creveling, J., Mitrovica, J., Clark, P., Waelbroeck, C., Pico, T. (2017) "Predicted bounds on peak global mean sea level during marine isotope stages 5a and 5c", *Quaternary Science Reviews*, 163, 193-208.

Cristofalo, G., Serravall, R. (1999) "On the presence of a coastal current of Levantine intermediate water in the central Tyrrhenian sea", *Oceanologica Acta*, 22(3), 281-290.

Cutler, K., Edwards, R., Taylor, F., Cheng, H., Adkins, J., Gallup, C., Cutler, P., Burr, G., Bloom, A. (2003) "Rapid sea-level fall and deep-ocean temperature change since the last interglacial period", *Earth and Planetary Science Letters*, 206(3-4), 253-271.

De Lange, G., Becker, J., Nijenhuis, I. (2001) "Geochemistry of coeval marine sediments in Mediterranean ODP cores and a land section: implications for sapropel formation models", *Palaeogeography, Palaeoclimatology, Palaeoecology*, 165(1-2), 97-112.

De Lange, G., Erba, E., Corselli, C., Slomp, C., Ziveri, P., Crudeli, D., Principato, M. (2006) "Phyto\_ and zooplankton paleofluxes during the deposition of sapropel S1 (eastern Mediterranean): Biogenic carbonate preservation and paleoecological implications", *Palaeogeography, Palaeoclimatology, Palaeoecology*, 235(1-3), 8-27.

De Lange, G., Nijenhuis, I. (2000) "Geochemical constraints on Pliocene sapropel formation in the eastern Mediterranean", *Marine Geology*, 163(1-4), 41-63.

De Lange, G., Thomson, J., Reitz, A., Slomp, C., Speranza Principato, M., Erba, E., Corselli, C. (2008) "Synchronous basin-wide formation and redox-controlled preservation of a Mediterranean sapropel", *Nature Geoscience*, 1(9), 606-610.

De Lange, G., Triantaphyllou, M., Filippidi, A. (2016) "Eastern-Mediterranean ventilation variability during

sapropel S1 formation, evaluated at two sites influenced by deep-water formation from Adriatic and Aegean seas", *Quaternary Science Reviews*, 144, 95-106.

De Rijk, S., Hayes, A., Rohling, E. (1999) "Eastern Mediterranean sapropel S1 interruption: an expression of the onset of climatic deterioration around 7 ka BP", *Marine Geology*, 153(1-4), 337-343.

De Vargas, C., Norris, R., de Garidel-Thoron, T., Ujiie, Y., Escarguel, G., Quillévéré, F., Morard, R. (2009) "Morphological recognition of cryptic species in the planktonic foraminifer *Orbulina universa*", *Marine Micropaleontology*, 71(3-4), 148-165.

De Vernal, A., Hillaire-Marcel, C. (2007) *Proxies in Late Cenozoic Paleoceanography, Vol. 1*, Elsevier Science: Amsterdam.

De Waal, A., Roodt, H., de Villiers, J., Koen, H. (2017) "An expert-driven causal model of the rhino poaching problem", *Ecological Modelling*, 347, 29-39.

Demirov, E., Pinardi, N. (2002) "Simulation of the Mediterranean Sea circulation from 1979 to 1993: Part I. The interannual variability", *Journal of Marine Systems*, 33-34, 23-50.

d-maps (2007) Mediterranean Sea: Free Map, Free Blank Map, Free Outline Map, Free Base Map: Hydrography, States [online], available: [http://d-maps.com/carte.php?num\\_car=3128&lang=en](http://d-maps.com/carte.php?num_car=3128&lang=en) [accessed 31 Jan 2017].

D'Ortenzio, F., Ribera d'Alcalà, M. (2009) "On the trophic regimes of the Mediterranean Sea: a satellite analysis", *Biogeosciences*, 6(2), 139-148.

Dowset, H., Robinson, M. (1998) Application of the Modern Analog Technique (MAT) Of Sea Surface Temperature Estimation to Middle Pliocene North Pacific Planktonic Foraminifer Assemblages [online], *Palaeo-electronica.org*, available: <http://palaeo-electronica.org/content/1-1-application-of-modern-analog> [accessed 5 Jun 2017].

Ducassou, E., Mulder, T., Migeon, S., Gonthier, E., Murat, A., Revel, M., Capotondi, L., Bernasconi, S., Masclé, J. and Zaragosi, S. (2008) "Nile floods recorded in deep Mediterranean sediments", *Quaternary Research*, 70(03), pp. 382-391. doi: 10.1016/j.yqres.2008.02.011.

El-Geziry, T., Bryden, I. (2010) "The circulation pattern in the Mediterranean Sea: Issues for modeller consideration", *Journal of Operational Oceanography*, 3(2), 39-46.

Emeis, K., Lourens, L., Ziegler, M., Grant, K., Adloff, F., Müller-Navarra, K., Schmiedl, G., Mikolajewicz, U., Maier-Reimer, E., Grimm, R. (2015) "Late glacial initiation of Holocene eastern Mediterranean sapropel formation", *Nature Communications*, 6, 7099.

Emeis, K., Robertson, A., Richter, C. (1996) "Proceedings of the Ocean Drilling Program", *Initial Reports*, 160.

Emeis, K., Sakamoto, T., Wehausen, R., Brumsack, H. (2000) "The sapropel record of the eastern Mediterranean Sea — results of Ocean Drilling Program Leg 160", *Palaeogeography, Palaeoclimatology, Palaeoecology*, 158(3-4), 371-395.

Emeis, K., Schmiedl, G., Maier-Reimer, E., Grimm, R., Kučera, M., Mikolajewicz, U., Adloff, F. (2011) "Upper ocean climate of the eastern Mediterranean sea during the Holocene Insolation maximum – a model study", *Climate of the Past*, 7(4), 1103-1122.

Emeis, K., Schulz, H., Struck, U., Rossignol-Strick, M., Erlenkeuser, H., Howell, M., Kroon, D., Mackensen, A., Ishizuka, S., Oba, T., Sakamoto, T., Koizumi, I. (2003) "Eastern Mediterranean surface water

temperatures and  $\delta^{18}\text{O}$  composition during deposition of sapropels in the late Quaternary", *Paleoceanography*, 18(1).

Emeis, K., Schulz, H., Struck, U., Sakamoto, T., Dooze, H., Erlenkeuser, H., Howell, M., Kroon, D., Paterne, M. (1998) "Stable isotope and alkenone temperature records of sapropels from Sites 964 and 967: constraining the physical environment of sapropel formation in the Eastern Mediterranean Sea", *Proceedings of the Ocean Drilling Program, 160 Scientific Results*.

Emeis, K., Struck, U., Schulz, H., Rosenberg, R., Bernasconi, S., Erlenkeuser, H., Sakamoto, T., Martinez-Ruiz, F. (2000) "Temperature and salinity variations of Mediterranean Sea surface waters over the last 16,000 years from records of planktonic stable oxygen isotopes and alkenone unsaturation ratios", *Palaeogeography, Palaeoclimatology, Palaeoecology*, 158(3-4), 259-280.

Ericson, D., Wollin, G., Wollin, J. (1955) "Coiling direction of Globorotalia truncatulinoides in deep-sea cores", *Deep Sea Research (1953)*, 2(2), 152-158.

European Commission (2017) European Atlas of the Seas [online], *Ec.europa.eu*, available: [http://ec.europa.eu/maritimeaffairs/atlas/maritime\\_atlas/#lang=EN;p=w;bkgd=6;theme=](http://ec.europa.eu/maritimeaffairs/atlas/maritime_atlas/#lang=EN;p=w;bkgd=6;theme=) [accessed 25 May 2017].

Facorellis, Y., Vardala-Theodorou, E. (2015) "Sea Surface Radiocarbon Reservoir Age Changes in the Aegean Sea from about 11,200 BP to Present", *Radiocarbon*, 57(03), 493-505.

Ferentinos, G., Papatheodorou, G., Ioakim, C., Tsaila-Monopolis, S., Geraga, M. (2000) "Evaluation of palaeoenvironmental changes during the last 18, 000 years in the Myrtoon basin, SW Aegean sea", *Palaeogeography, Palaeoclimatology, Palaeoecology*, 156(1-2), 1-17.

Ferentinos, G., Papatheodorou, G., Tsaila-Monopoli, S., Mylona, G., Geraga, M. (2008) "Northeastern Ionian Sea: Palaeoceanographic variability over the last 22 ka", *Journal of Marine Systems*, 74(1-2), 623-638.

Field, D. (2004) "Variability in vertical distributions of planktonic foraminifera in the California Current: Relationships to vertical ocean structure", *Paleoceanography*, 19(2).

Finné, M., Lindblom, M., Weiberg, E., Sundqvist, H., Holmgren, K. (2011) "Climate in the eastern Mediterranean, and adjacent regions, during the past 6000 years – A review", *Journal of Archaeological Science*, 38(12), 3153-3173.

Flohn, H., 1984. Climate evolution in the Southern Hemisphere and the equatorial region during the Late Cenozoic. *SASQUA International Symposium. Late Cainozoic Paleoclimates of the Southern Hemisphere*. AA Balkema, Rotterdam, pp.5-20.

Flower, B., Kennett, J. (1995) *Biotic Responses To Temperature And Salinity Changes During Last Deglaciation, Gulf Of Mexico*, National Academies Press, Washington (DC).

Font, J., Chic, O., Juliá, A., Salas, J., Millot, C. (1998) "The drift of Modified Atlantic Water from the Alboran Sea to the eastern Mediterranean", *Scientia Marina*, 62(3), 211-216.

Fontanier, C., Jorissen, F., Licari, L., Alexandre, A., Anschutz, P., Carbonel, P. (2002) "Live benthic foraminiferal faunas from the Bay of Biscay: faunal density, composition, and microhabitats", *Deep Sea Research Part I: Oceanographic Research Papers*, 49(4), 751-785.

Friedrich, O. (2010) "Benthic foraminifera and their role to decipher paleoenvironment during mid-Cretaceous Oceanic Anoxic Events – the “anoxic benthic foraminifera” paradox", *Revue de Micropaléontologie*, 53(3), 175-192.

- Fruehn, J., Reston, T., von Huene, R., Bialas, J. (2002) "Structure of the Mediterranean Ridge accretionary complex from seismic velocity information", *Marine Geology*, 186(1-2), 43-58.
- Frydas, D., Hemleben, C. (2007) "Opal phytoplankton assemblages of the Late Quaternary sapropel layers S5 and S7 from the southeastern Mediterranean Sea ("Meteor"-Cruise 40/4, Site 67)", *Revue de Micropaléontologie*, 50(2), 169-183.
- Gallego-Torres, D., Martínez-Ruiz, F., De Lange, G., Jimenez-Espejo, F., Ortega-Huertas, M. (2010) "Trace-elemental derived paleoceanographic and paleoclimatic conditions for Pleistocene Eastern Mediterranean sapropels", *Palaeogeography, Palaeoclimatology, Palaeoecology*, 293(1-2), 76-89.
- Gallego-Torres, D., Martínez-Ruiz, F., Paytan, A., Jiménez-Espejo, F., Ortega-Huertas, M. (2007) "Pliocene–Holocene evolution of depositional conditions in the eastern Mediterranean: Role of anoxia vs. productivity at time of sapropel deposition", *Palaeogeography, Palaeoclimatology, Palaeoecology*, 246(2-4), 424-439.
- Ganssen, G., Reichert, G., Wit, J. (2013) "Unmixing of stable isotope signals using single specimen  $\delta^{18}\text{O}$  analyses", *Geochemistry, Geophysics, Geosystems*, 14(4), 1312-1320.
- Garzanti, E., Andò, S., Vezzoli, G., Ali Abdel Megid, A., El Kammar, A. (2006) "Petrology of Nile River sands (Ethiopia and Sudan): Sediment budgets and erosion patterns", *Earth and Planetary Science Letters*, 252(3-4), 327-341.
- Geraga, M., Ioakim, C., Lykousis, V., Tsaila-Monopolis, S., Mylona, G. (2010) "The high-resolution palaeoclimatic and palaeoceanographic history of the last 24,000 years in the central Aegean Sea, Greece", *Palaeogeography, Palaeoclimatology, Palaeoecology*, 287(1-4), 101-115.
- Geraga, M., Mylona, G., Tsaila-Monopoli, S., Papatheodorou, G., Ferentinos, G. (2008) "Northeastern Ionian Sea: Palaeoceanographic variability over the last 22 ka", *Journal of Marine Systems*, 74(1-2), 623-638.
- Giunta, S., Negri, A., Maffioli, P., Sangiorgi, F., Capotondi, L., Morigi, C., Principato, M., Corselli, C. (2006) "Phytoplankton dynamics in the eastern Mediterranean Sea during Marine Isotopic Stage 5e", *Palaeogeography, Palaeoclimatology, Palaeoecology*, 235(1-3), 28-47.
- Grant, K., Grimm, R., Mikolajewicz, U., Marino, G., Ziegler, M., Rohling, E. (2016) "The timing of Mediterranean sapropel deposition relative to insolation, sea-level and African monsoon changes", *Quaternary Science Reviews*, 140, 125-141.
- Grant, K., Marino, G., Rohling, E. (2015) "Mediterranean climate and oceanography, and the periodic development of anoxic events (sapropels)", *Earth-Science Reviews*, 143, 62-97.
- Guasti, E., Speijer, R. (2008) "Acarinina multicamerata n. sp. (Foraminifera): a new marker for the Paleocene-Eocene thermal maximum", *Journal of Micropalaeontology*, 27(1), 5-12.
- Gudjonsson, L and van der Zwaan, G. (1986) "Middle Miocene—Pliocene stable isotope stratigraphy and paleoceanography of the Mediterranean", *Marine Micropaleontology*, 10(1-3), pp. 71-90. doi: 10.1016/0377-8398(86)90025-3.
- Guerra-Merchán, A., Serrano, F. (2012) "Sea-surface temperature for left-coiling Neoglobobulimina populations inhabiting the westernmost Mediterranean in the middle Pleistocene and the Pleistocene-Pliocene transition", *Geobios*, 45(2), 231-240.
- Gupta, B. (1999) "Systematics of modern Foraminifera", in Gupta, B., *Modern Foraminifera*, Kluwer Academic Publishers: Great Britain, 7-36.
- Halbach, P., Dittmer, J., De Lange, G., Hübner, A. (2003) "Geochemistry of an exotic sediment layer above sapropel S-1: Mud expulsion from the Urania basin, eastern Mediterranean?", *Marine Geology*, 197(1-4), 49-

61.

Hall, I., McCave, I. (2006) "Size sorting in marine muds: Processes, pitfalls, and prospects for paleoflow-speed proxies", *Geochemistry, Geophysics, Geosystems*, 7(10).

Hallock, P. (2000) Symbiont-Bearing Foraminifera: Harbingers Of Global Change? On JSTOR [online], *Jstor.org*, available: <http://www.jstor.org/stable/1486183>.

Hallock, P., Premoli Silva, I., Boersma, A. (1991) "Similarities between planktonic and larger foraminiferal evolutionary trends through Paleogene paleoceanographic changes", *Palaeogeography, Palaeoclimatology, Palaeoecology*, 83(1-3), 49-64.

Hamad, N., Millot, C., Taupier-Letage, I. (2005) "A new hypothesis about the surface circulation in the eastern basin of the mediterranean sea," *Progress in Oceanography*, 66(2-4), 287–298.

Hamann, Y., Ehrmann, W., Schmiedl, G., Krüger, S., Stuut, J., Kuhnt, T. (2008) "Sedimentation processes in the Eastern Mediterranean Sea during the Late Glacial and Holocene revealed by end-member modelling of the terrigenous fraction in marine sediments", *Marine Geology*, 248(1-2), 97-114.

Hammer, O., Harper, D., Ryan, P. (2004) "PAST — Palaeontological Statistics Version 1.20."

Hawkesworth, C., Matthews, A., Gilmour, M., Ayalon, A., Bar-Matthews, M. (2003) "Sea–land oxygen isotopic relationships from planktonic foraminifera and speleothems in the Eastern Mediterranean region and their implication for paleorainfall during interglacial intervals", *Geochimica et Cosmochimica Acta*, 67(17), 3181-3199.

Hayes, A., Kucera, M., Kallel, N., Sbaifi, L., Rohling, E. (2005) "Glacial Mediterranean sea surface temperatures based on planktonic foraminiferal assemblages", *Quaternary Science Reviews*, 24(7-9), 999-1016.

Hayes, A., Rohling, E., De Rijk, S., Kroon, D., Zachariasse, W. (1999) "Mediterranean planktonic foraminiferal faunas during the last glacial cycle", *Marine Geology*, 153(1-4), 239-252.

Helmke, J., Bauch, H., Röhl, U., Kandiano, E. (2008) "Uniform climate development between the subtropical and subpolar Northeast Atlantic across marine isotope stage 11", *Climate of the Past Discussions*, 4(2), 433-457.

Hemleben, C., Spindler, M., Anderson, O. (2012) *Modern Planktonic Foraminifera*, 1st ed, Springer: [Place of publication not identified].

Hennekam, R., De Lange, G., Schnetger, B., Jilbert, T. (2014) "Solar forcing of Nile discharge and sapropel S1 formation in the early to middle Holocene eastern Mediterranean", *Paleoceanography*, 29(5), 343-356.

Hernández-Almeida, I., Bárcena, M., Flores, J., Sierro, F., Sanchez-Vidal, A., Calafat, A. (2011) "Microplankton response to environmental conditions in the Alboran Sea (Western Mediterranean): One year sediment trap record", *Marine Micropaleontology*, 78(1-2), 14-24.

Higgs, N., Thomson, J., Wilson, T., Croudace, I. (1994) "Modification and complete removal of eastern Mediterranean sapropels by postdepositional oxidation", *Geology*, 22(5), 423.

Hilgen, F. (1991) "Extension of the astronomically calibrated (polarity) time scale to the Miocene/Pliocene boundary," *Earth and Planetary Science Letters*, 107(2), 349–368.

HMSO (1962) "Weather in the Mediterranean I: General Meteorology", 2d ed. *Her Majesty's Stationery Office*, 362.

Houpert, L. (2013) *Contribution To The Study Of Transfer Processes From The Surface To The Deep Ocean In The Mediterranean Sea Using In Situ Measurements*, available: <https://tel.archives-ouvertes.fr/tel->

01148986/file/These\_Houpert\_Loic\_2013.pdf [accessed 6 Mar 2017].

Hughen, K., Lehman, S., Southon, J., Overpeck, J., Marchal, O., Herring, C., Turnbull, J. (2004) "14C Activity and Global Carbon Cycle Changes over the Past 50,000 Years", *Science*, 303(5655), 202-207.

Huguen, C., Mascle, J., Chamillon, E., Kopf, A., Woodside, J., Zitter, T. (2004) "Structural setting and tectonic control of mud volcanoes from the Central Mediterranean Ridge (Eastern Mediterranean)", *Marine Geology*, 209(1-4), 245-263.

Hutson, W. (1978) "Application of Transfer Functions to Indian Ocean Planktonic Foraminifera", *Quaternary Research*, 9(01), 87-112.

HUTSON, W. (1980) "The Agulhas Current During the Late Pleistocene: Analysis of Modern Faunal Analogs", *Science*, 207(4426), 64-66.

Imbrie, J., Hays, J., Martinson, D., McIntyre, A., Mix, A., Morley, J., Pisias, N., Prell, W., Shackleton, N. (1984) "The orbital theory of Pleistocene climate: support from a revised chronology of the marine  $\delta^{18}\text{O}$  record", in Berger, A., *Milankovitch and Climate*, D. Riedel: Mass., 269-305.

Imbrie, J., Hays, J., Martinson, D., McIntyre, A., Mix, A., Morley, J., Pisias, N., Prell, W., Shackleton, N. (2017) The Orbital Theory Of Pleistocene Climate: Support From A Revised Chronology Of The Marine  $\Delta^{18}\text{O}$  Record [online], *Adsabs.harvard.edu*, available: <http://adsabs.harvard.edu/abs/1984mcur.conf..269I>

Imbrie, J., Kipp, J. (1971) "A new micropalaeontological method for quantitative paleoclimatology: application to a Late Pleistocene Caribbean core", in Turekian, K., *The Late Cenozoic Glacial Ages*, Yale University Press: New Haven, 71-181.

Incarbona, A., Sprovieri, M., Lirer, F., Sprovieri, R. (2011) "Surface and deep water conditions in the Sicily channel (central Mediterranean) at the time of sapropel S5 deposition", *Palaeogeography, Palaeoclimatology, Palaeoecology*, 306(3-4), 243-248.

İsler, E., Aksu, A., Hiscott, R. (2016) "Geochemistry of Aegean Sea sediments: implications for surface- and bottom-water conditions during sapropel deposition since MIS 5", *TURKISH JOURNAL OF EARTH SCIENCES*, 25, 103-125.

Ivanov, M., Cita, M., Woodside, j., Limonov, A. (1996) "The Mediterranean Ridge and related mud diapirism: a background", *Marine Geology*, 132.

Jian, Z., Li, B., Huang, B., Wang, J. (2000) "Globorotalia truncatulinoides as indicator of upper-ocean thermal structure during the Quaternary: evidence from the South China Sea and Okinawa Trough", *Palaeogeography, Palaeoclimatology, Palaeoecology*, 162(3-4), 287-298.

Jiang, Z., Liu, Z., Rohling, E., Roberts, A., Torrent, J., Larrasoana, J., Liu, Q. (2012) "New constraints on climate forcing and variability in the circum-mediterranean region from magnetic and geochemical observations of sapropels S1, S5 and S6", *Palaeogeography, Palaeoclimatology, Palaeoecology*, 333-334, 1-12.

Jiménez-Espejo, F., Pardos-Gené, M., Martínez-Ruiz, F., García-Alix, A., van de Flierdt, T., Toyofuku, T., Bahr, A., Kreissig, K. (2015) "Geochemical evidence for intermediate water circulation in the westernmost Mediterranean over the last 20kyrBP and its impact on the Mediterranean Outflow", *Global and Planetary Change*, 135, 38-46.

Jorissen, F. (1999) "Benthic foraminiferal microhabitats below the sediment-water interface", *Modern Foraminifera*, 161-179.

Jorissen, F. (1999) "Benthic foraminiferal successions across Late Quaternary Mediterranean

- sapropels", *Marine Geology*, 153(1-4), 91-101.
- Jouet, G., Jorry, S., Bassetti, M., Fontanier, C., Angue Minto'o, C., Toucanne, S. (2015) "Tracking rainfall in the northern Mediterranean borderlands during sapropel deposition", *Quaternary Science Reviews*, 129, 178-195.
- Jouet, G., Jorry, S., Bassetti, M., Fontanier, C., Minto'o, C., Toucanne, S. (2015) "Tracking rainfall in the northern Mediterranean borderlands during sapropel deposition", *Quaternary Science Reviews*, 129, 178-195.
- Kallel, N., Duplessy, J., Labeyrie, L., Fontugne, M., Paterne, M., Montacer, M. (2000) "Mediterranean pluvial periods and sapropel formation over the last 200 000 years", *Palaeogeography, Palaeoclimatology, Palaeoecology*, 157(1-2), 45-58.
- Kallel, N., Paterne, M., Duplessy, J., Vergnaudgrazzini, C., Pujol, C., Labeyrie, L., Arnold, M., Fontugne, M., Pierre, C. (1997) Enhanced Rainfall in The Mediterranean Region during the Last Sapropel Event [online], *Archimer.ifremer.fr*, available: <http://archimer.ifremer.fr/doc/00093/20427/> [accessed 5 Jun 2017].
- Kasten, S., Kriews, M., Römmermann, H., Hanebuth, T., Vogt, C., Wilhelms, F., Röhl, U., Westerhold, T., Wilhelms-Dick, D. (2012) "A comparison of mm scale resolution techniques for element analysis in sediment cores", *Journal of Analytical Atomic Spectrometry*, 27(9), 1574.
- Keller, J., Capotondi, L., Negri, A. (1999) "Calcareous nannofossils, planktonic foraminifera and oxygen isotopes in the late Quaternary sapropels of the Ionian sea", *Marine Geology*, 157(1-2), 89-103.
- Khanolkar, S., Saraswati, P. (2015) "Ecological response of shallow-marine foraminifera to early Eocene warming in equatorial India", *The Journal of Foraminiferal Research*, 45(3), 293-304.
- Kidd, R., Cita, M., Ryan, W. (1978) "Stratigraphy of eastern Mediterranean sapropel sequences recovered during Leg 42A and their paleoenvironmental significance", *Init. Rep. DSDP*, 42(A), 421-443.
- Kioroglou, S., Theocharis, A., Manca, B., Klein, B., Roether, W. (2007) "Transient eastern Mediterranean deep waters in response to the massive dense-water output of the Aegean sea in the 1990s", *Progress in Oceanography*, 74(4), 540-571.
- Klaeschen, D., Mascle, J., Kopf, A. (2003) "The Mediterranean ridge: A mass balance across the fastest growing accretionary complex on earth", *Journal of Geophysical Research*, 108(B8).
- Klein, B., Luchetta, A., Civitarese, G., Theocharis, A., Souvermezoglou, E., d'Alcala, M., Manca, B., Kress, N., Roether, W. (2003) "Accelerated oxygen consumption in eastern Mediterranean deep waters following the recent changes in thermohaline circulation", *Journal of Geophysical Research*, 108(C9).
- Klein, B., Nittis, K., Roether, W., Lascaratos, A. (1999) "Recent changes in deep water formation and spreading in the eastern Mediterranean sea: A review", *Progress in Oceanography*, 44(1-3), 5-36.
- Kontakiotis, G. (2015) "Late Quaternary paleoenvironmental reconstruction and paleoclimatic implications of the Aegean Sea (eastern Mediterranean) based on paleoceanographic indexes and stable isotopes", *Quaternary International*.
- Kopp, R., Simons, F., Mitrovica, J., Maloof, A., Oppenheimer, M. (2009) "Probabilistic assessment of sea level during the last interglacial stage", *Nature*, 462(7275), 863-867.
- Kroon, D., Jorissen, F., Hayes, A., Rogerson, M., Schiebel, R., Emeis, K., Bouloubassi, I., Cooke, S., Casford, J., Cane, T., Sprovieri, M., Rohling, E. (2004) "Reconstructing past planktic foraminiferal habitats using stable isotope data: A case history for Mediterranean sapropel S5", *Marine Micropaleontology*, 50(1-2), 89-123.
- Kucera, M. (2007) "Chapter Six Planktonic Foraminifera as tracers of past Oceanic environments", *Proxies in*

*Late Cenozoic Paleoceanography*, 213-262.

Kucera, M., Weinelt, M., Kiefer, T., Pflaumann, U., Hayes, A., Weinelt, M., Chen, M., Mix, A., Barrows, T., Cortijo, E., Duprat, J., Juggins, S., Waelbroeck, C. (2005) "Reconstruction of sea-surface temperatures from assemblages of planktonic foraminifera: multi-technique approach based on geographically constrained calibration data sets and its application to glacial Atlantic and Pacific Oceans", *Quaternary Science Reviews*, 24(7-9), 951-998.

Kuhlmann, J., Asioli, A., Trincardi, F., Klügel, A., Huhn, K. (2015) "Sedimentary response to Milankovitch-type climatic oscillations and formation of sediment undulations: evidence from a shallow-shelf setting at Gela Basin on the Sicilian continental margin", *Quaternary Science Reviews*, 108, 76-94.

Kuhnt, T., Stuetz, J., Krüger, S., Schmiedl, G., Ehrmann, W., Hamann, Y. (2008) "Sedimentation processes in the eastern Mediterranean sea during the late glacial and Holocene revealed by end-member modelling of the terrigenous fraction in marine sediments", *Marine Geology*, 248(1-2), 97-114.

Kuroyanagi, A., Kawahata, H. (2004) "Vertical distribution of living planktonic foraminifera in the seas around Japan", *Marine Micropaleontology*, 53(1-2), 173-196.

Lang, N., Wolff, E. (2011) "Interglacial and glacial variability from the last 800 ka in marine, ice and terrestrial archives", *Climate of the Past*, 7(2), 361-380.

Laskar, J., Joutel, F., Boudin, F. (1993) "Orbital, precessional, and insolation quantities for the Earth from -20 MYR to +10 MYR", *Astronomy and Astrophysics*, (270), 522-533.

Lea, D., Mashiotto, T., Spero, H. (1999) "Controls on magnesium and strontium uptake in planktonic foraminifera determined by live culturing", *Geochimica et Cosmochimica Acta*, 63(16), 2369-2379.

Leckie, R. (1987) "Paleoecology of Mid-Cretaceous Planktonic Foraminifera: A Comparison of Open Ocean and Epicontinental Sea Assemblages", *Micropaleontology*, 33(2), 164.

Limonov, A., Woodside, J., Cita, M., Ivanov, M. (1996) "The Mediterranean Ridge and related mud diapirism: a background", *Marine Geology*, 132(1-4), 7-19.

Lin, H. (2014) "The seasonal succession of modern planktonic foraminifera: Sediment traps observations from southwest Taiwan waters", *Continental Shelf Research*, 84, 13-22.

Linsley, B., Arbuszewski, J., deMenocal, P., Cléroux, C. (2013) "Reconstructing the upper water column thermal structure in the Atlantic ocean", *Paleoceanography*, 28(3), 503-516.

Lionello, P., Xoplaki, E., Ulbrich, U., Tsimplis, M., Trigo, R., May, W., Luterbacher, J., Li, L., Artale, V., Alpert, P., Boscolo, R., Malanotte-Rizzoli, P. (2006) "The Mediterranean climate: An overview of the main characteristics and issues", *Developments in Earth and Environmental Sciences*, 1-26.

Lionello, P., Giorgi, F. (2008) "Climate change projections for the Mediterranean region", *Global and Planetary Change*, 63(2-3), 90-104.

Lirer, F., Rettori, R., Pelosi, N., Magri, D., Lurcock, P., Lubritto, C., Florindo, F., Ferraro, L., Cascella, A., Cacho, I., Bonomo, S., Petrosino, P., Insinga, D., Bellucci, L., Capotondi, L., Di Rita, F., Vallefuoco, M., Margaritelli, G. (2016) "Marine response to climate changes during the last five millennia in the central Mediterranean sea", *Global and Planetary Change*, 142, 53-72.

Liu, Q., Larrasoana, J., Torrent, J., Roberts, A., Rohling, E., Liu, Z., Jiang, Z. (2012) "New constraints on climate forcing and variability in the circum-Mediterranean region from magnetic and geochemical observations of sapropels S1, S5 and S6", *Palaeogeography, Palaeoclimatology, Palaeoecology*, 333-334, 1-12.

Local Winds - Metlink Teaching Weather and Climate [online] (2017) [online].

- Löwemark, L., Lin, Y., Chen, H., Yang, T., Beier, C., Werner, F., Lee, C., Song, S., Kao, S. (2006) "Sapropel burn-down and ichnological response to late Quaternary sapropel formation in two 400 ky records from the eastern Mediterranean Sea", *Palaeogeography, Palaeoclimatology, Palaeoecology*, 239(3-4), 406-425.
- Luchetta, A., Kovacevic, V., Beitzel, V., Bregant, D., Manca, B., Roether, W., Klein, B. (1999) "The large deep water transient in the eastern Mediterranean", *Deep Sea Research Part I: Oceanographic Research Papers*, 46(3), 371-414.
- Maheras, P., Anagnostopoulou, C., Patrikas, I., Flocas, H. (2001) "A 40 year objective climatology of surface cyclones in the Mediterranean region: Spatial and temporal distribution", *International Journal of Climatology*, 21(1), 109-130.
- Maiorano, P., Aiello, G., Barra, D., Di Leo, P., Joannin, S., Lirer, F., Marino, M., Pappalardo, A., Capotondi, L., Ciaranfi, N., Stefanelli, S. (2008) "Paleoenvironmental changes during sapropel 19 (i-cycle 90) deposition: Evidences from geochemical, mineralogical and micropaleontological proxies in the mid-Pleistocene Montalbano Jonico land section (southern Italy)", *Palaeogeography, Palaeoclimatology, Palaeoecology*, 257(3), 308-334.
- Malaizé, B., Paillard, D., Jouzel, J., Raynaud, D. (1999) "The Dole effect over the last two glacial-interglacial cycles", *Journal of Geophysical Research: Atmospheres*, 104(D12), 14199-14208.
- Manca, B., Beitzel, V., Klein, B., Roether, W. (1998) "Property distributions and transient-tracer ages in Levantine intermediate water in the eastern Mediterranean", *Journal of Marine Systems*, 18(1-3), 71-87.
- Mangini, A., Schlosser, P. (1986) "The formation of Eastern Mediterranean sapropels", *Marine Geology*, 72(1-2), 115-124.
- Marino, G., Rohling, E., Rijpstra, W., Sangiorgi, F., Schouten, S., Damsté, J. (2007) "Aegean Sea as driver of hydrographic and ecological changes in the eastern Mediterranean", *Geology*, 35(8), 675.
- Marr, J., Bolton, A. (2013) "Trace element variability in crust-bearing and non-crust-bearing *Neogloboquadrina incompta*, *P-D* intergrade and *Globoconella inflata* from the southwest Pacific Ocean: Potential paleoceanographic implications", *Marine Micropaleontology*, 100, 21-33.
- Martinez-Ruiz, F., Sakamoto, T., Erlenkeuser, H., Bernasconi, S., Rosenberg, R., Schulz, H., Struck, U., Emeis, K. (2000) "Temperature and salinity variations of Mediterranean sea surface waters over the last 16,000 years from records of planktonic stable oxygen isotopes and alkenone unsaturation ratios", *Palaeogeography, Palaeoclimatology, Palaeoecology*, 158(3-4), 259-280.
- Martin-Vide, J., Lopez-Bustins, J.-A. (2006) "The Western Mediterranean Oscillation and rainfall in the Iberian Peninsula," *International Journal of Climatology*, 26(11), 1455-1475.
- McCormac, F., Reimer, P. (2002) "Marine radiocarbon reservoir corrections for the Mediterranean and Aegean seas", *Radiocarbon*, 44(01), 159-166.
- Meier, K., Zonneveld, K., Kasten, S., Willems, H. (2004) "Different nutrient sources forcing increased productivity during eastern Mediterranean S1 sapropel formation as reflected by calcareous dinoflagellate cysts", *Paleoceanography*, 19(1).
- Melki, T., Kallel, N., Fontugne, M. (2010) "The nature of transitions from dry to wet condition during sapropel events in the Eastern Mediterranean Sea", *Palaeogeography, Palaeoclimatology, Palaeoecology*, 291(3-4), 267-285.
- Meyers, P., Arnaboldi, M. (2008) "Paleoceanographic implications of nitrogen and organic carbon isotopic excursions in mid-Pleistocene sapropels from the Tyrrhenian and Levantine Basins, Mediterranean Sea", *Palaeogeography, Palaeoclimatology, Palaeoecology*, 266(1-2), 112-118.

- Mezger, E., de Nooijer, L., Boer, W., Brummer, G., Reichart, G. (2016) "Salinity controls on Na incorporation in Red Sea planktonic foraminifera", *Paleoceanography*, 31(12), 1562-1582.
- Millot, C., Benzohra, M., Taupier-Letage, I. (1997) "Circulation off Algeria inferred from the Médiprod-5 current meters," *Deep Sea Research Part I: Oceanographic Research Papers*, 44(9-10), 1467–1495.
- Millot, C., Taupier-Letage, I. (2005) "Additional evidence of LIW entrainment across the Algerian subbasin by mesoscale eddies and not by a permanent westward flow," *Progress in Oceanography*, 66(2-4), 231–250.
- Milner, A., Roucoux, K., Collier, R., Müller, U., Pross, J., Tzedakis, P. (2016) "Vegetation responses to abrupt climatic changes during the Last Interglacial Complex (Marine Isotope Stage 5) at Tenaghi Philippon, NE Greece", *Quaternary Science Reviews*, 154, 169-181.
- Möbius, J. (2013) "Isotope fractionation during nitrogen remineralization (ammonification): Implications for nitrogen isotope biogeochemistry", *Geochimica et Cosmochimica Acta*, 105, 422–432, available: <http://dx.doi.org/10.1016/j.gca.2012.11.048> [accessed 9 Jul 2015].
- Mohd, M., Murray, R., Plank, M., Godsoe, W. (2017) "Effects of biotic interactions and dispersal on the presence-absence of multiple species", *Chaos, Solitons & Fractals*, 99, 185-194.
- Mohtadi, M., Hebbeln, D., Marchant, M. (2005) "Upwelling and productivity along the Peru–Chile Current derived from faunal and isotopic compositions of planktic foraminifera in surface sediments", *Marine Geology*, 216(3), 107-126.
- Moller, T., Schulz, H., Hamann, Y., Dellwig, O., Kucera, M. (2012) "Sedimentology and geochemistry of an exceptionally preserved last interglacial sapropel S5 in the Levantine Basin (Mediterranean Sea)", *Marine Geology*, 291-294, 34-48.
- Moller, T., Schulz, H., Kucera, M. (2013) "The effect of sea surface properties on shell morphology and size of the planktonic foraminifer *Neoglobobulimina pachyderma* in the North Atlantic", *Palaeogeography, Palaeoclimatology, Palaeoecology*, 391, 34-48.
- Montacer, M., Paterne, M., Fontugne, M., Labeyrie, L., Duplessy, J., Kallel, N. (2000) "Mediterranean pluvial periods and sapropel formation over the last 200 000 years", *Palaeogeography, Palaeoclimatology, Palaeoecology*, 157(1-2), 45-58.
- Morard, R., Quillévéré, F., Escarguel, G., Ujiie, Y., de Garidel-Thoron, T., Norris, R., de Vargas, C. (2009) "Morphological recognition of cryptic species in the planktonic foraminifer *Orbulina universa*", *Marine Micropaleontology*, 71(3-4), 148-165.
- Morigi, C. (2009) "Benthic environmental changes in the Eastern Mediterranean Sea during sapropel S5 deposition", *Palaeogeography, Palaeoclimatology, Palaeoecology*, 273(3-4), 258-271.
- Mulder, T., Jouet, G., Toucanne, S., Ducassou, E., Morigi, C., Bassetti, M., Angue Minto'o, C. (2015) "Levantine intermediate water hydrodynamic and bottom water ventilation in the northern Tyrrhenian sea over the past 56, 000 years: New insights from benthic foraminifera and ostracods", *Quaternary International*, 357, 295-313.
- Murat, A. (1999) "Pliocene-Pleistocene occurrence of Sapropels in the Western Mediterranean Sea and their relation to Eastern Mediterranean Sapropels ", *Proceedings of the Ocean Drilling Program*, 161, 519-527.
- Mutti, M., Hallock, P. (2003) "Carbonate systems along nutrient and temperature gradients: some sedimentological and geochemical constraints", *International Journal of Earth Sciences*, 92(4), 465-475.
- Mylona, G., Tsaila-Monopolis, S., Lykousis, V., Ioakim, C., Geraga, M. (2010) "The high-resolution

palaeoclimatic and palaeoceanographic history of the last 24, 000years in the central Aegean sea, Greece", *Palaeogeography, Palaeoclimatology, Palaeoecology*, 287(1-4), 101-115.

Negri, A., Capotondi, L., Keller, J. (1999) "Calcareous nannofossils, planktonic foraminifera and oxygen isotopes in the late Quaternary sapropels of the Ionian Sea", *Marine Geology*, 157(1-2), 89-103.

Negri, A., Capozzi, R. (2009) "Role of sea-level forced sedimentary processes on the distribution of organic carbon-rich marine sediments: A review of the late Quaternary sapropels in the Mediterranean Sea", *Palaeogeography, Palaeoclimatology, Palaeoecology*, 273(3-4), 249-257.

Negri, A., Cobiachi, M., Luciani, V., Fraboni, R., Milani, A., Claps, M. (2003) "Tethyan Cenomanian pelagic rhythmic sedimentation and Pleistocene Mediterranean sapropels: is the biotic signal comparable?", *Palaeogeography, Palaeoclimatology, Palaeoecology*, 190, 373-397.

Negri, A., Corselli, C., Giunta, S., Principato, M. (2003) "Late Pleistocene–Holocene planktonic assemblages in three box-cores from the Mediterranean Ridge area (west–southwest of Crete): palaeoecological and palaeoceanographic reconstruction of sapropel S1 interval", *Palaeogeography, Palaeoclimatology, Palaeoecology*, 190, 61-77.

Negri, A., Morigi, C., Giunta, S. (2003) "Are productivity and stratification important to sapropel deposition? Microfossil evidence from late Pliocene insolation cycle 180 at Vrica, Calabria", *Palaeogeography, Palaeoclimatology, Palaeoecology*, 190, 243-255.

Niebler, H., Gersonde, R. (1998) "A planktic foraminiferal transfer function for the southern South Atlantic Ocean", *Marine Micropaleontology*, 34(3-4), 213-234.

Nijenhuis, I., de Lange, G. (2000) "Geochemical constraints on Pliocene sapropel formation in the eastern Mediterranean", *Marine Geology*, 163(1-4), 41-63.

Nolet, G., Corliss, B. (1990) "Benthic foraminiferal evidence for reduced deep-water circulation during sapropel deposition in the eastern Mediterranean", *Marine Geology*, 94(1-2), 109-130.

Nordlund, U., Malmgren, B. (1997) "Application of artificial neural networks to paleoceanographic data", *Palaeogeography, Palaeoclimatology, Palaeoecology*, 136(1-4), 359-373.

Nunez, N., Katsouras, G., Papanikolaou, M., Rosell-Melé, A., Dimiza, M., Kouli, K., Emeis, K., Bouloubassi, I., Lykousis, V., Marino, G., Gogou, A., Ziveri, P., Triantaphyllou, M. (2009) "Late Glacial–Holocene climate variability at the south-eastern margin of the Aegean sea", *Marine Geology*, 266(1-4), 182-197.

Olsson, R., Wade, B. (2009) "Investigation of pre-extinction dwarfing in Cenozoic planktonic foraminifera", *Palaeogeography, Palaeoclimatology, Palaeoecology*, 284(1-2), 39-46.

Omstedt, A., Shaltout, M. (2014) "Recent sea surface temperature trends and future scenarios for the Mediterranean sea", *Oceanologia*, 56(3), 411-443.

Oppo, D., Horowitz, M., Lehman, S. (1997) "Marine core evidence for reduced deep water production during Termination II followed by a relatively stable substage 5e (Eemian)", *Paleoceanography*, 12(1), 51-63.

O'Regan, M., Kroon, D., Pearson, P., Coxall, H., Birch, H. (2013) "Planktonic foraminifera stable isotopes and water column structure: Disentangling ecological signals", *Marine Micropaleontology*, 101, 127-145.

Ortega-Huertas, M., Jiménez-Espejo, F., Paytan, A., Martínez-Ruiz, F., Gallego-Torres, D. (2007) "Pliocene–Holocene evolution of depositional conditions in the eastern Mediterranean: Role of anoxia vs. Productivity at time of sapropel deposition", *Palaeogeography, Palaeoclimatology, Palaeoecology*, 246(2-4), 424-439.

Ortega-Huertas, M., Nieto-Moreno, V., Rodrigo-Gámiz, M., Gallego-Torres, D., Kastner, M., Martínez-Ruiz, F. (2015) "Paleoclimate and paleoceanography over the past 20, 000 yr in the Mediterranean sea basins as indicated by sediment elemental proxies", *Quaternary Science Reviews*, 107, 25-46.

Os, B.J.H.V., Lourens, L.J., Hilgen, F.J., Lange, G.J.D., Beaufort, L. (1995) "The formation of Pliocene sapropels and carbonate cycles in the Mediterranean: Diagenesis, dilution, and productivity," *Paleoceanography*, 9(4), 601–617.

Osborne, A., Marino, G., Vance, D., Rohling, E. (2010) "Eastern Mediterranean surface water Nd during Eemian sapropel S5: monitoring northerly (mid-latitude) versus southerly (sub-tropical) freshwater contributions", *Quaternary Science Reviews*, 29(19-20), 2473-2483.

Ozer, T., Herut, B., Silverman, J., Kress, N., Gertman, I. (2016) "Interannual thermohaline (1979–2014) and nutrient (2002–2014) dynamics in the Levantine surface and intermediate water masses, SE Mediterranean sea", *Global and Planetary Change*.

Ozsoy, E., Budillon, G., Brenner, S., Theocharis, A., d'Alcala, M., Manca, B., Malanotte-Rizzoli, P. (1999) "The eastern Mediterranean in the 80s and in the 90s: The big transition in the intermediate and deep circulations", *Dynamics of Atmospheres and Oceans*, 29(2-4), 365-395.

Özturgut, E. "The Source and Spreading of the Levantine Intermediate Water in the Eastern Mediterranean." *Saflant ASW Research Center Memorandum Sm-92, La Spezia, Italy* (1976).

Painter, S., Tsimplis, M. (2003) "Temperature and salinity trends in the upper waters of the Mediterranean Sea as determined from the MEDATLAS dataset", *Continental Shelf Research*, 23(16), 1507-1522.

Peeters, F. (2002) "The effect of upwelling on the distribution and stable isotope composition of *Globigerina bulloides* and *Globigerinoides ruber* (planktic foraminifera) in modern surface waters of the NW Arabian Sea", *Global and Planetary Change*, 34(3-4), 269-291.

Pelosi, N., Kucera, M., Marino, M., Girone, A., Maiorano, P. (2016) "Sea surface water variability during the Mid-Brunhes inferred from calcareous plankton in the western Mediterranean (ODP site 975)", *Palaeogeography, Palaeoclimatology, Palaeoecology*.

Pérez-Folgado, M., Sierro, F., Flores, J., Cacho, I., Grimalt, J., Zahn, R., Shackleton, N. (2003) "Western Mediterranean planktonic foraminifera events and millennial climatic variability during the last 70 kyr", *Marine Micropaleontology*, 48(1-2), 49-70.

Pianka, E. (1966) "Latitudinal Gradients in Species Diversity: A Review of Concepts", *The American Naturalist*, 100(910), 33-46.

Pika-Biolzi, M., Bernasconi, S. (2000) "A stable isotope study of multiple species of planktonic foraminifera across sapropels of the Tyrrhenian sea, ODP site 974", *Palaeogeography, Palaeoclimatology, Palaeoecology*, 158(3-4), 281-292.

Pika-Biolzi, M., Bernasconi, S. (2000) "A stable isotope study of multiple species of planktonic foraminifera across sapropels of the Tyrrhenian sea, ODP site 974", *Palaeogeography, Palaeoclimatology, Palaeoecology*, 158(3-4), 281-292.

Pinardi, N., Masetti, E. (2000) "Variability of the large scale general circulation of the Mediterranean Sea from observations and modelling: a review", *Palaeogeography, Palaeoclimatology, Palaeoecology*, 158(3-4), 153-173.

Pistek, P., Perkins, H. (1990) "Circulation in the Algerian basin during June 1986", *Journal of Geophysical Research*, 95(C2), 1577.

- Polonia, A., Romano, S., Çağatay, M., Capotondi, L., Gasparotto, G., Gasperini, L., Panieri, G., Torelli, L. (2015) "Are repetitive slumpings during sapropel S1 related to paleo-earthquakes?", *Marine Geology*, 361, 41-52.
- Price, J., Baringer, M. (1999) "A review of the physical oceanography of the Mediterranean outflow", *Marine Geology*, 155(1-2), 63-82.
- Price-Lloyd, N., Twitchett, R., Metcalfe, B. (2011) "Changes in size and growth rate of 'Lilliput' animals in the earliest Triassic", *Palaeogeography, Palaeoclimatology, Palaeoecology*, 308(1-2), 171-180.
- Principato, M., Crudeli, D., Ziveri, P., Slomp, C., Corselli, C., Erba, E., de Lange, G. (2006) "Phyto- and zooplankton paleofluxes during the deposition of sapropel S1 (eastern Mediterranean): Biogenic carbonate preservation and paleoecological implications", *Palaeogeography, Palaeoclimatology, Palaeoecology*, 235(1-3), 8-27.
- Principato, M., Giunta, S., Corselli, C., Negri, A. (2003) "Late Pleistocene–Holocene planktonic assemblages in three box-cores from the Mediterranean Ridge area (west–southwest of Crete): palaeoecological and palaeoceanographic reconstruction of sapropel S1 interval", *Palaeogeography, Palaeoclimatology, Palaeoecology*, 190, 61-77.
- Quillévéry, F., Morard, R., Escarguel, G., Douady, C., Ujiie, Y., de Garidel-Thoron, T., de Vargas, C. (2013) "Global scale same-specimen morpho-genetic analysis of *Truncorotalia truncatulinoides*: A perspective on the morphological species concept in planktonic foraminifera", *Palaeogeography, Palaeoclimatology, Palaeoecology*, 391, 2-12.
- Railsback, L., Gibbard, P., Head, M., Voarintsoa, N., Toucanne, S. (2015) "An optimized scheme of lettered marine isotope substages for the last 1.0 million years, and the climatostratigraphic nature of isotope stages and substages", *Quaternary Science Reviews*, 111, 94-106.
- Rasmussen, T., Thomsen, E. (2012) "Changes in planktic foraminiferal faunas, temperature and salinity in the Gulf Stream during the last 30,000 years: influence of meltwater via the Mississippi River", *Quaternary Science Reviews*, 33, 42-54.
- Rau, G., Krom, M., Voß, M., Emeis, K., Struck, U. (2001) "Biological productivity during sapropel S5 formation in the Eastern Mediterranean Sea: evidence from stable isotopes of nitrogen and carbon", *Geochimica et Cosmochimica Acta*, 65(19), 3249-3266.
- Rebotim, A., Voelker, A., Jonkers, L., Waniek, J., Meggers, H., Schiebel, R., Fraile, I., Schulz, M., Kucera, M. (2016) "Factors controlling the depth habitat of planktonic foraminifera in the subtropical eastern North Atlantic", *Biogeosciences Discussions*, 1-48.
- Reimer, P., McCormac, F. (2002) "Marine Radiocarbon Reservoir Corrections for the Mediterranean and Aegean Seas", *Radiocarbon*, 44(01), 159-166.
- Reimer, P., Stuiver, M., Taylor, R. (1996) "Development and extension of the calibration of the radiocarbon time scale: Archaeological applications", *Quaternary Science Reviews*, 15(7), 655-668.
- Renaud, S., Schmidt, D. (2003) "Habitat tracking as a response of the planktic foraminifer *Globorotalia truncatulinoides* to environmental fluctuations during the last 140 kyr", *Marine Micropaleontology*, 49(1-2), 97-122.
- Reolid, M., Sánchez-Quinónez, C., Alegret, L., Molina, E. (2016) "The biotic crisis across the Oceanic Anoxic Event 2: Palaeoenvironmental inferences based on foraminifera and geochemical proxies from the South Iberian Palaeomargin", *Cretaceous Research*, 60, 1-27.
- Revel, M., Sonzogni, C., Rouaud, G., Licari, L., Tachikawa, K., Vidal, L., Cornuault, M. (2016) "Deep water

circulation within the eastern Mediterranean sea over the last 95kyr: New insights from stable isotopes and benthic foraminiferal assemblages", *Palaeogeography, Palaeoclimatology, Palaeoecology*, 459, 1-14.

Rink, S., Kühl, M., Bijma, J., Spero, H. (1998) "Microsensor studies of photosynthesis and respiration in the symbiotic foraminifer *Orbulina universa*", *Marine Biology*, 131(4), 583-595.

Roberts, J. (1999) "Numerical Palaeobiology. Computer-Based Modelling and Analysis of Fossils and their Distributions", *Geological Magazine*, 137(4), 463-479.

Robinson, A., Leslie, W., Theocharis, A., Lascaratos, A. (2001) "Mediterranean Sea Circulation", *Encyclopedia of Ocean Sciences*, 1689-1705.

Roether, W., Klein, B., Beitzel, V., Manca, B.B. (1998) "Property distributions and transient-tracer ages in Levantine Intermediate Water in the Eastern Mediterranean," *Journal of Marine Systems*, 18(1-3), 71-87.

Roether, W., Schlitzer, R. (1991) "Eastern Mediterranean deep water renewal on the basis of chlorofluoromethane and tritium data", *Dynamics of Atmospheres and Oceans*, 15(3-5), 333-354.

Rohling, E. (1999) "Environmental control on Mediterranean salinity and  $\delta^{18}\text{O}$ ", *Paleoceanography*, 14(6), 706-715.

Rohling, E., Gieskes, W. (1989) "Late Quaternary changes in Mediterranean intermediate water density and formation rate", *Paleoceanography*, 4(5), 531-545.

Rohling, E., Haines, K., Myers, P. (1998) "Modeling the paleocirculation of the Mediterranean: The last glacial maximum and the Holocene with emphasis on the formation of sapropel S 1", *Paleoceanography*, 13(6), 586-606.

Rohling, E., Hayes, A., De Rijk, S., Kroon, D., Zachariasse, W., Eisma, D. (1998) "Abrupt cold spells in the northwest Mediterranean", *Paleoceanography*, 13(4), 316-322.

Rohling, E., Jorissen, F., De Stigter, H. (1997) "200 Year interruption of Holocene sapropel formation in the Adriatic Sea", *Journal of Micropalaeontology*, 16(2), 97-108.

Rohling, E., Jorissen, F., Grazzini, C., Zachariasse, W. (1993) "Northern Levantine and Adriatic Quaternary planktic foraminifera; Reconstruction of paleoenvironmental gradients", *Marine Micropaleontology*, 21(1-3), 191-218.

Rohling, E., Marino, G., Grant, K. (2015) "Mediterranean climate and oceanography, and the periodic development of anoxic events (sapropels)", *Earth-Science Reviews*, 143, 62-97.

Rohling, E., Myers, P. (2000) "Modeling a 200-Yr Interruption of the Holocene Sapropel S1", *Quaternary Research*, 53(1), 98-104.

Rohling, E., Scaffi, L., Kallel, N., Kucera, M., Hayes, A. (2005) "Glacial Mediterranean sea surface temperatures based on planktonic foraminiferal assemblages", *Quaternary Science Reviews*, 24(7-9), 999-1016.

Rohling, E., Sprovieri, M., Cane, T., Casford, J., Cooke, S., Bouloubassi, I., Emeis, K., Schiebel, R., Rogerson, M., Hayes, A., Jorissen, F., Kroon, D. (2004) "Reconstructing past planktic foraminiferal habitats using stable isotope data: a case history for Mediterranean sapropel S5", *Marine Micropaleontology*, 50(1-2), 89-123.

Rohling, E., Ziegler, M., Marino, G., Mikolajewicz, U., Grimm, R., Grant, K. (2016) "The timing of Mediterranean sapropel deposition relative to insolation, sea-level and African monsoon changes", *Quaternary Science Reviews*, 140, 125-141.

Rosignol-Strick, M. (1985) "Mediterranean Quaternary sapropels, an immediate response of the African monsoon to variation of insolation", *Palaeogeography, Palaeoclimatology, Palaeoecology*, 49(3-4), 237-263.

Roucoux, K., Tzedakis, P., Lawson, I., Margari, V. (2011) "Vegetation history of the penultimate glacial period (Marine isotope stage 6) at Ioannina, north-west Greece", *Journal of Quaternary Science*, 26(6), 616-626.

Rullkötter, J., Rinna, J., Bouloubassi, I., Scholz-Böttcher, B., Meyers, P., Johns, L., Rowland, S. (1998) "Biological marker significance of organic matter origin and transformation in sapropels from the Pisano Plateau, Site 964", *Proceedings of the Ocean Drilling Program, 160 Scientific Results*.

Russell, A., Hönisch, B., Spero, H., Lea, D. (2004) "Effects of seawater carbonate ion concentration and temperature on shell U, Mg, and Sr in cultured planktonic foraminifera", *Geochimica et Cosmochimica Acta*, 68(21), 4347-4361.

Said, M., Radwan, A., Hussein, M., Maiyza, I., Gerges, M. (2011) "Changes in Atlantic water characteristics in the south-eastern Mediterranean sea as a result of natural and anthropogenic activities", *Oceanologia*, 53(1), 81-95.

Sakamoto, T., Emeis, K. (1998) "The sapropel theme of leg 160", *Proceedings of the Ocean Drilling Program, 160 Scientific Results*.

Salmon, K., Anand, P., Sexton, P., Conte, M. (2016) "Calcification and growth processes in planktonic foraminifera complicate the use of B/Ca and U/Ca as carbonate chemistry proxies", *Earth and Planetary Science Letters*, 449, 372-381.

Sangiorgi, F., Bergami, C., Vigliotti, L., Capotondi, L. (2011) "The dark side of the Mediterranean geological record: The sapropel layers and a case study from the Ionian Sea", 658-669, available: <http://dx.doi.org/10.13140/RG.2.1.2637.7363> [accessed 12 Jan 2017].

Sangiorgi, F., Brinkhuis, H., de Lange, G., Bunnik, F., Donders, T., Hennekam, R., van Helmond, N. (2015) "Marine productivity leads organic matter preservation in sapropel S1: palynological evidence from a core east of the Nile River outflow", *Quaternary Science Reviews*, 108, 130-138.

Sangiorgi, F., Dinelli, E., Maffioli, P., Capotondi, L., Giunta, S., Morigi, C., Principato, M., Negri, A., Emeis, K., Corselli, C. (2006) "Geochemical and micropaleontological characterisation of a Mediterranean sapropel S5: A case study from core BAN89GC09 (south of Crete)", *Palaeogeography, Palaeoclimatology, Palaeoecology*, 235(1-3), 192-207.

Scheiderich, K., Zerkle, A., Helz, G., Farquhar, J., Walker, R. (2010) "Molybdenum isotope, multiple sulfur isotope, and redox-sensitive element behavior in early Pleistocene Mediterranean sapropels", *Chemical Geology*, 279(3-4), 134-144.

Schiebel, R., Hemleben, C. (2017) *Planktic Foraminifers in the Modern Ocean*, 1st ed, Springer.

Schiebel, R., Hiller, B., Hemleben, C. (1995) "Impacts of storms on Recent planktic foraminiferal test production and CaCO<sub>3</sub> flux in the North Atlantic at 47 °N, 20 °W (JGOFS)", *Marine Micropaleontology*, 26(1-4), 115-129.

Schiebel, R., Schmuker, B., Alves, M., Hemleben, C. (2002) "Tracking the Recent and late Pleistocene Azores front by the distribution of planktic foraminifers", *Journal of Marine Systems*, 37(1-3), 213-227.

Schiebel, R., Zeltner, A., Treppke, U., Waniek, J., Bollmann, J., Rixen, T., Hemleben, C. (2004) "Distribution

of diatoms, coccolithophores and planktic foraminifers along a trophic gradient during SW monsoon in the Arabian Sea", *Marine Micropaleontology*, 51(3-4), 345-371.

Schlitzer, R., Michelato, A., Johannsen, H., Hausmann, M., Junghans, H., Oster, H., Roether, W., (1991) "Chlorofluoromethane and oxygen in the eastern Mediterranean", *Deep Sea Research Part A. Oceanographic Research Papers*, 38(12), 1531-1551.

Schmidt, D., Elliott, T., Kasemann, S. (2008) "The influences of growth rates on planktic foraminifers as proxies for palaeostudies – a review", *Geological Society, London, Special Publications*, 303(1), 73-85.

Schmidt, D., Renaud, S., Bollmann, J., Schiebel, R., Thierstein, H. (2004) "Size distribution of Holocene planktic foraminifer assemblages: biogeography, ecology and adaptation", *Marine Micropaleontology*, 50(3-4), 319-338.

Schmiedl, G., Mitschele, A., Beck, S., Emeis, K., Hemleben, C., Schulz, H., Sperling, M., Weldeab, S. (2003) "Benthic foraminiferal record of ecosystem variability in the eastern Mediterranean Sea during times of sapropel S5 and S6 deposition", *Palaeogeography, Palaeoclimatology, Palaeoecology*, 190, 139-164.  
Send, U., Font, J., Krahmann, G., Millot, C., Rhein, M., Tintoré, J. (1999) "Recent advances in observing the physical oceanography of the western Mediterranean Sea", *Progress in Oceanography*, 44(1-3), 37-64.  
Shackleton, N. (1969) "The last interglacial in the marine and terrestrial records", *Proceedings of the Royal Society B: Biological Sciences*, 174(1034), 135-154.

Shackleton, N., Chapman, M., Sánchez-Goñi, M., Pailler, D., Lancelot, Y. (2002) "The Classic Marine Isotope Substage 5e", *Quaternary Research*, 58(01), 14-16.

Shaltout, M., Omstedt, A. (2014) "Recent sea surface temperature trends and future scenarios for the Mediterranean Sea", *Oceanologia*, 56(3), 411-443.

Shaw, A. (1964) *Time in Stratigraphy*, 1st ed, McGraw-Hill.

Siani, G., Paterne, M., Michel, E., Sulpizio, R., Sbrana, A., Arnold, M., Haddad, G. (2001) "Mediterranean Sea Surface Radiocarbon Reservoir Age Changes Since the Last Glacial Maximum", *Science*, 294(5548), 1917-1920.

Siebel, W., Hemleben, C., Kuhnt, T., Hamann, Y., Schmiedl, G., Ehrmann, W. (2007) "Clay minerals in late glacial and Holocene sediments of the northern and southern Aegean sea", *Palaeogeography, Palaeoclimatology, Palaeoecology*, 249(1-2), 36-57.

Sierro, F., Hodell, D., Curtis, J., Flores, J., Reguera, I., Colmenero-Hidalgo, E., Bárcena, M., Grimalt, J., Cacho, I., Frigola, J., Canals, M. (2005) "Impact of iceberg melting on Mediterranean thermohaline circulation during Heinrich events", *Paleoceanography*, 20(2).

Simon, D., Marzocchi, A., Flecker, R., Lunt, D., Hilgen, F., Meijer, P. (2017) "Quantifying the Mediterranean freshwater budget throughout the late Miocene: New implications for sapropel formation and the Messinian Salinity Crisis", *Earth and Planetary Science Letters*, 472, 25-37.

Soria, J., Corbí, H. (2016) "Late Miocene–early Pliocene planktonic foraminifer event-stratigraphy of the Bajo Segura basin: A complete record of the western Mediterranean", *Marine and Petroleum Geology*, 77, 1010-1027.

Sousa, S., de Godoi, S., Amaral, P., Vicente, T., Martins, M., Sorano, M., Gaeta, S., Passos, R., Mahiques, M. (2014) "Distribution of living planktonic foraminifera in relation to oceanic processes on the southeastern continental Brazilian margin (23°S–25°S and 40°W–44°W)", *Continental Shelf Research*, 89, 76-87.

Souvermezoglou, E., Scarazzato, P., Sansone, E., Michelato, A., Georgopoulos, D., Civitarese, G., Budillon, G., Bregant, D., Bergamasco, A., Theocharis, A., D'Alcalà, M., Manca, B., Malanotte-Rizzoli, P. (1997) "A synthesis of the Ionian sea hydrography, circulation and water mass pathways during POEM-phase I", *Progress in Oceanography*, 39(3), 153-204.

Spero, H. (1987) "Symbiosis in the planktonic foraminifer, *Orbulina Universa*, and the isolation of its symbiotic dinoflagellate, *Gymnodinium Beisp. Nov 1*", *Journal of Phycology*, 23, 307-317.

Spero, H. (1998) "Life history and stable isotope geochemistry of planktonic foraminifera", *Paleontological Society Paper*, (4), 7-36.

Spezzaferri, S., Hajdas, I., Ariztegui, D., Tamburini, F., Gennari, G. (2009) "Geochemical evidence for high-resolution variations during deposition of the Holocene S1 sapropel on the Cretan ridge, eastern Mediterranean", *Palaeogeography, Palaeoclimatology, Palaeoecology*, 273(3-4), 239-248.

Sprovieri, M., Manta, D., Sabatino, N., Ziveri, P., Incarbona, A. (2011) "Conflicting coccolithophore and geochemical evidence for productivity levels in the Eastern Mediterranean sapropel S1", *Marine Micropaleontology*, 81(3-4), 131-143.

Sprovieri, R., Pelosi, N., Ippolito, G., Di Stefano, E., Dinarès-Turell, J., Incarbona, A. (2013) "Orbital variations in planktonic foraminifera assemblages from the Ionian sea during the middle Pleistocene transition", *Palaeogeography, Palaeoclimatology, Palaeoecology*, 369, 303-312.

Stefanelli, S., Capotondi, L., Ciaranfi, N. (2005) "Foraminiferal record and environmental changes during the deposition of the Early–Middle Pleistocene sapropels in southern Italy", *Palaeogeography, Palaeoclimatology, Palaeoecology*, 216(1-2), 27-52.

Struck, U., Emeis, K., Voß, M., Krom, M., Rau, G. (2001) "Biological productivity during sapropel S5 formation in the Eastern Mediterranean Sea: evidence from stable isotopes of nitrogen and carbon", *Geochimica et Cosmochimica Acta*, 65(19), 3249-3266.

Sušelj K., Bergant K., Mediterranean Oscillation Index. *Geo-phys. Res. Abstr.*, 2006a, 8, 2145

Sutherland, H., Calvert, S., Morris, R. (1984) "Geochemical studies of the recent sapropel and associated sediment from the Hellenic Outer Ridge, eastern Mediterranean Sea. I: Mineralogy and chemical composition", *Marine Geology*, 56(1-4), 79-92.

Tachikawa, K., Revel, M., Menot, G., Bard, E., Sonzogni, C., Pothin, A., Garcia, M., Cornuault, M., Vidal, L. (2015) "Eastern Mediterranean sea circulation inferred from the conditions of S1 sapropel deposition", *Climate of the Past*, 11(6), 855-867.

Tachikawa, K., Vidal, L., Cornuault, M., Garcia, M., Pothin, A., Sonzogni, C., Bard, E., Menot, G., Revel, M. (2015) "Eastern Mediterranean Sea circulation inferred from the conditions of S1 sapropel deposition," *Climate of the Past*, 11(6), 855–867.

Tang, C., Stott, L. (1993) "Seasonal salinity changes during Mediterranean sapropel deposition 9000 years B.P.: Evidence from isotopic analyses of individual planktonic foraminifera", *Paleoceanography*, 8(4), 473-493.

Tanhua, T., Civitarese, G., Álvarez, M., Cardin, V., Schroeder, K., Hainbucher, D. (2013) "The Mediterranean Sea system: A review and an introduction to the special issue", *Ocean Science*, 9(5), 789-803.

Taylforth, J., McCay, G., Ellam, R., Raffi, I., Kroon, D., Robertson, A. (2014) "Middle Miocene (Langhian) sapropel formation in the easternmost Mediterranean deep-water basin: Evidence from northern Cyprus", *Marine and Petroleum Geology*, 57, 521-536.

Telford, R., Li, C., Kucera, M. (2013) "Mismatch between the depth habitat of planktonic foraminifera and the calibration depth of SST transfer functions may bias reconstructions", *Climate of the Past*, 9(2), 859-870.

Tesi, T., Asioli, A., Minisini, D., Maselli, V., Dalla Valle, G., Gamberi, F., Langone, L., Cattaneo, A., Montagna, P., Trincardi, F. (2017) "Large-scale response of the Eastern Mediterranean thermohaline circulation to African monsoon intensification during sapropel S1 formation", *Quaternary Science Reviews*, 159, 139-154.

Teutsch, N., Archer, C., Vance, D., Almogi-Labin, A., Bar-Matthews, M., Matthews, A., Azrieli-Tal, I. (2014) "Evidence from molybdenum and iron isotopes and molybdenum–uranium covariation for sulphidic bottom waters during eastern Mediterranean sapropel S1 formation", *Earth and Planetary Science Letters*, 393, 231-242.

Theocharis A, Gacic M, Kontoyiannis H. 1998. Physical and dynamical processes in the coastal and shelf areas of the Mediterranean. In *The Sea*, volume 11, RobinsonAR, BrinkKH (eds). John Wiley.

Thomson, J., Higgs, N., Wilson, T., Croudace, I., De Lange, G., Van Santvoort, P. (1995) "Redistribution and geochemical behaviour of redox-sensitive elements around S1, the most recent eastern Mediterranean sapropel", *Geochimica et Cosmochimica Acta*, 59(17), 3487-3501.

Thunell, R. (1978) "Distribution of recent planktonic foraminifera in surface sediments of the Mediterranean sea", *Marine Micropaleontology*, 3(2), 147-173.

Thunell, R., Reynolds, L. (1986) "Seasonal production and morphologic variation of *Neogloboquadrina pachyderma* (Ehrenberg) in the northeast pacific", *Micropaleontology*, 32(1), 1.

Thunell, R., Sautter, L. (1992) "Planktonic foraminiferal faunal and stable isotopic indices of upwelling: a sediment trap study in the San Pedro Basin, Southern California Bight", *Geological Society, London, Special Publications*, 64(1), 77-91.

Tierney, J., Russell, J., Huang, Y., Damste, J., Hopmans, E., Cohen, A. (2008) "Northern Hemisphere Controls on Tropical Southeast African Climate During the Past 60,000 Years", *Science*, 322(5899), 252-255.

Timm, O., Timmermann, A., Abe-Ouchi, A., Saito, F., Segawa, T. (2008) "On the definition of seasons in paleoclimate simulations with orbital forcing", *Paleoceanography*, 23(2).

Tintoré, J., Rhein, M., Millot, C., Krahnmann, G., Font, J., Send, U. (1999) "Recent advances in observing the physical oceanography of the western Mediterranean sea", *Progress in Oceanography*, 44(1-3), 37-64.

Toggweiler, J., Herbert, T., Sarmiento, J. (1988) "Mediterranean nutrient balance and episodes of anoxia", *Global Biogeochemical Cycles*, 2(4), 427-444.

Toledo, F., Cachão, M., Costa, K., Pivel, M. (2007) "Planktonic foraminifera, calcareous nannoplankton and ascidian variations during the last 25 kyr in the Southwestern Atlantic: A paleoproductivity signature?", *Marine Micropaleontology*, 64(1-2), 67-79.

Topa, P., Tyszka, J., Faber, Ł., Komosinski, M. (2017) "Modelling ecology and evolution of Foraminifera in the agent-oriented distributed platform", *Journal of Computational Science*, 18, 69-84.

Topper, R., Meijer, P. (2015) "Changes in Mediterranean circulation and water characteristics due to restriction of the Atlantic connection: a high-resolution ocean model", *Climate of the Past*, 11(2), 233-251.

Topper, R., Meijer, P. (2015) "Changes in Mediterranean circulation and water characteristics due to restriction of the Atlantic connection: a high-resolution ocean model", *Climate of the Past*, 11(2), 233-251.

- Törnros, T. (2013) "On the relationship between the Mediterranean oscillation and winter precipitation in the southern Levant", *Atmospheric Science Letters*, 14(4), 287-293.
- Toucanne, S., Angue Minto'o, C., Fontanier, C., Bassetti, M., Jorry, S., Jouet, G. (2015) "Tracking rainfall in the northern Mediterranean borderlands during sapropel deposition", *Quaternary Science Reviews*, 129, 178-195.
- Toucanne, S., Voarintsoa, N., Head, M., Gibbard, P., Railsback, B. (2015) "An optimized scheme of lettered marine isotope substages for the last 1.0 million years, and the climatostratigraphic nature of isotope stages and substages", *Quaternary Science Reviews*, 111, 94–106.
- Triantaphyllou, M., Antonarakou, A., Dimiza, M., Anagnostou, C. (2009) "Calcareous nannofossil and planktonic foraminiferal distributional patterns during deposition of sapropels S6, S5 and S1 in the Libyan Sea (Eastern Mediterranean)", *Geo-Marine Letters*, 30(1), 1-13.
- Triantaphyllou, M., Martínez-Botí, M., Antonarakou, A., Mortyn, P., Kontakiotis, G. (2011) "Field-based validation of a diagenetic effect on G. Ruber mg/ca paleothermometry: Core top results from the Aegean sea (eastern Mediterranean)", *Geochemistry, Geophysics, Geosystems*, 12(9).
- Triantaphyllou, M., Ziveri, P., Gogou, A., Marino, G., Lykousis, V., Bouloubassi, I., Emeis, K.-C., Kouli, K., Dimiza, M., Rosell-Melé, A., Papanikolaou, M., Katsouras, G., Nunez, N. (2009) "Late Glacial–Holocene climate variability at the south-eastern margin of the Aegean Sea," *Marine Geology*, 266(1-4), 182–197.
- Trigo, I., Bigg, G., Davies, T. (1999) "Objective Climatology of Cyclones in the Mediterranean region", *Journal of Climate*, 12(6), 1685-1696.
- Trincardi, F., Langone, L., Correggiari, A., Cattaneo, A. (2003) "The late-holocene Gargano subaqueous delta, Adriatic shelf: Sediment pathways and supply fluctuations", *Marine Geology*, 193(1-2), 61-91.
- Troelstra, S., Paterne, M., Siani, G., Croudace, I., Thomson, J., Mercone, D. (2000) "Duration of S1, the most recent sapropel in the eastern Mediterranean Sea, as indicated by accelerator mass spectrometry radiocarbon and geochemical evidence", *Paleoceanography*, 15(3), 336-347.
- Turley, C.M. (1999) "The changing Mediterranean Sea — a sensitive ecosystem?," *Progress in Oceanography*, 44(1-3), 387–400.
- Twitchett, R. (2007) "The Lilliput effect in the aftermath of the end-permian extinction event", *Palaeogeography, Palaeoclimatology, Palaeoecology*, 252(1-2), 132-144.
- Tyrlis, E., Lelieveld, J. (2013) "Climatology and dynamics of the Summer Etesian winds over the eastern Mediterranean\*", *Journal of the Atmospheric Sciences*, 70(11), 3374-3396.
- Ujjié, Y., de Garidel-Thoron, T., Watanabe, S., Wiebe, P., de Vargas, C. (2010) "Coiling dimorphism within a genetic type of the planktonic foraminifer *Globorotalia truncatulinoides*", *Marine Micropaleontology*, 77(3-4), 145-153.
- Urbanek, A. (1993) "Biotic crises in the history of upper Silurian graptoloids: A Palaeobiological model", *Historical Biology*, 7(1), 29-50.
- Vallina, S., Castro-Bugallo, A., Cermeño, P. (2013) "Diversification patterns of planktic foraminifera in the fossil record", *Marine Micropaleontology*, 104, 38-43.
- Vallis, G.K., Gerber, E.P. (2008) "Local and hemispheric dynamics of the North Atlantic Oscillation, annular patterns and the zonal index," *Dynamics of Atmospheres and Oceans*, 44(3-4), 184–212.

- Van Helmond, N., Hennekam, R., Donders, T., Bunnik, F., de Lange, G., Brinkhuis, H., Sangiorgi, F. (2015) "Marine productivity leads organic matter preservation in sapropel S1: palynological evidence from a core east of the Nile River outflow", *Quaternary Science Reviews*, 108, 130-138.
- Van Santvoort, P., De Lange, G., Mercone, ., Thomson, . (1999) "Review of recent advances in the interpretation of eastern Mediterranean sapropel S1 from geochemical evidence", *Marine Geology*, 153(1-4), 77-89.
- Van Santvoort, P., de Lange, G., Thomson, J., Cussen, H., Wilson, T., Krom, M., Ströhle, K. (1996) "Active post-depositional oxidation of the most recent sapropel (S1) in sediments of the eastern Mediterranean Sea", *Geochimica et Cosmochimica Acta*, 60(21), 4007-4024.
- Venancio, I., Franco, D., Belem, A., Mulitza, S., Siccha, M., Albuquerque, A., Schulz, M., Kucera, M. (2016) "Planktonic foraminifera shell fluxes from a weekly resolved sediment trap record in the southwestern Atlantic: Evidence for synchronized reproduction", *Marine Micropaleontology*, 125, 25-35.
- Vergnaud-Grazzini, C., Pujol, C., Den Dulk, M., Rohling, E. (1995) "Abrupt hydrographic change in the Alboran sea (western Mediterranean) around 8000 yrs BP", *Deep Sea Research Part I: Oceanographic Research Papers*, 42(9), 1609-1619.
- Vervatis, V., Somot, S., Özsoy, E., Gertman, I., Sofianos, S., Mantziafou, A., Georgiou, S. (2015) "Climate variability and deep water mass characteristics in the Aegean sea", *Atmospheric Research*, 152.
- Violette, P.E.L., Tintoré, J., Font, J. (1990) "The surface circulation of the Balearic Sea," *Journal of Geophysical Research*, 95(C2), 1559.
- Visbeck, M.H., Hurrell, J.W., Polvani, L., Cullen, H.M. (2001) "The North Atlantic Oscillation: Past, present, and future," *Proceedings of the National Academy of Sciences*, 98(23), 12876–12877.
- Wade, C., Kroon, D., Kucera, M., Darling, K. (2006) "A resolution for the coiling direction paradox in *Neogloboquadrina pachyderma*", *Paleoceanography*, 21(2).
- Walker, M. (2008) *Quaternary Dating Methods*, 1st ed, John Wiley & Sons: Chichester.
- Warner, J., Bever, A., Signell, R., Sherwood, C., Harris, C. (2008) "Sediment dispersal in the northwestern Adriatic sea", *Journal of Geophysical Research*, 113(C11).
- Wasserman, P. (1989) *Neural Computing*, 1st ed, Van Nostrand Reinhold: New York.
- Wehausen, R., Winkhofer, M., Rohling, E., Roberts, A., Larrasoana, J. (2003) "Three million years of monsoon variability over the northern Sahara", *Climate Dynamics*, 21(7-8), 689-698.
- Weldeab, S., Siebel, W., Wehausen, R., Emeis, K., Schmiedl, G., Hemleben, C. (2003) "Late Pleistocene sedimentation in the Western Mediterranean Sea: implications for productivity changes and climatic conditions in the catchment areas", *Palaeogeography, Palaeoclimatology, Palaeoecology*, 190, 121-137.
- Weldeab, S., Sperling, M., Schulz, H., Hemleben, C., Emeis, K., Beck, S., Mitschele, A., Schmiedl, G. (2003) "Benthic foraminiferal record of ecosystem variability in the eastern Mediterranean Sea during times of sapropel S5 and S6 deposition", *Palaeogeography, Palaeoclimatology, Palaeoecology*, 190, 139-164.
- Weston, K., Fernand, L., Mills, D., Delahunty, R., Brown, J. (2005) "Primary production in the deep chlorophyll maximum of the central North Sea", *Journal of Plankton Research*, 27(9), 909-922.
- Williams, M., Duller, G., Williams, F., Woodward, J., Macklin, M., El Tom, O., Munro, R., El Hajaz, Y., Barrows, T. (2015) "Causal links between Nile floods and eastern Mediterranean sapropel formation during the past 125 kyr confirmed by OSL and radiocarbon dating of Blue and White Nile sediments", *Quaternary Science Reviews*, 130, 89-108.

- Woodward, J. (2009) *The Physical Geography Of The Mediterranean*, Oxford University Press: New York.
- Woodward, J., Holt, T., Palutikof, J., Harding, A. (2009) in *The Climate System*, Oxford University Press: Oxford, 69-88.
- Woodward, J., Hoogakker, B., Hayes, A., Casford, J., Abu-Zied, R., Rohling, E. (2009) in *The Marine Environment: Present And Past*, Oxford University Press: Oxford, 33-67.
- Wu, J., Böning, P., Pahnke, K., Tachikawa, K., de Lange, G. (2016) "Unraveling North-African riverine and eolian contributions to central Mediterranean sediments during Holocene sapropel S1 formation", *Quaternary Science Reviews*, 152, 31-48.
- Wu, J., Liu, Z., Stuu, J., Zhao, Y., Schirone, A., de Lange, G. (2017) "North-African paleodrainage discharges to the central Mediterranean during the last 18,000 years: A multiproxy characterization", *Quaternary Science Reviews*, 163, 95-113.
- Wüst, G. (1961) "On the vertical circulation of the Mediterranean Sea," *Journal of Geophysical Research*, 66(10), 3261–3271.
- Xie, X., Duchamp-Alphonse, S., Cheng, X., Siani, G., Paterne, M., Colin, C., Liu, Z., Zhao, Y. (2011) "Variations of the Nile suspended discharges during the last 1.75Myr", *Palaeogeography, Palaeoclimatology, Palaeoecology*, 311(3-4), 230-241.
- Žarić, S., Donner, B., Fischer, G., Mulitza, S., Wefer, G. (2005) "Sensitivity of planktic foraminifera to sea surface temperature and export production as derived from sediment trap data", *Marine Micropaleontology*, 55(1-2), 75-105.